THE HYDROGEN ATOM

Doorway to Quantum Physics, its Symmetries and Radiative Shift

G. Jordan Maclay

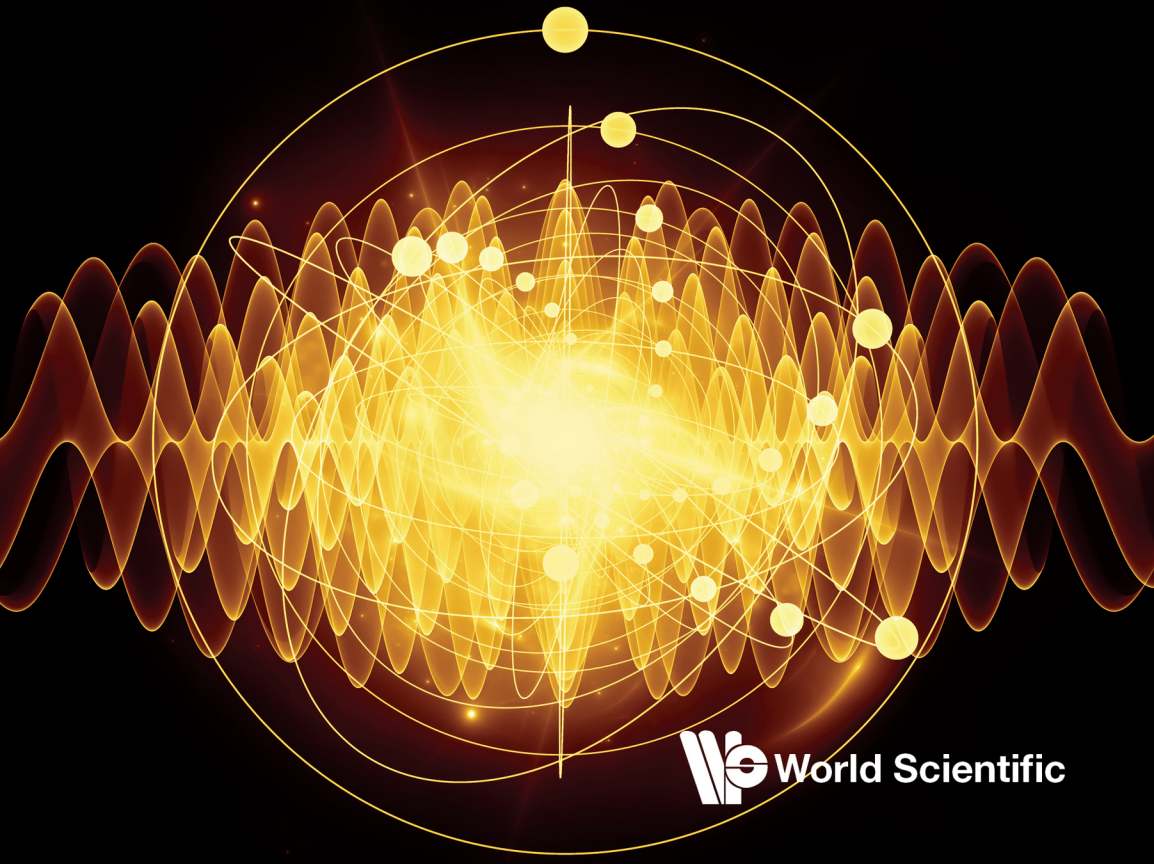

World Scientific

THE HYDROGEN ATOM

Doorway to Quantum Physics, its Symmetries and Radiative Shift

This page intentionally left blank

THE HYDROGEN ATOM

Doorway to Quantum Physics, its Symmetries and Radiative Shift

G. Jordan Maclay
University of Illinois at Chicago, USA
Quantum Fields LLC, USA

World Scientific
NEW JERSEY • LONDON • SINGAPORE • BEIJING • SHANGHAI • HONG KONG • TAIPEI • CHENNAI • TOKYO

Published by

World Scientific Publishing Co. Pte. Ltd.

5 Toh Tuck Link, Singapore 596224

USA office: 27 Warren Street, Suite 401-402, Hackensack, NJ 07601

UK office: 57 Shelton Street, Covent Garden, London WC2H 9HE

Library of Congress Control Number: 2025942253

British Library Cataloguing-in-Publication Data
A catalogue record for this book is available from the British Library.

THE HYDROGEN ATOM
Doorway to Quantum Physics, its Symmetries and Radiative Shift

Copyright © 2026 by World Scientific Publishing Co. Pte. Ltd.

All rights reserved. This book, or parts thereof, may not be reproduced in any form or by any means, electronic or mechanical, including photocopying, recording or any information storage and retrieval system now known or to be invented, without written permission from the publisher.

For photocopying of material in this volume, please pay a copying fee through the Copyright Clearance Center, Inc., 222 Rosewood Drive, Danvers, MA 01923, USA. In this case permission to photocopy is not required from the publisher.

ISBN 978-981-98-2036-8 (hardcover)
ISBN 978-981-98-2037-5 (ebook for institutions)
ISBN 978-981-98-2038-2 (ebook for individuals)

For any available supplementary material, please visit
https://www.worldscientific.com/worldscibooks/10.1142/14500#t=suppl

Desk Editor: Carmen Teo Bin Jie

Typeset by Stallion Press
Email: enquiries@stallionpress.com

Printed in Singapore

I dedicate this book to my wife Mary, my family, including Colin, Rachael, Zeev, Augie, Matthew, Eliza, Mona and Aaron, my brother Otis, my collaborators, my students, and myself, and to the betterment of all humanity.

This page intentionally left blank

Preface

Understanding the hydrogen atom is at the heart of modern physics. Exploring the energy levels and the symmetry of the most fundamental two-body system has led to advances in atomic physics, quantum mechanics, quantum electrodynamics, and elementary particle physics.

Regularities in the spectrum of atomic hydrogen inspired Bohr's theory of the atom and what has been called the *old quantum theory*, which described general features of the atom but not detailed behavior. A crucial success of the Schrodinger theory of wave mechanics, which was introduced about 1921, was the calculation of the absorption and emission of radiation and the second and third order Stark effect in the H atom. This non-relativistic theory had many successes but was unable to deal with the fine structure of the hydrogenic lines, a challenge solved by the relativistic Dirac theory, which explained the fine structure and gave a value for the spin component of the magnetic moment of the electron (g-2). Experiments by Lamb and Retherford in 1947 revealed problems with the Dirac theory, in particular that it incorrectly predicted that the $2s_{1/2}$ and $2p_{1/2}$ levels were degenerate. The method of renormalization was introduced by Bethe to compute the Lamb shift, paving the way for the computation of radiative effects due to the interaction of the electron with its own radiation field or with the quantum fluctuations of the electromagnetic field, while avoiding divergences. This was the birth of Quantum Electrodynamics (QED), today a mature theory that has predicted the energy levels of the hydrogen atom and the anomalous magnetic moment of the electron to unprecedented precision, the most precise physical theory in history [1, 2]. Today, significant effort has been focused on the calculation of higher-order radiative shifts. However, in this text, we focus on a deeper understanding of the H atom and the first-order radiative interaction that accounts for 96% of the shift.

Measurement and explanation of the properties of the hydrogen atom have been central to the development of modern physics over the last century. One of the most useful and profound ways to understand its properties is through its symmetries, which we explore, beginning with the symmetry of the Hamiltonian, which reflects the symmetry of the degenerate levels, then the larger non-invariance and spectrum-generating groups, which include all the states. The successes in using symmetry to explore the hydrogen atom led to the use of symmetry to understand and model other physical systems, particularly elementary particles.

In Part 1, we discuss the role of symmetry and group theory in understanding the H atom over the last century, and introduce some basic ideas about symmetry groups. We provide an integrated treatment of the symmetries of the classical and Schrödinger hydrogen atom, including the four-dimensional rotational symmetry group SO(4) (special orthogonal group in four dimensions), which is the degeneracy group, with the rotations in four dimensions generated by the angular momentum vector and Runge–Lenz vector, which points along the semi-major axis of the eliptical orbit. We calculate the energy levels using these symmetry operators and consider the wavefunctions in configuration space and in three- and four-dimensional momentum space, and how the wavefunctions are transformed by the generators. We introduce a novel set of wavefunctions that includes both the bound and scattering states and that uses the usual Schrodinger quantum numbers nlm. These wavefunctions allow for a simplified and integrated approach to quantum theory calculations. The semi-classical limit of the wavefunctions is explored.

In Part 2, we enlarge the degeneracy group to include all energy states of the H atom, bound and scattering, and consider the non-invariance group or spectrum-generating group SO(4,1), and the expanded group SO(4,2) that allows us to write Schrodinger's equation in terms of the generators. The group SO(p,q) is the group of orthogonal transformations that preserve the quantity $X = x_1^2 + x_2^2 + \cdots + x_p^2 - \cdots - x_{p+q}^2$, which may be viewed as the norm of a p+q-dimensional vector in a space that has a metric with p plus signs and q minus signs. The letters SO stand for special orthogonal, meaning the orthogonal transformations have a determinant equal to +1.

We present a unified treatment of the symmetries of the Schrodinger hydrogen atom that focuses on the physics of the atom, that gives explicit expressions for all the manifestly Hermitian generators in terms of position and momenta operators in a Cartesian space, that explains the action of the generators on the basis states, and that unifies the treatment of the bound

and continuum states in terms of wave functions with the same quantum numbers as the ordinary bound states. We evaluate the Casimir operators (group invariants that are numerical constants) that characterize the group representations. New group theoretical results are derived that are used in Part 3 for the analytical calculation of radiative shifts.

In Part 3, we discuss radiative shifts in general, including in classical physics for the Coulomb problem and for the simple harmonic oscillator. We discuss the historical context, the significance and impact of Bethe's seminal calculation of the Lamb shift that was done using second order perturbation theory. Then we take a different approach to calculate the radiative shift in field theory using only the equations of motion (Klein–Gordon equation), making none of the usual assumptions. We take the non-relativistic limit of the expression for the Lamb shift and use SO(4,2) methods to obtain an analytical expression for the first-order Lamb shift with no sum over all states, unlike the usual formulation. We obtain a generating function for the radiative shift for all energy levels. This unique analytical result allows us to determine the contribution to the shift from each frequency of virtual radiation and predicts the presence of a virtual radiation field that extends more than a thousand times the Bohr radius of the atom. If other atoms are nearby, this field results in the Casimir force and the van der Waals force [3].

We sometimes use the phrase "hydrogen-like atom", referring to atoms that are ionized with only one orbital electron like hydrogen. Such atoms, for example U^{238+}, have been measured to determine, for example, the role of the atomic number Z. Other hydrogen-like atoms include ionized helium, ionized deuterium, and positronium, which is made of a bound electron and positron, and muonium, made of a bound antimuon and an electron, or muonic atoms, in which an electron has been replaced by a muon. These unique atoms have radiative shifts like ordinary hydrogen, and although the qualitative behaviors are similar, the quantitative results are very different and give insight into fundamental physics [2]. Exploring muonic hydrogen spectra [4], and new physics using Rydberg states [5–10] using ultra-high precision measurement of the energy levels has led to new understanding of two-body systems with low Z, including muonium, positronium, and tritium [11]. Measurements of levels shifts are currently being used to determine the radius of the proton [1]. We will not discuss these hydrogen-like atoms in further detail.

The hydrogen atom will doubtlessly continue to be one of the testing grounds for fundamental physics. Researchers are exploring the relationship

between the hydrogen atom and quantum information [12], and the effect of non-commuting canonical variables $[x_i, x_j] \neq 0$ on energy levels [13–15]. We can expect that further investigations of the hydrogen atom and hydrogen-like atoms will continue to reveal new vistas of physics and that symmetry considerations will play an important part.

The first eight chapters of the text assume that the reader is familiar with quantum theory and classical mechanics at a first year graduate level. The remainder of the book, which is primarily on radiative shifts and quantum fluctuations of the electromagnetic field, assumes that the reader is also familiar with quantum field theory at a first year graduate level. The group theory is explained in the text. Students, non-experts, and the new generation of scientists may find the clearer, integrated presentation of the symmetries of the hydrogen atom helpful and illuminating, perhaps motivating some to use these methods in various new contexts. Senior researchers will find new perspectives, even some surprises and encouragements.

I am grateful to my friends, teachers, and collaborators for discussions over many years, with particular thanks to Peter Milonni and Lowell S. Brown, each of whom has been an important inspiration and a trusted source of knowledge for many years. I especially thank my good friend Peter Milonni, who read most of the book in draft form and gave me very helpful comments.

G. Jordan Maclay
Saint Charles, Illinois
USA, 2025

Contents

PART 1

Symmetry and Degeneracy of Energy Levels in a Coulomb Potential

In Chapter 1, we give an historical account of the role of symmetry in quantum mechanics and of the seminal work done to explore the symmetries of the Schrodinger hydrogen atom. Most of this work was done from 1920 to 1975, when physicists were using the H atom as a platform to explore symmetries that might be applicable to elementary particle physics. Why is symmetry important? Each symmetry in a physical system is associated with a conserved quantity, and conserved quantities characterize quantum systems. Symmetry in time corresponds to conservation of energy, symmetry with respect to translation in space corresponds to conservation of momentum, and isotropy in three-dimensional space corresponds to the conservation of angular momentum.

In Chapter 2, the theory of the classical H atom is presented. The classical equations of motion of the non-relativistic hydrogen atom in configuration and momentum space are derived from symmetry considerations alone.

In Chapter 3, we discuss the quantum theory of the H atom and provide some general background observations about symmetry groups and non-invariance groups. We discuss the degeneracy groups for the Schrodinger, Dirac, and Klein–Gordon equations, and introduce the novel $(Z\alpha)^{-1}$ eigenstates that allow us to treat the bound and scattering states in a uniform way, using the usual Schrodinger energy eigenstate quantum numbers nlm. The physical meaning of the symmetry transformations and the structure of the SO(4) degeneracy group are discussed.

In Chapter 4, symmetries are discussed using the language of quantum mechanics. In order to display the symmetries in quantum mechanics in the most elegant and uniform way we use as a basis our eigenstates of the inverse of the coupling constant, $(Z\alpha)^{-1}$. We discuss the wave functions in momentum and configuration space, how they transform, and their classical limit for Rydberg states.

In Chapter 5, we discuss the Dirac H atom and its symmetry operators, the generalized parity operator, and the conserved pseudoscalar operator, which together give a representation of the degeneracy group SO(4).

Chapter 1

Introduction to the H Atom and Symmetry Principles

1.1 Brief History of Symmetry in Quantum Mechanics and its Role in Understanding the Schrodinger Hydrogen Atom

The hydrogen atom is the fundamental two-body system and perhaps the most important tool of atomic physics, and the continual challenge is to continually improve our understanding of the hydrogen atom and to calculate its properties to the highest accuracy possible. The current QED theory is the most precise of any physical theory [1]:

> The study of the hydrogen atom has been at the heart of the development of modern physics . . . owing to the simplicity of the H atom, theoretical calculations reach precision up to the 12th decimal place . . . high resolution laser spectroscopy experiments . . . reach to the 15th decimal place for the 1S–2S transition . . . The Rydberg constant is known to 6 parts in 10^{12} [1, 16]. Today, the precision is so great that the measurement of the energy levels in the H atom has been used to determine the radius of the proton.

Continual progress in understanding the properties of the hydrogen atom has been a key to progress in quantum physics [17]. Understanding the atomic spectra of the hydrogen atom drove the discovery of quantum mechanics in the 1920s. The measurement of the Lamb shift in 1947 and its explanation in terms of the interaction of the atom with its own radiation field or, from a different perspective, with the quantum vacuum fluctuations, ushered in a revolution: the birth of quantum electrodynamics [18–20]. Exploring the symmetries of the hydrogen atom has been an essential part of this progress. Symmetry is a concept that has played a broader role in physics in general, for example, in understanding the

dynamics of the planets, atomic and molecular spectra, and the masses of elementary particles.

When applied to an isolated system, Newton's equations of motion imply the conservation of momentum, angular momentum, and energy. But the significance of these conservation laws was not really understood until 1911 when Emmy Noether established the connection between symmetry and conservation laws [21]. Rotational invariance in a system results in the conservation of angular momentum; translational invariance in space results in the conservation of momentum; and translational invariance in time results in the conservation of energy. We will discuss Nöther's theorem in more detail in Section 1.2.

Another critical ingredient of knowledge, on which Noether based her proof, was the idea of an infinitesimal transformation, such as a infinitesimal rotation generated by the angular momentum operators in quantum mechanics. These ideas of infinitesimal transformations originated with the Norwegian mathematician Sophus Lie, who studied differential equations in the latter half of the nineteenth century. He studied the collection of infinitesimal transformations that would leave a differential equation invariant [22]. In 1918, German physicist and mathematician Hermann Weyl, in his classic book *The Theory of Groups and Quantum Mechanics*, would refer to this collection of differential generators leaving an operator invariant as a linear algebra, ushering in a little of the terminology of modern group theory [23]. Still, this was a very early stage in understanding the role of symmetry in the language of quantum theory. When he introduced the new idea of a commutator on page 264, he put the word "commutator" in quotes. In the preface, Weyl made a prescient observation: "...the essence of the new Heisenberg–Schrodinger–Dirac quantum mechanics is to be found in the fact that there is associated with each physical system a set of quantities, constituting a non-commutative algebra in the technical mathematical sense, the elements of which are the physical quantities themselves."

A few years later Eugene Wigner published in German *Group Theory and Its Application to the Quantum Mechanics of Atomic Spectra* [24]. One might ask why this classic was not translated into English until 1959. In the preface to the English edition, Prof. Wigner recalled: "When the first edition was published in 1931, there was a great reluctance among physicists toward accepting group theoretical arguments and the group theoretical point of view. It pleases the author that this reluctance has virtually vanished..." It was the application of group theory in particle physics in the early

sixties, such as SU(3) and chiral symmetry, that reinvigorated interest in Wigner's book and the field in general. In the 1940s, Wigner and Bargmann developed the representation theory of the Poincare group that provided an infrastructure for the development of relativistic quantum mechanics [24, 25].

The progress in understanding the symmetries of the hydrogen atom has some parallels to the history of symmetry in general: there were some decades of interest, but after the 1930s interest waned for about three decades in both fields, until stimulated by the work on symmetry in particle physics.

Probably the first major advance in understanding the role of symmetry in the classical treatment of the Kepler problem after Newton's discovery of universal gravitation, elliptical orbits and Kepler's laws (1687), was made 150 years later by Laplace. He discovered the existence of three new constants of motion in addition to the components of the angular momentum [26]. These additional conserved quantities are the components of a three-dimensional vector which determines the direction of the perihelion of the motion (point closest to the focus) and whose magnitude is the eccentricity of the orbit. The Laplace vector was rediscovered by Jacobi and has since been rediscovered numerous times under different names. Today, it is generally referred to as the Runge-Lenz vector. But the significance of this conserved quantity, which determines the semi-major axis of the elliptical orbit, was not well understood until the 1930s.

In 1924, Pauli made the next major step forward in understanding the role of symmetry in the hydrogen atom [27, 28]. He used the conserved Runge–Lenz vector $\boldsymbol{A}$ and the conserved angular momentum vector $\boldsymbol{L}$ to derive the energy spectrum of the hydrogen atom by purely algebraic means, a beautiful result, yet he did not explicitly identify that $\boldsymbol{L}$ and $\boldsymbol{A}$ formed the symmetry group $\mathrm{SO}(4) \approx \mathrm{SU}(2) \bigotimes \mathrm{SU}(2)$ corresponding to the degeneracy.[1] At this time, the degree of degeneracy in hydrogen energy levels was believed to be n^2 for a state with the principal quantum number n, clearly greater than the degeneracy due to rotational symmetry, which is $(2l+1)$. The degeneracy n^2 arises from the possible values of the angular

[1] The group SU(2), special unitary group in two dimensions, corresponds to rotations in a complex two dimensional space that are isomorphic to rotations in a 3-dimensional space [29]. The group SO(4) is the group of special orthogonal transformations (rotations) in a four dimensional vector space. Special means the determinant of the rotation matrix is +1.

momentum $l = 0, 1, 2, \ldots n-1$, and the $2l+1$ values of the component of angular momentum along the azimuthal axis $m = -l, -l+1, \ldots 0, 1, 2, l+1$. The additional degeneracy was called an "accidental degeneracy" [30].

Six years after Pauli's paper, Hulthen used the new Heisenberg matrix mechanics to simplify the derivation of the energy eigenvalues of Pauli by showing that the sum of the squares $\boldsymbol{L}^2 + \boldsymbol{A}^2$ could be used to express the Hamiltonian and derive the energy eigenvalues [31]. In a one sentence footnote in this three page paper, Hulthen gives probably the most important information in the paper: Prof. Otto Klein, who had collaborated for years with Sophus Lie, had noticed that the two conserved vectors formed the generators of the Lorentz group, which we can describe as rotations in four dimensions, the fourth dimension being time. This is the non-compact group SO(3,1), the special orthogonal group in four dimensions whose transformations leave the magnitude $g_{\mu\nu}z^\mu z^\nu = -t^2 + x^2 + y^2 + z^2$ unchanged.[2] Klein's perceptive observation triggered the introduction of group theory to understanding the hydrogen atom.

About a decade later, in 1935, the Russian physicist Vladimir Fock published a major article in Zeitshrift für Physik, the journal in which all key articles about the hydrogen atom cited were published [32]. He transformed Schrodinger's equation for a given energy eigenvalue from configuration space to momentum space, and did a stereographic projection onto a unit sphere, and showed that the bound state momentum space wave functions were spherical harmonics in four dimensions. He stated that this showed that rotations in four dimensions corresponded to the symmetry of the degenerate bound state energy levels in momentum space, realizing the group SO(4), the group of special orthogonal transformations which leaves the norm of a four-vector $U_0^2 + U_1^2 + U_2^2 + U_3^2$ constant. By counting the number of four-dimensional spherical harmonics Y_{nlm} in momentum space ($m = -l, -l+1 \ldots 0, 1, \ldots, l$, where the angular momentum l can equal $l = n-1, n-2, \ldots 0$) he determined that the degree of degeneracy for the energy level characterized by the principal quantum number n was n^2. It is interesting that Fock did not cite the work by Pauli implying the four-dimensional rotational symmetry in configuration space. Fock also presented some ideas about using this symmetry in calculating form factors for atoms.

[2] We employ natural Gaussian units so $\hbar = 1$, $c = 1$, and $\alpha = (e^2/\hbar c) \approx 1/137$. The notation for indices and vectors is $\mu, \nu, \ldots = 0, 1, 2, 3$; $i, j, . = 1, 2, 3$; $p_\mu p^\mu = -p_0^2 + \boldsymbol{p}^2$, $\boldsymbol{p} = (p_1, p_2, p_3)$, $g_{\mu\nu} = (-1, 1, 1, 1)$.

A year later, the German-American mathematician and physicist Valentine Bargmann showed that for bound states ($E < 0$) Pauli's conserved operators, the angular momentum $\boldsymbol{L}$ and the Runge–Lenz vector $\boldsymbol{A}$, obeyed the commutation rules of SO(4) [25]. His use of commutators was so early in the field of quantum mechanics that Bargmann explained the square bracket notation he used for a commutator in a footnote [33]. He gave a differential expression for the operators, adapting the approach of Lie generators in the calculation of the commutators. He linked solutions to Schrodinger's equation in parabolic coordinates to the existence of the conserved Runge–Lenz vector and was thereby able to establish the relationship of Fock's results to the algebraic representation of SO(4) for bound states implied by Fock and Pauli [25]. He also pointed out that the scattering states ($E > 0$) could provide a representation of the group SO(3,1). In a note at the end of the paper, Bargmann, who was at the University in Zurich, thanked Pauli for pointing out the paper of Hulthen and the observation by Klein that the Lie algebra of $\boldsymbol{L}$ and $\boldsymbol{A}$ was the same as the infinitesimal Lorentz group, which is how he referred to a Lie algebra. Bargmann's work was a milestone demonstrating the relationship of symmetry to conserved quantities, and it clearly showed that, to fully understand a physical system, one needed to go beyond the usual ideas of geometrical symmetry. This work was the birth, in 1936, without much fanfare, of the idea of dynamical symmetry.

Little attention was paid to these developments until the 1960's when interest arose primarily because of the application of group theory in particle physics, particularly modeling for the mass spectra of hadrons. Particle physicists faced the challenge of achieving a quantitative description of hadron properties, particularly the mass spectra and form factors, in terms of quark models. Since little was known about quark dynamics, they turned to group-theoretical arguments, exploring groups like SU(3), chiral $\mathrm{U}(3) \otimes \mathrm{U}(3)$, $\mathrm{U}(6) \otimes \mathrm{U}(6)$ etc. The success of the eight-fold way of SU(3) (special unitary group in three dimensions) of American physicist Murray Gell-Mann in 1962 brought attention to the use of symmetry considerations and group theory as important tools for exploring systems in which one was unsure of the exact dynamics [34].

In 1964, three decades after Fock's work, American physicist Julian Schwinger published a paper using SO(4) symmetry to construct a Green function for the Coulomb potential, which he noted was based on a class he taught at Harvard in 1949 [35]. The publication was a response to the then current emphasis on group theory and symmetry which led, as Israeli physicist Yuval Ne'eman described it, "to the great-leap-forward"

in particle physics during the years 1961–66 [36]. Some of the principal investigators leading this effort were Ne'eman [36], Gell-Mann [34, 37, 38], and Israeli physicist Y. Dothan [39], Japanese physicist Yochiri Nambu [40], and English-American Freeman Dyson [41]. Advantage was taken of the mathematical infrastructures of group theory developed years earlier [23–25, 42, 43].

Interest was particularly strong in systems with wave equations that had an infinite number of components, which characterize non-compact groups. In about 1965, this interest in particle physics gave birth to the identification of the non-compact groups SO(4,1) and SO(4,2) as providing Spectrum Generating Algebras (SGA) that might serve as models for hadronic masses. The hydrogen atom was seen as a model for exploring the infinite-dimensional representations of non-compact groups. The first mention of SO(4,1) was by Barut, Budini, and Fronsdal [44], where the H atom was presented as an illustration of a system characterized by non-compact representation, and so comprising an infinite number of states. The first mention of a six-dimensional symmetry, referred to as the "non-compact group O(6)", appears to be by the Russian physicists I. Malin and V. Man'ko of the Moscow Physico-technical Institute [45]. In a careful three page paper, they showed that all the bound states of the H atom energy spectrum in Fock coordinates provided a representation of this group, and they calculated the Casimir operators for their symmetric tensor representation in parabolic coordinates.

Very shortly thereafter, Turkish-American theoretical physicist Asim Barut and his student at the University of Colorado, German theoretical physicist Hagen Kleinert, showed that including the dipole operator er as a generator led to the expansion of SO(4,1) to SO(4,2), and that all the bound states of the H atom formed a representation of SO(4,2) [46]. This allowed them to calculate dipole transition matrix elements algebraically. They give a position representation of the generators based on the use of parabolic coordinates. The generators of the transformations are given in terms of the raising and lowering operators for the quantum numbers for solutions to the H atom in parabolic coordinates. The dilation operator is used to go from one SO(4) subspace with one energy to a SO(4) subspace with a different energy, and it has a rather complicated form. They also used SO(4,2) symmetry to compute form factors [47].

The papers of Polish-American physicist Myron Bander and French physicist Claude Itzakson published in 1966, when both were working at SLAC (Stanford Linear Accelerator in California), provided the first

mathematically rigorous and "succinct" review of the O(4) symmetry of the H atom, and provided an introduction to SO(4,1) [48, 49], which is referred to as Spectrum Generating Algebra because it can be used to generate all states of the H atom. They used two approaches in their mathematical analysis, the first was referred to as "the infinitesimal method," based on the two symmetry operators, $\boldsymbol{L}$ and $\boldsymbol{A}$ and the O(4) group they form, and the other, referred to as the "global method," first done by Fock, converted the Schrodinger equation to an integral equation with a manifest four-dimensional symmetry in momentum space. They established the equivalence of the two approaches by appealing to the solutions of the H atom in parabolic coordinates and demonstrated that the symmetry operators in the momentum space correspond to the symmetry operators in the configuration space. As noted, the stereographic projection depends on the energy, so the statements for a SO(4) subgroup were valid only in a subspace of constant energy. They then explored the expansion of the SO(4) group to include scale changes so that the energy can be changed, transforming between states of different principal quantum number, which correspond to different subspaces of SO(4). To ensure that this expansion results in a group, they included other transformations which led to the generators forming the conformal group O(4,1). Their mathematical analysis introducing SO(4,1) was based on the projection of a p-dimensional space (4 in the case of interest) on a paraboloid in p + 1 dimensions (5 dimensions). In their derivation, they treated bound states in their first paper [48] and scattering states in their second paper [49].

As we have indicated, interest in the SO(4,2) symmetry of the Schrodinger equation was driven by a program focused on developing equations for composite systems that had infinite multiplets of energy solutions and ultimately could lead to equations that could be used to predict masses of elementary particles, perhaps using other dimensions [40, 48–53]. In 1969, Jordan and Pratt showed that one could add spin to the generators $\boldsymbol{A}$ and $\boldsymbol{L}$, and still form a SO(4) degeneracy group. Defining $\boldsymbol{J} = \frac{1}{2}(\boldsymbol{L} + \boldsymbol{A}) + \boldsymbol{S}$, they showed that one could obtain a representation of O(4,1) for any spin S [54].

In their review of the symmetry properties of the hydrogen atom, Bander and Itzakson emphasized their purpose for exploring the group theory of the hydrogen atom [48]:

> The construction of unitary representations of non-compact groups which have the property that the irreducible representations of their maximal subgroup appear at most with multiplicity one is of certain

interest for physical applications. The method of construction used here in the Coulomb potential case can be extended to various other cases. The geometrical emphasis may help visualize things and provide a global form of the transformations.

Special attention was also given to solutions for the hydrogen atom from the two-body Bethe–Salpeter equation, which allows for detailed nuclear dynamics with a proton and electron interacting by a Coulomb potential, since the symmetry was that of a relativistic non-compact group [40, 53, 55, 56].

Finally in 1969, five years after it was published, Schwinger's form of the Coulomb Green function based on the SO(4) symmetry was used to calculate the Lamb shift by Michael Lieber, one of Schwinger's students at Harvard [35, 57]. A year later, Robert Huff, a student of Christian Fronsdal at UCLA, focused on SO(4,2) group theory to compute the Lamb shift [58]. He converted the conventional expression for the Lamb shift into a matrix element containing generators of SO(4,2), and was able to perform rotations and scale changes to simplify and evaluate the matrix elements. After clever mathematical manipulation, he obtained an expression for the Bethe log in terms of a rapidly terminating series for the level shifts.

In the next few years, researchers published a few mathematically oriented papers [54, 59–63], a short book [64] dealing with the symmetries of the Coulomb problem, and a paper by Barut presenting a SO(4,2) formulation of symmetry breaking in relativistic Kepler problems, with a 1 page summary of the application of SO(4,2) to the non-relativistic hydrogen atom [47, 65]. Bednar published a paper applying group theory to a variety of modified Coulomb potentials which included some matrix elements of SO(4,2) using hydrogen atom basis states with quantum numbers nlm [66]. There was also interest in the application of symmetry methods and dynamical groups in molecular chemistry [67] and atomic spectroscopy [68].

In the 1970s researchers focused on developing methods of group theory and on understanding dynamical symmetries in diverse systems [69–71]. A book on group theory and its applications appeared in 1971 [72]. Barut and his collaborators published a series of papers dealing with the hydrogen atom as a relativistic elementary particle, leading to an infinite component wave equation and mass formula [73–76].

Papers on the classical Kepler problem, the Runge–Lenz vector, and SO(4) for the hydrogen atom have continued to appear sporadically over the years, from 1959 to today. Many were published in the 1970s [77–83] and some since 1980, including [28, 84–87]. Papers dealing with SO(4,2) are

much less frequent. In 1986 Barut, A. Bohm, and Ne'eman published a book on dynamical symmetries that included some material on the hydrogen atom [88]. In 1986, Greiner and Muller published the second edition of Quantum Mechanics Symmetries, which had six pages on the hydrogen atom, covering only the SO(4) symmetry [89]. The 2005 book by Gilmore on Lie algebras has four pages of homework problems on the H atom to duplicate the results in early papers [90]. The last papers I know of using SO(4,2) were applications in molecular physics [91, 92] and more general in scope [93].

Carl Wulfman published a book on dynamical symmetries in 2011, which provides a helpful mathematical discussion of dynamical symmetries for the hydrogen atom [94]. He regularizes the Schrodinger equation, essentially multiplying by r, obtaining Sturmian wave functions in parabolic coordinates. This approach allows him to treat bound and scattering states for SO(4,2) at one time, but requires redefining the inner product and leads to a non-Hermitian position operator [94]. This method is also mentioned in [95, p. 18]. We discuss it briefly in Section 3.4.2 and contrast it to our approach using wave functions of the inverse of the coupling constant that have the usual nlm quantum numbers, the usual inner product and produce Hermitian generators. Our presentation benefits from all previous research and, as a consequence, is hopefully clearer, more comprehensive, and reveals a deeper understanding.

1.2 Symmetry of the Dirac Hydrogen Atom

We have focused our discussion on the symmetries of the non-relativistic hydrogen atom described by the Schrodinger equation. Quantum mechanics also describes the hydrogen atom in terms of the relativistic Dirac equation, which we will discuss briefly in this section and in more detail in Chapter 5.

The gradual understanding of the dynamical symmetry of the Dirac atom parallels that of the Schrodinger atom, but it has received much less attention, probably because the system has less relevance for particle physics and for other applications. The rotational symmetry was known to be present and the equation predicted that the energy depended on the principal quantum number and the quantum number for the total angular momentum j, but not the spin s or the orbital angular momentum l separately. This remarkable fact meant that, in some sense, angular momentum contributed the same to the total energy, regardless of whether

it was intrinsic or orbital in origin. This degeneracy is lifted if we include the radiative interactions which lead to the Lamb shift.

To understand the symmetry group for the Dirac equation, consider that for a given total angular momentum quantum number $j > 0$ there are two degenerate levels for each energy level of the Dirac hydrogen atom: one level has $l = j + 1/2$ and the other has $l = j - 1/2$. Since the l values differ by unity, the two levels have opposite parity. Dirac described a generalized parity operator K, which was conserved [33]. For an operator Λ to transform one degenerate state into the other, it follows that the operator has to commute with j and have parity -1. This means it has to anti-commute with K, and so it is a conserved pseudoscalar operator.

In 1950, M. Johnson and B. Lippman discovered the operator Λ [96]. More work was done on understanding Λ by Biedenharn [97]. The Johnson–Lippman operator has been rediscovered (including by us!) and reviewed several times over the decades [98–100]. It has been interpreted in the non-relativistic limit as the projection of the Runge–Lenz vector onto the spin angular momentum [99, 101, 102].

The parity $(-1)^{l+j-1/2}$ is conserved in time, so the states are parity eigenstates. Using the two symmetry operators Λ and K, one can build a SU(2) algebra. If we include the O(3) symmetry due to the conservation of angular momentum, we obtain the full symmetry group $\mathrm{SU}(2)\otimes\mathrm{O}(3)$ which is isomorphic to SO(4) for the degeneracy of the Dirac hydrogen atom.

The SO(4) group can be expanded to include all states, obtaining the spectrum generating group SO(4,1) or SO(4,2), depending on the assumptions regarding the relativistic properties and the charges present [46, 51].

1.3 Background on Symmetry Principles

1.3.1 *The relationship between symmetry and conserved quantities*

The nature of the relationship between symmetry, degeneracy, and conserved operators is implicit in the equation

$$[H, S] = 0, \tag{1.1}$$

where H is the Hamiltonian of our system, which we assume is Hermitian, S is a Hermitian symmetry operator, and the brackets signify a commutator if we are discussing a quantum mechanical system, or i times a Poisson bracket if we are discussing a classical system. If S is viewed as the generator of

a transformation on H, then Eq. (1.1) says that the transformation leaves H unchanged.[3] We therefore say that S is a symmetry operator of H and leaves the energy invariant. The fact that a non-trivial S exists means that there is a degeneracy. To show this, consider the action of the commutator on an energy eigenstate $|E\rangle$:

$$[H, S]|E\rangle = 0 \tag{1.2}$$

or

$$H(S|E\rangle) = E(S|E\rangle). \tag{1.3}$$

If S is non-trivial then $S|E\rangle$ is a different state than $|E\rangle$ but has the same energy eigenvalue. If we label all such degenerate states by

$$|E, m\rangle, m = 1, \ldots, N \tag{1.4}$$

then clearly $S|E, m\rangle$ is a linear combination of degenerate states:

$$S|E, m\rangle = S_{mn}|E, n\rangle \equiv \sum_n S_{mn}|E, n\rangle. \tag{1.5}$$

The repeated index n means there is a summation over n. S_{mn} is a matrix representation of S in the subspace of degenerate states. In a classical Kepler system, S generates an orbit deformation that leaves H invariant (for example, a rotation or a change in eccentricity keeping the same length semi-minor axis). The existence of a non-trivial S therefore implies a degeneracy in which multiple states have the same energy eigenvalue. We can show that the complete set of symmetry operators for H forms a Lie algebra by applying Jacobi's identity to our set of Hermitian operators S_i:

$$[H, S_i] = 0, \quad i = 1, \ldots, L. \tag{1.6}$$

$$[S_j, [H, S_i]] + [S_i, [S_j, H]] + [H, [S_i, S_j]] = 0, \tag{1.7}$$

so

$$[H, [S_i, S_j]] = 0. \tag{1.8}$$

The commutator of S_i and S_j is therefore a symmetry operator of H. Either the commutator is a linear combination of all the symmetry operators

[3] The commutator arises if one does a similarity transformation $\exp(iS\theta)$ on H, namely $\exp(iS\theta)H\exp(-iS\theta) = H + i[S, H]\theta +$ higher order terms in θ.

$S_i, i = 1, \ldots, L$:

$$[S_i, S_j] = C_{ij}^k S_k \tag{1.9}$$

or the commutator defines a new symmetry operator which we label S_{L+1}. We repeat this procedure until the Lie algebra closes as in Eq. (1.9).

By exponentiation, we assume that we can locally associate a group of unitary transformations

$$\exp(iS_i a^i) \tag{1.10}$$

for real a^i with our Lie algebra and so conclude that there is a group of transformations under which the Hamiltonian is invariant [103]. We call this the symmetry or degeneracy group of H. Our energy eigenstates form a representation of this group.

It is possible to form scalar operators, called Casimir operators, from the generators of the group that commute with all the generators of the group and therefore have numerical values. The values of the Casimir operators characterize the particular representation of the group. For example, for the rotation group in three dimensions, O(3), the generators are $\boldsymbol{L} = (L_1, L_2, L_3)$ and the quantity $\boldsymbol{L}^2 = L(L+1)$ commutes with all the generators. L can have any positive integer value for a particular representation. The Casimir operator for O(3) is $\boldsymbol{L}^2$. The number of Casimir operators that characterize a group is called the rank of the group. O(3) is rank 1 and SO(4,2) is rank 3.

Now, let us consider Eq. (1.1) in a different way. If we view H as the generator of translations in time, then we recall that the total time derivative of an operator S_i is

$$\frac{\mathrm{d}S_i}{\mathrm{d}t} = \frac{i}{\hbar}\,[H,\, S_\mathrm{i}] + \frac{\partial S_\mathrm{i}}{\partial t}, \tag{1.11}$$

where the commutator and the partial derivative give the implicit and explicit time dependence, respectively. Provided that the symmetry operators have no explicit time dependence ($\frac{\partial S_i}{dt} = 0$), then Eq. (1.11) implies that the symmetry operators S_i are conserved in time and $\frac{dS_i}{dt} = 0$. For example, if the angular momentum vector generates rotations that leave the energy unchanged, then the angular momentum is conserved. Conversely, we can say that conserved Hermitian operators with no explicit time dependence are symmetry operators of H. This very important relationship between conserved Hermitian operators and symmetry was first discovered

by German mathematician Emmy Noether in 1917, and is called Noether's Theorem [21, 21, 104–106].[4]

1.3.2 *Non-invariance groups and spectrum generating groups*

As we have discussed, the symmetry algebra contains conserved generators S_i that transform an energy eigenstate into a linear combination of eigenstates all with the same energy E_n. To illustrate with hydrogen atom eigenstates:

$$S_i|nlm\rangle = S_{nlm}^{nl'm'}|nl'm'\rangle, \tag{1.12}$$

where $|nlm\rangle$ refers to a state with energy E_n, squared angular momentum $l(l+1)$ and azimuthal angular momentum $l_z = m$. Summation is implied over repeated indices. Since the Hamiltonian for the H atom is Hermitian and is bounded from below, the set of states $|nlm\rangle$ is complete. Since the H is not bounded above, the complete set will include scattering states of all positive energies.

A non-invariance algebra contains generators D_i that can be used to transform one energy eigenstate $|nlm\rangle$ into a linear combination of other eigenstates, with the same or a different energy, different angular momentum l and different azimuthal angular momentum m:

$$D|nlm\rangle = D_{nlm}^{n'l'm'}|n'l'm'\rangle. \tag{1.13}$$

Since the set of energy eigenstates is complete, the action of the most general operator would be identical to that shown in Eq. (1.13). Therefore, this requirement alone is not sufficient to determine the generators needed.

The goal is to expand the degeneracy group with its generators S_i into a larger group, so that some or all of the eigenstates form a representation of

[4]The daughter of a mathematician, she wanted to be a mathematician, but since women were not allowed to take classes at the University of Erlangen in Germany, she audited courses. She did so well in the exams that she received a degree and was allowed to enroll in the University and received a Ph.D. in 1907. She remained at the University, unpaid, in an unofficial status, for 8 years. Then she went to the University at Gottengen, where she worked for 8 years with no pay or status before being appointed as Lecturer with a modest salary. She was invited in 1915 by Felix Klein and David Hilbert, two of the most famous mathematicians in the world at the time, to work with them and address issues in Einstein's theory of General Relativity about energy conservation. She discovered Noether's First Theorem (and a second theorem also). She remained there until 1933 when she, as a Jew, lost her job. At Einstein's suggestion, she went to Bryn Mawr College in Pennsylvania. She died of ovarian cancer two years later.

the larger group with the degeneracy group as a subgroup. Thus, we need to add generators G_i such that the combined set of generators

$$\{S_i, G_j \text{ for all } i, j\} \equiv \{D_k; \text{ for all } k\}$$

forms an algebra that closes

$$[D_i, D_j] = i\epsilon_{ijk} D_k. \tag{1.14}$$

This is the Lie algebra for the expanded group. To illustrate with a specific example, consider the O(4) degeneracy group of the H atom with 6 generators.[5] One can expand the group to O(5) or O(4,1), which has ten generators by adding a four-vector of generators, some or all of which do not commute with the Hamiltonian. The question then is: Do some or all of the energy eigenstates with different principal quantum numbers n provide a representation of O(5)? If so, then this would be considered a non-invariance group. The group might be expanded further in order to obtain generators of a certain type or to include all states in the representation. For the H atom, the generators D_i can transform between different energy eigenvalues, meaning between eigenstates with different principal quantum numbers.

Another way to view the expansion of the Lie algebra of the symmetry group is to consider additional generators D_i that are constants in time [107] but do not commute with the Hamiltonian, so

$$\frac{\mathrm{d}D_i}{\mathrm{d}t} = 0 = \frac{i}{\hbar}[H,\, D_i] + \frac{\partial D_i}{\partial t}. \tag{1.15}$$

If we make the additional assumption that the partial time dependence of the generators is harmonic

$$\frac{\partial^2 D_i(t)}{\partial t^2} = \omega_{in} D_n(t). \tag{1.16}$$

then generators D_i, and the first and second partial derivatives with respect to time could close under commutation, forming an algebra. This approach does not tell us what generators to add, but as we demonstrate in Section 7.5, it does reflect the behavior of the generators that have been added to form the spectrum generating group in the case of the hydrogen atom.

We may look for the largest set of generators D_i that can transform the set of solutions into itself in an irreducible fashion (that is, there are no

[5] An O(4) rotation can be implemented by an antisymmetric 4×4 matrix, which has six independent off-diagonal components, hence six generators.

more generators than necessary). These generators form the Lie algebra for the non-invariance or spectrum generating algebra [45, 108]. If the generators for the spectrum generating algebra can be exponentiated, then we have a group of transformations for the spectrum generating group. The corresponding wave functions form the basis for a single irreducible representation of this group. This group generates transformations among all solutions for all energy eigenvalues and is called the Spectrum Generating Group [109]. For the H atom, SO(4,1) is a spectrum generating group or non-invariance group, which can be reduced to contain one separate SO(4) subgroup for each value of n.

To get a representation of SO(4,1) we need an infinite number of states, which we have for the H atom. This group can be expanded by adding a five-vector to form SO(4,2). The additional generators can be used to express the Hamiltonian and the dipole transition operator. The group $\mathrm{SO}(p,q)$ is the group of orthogonal transformations that preserve the quantity $X = x_1^2 + x_2^2 + \cdots + x_p^2 - \cdots - x_{p+q}^2$, which may be viewed as the norm of a $p+q$-dimensional vector in a space that has a metric with p plus signs and q minus signs. The letters SO stand for special orthogonal, meaning the orthogonal transformations have a determinant equal to +1.

In terms of group theory, there is a significant difference between a group like SO(4) and SO(4,1). SO(4) and SO(3) are both compact groups, while SO(4,1) and SO(4,2) are non-compact groups. A continuous group G is compact if each function $f(g)$, continuous for all elements g of the group G, is bounded. The rotation group in three dimensions O(3), which conserves the quantity $r^2 = x_1^2 + x_2^2 + x_3^2$, is an example of a compact group.

For a non-compact group consider the Lorentz group O(3,1) of transformations to a coordinate system moving with a velocity v. The transformations preserve the quantity $r^2 - c^2t^2$. The matrix elements of the Lorentz transformations are proportional to $1/\sqrt{1-\beta^2}$, where $\beta = v/c$, and are not bounded as $\beta \to 1$. Therefore, r and ct may increase without bound while the difference of the squares remains constant. Unitary representations of non-compact groups are infinite dimensional. For example, the representation of the non-invariance group SO(4,1) has an infinite number of states. Unitary representations of compact groups can be finite-dimensional; for example, our representation of SO(4) for an energy level E_n has dimension n^2.

In the 1960s and beyond, the spectrum generating group was of special interest in particle physics because it was believed to provide guidance where the precise particle dynamics were not known. The hydrogen atom

provided a physical system as a model. Because the application was in particle physics, there was less interest in exploring representations in terms of the dynamical variables for position and momentum.

The expansion of the group from SO(4,1) to SO(4,2) was motivated by the fact that the additional generators could be used to write Schrodinger's equation entirely in terms of the generators, and to express the dipole transition operator. This allowed algebraic techniques and group theoretical methods to be used to obtain solutions, calculate matrix elements, and other quantities [46, 51].

1.4 Basic Idea of Eigenstates of $(Z\alpha)^{-1}$

We introduce the idea behind these states since they are unfamiliar [110]. The full derivation is given in Chapter 3, Section 3.4. The Schrodinger equation in momentum space for bound states can be written as[6]

$$\left[p^2 + a^2 - \frac{2mZ\alpha}{r}\right] |a\rangle = 0. \tag{1.17}$$

where where m = mass of the electron, r is the location of the electron, p is its momentum, α is the fine structure constant, E is the total non-relativistic energy, $a^2 = -2mE > 0$ and $Z\alpha$ is the coupling constant, which we will now view as a parameter rather than a constant. Although this is physically impossible, it is mathematically possible and very useful. This equation has well behaved solutions for certain discrete eigenvalues of the energy or a^2, namely

$$a_n^2 = -2mE_n - m^2(Z\alpha)^2/n^2$$

or equivalently,

$$\left(\frac{a_n}{mZ\alpha}\right) = \frac{1}{n}. \tag{1.18}$$

This last equation shows that solutions exist for certain values a_n of the RMS momentum a. To introduce eigenstates of $(Z\alpha)^{-1}$ we simply take a different view of this last equation and say that instead of quantizing a and obtaining a_n, we imagine that we quantize $(Z\alpha)^{-1}$, and let a remain unchanged, obtaining

$$\frac{a}{m(Z\alpha)_n} = \frac{1}{n}. \tag{1.19}$$

[6] We employ natural Gaussian units so $\hbar = 1$, $c = 1$, and $\alpha = (e^2/\hbar c) \approx 1/137$.

So, now we can interpret Schrodinger's equation as an eigenvalue equation that has solutions for certain values of $(Z\alpha)^{-1}$ namely

$$(Z\alpha)_n^{-1} = \frac{m}{an}. \tag{1.20}$$

We have the same equation but can view the eigenvalues differently but equivalently. Instead of quantizing a we quantize $(Z\alpha)^{-1}$.

This roughly conveys the basic idea of eigenstates of the inverse of $(Z\alpha)$, but this simplified version does not reveal the advantages of our reformulation because we have left the Hamiltonian unchanged. In Section 3.4 (Chapter 3, Section 4), we transform Schrodinger's equation to an eigenvalue equation in $a/mZ\alpha$ so that the kernel is bounded from below and from above, which means that there are no states with $E > 0$ (no scattering states) and all states have the usual bound state quantum numbers. Other important advantages to this approach will also be discussed.

1.5 Degeneracy Groups for Schrodinger, Dirac and Klein–Gordon Equations

The degeneracy groups for the bound states described by the different equations of the hydrogen atom are summarized in Table 1.1. The degeneracy (column 2) is due to the presence of conserved operators which are also symmetry operators (column 3), forming a degeneracy symmetry group (column 4). For example, The symmetry operators for the degeneracy group in the Schrodinger hydrogen atom are the angular momentum $\boldsymbol{L}$ and the Runge–Lenz vector $\boldsymbol{A}$. In Chapter 3, it will be shown that together these are the generators of the direct product $\mathrm{SO}(3)\otimes\mathrm{SO}(3)$, which is isomorphic to SO(4). Column 5 gives the particular representations present. These numbers are determined by the allowed values of the Casimir operators for the group and they determine the degree of degeneracy (last column) and the corresponding allowed values of the quantum numbers for the degenerate states.

As we mentioned earlier, the Casimir operators, which are made from generators of the group, have to commute with all the members of the group, and the only way this can happen is if they are actually constants for the representation. The generators are formed from the dynamical variables of the H atom, so the Casimir operators are invariants under the group composed of the generators, and their allowed numerical values reflect the underlying physics of the system and determine the appropriate

representations of the group [22, 94, 111]. For example, $\boldsymbol{L}^2$ is the Casimir operator for the group O(3) and can have the values $l(l+1)$. The relationship between Casimir operators and group representations is true for all irreducible group representations, including the SO(4) degeneracy group, as well as the spectrum generating group SO(4,2) [56, 66].

For the Schrodinger equation there are n^2 states $|nlm\rangle$ that form a representation of the degeneracy group SO(4) with generators $\boldsymbol{L}$ and $\boldsymbol{A}$. These states correspond to the principal quantum number n, the n different values of the angular momentum quantum number l, and $2l+1$ different values of the z component of the angular momentum $l_Z = m$.

For the Dirac equation, the $2(2J+1)$ dimensional degeneracy group for bound states is realized by the total angular momentum operator $\boldsymbol{J}$, the generalized parity operator K, and the Johnson–Lippman operator Λ, which together form the Lie algebra for SO(4).

For the fully relativistic Klein–Gordon equation, only the symmetry from rotational symmetry survives, leading to the degeneracy group O(3). If the V^2 term, the four-potential term squared, is dropped in a semi-relativistic approximation as we describe in Section 3.3, then the equation can be rewritten in the same form as the non-relativistic Schrödinger equation, so a Runge–Lenz vector can be defined and the degeneracy group is again SO(4).

Table 1.1. In the table $\boldsymbol{L} = \boldsymbol{rxp}$ is the orbital angular momentum; $\boldsymbol{A}$ is the Runge–Lenz vector; $\boldsymbol{J} = \boldsymbol{L} + \sigma/2$ is the total angular momentum; K is the generalized parity operator; Λ is the conserved pseudoscalar operator.

Degeneracy Groups for Bound States in A Coulomb Potential					
Equation	Degeneracy	Conserved Quantities	Degeneracy Group	Representation	Dimension
Schrodinger	E indep. of l, l_z	$\boldsymbol{A}$, $\boldsymbol{L}$	SO(4)	$(\frac{n-1}{2}, \frac{n-1}{2})$	n^2
Klein–Gordon	E indep. of l_z	$\boldsymbol{L}$	O(3)	Casimir op. is $l(l+1)$	$2l+1$
Klein–Gordon without V^2 term	E indep. of l, l_z	$\boldsymbol{A}$, $\boldsymbol{L}$	SO(4)	$(\frac{n-1}{2}, \frac{n-1}{2})$	n^2
Dirac	E depends on J, n only	$\Lambda, K, \boldsymbol{J}$	SO(4)	$(1/2, J)$	$2(2J+1)$

This page intentionally left blank

Chapter 2

Classical Theory of the H Atom

In order to address orbital motion and the continuous deformation of orbits, we give this discussion in terms of classical mechanics, but much of it is valid in terms of the Heisenberg representation of quantum mechanics if the Poisson brackets are converted to commutators, as will be discussed in Section 2.4.

For a charged particle in a Coulomb potential, there are two classical conserved vectors: the angular momentum $\boldsymbol{L}$, which is perpendicular to the plane of the orbit, and the Runge–Lenz vector $\boldsymbol{A}$, which goes from the focus corresponding to the center of mass and force along the semi-major axis to the perihelion (closest point) of the elliptical orbit. The conservation of $\boldsymbol{A}$ is related to the fact that non-relativistically the orbits do not precess. The Hamiltonian of our bound state classical system with an energy $E < 0$ is[1]

$$H = \frac{p^2}{2m} - \frac{Z\alpha}{r} = E, \tag{2.1}$$

where m = mass of the electron, r is the location of the electron, p is its momentum, α is the fine structure constant, E is the total non-relativistic energy.

The Runge–Lenz vector is

$$\boldsymbol{A} = \frac{1}{\sqrt{-2mH}} \left(\boldsymbol{p} \times \boldsymbol{L} - mZ\alpha \frac{\boldsymbol{r}}{r} \right), \tag{2.2}$$

[1]We employ natural Gaussian units so $\hbar = 1$, $c = 1$, and $\alpha = (e^2/\hbar c) \approx 1/137$. The notation for indices and vectors is $\mu, \nu, .. = 0, 1, 2, 3$; $i, j, . = 1, 2, 3$; $p_\mu p^\mu = -p_0^2 + \boldsymbol{p}^2$, $\boldsymbol{p} = (p_1, p_2, p_3)$, $g_{\mu\nu} = (-1, 1, 1, 1)$.

where L is the angular momentum. From Hamilton's equation, for a subspace of energy E, $H = E$ so

$$\boldsymbol{A} = \frac{\boldsymbol{p} \times \boldsymbol{L}}{a} - \frac{mZ\alpha}{a}\frac{\boldsymbol{r}}{r}, \tag{2.3}$$

where a is defined by

$$a = \sqrt{-2mE}. \tag{2.4}$$

From the virial theorem, the average momentum $\langle p^2 \rangle = -2mE$ so a is the root mean square momentum. Since we are discussing bound states, $E < 0$. It is straightforward to verify that $\boldsymbol{A}$ is conserved in time:

$$[\boldsymbol{A}, H] = \frac{d\boldsymbol{A}}{dt} = 0, \tag{2.5}$$

where the brackets mean i times the Poisson bracket, the classical limit of a commutator. From the definition of $\boldsymbol{A}$ and the definition of angular momentum

$$\boldsymbol{L} = \boldsymbol{r} \times \boldsymbol{p}, \tag{2.6}$$

it follows that $\boldsymbol{A}$ is orthogonal to the angular momentum vector

$$\boldsymbol{A} \cdot \boldsymbol{L} = 0. \tag{2.7}$$

Using the fact that $\boldsymbol{A}$ and $\boldsymbol{L}$ are conserved, we can easily obtain equations for the orbits in configuration and momentum space and the eccentricity, and other quantities, all usually derived by solving the equations of motion directly.

$\boldsymbol{A}$ and $\boldsymbol{L}$ are the generators of the group O(4). If we introduce the linear combinations $\boldsymbol{N} = \frac{1}{2}(\boldsymbol{L} + \boldsymbol{A})$ and $\boldsymbol{M} = \frac{1}{2}(\boldsymbol{L} - \boldsymbol{A})$, we find that $\boldsymbol{N}$ and $\boldsymbol{M}$ commute, reducing the non-simple group O(4) to the direct product O(3) $\otimes$ O(3), which we will discuss in Section 3.2 in the language of quantum mechanics.

2.1 Orbit in Configuration Space

To obtain the equation of the orbit one computes

$$\boldsymbol{r} \cdot \boldsymbol{A} = rAcos\phi_r = -r\frac{mZ\alpha}{a} + \boldsymbol{r} \cdot \boldsymbol{p} \times \boldsymbol{L}. \tag{2.8}$$

Noting that $\boldsymbol{r} \cdot \boldsymbol{p} \times \boldsymbol{L} = L^2$ we can solve for r

$$r = \frac{L^2/mZ\alpha}{(a/mZ\alpha)A\ cos\phi_r + 1}. \tag{2.9}$$

This is the equation of an ellipse with eccentricity $e = (a/mZ\alpha)A$ and a focus at the origin (Fig. 2.1). To find e, in terms of the energy, we calculate $\boldsymbol{A} \cdot \boldsymbol{A}$ using the identity $\boldsymbol{p} \times \boldsymbol{L} \cdot \boldsymbol{p} \times \boldsymbol{L} = p^2 L^2$ and obtain

$$A^2 = \frac{p^2 L^2}{a^2} - \frac{2mZ\alpha}{a^2}\frac{L^2}{r} + \left(\frac{mZ\alpha}{a}\right)^2. \tag{2.10}$$

Substituting E from Eq. (2.1) gives the eccentricity

$$\frac{a}{mZ\alpha}A = e = \sqrt{\frac{2EL^2}{m(Z\alpha)^2} + 1}. \tag{2.11}$$

The length r_c of the semi-major axis is the average of the radii at the turning points at $\phi_r = (0, \pi)$

$$r_c = \frac{r_1 + r_2}{2}. \tag{2.12}$$

Using the orbit equation we find

$$r_c = \frac{L^2}{mZ\alpha}\frac{1}{1 - e^2} \tag{2.13}$$

or

$$r_c = -\frac{Z\alpha}{2E} = \frac{mZ\alpha}{a^2}. \tag{2.14}$$

The energy depends only on the length of the semi-major axis r_c, not on the eccentricity. This important result is a consequence of the symmetry of the problem. It is convenient to parameterize the eccentricity in terms of the angle ν (see Fig. 2.1) where

$$e = \sin\nu. \tag{2.15}$$

From this definition and from Eqs. (2.11), (2.13), and (2.14) follow the useful results

$$L = r_c a \cos\nu, \quad A = r_c a \sin\nu \tag{2.16}$$

which immediately imply

$$L^2 + A^2 = (r_c a)^2 = \left(\frac{mZ\alpha}{a}\right)^2. \tag{2.17}$$

This equation is the classical analogue of an important quantum mechanical result first obtained by Pauli and Hulthen allowing us to determine the energy levels from symmetry properties alone [27, 31]. From

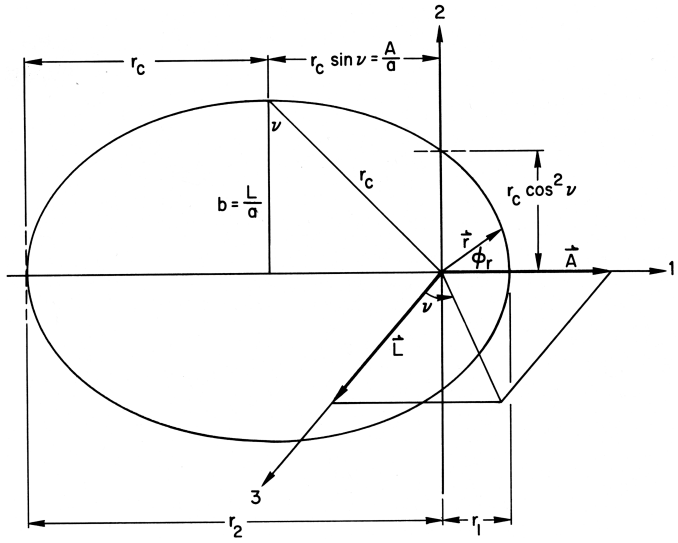

Fig. 2.1. Classical Kepler orbit in configuration space. The orbit is in the 1–2 plane (plane of the paper). One focus, where the proton charge is located, is the origin. The semi-minor axis is $b = r_c \sin\nu$. The semi-major axis is r_c.

Fig. 2.1, it is apparent that this equation is a statement of Pythagoras' theorem for right triangles.

The energy equation (Eq. (2.1)) and the orbit equation (Eq. (2.9)) respectively may be rewritten in terms of a, r, and ν:

$$\frac{r_c}{r} = \frac{p^2 + a^2}{2a^2} \tag{2.18}$$

$$r = \frac{r_c \cos^2\nu}{1 + \sin\nu\cos\phi_r}. \tag{2.19}$$

2.2 The Period

To obtain the period we use the geometrical definition of the eccentricity

$$e = \sqrt{1 - (b/r_c)^2}, \tag{2.20}$$

where b is the semi-minor axis. Using $e = \sin\nu$ we find

$$b = r_c \cos\nu \tag{2.21}$$

so from Eq. (2.16) we obtain

$$L = ab. \tag{2.22}$$

From classical mechanics we know the magnitude of the angular momentum is equal to twice the mass times the area swept out by the radius vector per unit time. The area of the ellipse is $\pi b r_c$. If the period of the classical motion is T, then $L = 2m\pi b r_c/T = ab$. Therefore, the classical period is

$$T = 2\pi \frac{m r_c}{a} = 2\pi \sqrt{\frac{m(Z\alpha)^2}{-8E^3}}. \tag{2.23}$$

and the classical frequency $\omega_{cl} = 2\pi/T$ is

$$\omega_{cl} = \frac{a}{m r_c}. \tag{2.24}$$

Expressing the root mean square momentum $a = m v_{\text{mean}}$ in terms of a mean velocity v_{mean} shows that

$$v_{\text{mean}} = r_c \omega_{cl}$$

as expected.

2.3 Group Structure SO(4)

The generators of our symmetry operations form the closed Poisson bracket algebra of O(4):

$$[L_i, L_j] = i\epsilon_{ijk} L_k, \quad [L_i, A_j] = i\epsilon_{ijk} A_k, \quad [A_i, A_j] = i\epsilon_{ijk} L_k. \tag{2.25}$$

The brackets mean i times the Poisson bracket, which is the classical limit of a commutator. The first bracket says that the angular momentum generates rotations and forms a closed Lie algebra corresponding to O(3). The second bracket says that the Runge–Lenz vector transforms as a vector under rotations generated by the angular momentum. The last bracket says that the multiple transformations generated by the Runge–Lenz vector are equivalent to a rotation. Taken together the Poisson brackets form the Lie algebra of O(4). The connected symmetry group for the classical bound state Kepler problem is obtained by exponentiating our algebra giving the symmetry group SO(4). The scattering states with $E > 0$ form a representation of the non-compact group SO(3,1).

We now want to determine the nature of the transformations generated by A_i and L_i. Clearly, $\boldsymbol{L} \cdot \boldsymbol{\delta\omega}$ generates a rotation of the elliptical orbit about the axis $\boldsymbol{\delta\omega}$ by an amount $\delta\omega$. To investigate the transformations generated by $\boldsymbol{A} \cdot \boldsymbol{\delta\nu}$ we assume a particular orientation of the orbit, namely that it is in the 1–2 (or x–y) plane and that $\boldsymbol{A}$ is along the 1-axis (see Fig. 2.1). The more general problem is obtained by a rotation generated

by L_i. For an example, we choose a transformation with $\boldsymbol{\delta\nu}$ pointing along the 2-axis so that $\boldsymbol{A}\cdot\boldsymbol{\delta\nu} = A_2\delta\nu$. The change in $\boldsymbol{A}$ is defined by $\boldsymbol{\delta A}$ where

$$\boldsymbol{\delta A} = i[\boldsymbol{A}\cdot\boldsymbol{\delta\nu}, \boldsymbol{A}]. \tag{2.26}$$

From the Poisson bracket relations we find for this particular case:

$$\delta A_1 = L_3\delta\nu, \quad \delta A_2 = 0, \quad \delta A_3 = -L_1\delta\nu. \tag{2.27}$$

For our orbit, $L_1 = 0$ so $\delta A_3 = 0$. We perform a similar computation to find $\boldsymbol{\delta L}$. We find we can characterize the transformation by

$$\begin{array}{lll} \delta A_1 = L_3\delta v & \text{or} & \delta A = L\delta\nu \\ \delta L_3 = -A_1\delta\nu & \text{or} & \delta L = -A\delta\nu \\ \delta e = \sqrt{1-e^2}\delta\nu & \text{or} & \delta(\sin\nu) = \cos\nu\delta\nu \end{array} . \tag{2.28}$$

Recalling $e = \sin\nu$ and Eq. (2.16) we see that these transformations are equivalent to the substitution

$$\nu \longrightarrow \nu + \delta\nu. \tag{2.29}$$

The eccentricity of the orbit, and therefore $\boldsymbol{A}$ and $\boldsymbol{L}$ are all changed in such a way that the energy, a and r_c (length of the semi-major axis) remain constant. In our example, both $\boldsymbol{L}$ and $\boldsymbol{A}$ change in length but not direction, so the plane and orientation of the orbit are unchanged. The general transformation $\boldsymbol{A}\cdot\boldsymbol{\delta\mu}$ will also rotate the plane of the orbit or the semi-major axis.

Figure 2.2 shows a set of orbits in configuration space with different values of the eccentricity $e = \sin\nu$ but the same total energy and the same semi-major axis r_c, which is the bold hypotenuse. The bold vertical and horizontal legs are A/a and L/a and are related to the hypotenuse r_c by Pythagoras's theorem. The generator $A_2\nu$ produces a deformation of the circular orbit into the various elliptical orbits shown. This classical degeneracy corresponds to the quantum mechanical degeneracy in energy levels that occurs for different eigenvalues of the angular momentum with a fixed principal quantum number.

We can visualize all possible elliptical orbits for a fixed total energy or semi-major axis through a simple device. It is possible to produce an elliptical orbit with eccentricity $\sin\nu$ as the shadow of a circle of radius r_c which is rotated an amount ν about an axis perpendicular to the illuminating light. With a complete rotation of the circle we will see all possible classical elliptical orbits corresponding to a given total energy. In quantum mechanics only certain angles of rotation would be possible

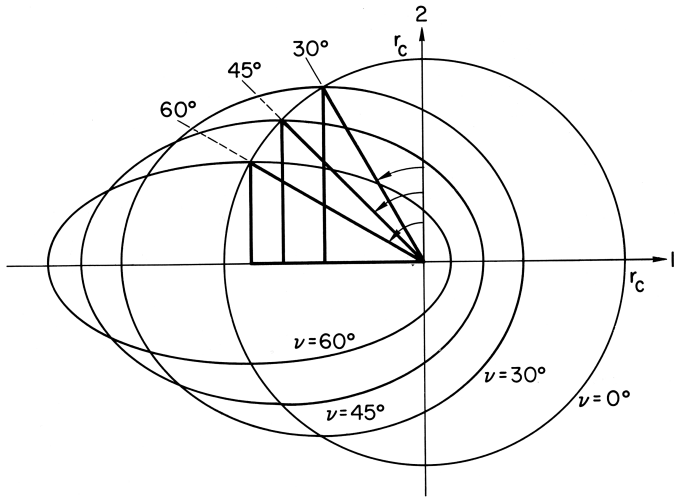

Fig. 2.2. Kepler bound state orbits in configuration space for a fixed energy and different values of the eccentricity $e = \sin\nu$. The bold hypotenuse is the semi-major axis r_c which makes an angle ν with the vertical 2-axis. From Eq. (2.17), $r_c^2 = (A/a)^2 + (L/a)^2$ as illustrated. The vector $\boldsymbol{L}$ is along the 3-axis, pointing out of the paper, perpendicular to the orbit, and $\boldsymbol{A}$ is along the 1-axis.

corresponding to the quantized values of L. As the circle is rotated we must imagine that the force center shifts as the sine of the angle of rotation so that it always remains at the focus.[2]

2.4 The Classical Hydrogen Atom in Momentum Space

We can derive the equation for the classical orbit in momentum space of a particle bound in a Coulomb potential using the conserved operators $\boldsymbol{L}$ and $\boldsymbol{A}$. For convenience, we assume that we have rotated our axes so that $\boldsymbol{L}$ lies along the 3-axis and $\boldsymbol{A}$ lies along the 1-axis as shown in Fig. 2.1. We compute

$$\boldsymbol{p}\cdot\boldsymbol{A} = p_1 A = \frac{-mZ\alpha}{a}\boldsymbol{p}\cdot\frac{\boldsymbol{r}}{r} \equiv \frac{-mZ\alpha}{a}p_r \tag{2.30}$$

[2]Were it not for this displacement of the force center, the observation that a rotated circle projects onto a plane as an ellipse would manifest the four-dimensional symmetry of the hydrogen-like atom directly in configuration space. The elliptical orbits could be viewed as projections of a rotated hypercircle onto a three-dimensional hyperplane. These considerations can be applied with some modification to the three-dimensional harmonic oscillator for which the force center and the center of the ellipse coincide.

and employ Eq. (2.11), $A = \frac{mZ\alpha}{a}\sin\nu$, to obtain[3]

$$p_r = -\sin\nu p_1, \tag{2.31}$$

which we substitute into the identity

$$p_r^2 + \frac{\boldsymbol{L}^2}{r^2} = p^2 = p_1^2 + p_2^2. \tag{2.32}$$

Using Eqs. (2.16) and (2.18) we find

$$1 = \left(\frac{2ap_1}{p^2+a^2}\right)^2 + \left(\frac{2ap_2}{p^2+a^2}\right)^2 \frac{1}{\cos^2 v}, \tag{2.33}$$

and

$$p^2 - a^2 = 2ap_2\tan\nu, \tag{2.34}$$

which may also be written as

$$p_1^2 + (p_2 - a\tan\nu)^2 = \frac{a^2}{\cos^2\nu}. \tag{2.35}$$

From Eq. (2.35), we see the orbit in momentum space is a circle of radius $a/\cos\nu$ with its center displaced from the origin a distance $a\tan\nu$ along the 2-axis. Figure 2.3 shows the momentum space orbit that corresponds to the configuration space orbit in Fig. 2.1. As an alternative method of showing the momentum space orbits are circular we can compute [112]

$$\left(\boldsymbol{p} - a\frac{\boldsymbol{L}\times\boldsymbol{A}}{\boldsymbol{L}^2}\right)^2 = C^2. \tag{2.36}$$

Using the lemma

$$\boldsymbol{p}\times\boldsymbol{A} = -\frac{\boldsymbol{L}}{2a}(p^2 - a^2), \tag{2.37}$$

the fact that $\boldsymbol{L}\cdot\boldsymbol{A} = 0$, and Eq. (2.16), we find $C = a/\cos\nu$. The orbit is a circle of radius $a/\cos\nu$ whose center lies at $a\boldsymbol{L}\times\boldsymbol{A}/\boldsymbol{L}^2$, in agreement with the previous result.

We now consider what the generators A_i and L_i do to the orbit in momentum space. Clearly, $\boldsymbol{L}$ generates a rotation of the axes. For an A_i transformation consider the same situation we considered in our discussion

[3]This equation and any other equation written in this specific coordinate system can be generalized to an arbitrary coordinate system by noting that the Cartesian unit vectors may be written in a manner that is independent of the coordinate system: $\boldsymbol{i} = \frac{\boldsymbol{A}}{A}$, $\boldsymbol{j} = \frac{\boldsymbol{L}\times\boldsymbol{A}}{LA}$, $\boldsymbol{k} = \frac{\boldsymbol{L}}{L}$.

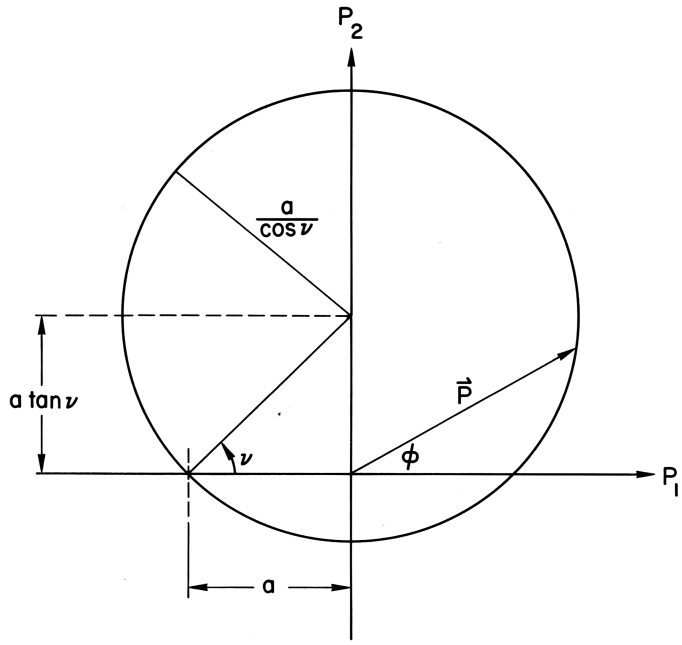

Fig. 2.3. Kepler orbit in momentum space of radius $a/\cos\nu$, with its center at $p_2 = a\tan\nu$, corresponding to the orbit in configuration space shown in Fig. 2.1. A circular orbit in configuration space corresponds to a circular orbit in momentum space centered on the origin with radius a.

of the configuration space orbit (see Figs. 2.1 and 2.3). Since the generator $A_2\delta\nu$ changes ν to $\nu + \delta\nu$, we conclude that in momentum space this shifts the center of the orbit along the p_2-axis and changes the radius of the circle. However, the distance a from the p_2-axis to the intersection of the orbit with the p_1-axis remains unchanged. Figure 2.4 shows a set of momentum space orbits for a fixed energy which correspond to the set of orbits in configuration space shown in Fig. 2.2.

2.5 Four-Dimensional Stereographic Projection in Momentum Space

It is interesting that in classical mechanics the bound state orbits in a Coulomb potential are simpler in momentum space than in configuration space. In quantum mechanics, the momentum space wave functions become simply four-dimensional spherical harmonics if one normalizes the

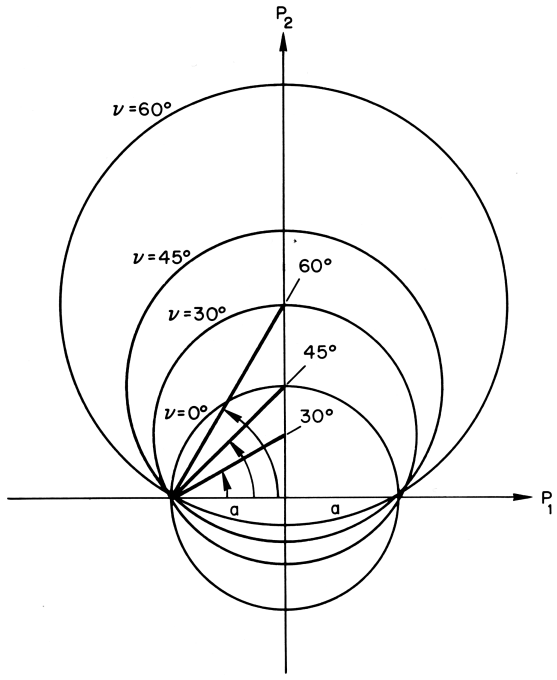

Fig. 2.4. Kepler orbits in momentum space for a fixed energy and RMS momentum a with different values of the eccentricity $e = \sin\nu$ corresponding to the orbits in configuration space shown in Fig. 2.2. The straight lines locate the center of the corresponding circular orbit on the p_2-axis. For a circular orbit, ν is zero and the eccentricity is zero.

momentum $\boldsymbol{p}$ by dividing by the RMS momentum $a = \sqrt{-2mE}$, so it becomes dimensionless, and performs a stereographic projection onto a unit hypersphere in a four-dimensional space [32, 48, 94]. We will do the analogous projection procedure for the classical orbits. As shown in Fig. 2.5, the three-dimensional momentum space hyperplane passes through the center of the four-dimensional hypersphere. The unit vector in the fourth direction is $\hat{n} = (1, 0, 0, 0)$. The unit vector $\hat{U}$ goes from the center of the sphere to the surface of the hypersphere where it is intersected by the line connecting the vector $\boldsymbol{p}/a$ to the north pole of the sphere.

We find

$$U_i = \frac{2ap_i}{p^2 + a^2} \quad i = 1, 2, 3. \quad U_4 = \frac{p^2 - a^2}{p^2 + a^2}. \tag{2.38}$$

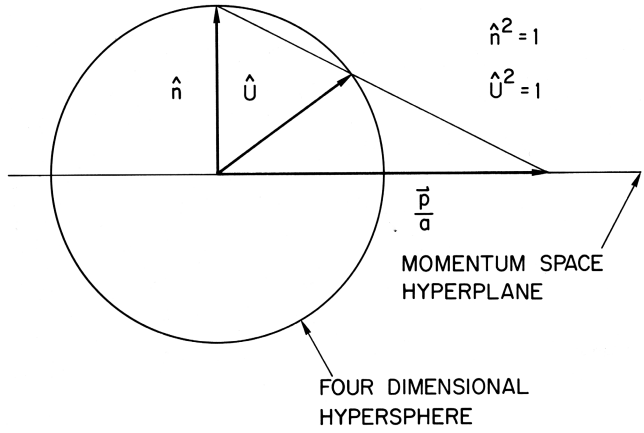

Fig. 2.5. Stereographic projection in momentum space for a fixed energy, mapping $\boldsymbol{p}/a$ into $\hat{U}$. The unit vector in the 4 direction is $\hat{n}$ and $\hat{n} \cdot \hat{U} = \cos\Theta_4$.

Note that the four-vector U has been normalized to 1. Inverting the equations gives the following result.

$$p_i = \frac{aU_i}{1 - U_4} \qquad p^2 = a^2 \frac{1 + U_4}{1 - U_4}. \tag{2.39}$$

Momentum space vectors for which $p/a < 1$ are mapped onto the lower hyperhemisphere. The advantage of this projection over one in which the hypersphere is tangent to the hyperplane is that we may have $|\hat{n}| = |\hat{U}| = 1$. At times, it is convenient to describe $\hat{U}$ in terms of spherical polar coordinates in four dimensions. Since $\hat{U}$ is a unit vector we define

$$\begin{aligned} U_4 &= \cos\theta_4, \\ U_3 &= \sin\theta_4 \cos\theta, \\ U_2 &= \sin\theta_4 \sin\theta \sin\phi, \\ U_1 &= \sin\theta_4 \sin\theta \cos\phi. \end{aligned} \tag{2.40}$$

where θ and ϕ are the usual coordinates in three dimensions. By comparison to Eq. (2.38), we have

$$\theta_4 = 2\cot^{-1}\frac{p}{a} \qquad \theta = \cos^{-1}\frac{p_3}{p} \qquad \phi = \tan^{-1}\frac{p_2}{p_1}. \tag{2.41}$$

2.6 Orbit in U-Space

We want to find the trajectory of the particle on the surface of the hypersphere corresponding to the Kepler orbits in configuration space or

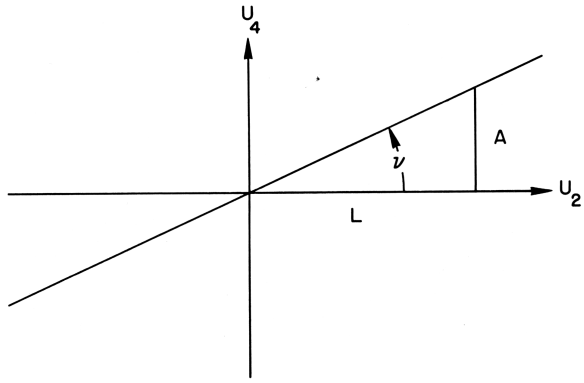

Fig. 2.6. Showing the hyperplane containing the orbit making an angle ν with the U_2 plane. Note $\tan\nu = A/L$ as required by Eq. (2.16).

the displaced circles in momentum space. We assume that we have rotated the axes in configuration space so that $\boldsymbol{L}$ is along the 3-axis and $\boldsymbol{A}$ is along the 1-axis, as shown in Fig. 2.1. The equation for the orbit in the three-dimensional momentum space is given by Eqs. (2.34) or (2.36). Dividing Eq. (2.34) by $p^2 + a^2$ immediately gives a parametric equation for the projected orbit in U space:

$$U_4 = U_2 \tan\nu. \tag{2.42}$$

Since the orbit is in the 1–2 plane in configuration space, it follows that $U_3 = 0$. The orbit lies in a hyperplane perpendicular to the 2–4 plane that goes through the origin and makes an angle $\pi/2 - \nu$ with the U_4-axis as shown in Fig. 2.6.[4] The orbit is the intersection of this plane with the hypersphere and is therefore a great circle. To derive the exact equation for the projected orbit we express p in Cartesian components p_1 and p_2 in Eq. (2.34) and substitute Eq. (2.39) obtaining

$$U_l^2 + U_2^2 - 2\tan\nu\, U_2(l - U_4) = (1 - U_4)^2. \tag{2.43}$$

To interpret this equation we consider it in a rotated coordinate system. We perform a rotation by an amount $\delta\nu$ about the 1–3 plane; $A_2\delta\nu$ is the generator of this rotation which mixes the components along the U_2 and

[4] We define the angle between a three-dimensional hyper-plane and a line as $\pi/2$ minus the angle between the line and the normal to the hyperplane.

U_4 axes. The equations of transformation may be written[5]

$$\begin{aligned} U_2 &= U_2' \cos\delta\nu + U_4' \sin\delta\nu, \quad U_3 = U_3' \\ U_4 &= U_4' \cos\delta\nu - U_2' \sin\delta\nu, \quad U_1 = U_1'. \end{aligned} \tag{2.44}$$

This transformation is equivalent to making the substitution $\nu \longrightarrow \nu + \delta\nu$ in the equations relating to the orbit. For example, Eq. (2.42) becomes

$$U_4' = U_2' \tan(\nu + \delta\nu). \tag{2.45}$$

We choose $\delta\nu = -\nu$, which means the orbital plane becomes $U_4' = 0$. Writing Eq. (2.43) in terms of the primed coordinates, we find

$$U_1'^2 + U_2'^2 = 1, \tag{2.46}$$

which in the original system is

$$U_1^2 + (U_2 \cos\nu + U_4 \sin\nu)^2 = 1. \tag{2.47}$$

This is the equation of a great hypercircle $(\nu, 0)$ centered at the origin and lying in a hyperplane making an angle $\pi/2 - \nu$ with the U_4-axis and an angle $\pi/2$ with the U_3-axis. If $\boldsymbol{L}$ did not lie along the U_3-axis but, for example, was in the 1–3 plane, at an angle Θ from the U_3-axis, then Eq. (2.47) would be modified by the substitution

$$U_1 \longrightarrow U_1 \cos\Theta + U_3 \sin\Theta, \tag{2.48}$$

which follows since U_i transforms as a three-vector. The corresponding great circle (ν, Θ) lies in a hyperplane making an angle $\pi/2 - \nu$ with the U_4-axis and $\pi/2 - \Theta$ with the 3-axis.

The motion of the orbiting particle corresponds to a dot moving along the great circle ($\nu, 0$ or Θ) with a period T given by the classical period Eq. (2.23). The velocity in configuration space can be expressed in terms of U_4 by using its definition in terms of p^2 Eq. (2.39) or in terms of θ_4 Eq. (2.41). The particle is moving at maximum velocity when θ_4 is a minimum, which occurs at the perihelion when $\theta_4 = \pi/2 - \nu$:

$$max\left(\frac{p}{a}\right) = \sqrt{\frac{1+e}{1-e}} = \sqrt{\frac{r_2}{r_1}} \tag{2.49}$$

[5]It is desirable to first show that $\boldsymbol{A}$ (and of course $\boldsymbol{L}$) generate rotations of the hypersphere or $\hat{U}$. However, since we prefer to do the necessary calculations in terms of commutators rather than Poisson brackets, we defer these considerations to Section 2.4. There we show that the generator L_i rotates $\hat{U}$ about the $i-4$ plane; the generator A_1 rotates $\hat{U}$ about the 2–3 plane, etc., thereby changing the orbit with respect to the U_4-axis and changing the eccentricity.

and at a minimum velocity when $\theta_4 = \pi/2 + \nu$:

$$min\left(\frac{p}{a}\right) = \sqrt{\frac{1-e}{1+e}}. \tag{2.50}$$

These values of θ_4 correspond to turning points at which r and p have extreme values. This is apparent when we use the definition of U_4 Eq. (2.36) and Eq. (2.18) for the total energy to show

$$U_4 = \frac{r_c - r}{r_c}. \tag{2.51}$$

When $r > r_c$ then $p^2 < a^2$, so the particle is moving more slowly than the RMS velocity. Applying the virial theorem to any orbit we find $\langle p^2 \rangle = a^2$, so, as expected, a is the RMS momentum and $\langle 1/(1-U_4) \rangle = 1 = \langle r_c/r \rangle$.

Figure 2.7 is a picture of a simple device illustrating the stereographic projection of the orbit in p/a-space onto the four-dimensional hypersphere in U-space. We assume that the orbit is in the 1–2 plane and that $\boldsymbol{A}$ lies along the 1-axis, so $p_3 = 0$, $U_3 = 0$. Due to this trivial dependence on p_3, we have omitted the 3-axis. The vertical pin or rod represents the unit

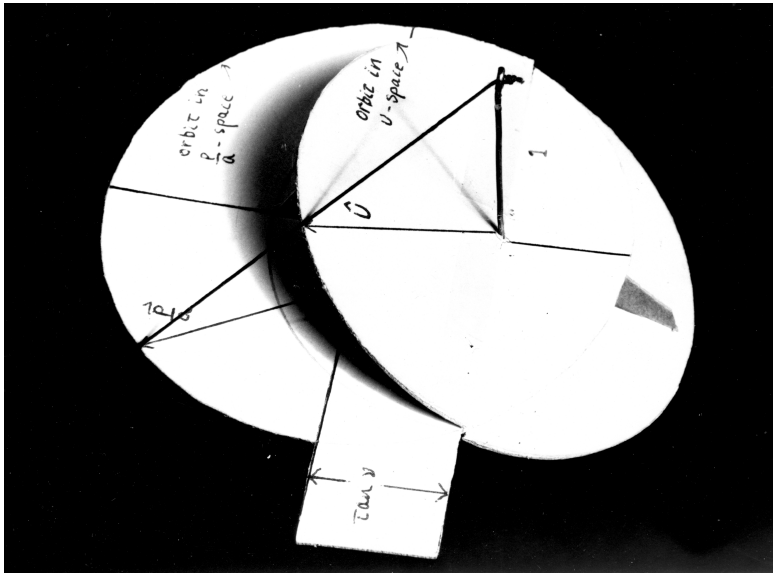

Fig. 2.7. Model illustrating the stereographic projection from the 1–2 plane to a four-dimensional hypersphere. The pin represents the unit vector $\hat{n}$ along the 4-axis, normal to the 1–2 plane.

vector $\hat{n}$ that lies along the 4-axis. The circumference of the larger circle perpendicular to the 4-axis represents the orbit in p/a-space. One can see that it is displaced from the origin along the 2-axis. Centered at the origin, we must imagine a hypersphere of unit radius $\hat{U}^2 = 1$. The stereographic projection $\hat{U}$ of the vector $\boldsymbol{p}/a$ is obtained by placing the string coming from the top of n directly at the head of the vector $\boldsymbol{p}/a$. The intersection of the string with the unit hypersphere defines $\hat{U}$. As the string is moved along the orbit in p/a-space, it intersects the hypersphere along a great circle shown by the circumference of the unit circle making an angle ν with the 1–2 plane. We can see, for example, that at the closest approach θ_4 is a minimum and U_4 is a maximum, $\hat{U} \cdot \boldsymbol{A} = U_1$ is a minimum and p/a is a maximum.

2.7 Classical Time Dependence of Orbital Motion

We can determine the time dependence of the orbital motion by integrating the expression for the angular momentum $L = mr^2 d\phi_r/dt$

$$\int dt = \int \frac{mr^2}{L} d\phi_r, \tag{2.52}$$

where r is given by the orbit equation Eq. (2.19) and we are assuming that the orbit is in the 1–2 plane. After integrating, we can use the equations relating the momentum space and configuration space variables to obtain the time dependence in p-space and U-space. We obtain

$$\frac{1}{r_c^2} \frac{1}{\cos\nu} \frac{L}{m} \int_0^t dt = \cos^3\nu \int_0^{\phi_r(t)} \frac{d\phi_r}{(1 + \sin\nu \cos\phi_r)^2}. \tag{2.53}$$

We can show that the left-hand side of this equation is equal to $\omega_{cl} t$, where ω_{cl} is the classical frequency, substituting Eqs. (2.16) and (2.24)

$$L = a r_c \cos\nu \quad \omega_{cl} = \frac{a}{m r_c}. \tag{2.54}$$

The integral on the right side gives [113]

$$\omega_{cl} t = -\frac{\sin\nu \cos\nu \sin\phi_r}{1 + \sin v \cos\phi_r} - \tan^{-1} \frac{\cos\nu \sin\phi_r}{\sin\nu + \cos\phi_r}, \tag{2.55}$$

which may be simplified as

$$\omega_{cl} t = -\frac{A}{L} \frac{y}{r_c} - \tan^{-1} \frac{A}{L} \frac{y}{r_c - r}, \tag{2.56}$$

where $y = r \sin\phi_r$.

We can convert Eq. (2.55) to obtain the time dependence in U-space. The relationship between the angle $\phi \equiv \phi_p$ in momentum space and ϕ_r in configuration space follows by differentiating the orbit equation Eq. (2.34) with respect to time and using $L = mr^2\dot{\phi}_r$ or by solving simultaneously the configuration space orbit Eq. (2.19), the momentum space orbit Eq. (2.34) and the energy equation Eq. (2.18). We find

$$\sin\phi_r = -p\cos\phi\frac{\cos\nu}{a} \qquad \cos\phi_r = p\sin\phi\frac{\cos v}{a} - \sin\nu. \tag{2.57}$$

From these equations, the definitions of the U_i, Eq. (2.38), and the orbit and energy equations, it follows that for the classical orbit in the 1–2 plane

$$\begin{aligned} U_1 &= -\frac{r\sin\phi_r}{r_c\cos\nu}, \\ U_2 &= \frac{r}{r_c}\frac{\sin\nu + \cos\phi_r}{\cos v} = U_4\cot\nu, \\ U_3 &= 0, \\ U_4 &= \frac{r_c - r}{r_c}. \end{aligned} \tag{2.58}$$

Using these results in Eq. (2.55) gives

$$\omega_{cl}t = U_1\sin\nu + \tan^{-1}\left(\frac{U_2}{U_1\cos\nu}\right), \tag{2.59}$$

which gives the time dependence in U space, and agrees with the results of [39, 107]. We can also rewrite the inverse tangent as $\cos^{-1}U_1$ using

$$U_1^2 + \frac{U_2^2}{\cos^2\nu} = 1 \tag{2.60}$$

and obtain

$$\omega_{cl}t = U_1\sin\nu + \cos^{-1}U_1. \tag{2.61}$$

Using Eq. (2.30), we can generalize this result to an arbitrary orbit in configuration space.

$$\omega_{cl}t = -\frac{\boldsymbol{p}\cdot\boldsymbol{r}}{ar_c} + \cos^{-1}\frac{\boldsymbol{U}\cdot\boldsymbol{A}}{A}. \tag{2.62}$$

If we consider Eqs. (2.59)–(2.61) for circular orbits with $e = \sin\nu = 0$, we obtain $\tan^{-1}(U_2/U_1) = \cos^{-1}\mathrm{U}_1 = \phi(t) = \omega_{cl}t = \phi_r(t) + \pi/2$, and $U_1^2 + U_2^2 = 1$, representing uniform motion in a circle. For this orbit, $U_4 = 0$, so $\theta_4 = \pi/2$.

2.8 Symmetry of the Harmonic Oscillator

We can find a conserved Runge–Lenz vector for the non-relativistic hydrogen atom because the elliptical orbit does not precess, as it does for the relativistic atom. The only central force laws which yield classical elliptical orbits that do not precess are the inverse Kepler force and the linear harmonic oscillator force [110]. Thus, it seems reasonable that one could construct a constant vector similar to $\boldsymbol{A}$ for the oscillator, although the force center for the atom is at a focus and for the oscillator it is at the center of the ellipse. However, it is not possible to define a vector that corresponds to the Runge–Lenz vector for the oscillator [114]. However, it is possible to construct a constant Hermitian second-rank tensor T_{ij}:

$$T_{ij} = \frac{1}{m\omega_0} p_i p_j + m\omega_0 x_i x_j. \tag{2.63}$$

This constant tensor is analogous to the moment of inertia tensor for rigid body motion. The eigenvectors of the tensor will be constant vectors along the principal axes for the particular orbit being considered. The existence of the conserved tensor leads to the U(3) symmetry algebra of the oscillator. The generators are $\lambda^a_{ij} T_{ij}$ where the λ's are the usual U(3) matrices [36]. The spectrum generating algebra is SU(3,1).

In another approach, the Schrodinger equation for the hydrogen atom has been transformed into an equation for a four-dimensional harmonic oscillator or two two-dimensional harmonic oscillators. This approach fits well with parabolic coordinates and was used especially in the 1980s to analyze the group structure of the atom and relate it to SU(3) [52, 115–123]. We will not discuss this approach further.

In the next chapter, we describe the H atom in terms of quantum mechanics.

This page intentionally left blank

Chapter 3

The Hydrogen-like Atom in Quantum Mechanics

In this section, we switch from classical dynamics to quantum mechanics and discuss the group structure and exploit it to determine the bound state energy spectrum directly, as Pauli and his followers did almost a century ago [27, 31]. In Section 3.4, we introduce a new set of basis states for the hydrogen-like atom, eigenstates of the coupling constant. Using these states allows us to display the symmetries in the most convenient manner and to treat bound and scattering states uniformly.

3.1 The Degeneracy Group SO(4)

The quantum mechanical Hamiltonian is

$$H = \frac{p^2}{2m} - \frac{Z\alpha}{r} = E. \tag{3.1}$$

The classical expression for the Runge–Lenz vector must be symmetrized to ensure the corresponding quantum mechanical operator $\boldsymbol{A}$ is Hermitian:

$$\boldsymbol{A} = \frac{1}{\sqrt{-2mH}} \left(\frac{\boldsymbol{p} \times \boldsymbol{L} - \boldsymbol{L} \times \boldsymbol{p}}{2} - mZ\alpha \frac{\boldsymbol{r}}{r} \right). \tag{3.2}$$

We may verify that $\boldsymbol{A}$ and $\boldsymbol{L} = \boldsymbol{r} \times \boldsymbol{p}$ both commute with the Hamiltonian H. The commutation relations of L_i and A_i are the same as the corresponding classical Poisson bracket relations for bound states:

$$[L_i, L_j] = i\epsilon_{ijk} L_k, \quad [L_i, A_j] = i\epsilon_{ijk} A_k, \quad [A_i, A_j] = i\epsilon_{ijk} L_k \tag{3.3}$$

and form the algebra of O(4) [48]. We can write the commutation relations in a single equation that makes the O(4) symmetry explicit. If we define

$$S_{ij} = \epsilon_{ijk} L_k \quad S_{i4} = A_i \tag{3.4}$$

then

$$[S_{ab}, S_{cd}] = i(\delta_{ac}S_{bd} + \delta_{bd}S_{ac} - \delta_{ad}S_{bc} - \delta_{bc}S_{ad}) \quad a, b = 1, 2, 3, 4. \quad (3.5)$$

The Kronecker delta function δ_{ab} acts like a metric tensor.

3.2 Derivation of the Energy Levels

We can obtain the energy levels by determining which representations of the SO(4) group are realized by the degenerate eigenstates of the hydrogen-like atom [25, 27, 48]. The representations of SO(4) can be characterized by the numerical values of the two Casimir operators for SO(4):

$$C_1 = \boldsymbol{L} \cdot \boldsymbol{A} \qquad C_2 = \boldsymbol{L}^2 + \boldsymbol{A}^2. \quad (3.6)$$

Once we know the value of C_2, then the eigenvalues of H follow from the quantum mechanical form of Eq. 2.17, namely

$$\boldsymbol{L}^2 + \boldsymbol{A}^2 + 1 = \frac{(mZ\alpha)^2}{-2mH}. \quad (3.7)$$

In order to determine the possible values of C_2 we factor the O(4) algebra into two disjoint SU(2) algebras [124], each of which has the same commutation relations as the ordinary angular momentum operators,

$$\boldsymbol{N} = \tfrac{1}{2}(\boldsymbol{L} + \boldsymbol{A}) \qquad \boldsymbol{M} = \tfrac{1}{2}(\boldsymbol{L} - \boldsymbol{A}). \quad (3.8)$$

The commutation relations are

$$[M_i, N_j] = 0 \quad [M_i, M_j] = i\epsilon_{ijk}M_k \quad [N_i, N_j] = i\epsilon_{ijk}N_k. \quad (3.9)$$

In analogy with the results for the ordinary angular momentum operators, the Casimir operators are

$$\begin{aligned} M^2 &= j_1\,(j_2 + 1)\,, \quad j_1 = 0, \tfrac{1}{2}, 1, \ldots \\ N^2 &= j_2\,(j_2 + 1)\,, \quad j_2 = 0, \tfrac{1}{2}, 1, \ldots \end{aligned} \quad (3.10)$$

The numbers j_1 and j_2, which may have half-integral values for SU(2) but not O(3), define the (j_1, j_2) representation of SO(4). From the definitions of $\boldsymbol{A}$ and $\boldsymbol{L}$ in terms of the canonical variables, it follows that $C_1 = \boldsymbol{L} \cdot \boldsymbol{A} = 0$ which means $j_1 = j_2 = j$ as in the classical case. For our representations, we find

$$\boldsymbol{M}^2 = \boldsymbol{N}^2 = \tfrac{1}{4}(\boldsymbol{L}^2 + \boldsymbol{A}^2) = j(j+1), j = 0, \tfrac{1}{2}, 1, .. \quad (3.11)$$

and therefore

$$\boldsymbol{L}^2 + \boldsymbol{A}^2 + 1 = (2j+1)^2. \tag{3.12}$$

Substituting this result into Eq. (3.7) gives the usual formula for the bound state energy levels of the hydrogen atom:

$$H' = -\frac{m(Z\alpha)^2}{2n^2} = E_n, \tag{3.13}$$

where the principal quantum number $n = 2j + 1 = 1, 2, \ldots$ and the prime on H signifies an eigenvalue of the operator H.

Within a subspace of energy E_n, the Runge–Lenz vector is

$$\boldsymbol{A} = \frac{1}{a_n}\left(\frac{\boldsymbol{p}\times\boldsymbol{L} - \boldsymbol{L}\times\boldsymbol{p}}{2} - mZ\alpha\frac{\boldsymbol{r}}{r}\right), \tag{3.14}$$

where

$$a_n = \sqrt{-2mE_n} = \frac{mZ\alpha}{n}. \tag{3.15}$$

Our considerations of the Casimir operators have shown that the hydrogen atom provides completely symmetric tensor representations of SO(4), namely, $(j, j) = (\frac{n-1}{2}, \frac{n-1}{2})$, $n = 1, 2, \ldots$ The dimensionality is $(2j+1)^2 = n^2$, corresponding to the n^2 degenerate states. The appearance of only symmetrical tensor representations ($j_1 = j_2$) can be traced to $\boldsymbol{L}\cdot\boldsymbol{A}$ vanishing, which is a consequence of the structure of $\boldsymbol{L}$ and $\boldsymbol{A}$ in terms of the dynamical variables for the hydrogen-like atom. For systems other than the hydrogen-like atom, it is not generally possible to find the expression for the energy levels in terms of all the different quantum numbers alone. It worked here since we could express the Hamiltonian as a function of the Casimir operators which contained all quantum numbers explicitly.

There are a variety of possible basis states. We could choose basis states for the SO(4) representation that reflect the SU(2) decomposition, namely eigenstates of $\boldsymbol{M}^2$, $\boldsymbol{N}^2$, M_3 and N_3 [124]. Another possibility is to have a basis with the eigenstates of the Casimir operator C_2, and A_3, and M_3. This choice fits well with the use of parabolic coordinates [73]. A more physically understandable choice is to choose the common basis states $|nlm\rangle$ that are eigenstates of C_2, $\boldsymbol{L}^2$, and L_3. For this set of basis states, we have

$$\sqrt{(\boldsymbol{L}^2 + \boldsymbol{A}^2 + 1)}|nlm\rangle = n|nlm\rangle \tag{3.16}$$

$$\boldsymbol{L}^2|nlm\rangle = l(l+1)|nlm\rangle \tag{3.17}$$

$$L_3|nlm\rangle = m|nlm\rangle. \tag{3.18}$$

We can define raising and lowering operators for m:

$$L_\pm = L_1 \pm iL_2, \tag{3.19}$$

which obeys the commutation relations

$$[\boldsymbol{L}^2, L_\pm] = 0 \qquad [L_3, L_\pm] = \pm L_\pm. \tag{3.20}$$

Therefore, we can use $L_\pm$ to change the value of m for the basis states

$$L_\pm|nlm\rangle = \sqrt{(l(l+1) - m(m\pm 1)}|nl\ m\pm 1\rangle \tag{3.21}$$

for $l \geq 1$. We can also use the generators $\boldsymbol{A}$ to change the angular momentum. A general SO(4) transformation can be expressed as a rotation induced by $\boldsymbol{L}$, followed by a rotation induced by A_3, followed by another rotation generated by $\boldsymbol{L}$ [125]. Our interest is primarily in changing the angular momentum l, which is most directly done using A_3, which commutes with L_3 and C_2, and so it only changes l:

$$\begin{aligned} A_3|nlm\rangle = &\left(\frac{(n^2-(l+1)^2)((l+1)^2-m^2)}{4(l+1)^2-1}\right)^{\frac{1}{2}}|nl+1m\rangle \\ &+\left(\frac{(n^2-l^2)(l^2-m^2)}{4l^2-1}\right)^{\frac{1}{2}}|nl-1m\rangle \end{aligned} \tag{3.22}$$

for $l \geq 1$.

3.3 Relativistic and Semi-relativistic Spinless Particles in the Coulomb Potential Described by the Klein-Gordon Equation

As we mentioned in Chapter 1, in the discussion of Table 1, the relativistic Klein–Gordon equation may be approximated by dropping the V^2 term to obtain an equation of the same form as the non-relativistic Schrodinger equation. The Klein–Gordon equation

$$(p^2 - (\tilde{E} - V)^2 + m^2)\tilde{\psi} = 0$$

where $\tilde{E}$ is the relativistic total energy, may be solved exactly for a Coulomb potential, $V = -(Z\alpha)/r$ [126]. The energy levels depend on a principal quantum number and on the magnitude of the angular momentum but not

on its direction. The only degeneracy present is associated with the O(3) symmetry of the Hamiltonian. For a relativistic scalar particle, there is no degeneracy to be lifted by a Lamb shift.

If we neglect the V^2 term the resulting equation can be written in the form

$$\left(\frac{p^2}{2\tilde{E}} + V - \frac{\tilde{E}^2 - m^2}{2\tilde{E}}\right)\tilde{\psi} = 0.$$

This is exactly the same as the nonrelativistic Schrodinger equation with the substitutions

$$m \to \tilde{E} \qquad E \to \frac{\tilde{E}^2 - m^2}{2\tilde{E}}.$$

Thus, we regain the O(4) symmetry of the non-relativistic hydrogen atom, and can define two conserved vectors, as indicated in Table 1. It is possible to take the "square root" of this approximate Klein-Gordon equation (in the same sense that the Dirac equation is the square root of the Klein–Gordon equation) and obtain an approximate Dirac equation whose energy eigenvalues are independent of the orbital angular momentum [127].

3.4 Eigenstates of the Inverse Coupling Constant $(Z\alpha)^{-1}$

We introduced the unusual idea of eigenstates of the coupling constant $(Z\alpha)^{-1}$ in Section 1.3. We are allowing the coupling constant to vary while we keep the energy $\mathrm{a}^2/2\mathrm{m}$ constant. Mathematics allows this unusual treatment of a constant as a parameter, while of course it is physically impossible.

Solutions to Schrodinger's equation for a particle of energy $E = -a^2/2m$ in a Coulomb potential

$$\left[p^2 + a^2 - \frac{2mZ\alpha}{r}\right]|a\rangle = 0 \tag{3.23}$$

may be found for certain critical values of the energy $E_n = -a_n^2/2m$ where $a_n = mZ\alpha/n$. The corresponding eigenstates of the Hamiltonian are $|n\ell m\rangle$ which satisfy Eq. (3.23) with a replaced by a_n. In addition to the bound states because there is no upper bound on p^2 in the Hamiltonian, we also have the continuum of scattering states that have $E > 0$.

Since the quantity which must have discrete values for a solution to exist is actually $a/mZ\alpha$, as noted in Section 1.4, we might ask if eigensolutions to Eq. (3.23) exist for certain critical values of $Z\alpha$ while keeping a and

the energy fixed [110]. To investigate such solutions it is convenient to algebraically transform (3.23):

$$\left[\frac{1}{\sqrt{\rho(a)}}\left(\frac{p^2+a^2}{a}\right)\frac{1}{\sqrt{\rho(a)}}-\frac{1}{\sqrt{\rho(a)}}\left(\frac{2mZ\alpha}{ar}\right)\frac{1}{\sqrt{\rho(a)}}\right]\sqrt{\rho(a)}|a\rangle=0,$$

where

$$\rho(a)=\frac{p^2+a^2}{2a^2}. \tag{3.24}$$

Since $\rho(a)$ commutes with p^2 we obtain the eigenvalue equation

$$\left[\left(\frac{a}{mZ\alpha}\right)-K(a)\right]|a)=0, \tag{3.25}$$

where the totally symmetric and real kernel is

$$K(a)=\sqrt{\frac{2a^2}{p^2+a^2}}\frac{1}{ar}\sqrt{\frac{2a^2}{p^2+a^2}} \tag{3.26}$$

and we define the transformed eigenstates $|nlm)$ in terms of the old eigenstates $|nlm\rangle$

$$|a)=(\rho(a))^{\frac{1}{2}}|a\rangle. \tag{3.27}$$

As before, solutions to this transformed equation may found for the eigenvalues

$$K'(a)=\left(\frac{a}{mZ\alpha}\right)'=\frac{1}{n}. \tag{3.28}$$

If we hold $Z\alpha$ constant and let a vary, we obtain the usual spectrum $a_n=\sqrt{-2mE_n}=mZ\alpha/n$. For $a=a_n$, Eq. (3.27) reduces to the equation for the eigenstates

$$\sqrt{\rho(a_n)}|nlm\rangle=|nlm;a_n). \tag{3.29}$$

Alternatively, if we hold a constant, then $Z\alpha$ has the spectrum

$$(Z\alpha)_n=\frac{na}{m} \tag{3.30}$$

with the corresponding eigenstates of $(Z\alpha)^{-1}$ being

$$|nlm;a). \tag{3.31}$$

The relationship between the usual energy eigenstates $|nlm\rangle$ and the eigenstates $|nlm;a)$ of $(Z\alpha)^{-1}$ is

$$|nlm\rangle = \frac{1}{\sqrt{\rho(a_n)}}|nlm;a_n) = \left[\frac{p^2+a_n^2}{2a_n^2}\right]^{-1/2}|nlm;a_n), \tag{3.32}$$

which requires that both sets of states have precisely the same quantum numbers.

Note that the magnitude $(a|K(a)|a)$ is proportional to $\langle 1/ar\rangle_n = (1/a_n)(1/n^2a_0)$ where a_0 is the Bohr radius for the ground state and so is positive and bounded. The kernel K(a) is real and symmetric in p and r and is manifestly Hermitean. Since the kernel K in Eq. (3.25) is bounded, definite, and Hermitian with respect to the eigenstates $|nlm;a_n)$ the set of normalized eigenstates

$$\begin{aligned}&|nlm;a) \quad n=0,1,2,\ldots; \quad l=0,1,\ldots,n-2,n-1;\\ &m=-l,-l+1,\ldots,l-1,l,\end{aligned} \tag{3.33}$$

where

$$\left(\frac{1}{n}-K(a)\right)\ |nlm;a) = 0 \tag{3.34}$$

is a complete orthonormal basis for the hydrogen-like atom [94, p. 340; 110; 128, p. 19]:

$$(nlm;a|n'l'm';\ a) = \delta_{nn'}\delta_{ll'}\delta_{mm'} \tag{3.35}$$

$$\sum_{nlm}|nlm;\ a)(nlm;\ a| = 1. \tag{3.36}$$

There are several important points to notice with regard to these eigenstates of the inverse of the coupling constant:

(1) **Because of the boundedness of K, there is no continuum portion in the eigenvalue spectrum of $(Z\alpha)^{-1}$, the eigenvalues are discrete**. Since K is a positive definite Hermitian operator, all eigenvalues are positive real numbers. This feature leads to a unified treatment of all states of the hydrogen-like atom as opposed to the treatment in terms of energy eigenstates in which we must consider separately the bound states and the continuum of scattering states.

(2) It follows from Eq. (3.32) that **the quantum numbers, multiplicities, and degeneracies of these states $|nlm;a)$ are precisely the same as those of the usual bound energy eigenstates**. For

example, there are n^2 eigenstates of $(Z\alpha)^{-1}$ that have the principal quantum number equal to n or $(Z\alpha)$ equal to na/m.

(3) **A single value of the RMS momentum a or the energy $E = -a^2/2m$ applies to all states in our complete basis** as opposed to the usual energy eigenstates where each non-degenerate state has a different value of a. We have made this explicit by including a in the notation for the states: $|nlm; a)$. Sometimes, for simplicity, we will write the states as $|nlm)$, provided that the value of a has been specified. This behavior in which a single value of a applies to all states will prove to be very useful. In essence, it allows us to generalize from statements applicable in a subspace of Hilbert space with energy E_n or energy parameter a_n to the entire Hilbert space.

(4) **By a suitable scale change or dilation we can give the quantity a any positive value we desire**. This is effected by the unitary operator

$$D(\lambda) = e^{i\frac{1}{2}(\boldsymbol{p}\cdot\boldsymbol{r}+\boldsymbol{r}\cdot\boldsymbol{p})\lambda}, \tag{3.37}$$

which transforms the canonical variables

$$D(\lambda)\boldsymbol{p}D^{-1}(\lambda) = e^{-\lambda}\boldsymbol{p} \quad D(\lambda)\boldsymbol{r}D^{-1}(\lambda) = e^{\lambda}\boldsymbol{r} \tag{3.38}$$

and the kernel K(a)

$$D(\lambda)K(a)D^{-1}(\lambda) = K(ae^{\lambda}) \tag{3.39}$$

and the eigenvalue equation

$$\left(\frac{1}{n} - K(ae^{\lambda})\right) D(\lambda)|nlm;\ a) = 0. \tag{3.40}$$

Therefore, the states transform as

$$D(\lambda)|nlm; a) = |nlm; ae^{\lambda}). \tag{3.41}$$

These transformed states form a new basis corresponding to the new value $e^{\lambda}a$ of the RMS momentum.

The relationship between the energy eigenstates and the $(Z\alpha)^{-1}$ eigenstates can be written using the dilation operator:

$$|nlm\rangle = \frac{1}{\sqrt{\rho\,(a_n)}} D(\lambda_n)|n\ell m;\ a), \quad \text{where } e^{\lambda_n} = \frac{a_n}{a}. \tag{3.42}$$

The usual energy eigenstates $|nlm\rangle$ are obtained from the eigenstates of $(Z\alpha)^{-1}$ by first performing a scale change to insure that the energy

parameter a has the value a_n and then multiplying by a factor $\rho^{-1/2}$. The $(Z\alpha)^{-1}$ eigenvalue equation Eq. (3.25) indicates that the eigenfunctions are functions of p/a or ar, while the energy eigenvalue equation Eq. (3.23) indicates that the eigenfunctions are functions of p/a_n and $a_n r$ if we note that $mZ\alpha = na_n$. Hence, the scale change from a to a_n is needed. The factor $\rho^{-1/2}$ is required to convert Schrodinger's equation to one involving a bounded Hermitean operator.

Using the eigenstates of $(Z\alpha)^{-1}$ as our basis allows us to analyze the mathematical and physical structure of the hydrogen-like atom in the easiest and clearest way.

3.4.1 *Another set of eigenstates of* $(Z\alpha)^{-1}$

We can transform Schrodinger's equation Eq. (3.23) to an eigenvalue equation for $(Z\alpha)^{-1}$ that differs from Eq. (3.34):

$$\left(\frac{1}{n} - K_1(a)\right) \; |nlm;\; a) = 0, \tag{3.43}$$

where

$$K_1(a) = \frac{1}{\sqrt{ar}} \frac{2a^2}{p^2 + a^2} \frac{1}{\sqrt{ar}}, \tag{3.44}$$

and

$$|nlm\rangle = \frac{1}{\sqrt{\rho(a_n)}} D(\lambda_n)|nlm; a_n) \quad \rho(a) = n/ar. \tag{3.45}$$

The kernel K_1(a) is bounded from below and is a positive definite Hermitian operator so the eigenstates form a complete basis. K_1(a) is also bounded from above and there are no scattering states with arbitrary large energies. The relationship of these basis states to the energy eigenstates is the same as that of the previously discussed eigenstates of $(Z\alpha)^{-1}$ Eq. (3.41) but with $\rho(a) = n/ar$. The n guarantees that the two sets of eigenstates have consistent normalization, which may be checked by means of the virial theorem. The n cancels out when similarity transforming from the basis of energy eigenstates to the basis of $(Z\alpha)^{-1}$. Note that, classically, both kernels equal $1/ar_c$.

The first set of basis states of $(Z\alpha)^{-1}$ with $\rho(a) = p^2 + a^2/2a^2$ is more convenient to use when working in the momentum space, and the second set with $\rho(a) = n/ar$ is more convenient in configuration space.

Other researchers have used other approaches to secure a bounded kernel for the Schrodinger hydrogen atom, for example, by multiplying the equation on the left by r to regularize it [94]. However, the methods used have not symmetrized the kernels to make them Hermitian, nor are all the generators of the corresponding groups Hermitian, and they have to redefine the inner product [51, 94].

3.4.2 *Transformation of A and L to the new basis states*

We must transform the defining equation for $\boldsymbol{A}$ as given in Eq. (3.2) and $\boldsymbol{L} = \boldsymbol{r} \times \boldsymbol{p}$ when we change our basis states from eigenstates of the energy to eigenstates of the inverse coupling constant. The correct transformation may be derived by requiring that the transformed generators produce the same linear combination of new states as the original generators produced of the old states. Thus, since

$$\boldsymbol{A}|nlm\rangle = \sum_{l',m'} |nl'm'\rangle A^{lm}_{l'm'}, \tag{3.46}$$

where the coefficients $A^{lm}_{l'm'}$ are the matrix elements of $\boldsymbol{A}$, we require that the transformed generator $\boldsymbol{a}$ satisfies the equation

$$\mathbf{a}|nlm) = \sum_{l'm'} |nl'm')A^{lm}_{l'm'}. \tag{3.47}$$

In other words, since the Runge–Lenz vector $\boldsymbol{A}$ is a symmetry operator of the original energy eigenstates, $\mathbf{a}$ will be a symmetry operator of the new states with precisely the same properties and matrix elements. Since $\boldsymbol{A}$ is Hermitian, $\mathbf{a}$ is Hermitian.

To obtain a differential expression for $\mathbf{a}$ acting on the new states, we need to transform the generator using Eq. (3.42):

$$\mathbf{a} = D^{-1}(\lambda_n)\left(\sqrt{\rho(a_n)}\boldsymbol{A}\frac{1}{\sqrt{\rho(a_n)}}\right)D(\lambda_n). \tag{3.48}$$

The effect of the scale change from $D(\lambda_n)$ on the quantity in large parenthesis is to replace a_n everywhere by a. By explicit calculation, we find

$$\mathbf{a} = \frac{1}{2a}\left(\frac{\boldsymbol{r}p^2 + p^2\boldsymbol{r}}{2} - \boldsymbol{r}\cdot\boldsymbol{p}\boldsymbol{p} - \boldsymbol{p}\boldsymbol{p}\cdot\boldsymbol{r}\right) - \frac{a\mathbf{r}}{2} \tag{3.49}$$

for $\rho(a) = (p^2 + a^2)/2a^2$. And we obtain

$$\mathbf{a} = \frac{1}{2a}\left(\frac{\boldsymbol{r}p^2 + p^2\boldsymbol{r}}{2} - \boldsymbol{r}\cdot\boldsymbol{p}\boldsymbol{p} - \boldsymbol{p}\boldsymbol{p}\cdot\boldsymbol{r} - \frac{\mathbf{r}}{4r^2}\right) - \frac{a\mathbf{r}}{2} \tag{3.50}$$

for $\rho(a) = n/ar$.

Both of these expressions for $\mathbf{a}$ are manifestly Hermitian. In addition, since there is no dependence on the principal quantum number, these expressions are valid in the entire Hilbert space, and not just in a subspace spanned by the degenerate states, as was the case when we used the energy eigenstates as a basis using Eq. (3.14).

The angular momentum operator is invariant under scale changes, and it commutes with scalar operators. Therefore, $\boldsymbol{L}$ is invariant under the similarity transformation $\frac{1}{\sqrt{\rho(a_n)}}D(\lambda_n)$ and the expression for the angular momentum operator with respect to the eigenstates of $(Z\alpha)^{-1}$ is the same as the expression with respect to the eigenstates of the energy.

3.5 The $\langle U'|$ Representation

The U' coordinates provide the natural four-dimensional representation for the investigation of the symmetries of the hydrogen-like atom in quantum mechanics, as in classical mechanics.[1] Therefore, we briefly consider the relevant features of this representation and, in particular, its relationship to the momentum representation. The eigenstate $\langle U'|$ of U_b, $b = 1, 2, 3, 4$, is defined by

$$\langle U'| \quad U_b = U'_b \quad \langle U'|. \tag{3.51}$$

These states are complete on the unit hypersphere in four dimensions:

$$\int |U'\rangle\langle U'|\ d^3\Omega' = \int |U'\rangle\langle U'|\ \sin^2\theta_4 \sin\theta d\theta_4 d\theta d\phi = 1, \tag{3.52}$$

where Ω refers to the angles (θ_4, θ, ϕ) defined in Eq. (2.41). The U variables are defined in terms of the momentum variables and the quantity a in Eq. (2.38). Therefore the momentum and the U operators commute

$$[p_i, U_b] = 0 \tag{3.53}$$

and the state $\langle U'|$ is proportional to a momentum eigenstate $\langle p'|$:

$$\langle U'| = \langle p'|\ \sqrt{J(p)}, \tag{3.54}$$

[1] The prime indicates eigenvalues of operators, and the unprimed quantities indicate abstract operators. The quantity x′ means the four-vector (t′, x′).

where the momentum eigenstate is defined by $\langle p'|\boldsymbol{p} = \boldsymbol{p'}\langle p|$ and

$$\int d^3p'|p'\rangle\langle p'| = 1. \tag{3.55}$$

The function $J(p')$ may be determined by equating the completeness conditions and substituting Eq. (3.54):

$$1 = \int d^3p'|p'\rangle\langle p'| = \int d^3\Omega'|U'\rangle\langle U'| = \int d^3\Omega' J(p')|p'\rangle\langle p'|, \tag{3.56}$$

which leads to the identification of the differential quantities

$$d^3p' = d^3\Omega' J(p') \tag{3.57}$$

demonstrating that $J(p')$ is the Jacobian of the transformation from the p- to the U-space. The volume element in momentum space is

$$d^3p' = p'^2 dp' \sin\theta' d\theta' d\phi' \tag{3.58}$$

Substituting the expression for $d^3\Omega'$ from Eq. (3.52) we find

$$d^3p' = p'^2 \frac{dp'}{d\theta'_4} \frac{1}{\sin^2\theta'_4} d\Omega'. \tag{3.59}$$

Using Eq. (2.38) and (2.40) we can evaluate $dp'/d\theta_4$ and $\sin\theta_4$ in terms of p, obtaining the Jacobian

$$J(p') = \left[\frac{p'^2 + a^2}{2a}\right]^3. \tag{3.60}$$

Therefore from Eq. (3.54) we have the important result

$$\langle U'| = \langle p'| \left[\frac{p^2 + a^2}{2a}\right]^{3/2}. \tag{3.61}$$

We can use this result to compute the action of $\boldsymbol{r}$ on $\langle U'|$ in terms of differential operators. Using the equation

$$\langle p'|\boldsymbol{r} = i\boldsymbol{\nabla}_{p'}\langle p'|, \tag{3.62}$$

we obtain

$$\langle U'|\boldsymbol{r} = \left(i\boldsymbol{\nabla}_{p'} - \frac{3i\boldsymbol{p'}}{p'^2 + a^2}\right)\langle U'|. \tag{3.63}$$

3.5.1 *Action of a and L on* $\langle U'|$

Using Eq. (3.62) for the action of $\boldsymbol{r}$ on $\langle U'|$ and using the expression Eq. (3.49) for $\boldsymbol{a}$, we immediately find that when acting on $\langle U'|$, $\boldsymbol{a}$ has the differential representation

$$\boldsymbol{a}' = \frac{i}{2a}((p'^2 - a^2)\boldsymbol{\nabla}_{p'} - 2\boldsymbol{p}'\boldsymbol{p}' \cdot \boldsymbol{\nabla}_{\boldsymbol{p}'}), \tag{3.64}$$

where

$$\langle U'|\boldsymbol{a} = \boldsymbol{a}'\langle U'|. \tag{3.65}$$

We can also write $\boldsymbol{a}'$ in terms of the U' variables by using the relationship Eq. 2.39 between the p and U variables:

$$\boldsymbol{a}' = U_4' i\boldsymbol{\nabla}_{U'} - \boldsymbol{U}' i\partial/\partial_4', \tag{3.66}$$

where the spatial part of the four vector U' is $\boldsymbol{U} = (U_1, U_2, U_3)$ and U_4 is the fourth component. This is the differential representation of a rotation operator mixing the spatial and the fourth components of U'. When acting on the state $\langle U'|$, clearly $e^{i\boldsymbol{a}\cdot\boldsymbol{\nu}}$ generates a four-dimensional rotation that produces a new eigenstate $\langle U''|$. To derive the form of the finite transformation explicitly we compute

$$[a_j', U_j'] = iU_4'\delta_{ij} \qquad [a_j', U_4'] = -iU_i'. \tag{3.67}$$

For a finite transformation $a^{i\boldsymbol{a}\cdot\boldsymbol{n}\nu}$ with $\boldsymbol{n}^2 = 1$, for the transformation of the spatial components of U we have

$$\begin{aligned} \boldsymbol{U}'' &= e^{i\boldsymbol{a}'\cdot\boldsymbol{n}\nu}\boldsymbol{U}'e^{-i\boldsymbol{a}'\cdot\boldsymbol{n}\nu} \\ &= \boldsymbol{U}' - \boldsymbol{n}\boldsymbol{n}\cdot\boldsymbol{U}' + \boldsymbol{n}\boldsymbol{n}\cdot\boldsymbol{U}'\cos\nu - \boldsymbol{n}U_4'\sin\nu \end{aligned} \tag{3.68}$$

and for the fourth component of U we have

$$\begin{aligned} U_4'' &= e^{i\boldsymbol{a}'\cdot\boldsymbol{n}\nu}U_4'e^{-i\boldsymbol{a}'\cdot\boldsymbol{n}\nu} \\ &= U_4'\cos\nu + \boldsymbol{n}\cdot\boldsymbol{U}'\sin\nu. \end{aligned} \tag{3.69}$$

These equations of transformation are like those for a Lorentz transformation of a four-vector $(r,\ it)$. We can illustrate the equations for $e^{ia_2\nu}$ (cf Eq. (2.44)) which mixes the 2 and 4 components of U':

$$\begin{aligned} &U_1'' = U_1' \quad U_3'' = U_3' \\ &U_2'' = U_2'\cos\nu - U_4'\sin\nu \quad U_4'' = U_2'\sin\nu + U_4'\cos\nu. \end{aligned} \tag{3.70}$$

When $\boldsymbol{L}$ acts on $\langle U'|$ it has the differential representation

$$\boldsymbol{L}' = \boldsymbol{U}' \times i\boldsymbol{\nabla}_{U'} \tag{3.71}$$

This result follows directly since U'_i equals p'_i times a factor that is a scalar under rotations in three dimensions. When $e^{i\boldsymbol{L}\cdot\boldsymbol{\omega}}$ acts on $\langle U'|$ it produces a new state $\langle U''|$, where the spatial components of U' have been rotated to produce U''.

In summary, we see that U' is a four-vector under rotations generated by $\boldsymbol{a}'$ and $\boldsymbol{L}'$. Therefore the states $\langle U'|$ provide a vector representation of the group of rotations in four dimensions SO(4), with the generators $\boldsymbol{a}$ and $\boldsymbol{L}$.

In the next chapter, we describe the wave functions of the hydrogen atom.

Chapter 4

Wave Functions for the Hydrogen-like Atom

In this chapter, we analyze the wave functions of the hydrogen-like atom, working primarily in the $\langle U'|$ representation and using eigenstates of the inverse of the coupling constant $(Z\alpha)^{-1}$ for the basis states. In this representation, the wave functions are spherical harmonics in four dimensions. We derive the relationship of the usual energy eigenfunctions in momentum space to the spherical harmonics and discuss the classical limits in momentum and configuration space.

4.1 Transformation Properties of the Wave Functions under the Symmetry Operations

We can show that the wave functions $Y_{nlm}(U')$ in the $\langle U'|$ representation with respect to the eigenstates of $(Z\alpha)^{-1}$

$$Y_{nlm}(U') \equiv \langle U'|nlm) \tag{4.1}$$

transform as four-dimensional spherical harmonics under the four-dimensional rotations generated by the Runge–Lenz vector $\boldsymbol{a}$ and the angular momentum $\boldsymbol{L}$. We note that the quantity a is implicit in both the bra and the ket in Eq. (4.1). For our basis states we employ the set of $(Z\alpha)^{-1}$ eigenstates $|nlm)$ of the inverse coupling constant that are convenient for momentum space calculations ($\rho = (p^2 + a^2)/2a^2$). We choose these states rather than those convenient for configuration space calculations because the $\langle U'|$ eigenstates are proportional to the $\langle p'|$ eigenstates (Eq. 3.61).

If we transform our system by the unitary operator $e^{i\theta}$, where $\theta = \boldsymbol{L}\cdot\boldsymbol{\omega} + \boldsymbol{a}\cdot\boldsymbol{\nu}$, then the wave function in the new system is

$$Y'_{nlm}(U') = \langle U'|e^{i\theta}|nlm). \tag{4.2}$$

There are two ways in which we may interpret this transformation, corresponding to what have been called the active and the passive interpretations. In the passive interpretation, we let $e^{i\theta}$ act on the coordinate eigenstate $\langle U'|$. As we have seen in Section 3.5.1, this produces a new eigenstate $\langle U''|$, where the four-vector U'' is obtained by a four-dimensional rotation of U' (Eqs. 3.68–3.70). Thus we have

$$Y'_{nlm}(U') = \langle U''|nlm) = Y_{nlm}(U''). \tag{4.3}$$

In the active interpretation, we let $e^{i\theta}$ act on the basis state $|nlm)$. Since $\boldsymbol{L}$ and $\boldsymbol{a}$ are symmetry operators of the system, which transform degenerate states into each other, it follows that $e^{i\theta}|nlm)$ must be a linear combination of states with a principal quantum number equal to n. Therefore, we have

$$Y'_{nlm}(U') = \sum_{l'm'} \langle U'|R^{nlm}_{nl'm'}|nl'm') \;\; = \;\; \sum_{l'm'} R^{nlm}_{nl'm'} Y_{nl'm'}(U'). \tag{4.4}$$

The wave functions for degenerate states with a given n transform irreducibly among themselves under the four-dimensional rotations, forming a basis for an irreducible representation of SO(4) of dimensions n^2. Equating the results of the two different interpretations gives

$$Y_{nlm}(U'') = \sum_{l'm'} R^{nlm}_{nl'm'} Y_{nl'm'}(U'). \tag{4.5}$$

The transformation properties Eq. (4.5) of Y_{nlm} are precisely analogous to those of the three-dimensional spherical harmonic functions. It follows that Y_{njm} are four-dimensional spherical harmonics [48, 129].

4.2 Differential Equation for the Four-Dimensional Spherical Harmonics $Y_{nlm}(U')$

The differential equation for the $Y_{nlm}(U')$ may be obtained from the equation

$$(\boldsymbol{L'}^2 + \boldsymbol{a'}^2) Y_{nlm}(U') = (n^2 - 1) Y_{nlm}(U'), \tag{4.6}$$

which follows from $C_2 = n^2 - 1$ and the definition $C_2 = \boldsymbol{L}^2 + \boldsymbol{A}^2$, Eq. (3.6). Substituting in the differential expressions Eqs. (3.66) and (3.71) for $\boldsymbol{a'}$ and $\boldsymbol{L'}$ we find that $\boldsymbol{L'}^2 + \boldsymbol{a'}^2$ equals $\nabla^2_{U'} - (\boldsymbol{U'} \cdot \boldsymbol{\nabla}_{U'})^2$, which is the angular part of the Laplacian operator in four dimensions (cf in three dimensions, $\boldsymbol{L}^2/r^2 = p^2 - p_r^2$). Thus Eq. (4.6) is the differential equation

for four-dimensional spherical harmonics with the degree of homogeneity equal to $n-1$, which means n^2 such functions exist, in agreement with the know degree of degeneracy.

4.3 Energy Eigenfunctions in Momentum Space

We want to determine the relationship between the usual energy eigenfunctions in the momentum space $\psi_{nlm}(p') \equiv \langle p'|nlm\rangle$ (with $a = a_n$) and the four-dimensional spherical harmonic eigenfunctions $Y_{nlm}(U';a) = \langle U'|nlm;a)$.

We choose the RMS momentum a to have the value a_n. If we use the expression Eq. (3.61) for $\langle U'|$ in terms of $\langle p'|$

$$\langle U'| = \langle p'| \left(\frac{p^2 + a_n^2}{2a_n}\right)^{3/2} \tag{4.7}$$

and the expression Eq. (3.32) for the eigenstates of $(Z\alpha)^{-1}$ in terms of the energy eigenstates

$$|nlm;a_n) = \sqrt{\frac{p^2 + a_n^2}{2a_n^2}}|nlm\rangle \tag{4.8}$$

we find the desired result

$$Y_{nlm}(U';a_n) = \left(\frac{p^2 + a_n^2}{2a_n}\right)^2 \frac{1}{\sqrt{a_n}}\psi_{nlm}(p'). \tag{4.9}$$

The usual method of deriving this relationship between the wave function in momentum space and the corresponding spherical harmonics in four dimensions involves transforming the Schrodinger wave equation to an integral equation in momentum space [32, 48]. As in the classical case, we first replace $\boldsymbol{p}$ by $\boldsymbol{p}/a$ and perform a stereographic projection from the hyperplane corresponding to the three-dimensional momentum space to a unit hypersphere in a four-dimensional space. The resulting integral equation manifests a four-dimensional invariance. When the wave functions are normalized as in Eq. (4.9), the solutions are spherical harmonics in four dimensions. As another alternative to this procedure, we can Fourier transform the configuration space wave functions directly [129].

4.4 Explicit Form for the Spherical Harmonics

The spherical harmonics in four dimensions can be expressed as [130]:

$$Y_{nlm}(\Omega) = N_1(n,l)(\sin\theta_4)^l C_{n-1-l}^{l+1}(\cos\theta_4) \cdot \left[N_2(l,m)(\sin\theta)^m C_{l-m}^{m+1/2}(\cos\theta) \frac{e^{im\phi}}{\sqrt{2\pi}} \right]. \tag{4.10}$$

The factor in brackets is equal to $Y_l^m(\theta,\phi)$, the usual spherical harmonic in three-dimensions [130]. The Gegenbauer polynomials $C_n^\lambda(x)$ of degree n and order λ are defined in terms of a generating function:

$$\frac{1}{(1-2tx+t^2)^\lambda} = \sum_{n=0} t^n C_n^\lambda(x). \tag{4.11}$$

$N_1(n,l)$ and $N_2(l,m)$ are chosen to normalize the Y_{nlm} on the surface of the unit sphere:

$$\int |Y_{nlm}(\Omega)|^2 d^3\Omega_U = 1, \tag{4.12}$$

where $d^3\Omega_U = \sin^2\theta_4 \sin\theta d\theta d\phi$. We find

$$N_1(n,l) = \sqrt{\frac{2^{2l+1}}{\pi} \frac{n(n-l-1)!(l!)^2}{(n+l)!}} \tag{4.13}$$

$$N_2(l,M) = \sqrt{\frac{2^{2m}}{\pi} \left(l+\frac{1}{2}\right) \frac{(l-m)!}{(l+m)!} \left[\Gamma\left(m+\frac{1}{2}\right)\right]^2}. \tag{4.14}$$

In the next section, we discuss the asymptotic behavior of Y_{nlm} for large quantum numbers and compare it to the classical results of Chapter 2. We first mention experiments with Rydberg atoms, which are atoms with a very large radius that approximate the classical behavior.

4.5 Wave Functions in the Semi-classical Limit

4.5.1 *Rydberg atoms*

Advances in quantum optics, such as the development of ultra-short laser pulses, microwave spectroscopy, and atom interferometry, have opened new possibilities for experiments with atoms and Rydberg states, meaning hydrogen-like atoms in states with very large principal quantum numbers and correspondingly large diameter electron orbits. The pulsed electromagnetic fields can be used to modify the behavior of the orbital electrons. Semi-classical electron wave packets in hydrogen-like atoms were first generated

in 1988 by ultrashort laser pulses, and today are often generated by unipolar teraherz pulses [131–133].

Rydberg states of alkalai metals, which have one outer electron, have been employed recently in systems of entangled atoms to perform quantum computation. Two atoms, micrometers apart, can interact a billion times more strongly than normal if one is excited to a high-energy Rydberg state, for example with n about 79. Now much bigger, that atom shifts the energy levels in the second atom so it cannot be excited, the so-called Rydberg blockade [278].

Over the last few decades, there has been a broad interest in the classical limit of the hydrogen-like atom for n very large, Rydberg states, for a number of reasons [134]: (1) Rydberg states are at the border between bound states and the continuum, and any process that leads to excited bound states, ions, or free electrons usually leads to the production of Rydberg states. This includes, for example, photo-ionization or the application of microwave fields. The very large cross section for scattering is unique. (2) Rydberg states can be used to model atoms with a higher atomic number that have an excited valence electron that orbits beyond the core. (3) In Rydberg states, the application of electric and magnetic fields breaks the symmetry of the atom and allows the study of different phenomena, including the transition from classical chaos to quantum chaos [135]. (4) Rydberg atoms can be used to study coherent transient excitation and relaxation, for example the response to short laser pulses creating coherent quantum wave packets that behave like a classical particle.

The square of the wave function for a given quantum state gives a probability distribution for the electron that is independent of time. The wave function is the appropriate description for Rydberg states for which the principal quantum number is not too high.

If we want to describe the movement of an electron in a semiclassical state, with a large radius, going around the nucleus with a classical time dependence, then we need to form a wave packet. The wave packet is built as a superposition of many wave functions with a band of principal quantum numbers.

A variety of theoretical methods have been used to derive expressions for the hydrogen atom wave functions and wave packets for highly excited states. There is general agreement on the wave functions for large n, and that the wave functions display the expected classical behavior: elliptical orbits in the configuration space and great circles in the four-dimensional momentum space [136–139].

Researchers have proposed a variety of wave packets to describe semi-classical Rydberg states. There are general similarities in the wave packets that describe electrons traveling in circular or elliptical orbits with a classical time dependence for some characteristic number of orbits, and it is maintained that the quantum mechanical wave packets provide results that agree with the classical results [112, 132, 133, 136–141]. Most of the approaches exploit the SO(4) or SO(4,2) symmetry of the hydrogen atom, which is used to rotate a circular orbit to an elliptical orbit. The starting orbital is often taken as a coherent state, which is usually considered a classical-like state. The most familiar example of a coherent state is for a one-dimensional harmonic oscillator characterized by creation and annihilation operators $a^\dagger$ and a. The coherent state $|\alpha\rangle$ is a superposition of energy eigenstates that is an eigenstate of a where $a|\alpha\rangle = \alpha|\alpha\rangle$ for a complex α. This coherent state will execute harmonic motion like a classical particle [142]. To obtain a coherent state for the hydrogen-like atom, eigenstates of the operator that lowers the principal quantum number n (which will be discussed in Section 7.4) have been used [143], as well as lowering operators based on the equivalence of the four-dimensional harmonic oscillator representation of the hydrogen atom [137, 138, 144].

In either case, this coherent eigenstate is characterized by a complex eigenvalue, which needs to be specified. Several constraints have been used to obtain the classical wave packet that presumably obeys Kepler's laws, such as requiring that the orbit lie in a plane so $\langle z\rangle = 0$ for the orbital, or that $\langle r - r_{\text{classical}}\rangle$ be a minimum, or that some minimum uncertainty relationship is obtained. In addition, there are issues regarding the approximations used, in particular, those that relate to time. For times characteristic of the classical hydrogen atom, the wave packets act like a classical system. For longer times, the wave packet spreads in the azimuthal direction and after some number of classical revolutions of order 10 to 100 the spread is 2π so the electron is uniformly spread over the entire orbit. The spread arises because the component wave functions that form the wave packet have different momenta. In two derivations, still longer times were considered, and recoherence was predicted to occur after about $n/3$ revolutions, where n is the approximate principal quantum number, although there is some difference in the predicted amount of recoherence [134, 139]. Due to the conservation of $\boldsymbol{L}$ and $\boldsymbol{A}$ the spread of the wave packets is inhibited except in the azimuthal direction.

Brown took a different approach to develop a wave packet for a circular orbit [112]. He first developed the asymptotic wave function for large n and then optimized the coefficients in a Gaussian superposition to minimize the spread in ϕ, obtaining a predicted characteristic decoherence time of about 10 minutes, considerably longer than any other predicted decoherence time.

Other authors have explored the problem from the perspective of classical physics and the Bohr Correspondence Principle [136, 140, 145, 146] Results from the different methods support the basic conclusion that the wave functions are peaked on the corresponding classical Kepler trajectories: "atomic elliptic states sew the wave flesh on the classical bones" [132].

With the variety of experimental methods used to generate Rydberg states, a variety of Rydberg wave packets are created, and it is not clear which theoretical model, if any, is preferred [134]. We take a very simple approach to forming a wave packet and simply use a Gaussian weight for the different frequency components. This does not give an intentionally optimized wave packet, but it is a much simpler approach and the result has all the expected classical behavior that is very similar to that obtained from much more complicated derivations. We start with a circular orbit and then do a SO(4) rotation to secure an elliptical orbit. We show that it has the classical period of rotation.

4.5.2 *Formation of semi-classical wave packets*

We need to derive the semi-classical limit of the wave functions that correspond to circular orbits in configuration space. For this case, $\sin\nu$, which we interpret as the expectation value of the eccentricity, vanishes. We derive expressions for the wave functions in momentum space and then form a wave packet. To obtain corresponding expressions for elliptical orbits, we perform a rotation by $e^{i\boldsymbol{a}\cdot\nu}$ which does not alter the energy but changes the eccentricity and the angular momentum.

Case 1: Circular orbits, $\sin\nu = e = 0$

We derive the asymptotic form of Y_{nlm}, the spherical harmonic in four dimensions, for large quantum numbers, where for simplicity we choose the quantum numbers $n-1 = l = m$ corresponding to a circular orbit in the 1–2 plane. From Eq. (4.10) we see that we encounter Gegenbauer polynomials of the form C_0^λ, which represents the first term in the expansion of the left

side of Eq. (4.11), and therefore are unity. For a very large l, $\sin^l\theta$ will have a very strong peak at $\theta = \pi/2$ so we make the expansion [112]

$$\sin\theta = \sin\left(\frac{\pi}{2} + \left(\theta - \frac{\pi}{2}\right)\right) = 1 - \frac{1}{2}\left(\theta - \frac{\pi}{2}\right)^2 + \cdots \approx e^{-(1/2)(\theta-\pi/2)^2} \tag{4.15}$$

to obtain

$$\sin^l\theta \approx e^{-(1/2)l(\theta-\pi/2)^2}. \tag{4.16}$$

The asymptotic forms for N_1 and N_2 can be computed using the properties of Γ functions:

$$\lim_{z\to\infty}\Gamma(az+b) \simeq \sqrt{2\pi}e^{-az}(az)^{az+b-\frac{1}{2}}, \tag{4.17}$$

and the Stirling approximation for the factorial function

$$n! \approx \sqrt{2\pi n}(n/e)^n \text{ for large } n. \tag{4.18}$$

We obtain[1]

$$Y_{n,n-1,n-1}(\Omega) = \sqrt{\frac{n}{2\pi^2}}e^{-\frac{1}{2}n\left(\theta_4-\frac{\pi}{2}\right)^2}\cdot e^{-\frac{1}{2}n\left(\theta-\frac{\pi}{2}\right)^2}e^{i(n-1)\phi}. \tag{4.19}$$

which gives the probability density

$$|Y_{n,n-1,n-1}(\Omega)|^2 = \frac{n}{(2\pi^2)}e^{-n\left(\theta_4-\frac{\pi}{2}\right)^2}\cdot e^{-n\left(\theta-\frac{\pi}{2}\right)^2}. \tag{4.20}$$

We have Gaussian probability distributions in θ_4 and θ about the value $\pi/2$. The distributions are quite narrow with widths $\Delta\theta_4 \approx \Delta\theta \approx 1/\sqrt{n}$. The spherical harmonic essentially describes a circle ($\theta_4 = \theta = \pi/2$) on the unit hypersphere in the 1–2 plane. As n becomes very large, both $U_4 = \cos\theta_4 \approx (r - r_c)/r$ (Eqs. (2.40) and (2.51)) and $U_3 = \sin\theta_4\cos\theta$, which is proportional to p_3, go to zero as $1/\sqrt{n}$. The distribution approaches the great circle $U_1^2 + U_2^2 = 1$ that we saw in Eq. (2.46) for a classical particle moving in a circular orbit in the 1–2 plane in configuration space. Note that this state is a quantum mechanical stationary state with a constant probability density. To get the classical time dependence, we need to form a wave packet.

[1] According to Eq. (4.9), the corresponding wavefunction in momentum space $\psi(p)$ is obtained by multiplying $Y_{n,n-1,n-1}(\Omega)$ by $4a_n^{5/2}/(p^2+a^2)^2$.

Forming a Wave packet

We form a time dependent wave packet for circular orbits by superposing circular energy eigenstates:

$$\chi(\Omega, t) = \sum_n e^{itE_n} Y_{n,n-1,n-1} A_{n-N}, \tag{4.21}$$

where A_{n-N} is an amplitude peaked about $n = N >> 1$. For $n >> 1$ we expand E_n about E_N:

$$E_n = E_N + \left.\frac{\partial E}{\partial n}\right|_N s + \left.\frac{\partial^2 E}{\partial n^2}\right|_N s^2 + \cdots, \tag{4.22}$$

where $s = n - N$. From the equation for the energy levels, $E = -m(Z\alpha)^2/(2n^2)$ we compute

$$\left.\frac{\partial E_n}{\partial n}\right|_N = \frac{m(Z\alpha)^2}{N^3} = \sqrt{\frac{-8E_N^3}{m(Z\alpha)^2}}. \tag{4.23}$$

In agreement with the Bohr Correspondence Principle, the right-hand side of Eq. (4.23) is just the classical frequency ω_{cl} as given in Eq. (2.24). For the second order derivative we have

$$\left.\frac{\partial^2 E}{\partial n^2}\right|_N = -\frac{3}{N}\omega_{cl} \equiv \beta, \tag{4.24}$$

which gives

$$\chi(\Omega, t) = e^{-itE_N} e^{i\phi(N-1)} \sum_{s=-N+1}^{\infty} e^{-i\left(\omega_{cl} s t - \left(\frac{\beta}{2}\right) s^2 t - s\phi\right)} \cdot A_s |Y_{N+s,N+s-1,N+s-1}|. \tag{4.25}$$

We choose a simple Gaussian form for A_s

$$A_s = \frac{1}{\sqrt{2\pi N}} e^{-s^2/(2N)}. \tag{4.26}$$

Brown used $A_s = Ce^{-s^2 3\omega_{cl} t/N}$ which minimizes the diffusion in ϕ at time t [112]. Since $|Y_{N+s,N+s-1,N+s-1}|$ varies slowly with s for $N >> 1$, we can take it outside of the summation in Eq. (4.25). We now replace the sum by an integral over s. Since A_s is peaked about $s = N$, we can integrate from $s = -\infty$ to $s = +\infty$. We perform the integral by completing the square in

the usual way. The final result for the probability amplitude for a circular orbital wave packet is

$$|x(\Omega,t)|^2 = |Y_{N,N-1,N-1}|^2 \left(1+\beta^2 t^2 N^2\right)^{-1} \cdot \exp\left[-(\phi-\omega_{cl}t)^2 \frac{N}{1+(\beta t N)^2}\right]. \tag{4.27}$$

This represents a Gaussian distribution in ϕ that is centered about the classical value $\phi = \omega_{cl}t$, which means that the wavepacket is traveling in the classical trajectory with the classical time dependence. The width of the ϕ distribution is

$$\Delta\phi = (N)^{(-1/2)}(1+\beta^2 t^2 N^2)^{1/2} = (N)^{(-1/2)}(1+9\omega_{cl}^2 t^2)^{1/2}. \tag{4.28}$$

The distribution in ϕ at $t=0$ is very narrow, proportional to $1/\sqrt{N}$, but $\Delta\phi$ increases approximately linearly over time.

The distributions in θ_4 and θ are Gaussian and centered about $\pi/2$ in each case, as for the circular wave function (cf. Eq. (4.20)) with widths equal to $(N)^{-1/2}$. The spread of these distributions in time is inhibited because of the conservation of angular momentum and energy. The detailed behavior of the widths depends on our use of the Gaussian distribution. Other distributions will give different widths, although the general behavior is expected to be similar.

As a numerical example, consider a hydrogen atom that is in the semiclassical region when the orbital diameter is about 1 cm. The corresponding principal quantum number is about 10^4, the mean velocity is about 2.2×10^4 cm/sec, and the period about 1.5×10^{-4} sec. After about 34 revolutions or 5×10^{-3} sec, the spread in ϕ is about 2π, which means that the electron is spread uniformly throughout the circular orbit. This characteristic spreading time can be compared to 1.6×10^{-3} sec for a fully optimized wave packets formed from coherent SO(4,2) states [139, 147]. In order to make predictions about significantly longer times, we would need to retain more terms in the expansion Eq. (4.22) of E_n.

Case 2: Elliptical orbits $\sin\nu = e \neq 0$

We can obtain the classical limit of the wave function for elliptical orbits by first writing our asymptotic form Eq. (4.19) for $Y_{n,n-1,n-1}$ in terms of the U variables instead of the angular variables by using definitions Eq. (2.40),

and setting $a = a_n$. Retaining only the lowest order terms in $(\theta_4 - \pi/2)$ and $(\theta - \pi/2)$, we find

$$Y_{n,n-1,n-1}(\hat{U}) = \left(\frac{n}{2\pi^2}\right)^{\frac{1}{2}} e^{i(n-1)\tan^{-1}\left(\frac{U_2}{U_1}\right)} \cdot e^{-\frac{1}{2}n(U_4)^2} e^{-\frac{1}{2}n(U_3)^2}. \quad (4.29)$$

For large n, this represents a circular orbit in the 1-2 plane. The exponential in U_3 indicates p_3 is near zero; the exponential in U_4 indicates that $U_4 = (r_c - r)/r_c$ (Eq. 2.51) is near zero so the trajectory is approximately the classical trajectory. The quantity r_c is the length of the classical semi-major axis given by Eq. (2.14). We now perform a rotation by $A_2\nu$. which will change the eccentricity to $\sin\nu$, and change the angular momentum, but will not change the energy or the orbital plane. Using Eq. (3.70) to express the old coordinates in terms of the new coordinates, we find to lowest order

$$Y'_{n,n-1,n-1}(U) = \left(\frac{n}{2\pi^2}\right)^{1/2} e^{i(n-1)\tan^{-1}\left(\frac{U_2}{U_1\cos v}\right)} \cdot e^{-\frac{1}{2}n\{U_2\sin\nu - U_4\cos\nu\}^2} \cdot e^{-\frac{1}{2}n(U_3)^2}. \quad (4.30)$$

In Section 2.6, we found that the vanishing of the term in braces $(0 = U_2\sin\nu - U_4\cos\nu)$, along with U_3 approximately zero, specifies the classical great hypercircle orbit (Eq. (2.42)) corresponding to an ellipse in configuration space with eccentricity $e = \sin\nu$ and lying in the 1–2 plane. The probability density $|Y'_{n,n-1,n-1}(U)|^2$ vanishes except within a hypertorus with a narrow cross section of radius approximately $\frac{1}{\sqrt{n}}$ which is centered about the classical distribution. Since the width $\frac{1}{\sqrt{n}}$ of the distribution is constant in U space, it will not be constant when projected onto p space.

In terms of the original momentum space variables (Eq. 2.38), the asymptotic spherical harmonic is

$$\begin{aligned} &Y_{n,n-1,n-1}(\boldsymbol{p}) \\ &= \left(\frac{n}{2\pi^2}\right)^{\frac{1}{2}} e^{i(n-1)\tan^{-1}\left(\frac{p_2}{p_1\cos\nu}\right)} \\ &\quad \cdot \exp\left\{-\left(\frac{n}{2}\right)\left[p_1^2 + (p_2 - a\tan\nu)^2 - \frac{a^2}{\cos^2\nu}\right]^2 \left(\frac{\cos\nu}{p^2+a^2}\right)\right\}^2 \\ &\quad \cdot \exp\left\{-\left(\frac{n}{2}\right)\left(\frac{2p_3 a}{p^2+a^2}\right)\right\}^2 \Big| a = a_n. \end{aligned} \quad (4.31)$$

The expression in brackets corresponds to the momentum space classical orbit equation we found previously (Eq. 2.35). As we expect, p_3 is Gaussian

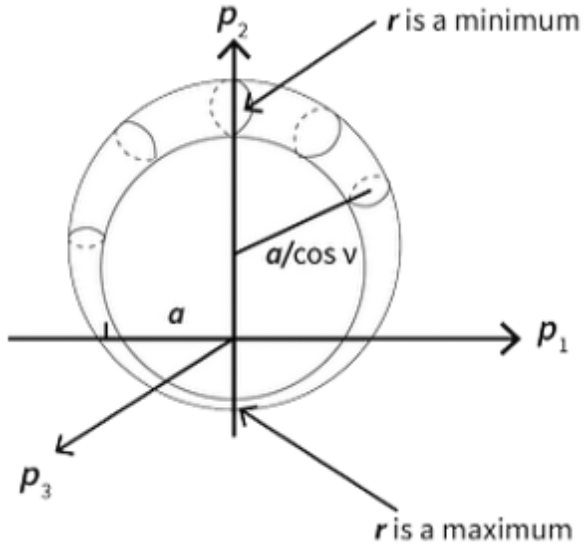

Fig. 4.1. Wave function probability distribution $|Y'_{n,n-1,n-1}(\boldsymbol{p})|^2$ in momentum space for large n, showing the variation in the width of the momentum distribution about the classical circular orbit. The center of the distribution is at $p_2 = a\tan\nu$. The classical orbit is in the 1–2 plane.

about zero since the classical orbit is in the 1–2 plane. We can simplify the expressions for the widths by observing that to lowest order we can use Eq. (2.34), which implies $p^2 + a^2 = 2a^2 + 2ap_2\tan\nu$ in the exponentials. The widths of both distributions therefore increase linearly with p_2. We also note that since classically there exists a one-to-one correspondence between each point of the trajectory in momentum space and each point in configuration space, we may interpret the widths of the distributions using Eq. (2.18) $(p^2 + a^2)/a^2 = 2r_c/r$. Accordingly the widths increase as the momentum increases or as the distance to the force center decreases (Fig. 4.1).

Forming a Wave packet for Elliptical Motion

We may form a time dependent wave packet superposing the wave functions of Eq. (4.30). Care must be taken to include the first-order dependence (through a_n) of $\tan^{-1}(U_2/U_1\cos\nu)$ on the principal quantum number when integrating over the Gaussian weight function. The result for the probability density is the same as before (Eq. 4.27) except $|Y'_{N,N-1,N-1}|^2$ (given in

Eq. 4.30) replaces $|Y_{N,N-1,N-1}|^2$ and

$$\omega_{cl}t = \tan^{-1}\left(\frac{U_2}{U_1\cos\nu}\right) + \sin\nu\,(U_1) \tag{4.32}$$

replaces $\omega_{cl}t = \phi$, The final result for large $n = N$ is

$$|\chi(\Omega,t)|^2 = \frac{n}{2\pi^2}(1+\beta^2t^2n^2)^{-1}\exp[-n(U_2\sin\nu - U_4\cos\nu)].$$
$$\exp[-nU_3^2]\cdot exp\left[-\left(\phi - \tan^{-1}\frac{U_2}{U_1\cos\nu} + U_1\sin\nu\right)^2\frac{n}{1+(\beta tn)^2}\right]. \tag{4.33}$$

The result has the same time dependence as the classical result Eq. (2.59) and the orbit is approximating the classical orbit (Eq. 2.42). The spread of the wave packet will be controlled by the same factor as for the circular wave packet.

Remark on the Semiclassical Limit in Configuration Space

The time dependent quantum mechanical probability density follows the classical trajectory in momentum space, meaning that the probability is greatest at the classical location of the particle in momentum space. Since the configuration space wave function is the Fourier transform of the momentum space wave function, the classical limit must also be obtained in configuration space. That this limit is obtained is made explicit by observing that the momentum space probability density is large when

$$(U_2\sin\nu - U_4\cos\nu)^2 \approx 0. \tag{4.34}$$

However, from Section 2.6 we know that a parametric equation for the classical orbit in $U =$ space is

$$U_2\sin\nu - U_4\cos\nu = 0. \tag{4.35}$$

Accordingly we conclude that the configurations space probability will be large when

$$\left[\frac{r - r_{\text{classical}}}{r_{\text{classical}}}\right]^2 \approx 0. \tag{4.36}$$

4.6 Quantized Semiclassical Orbits

It is convenient at times to have a semiclassical model for the orbitals of the hydrogen-like atom. Historically, this was first done by Pauling and

Wilson [148, p. 36]. We can obtain a model by interpreting the classical formulae for the geometrical properties of the orbits as corresponding to the expectation values of the appropriate quantum mechanical expressions. Thus, when the energy $E = -a^2/2m$ appears in a classical formula, we employ the expression for a for the quantized energy levels $a = 1/nr_0$ where $r_0 = (mZ\alpha)^{-1}$ which is the radius 0.53 Angstrom of the ground state. Similarly, if $\boldsymbol{L}^2$ appears in a classical formula, we substitute $l(l+1)$ where l is quantized $l = 0, 1, 2, \ldots, n-2, n-1$; and m , the component of $\boldsymbol{L}$ along the 3-axis is quantized: $m = -l, -l+1, -l+2, \ldots, l$.

Orbits in Configuration Space

Recalling Eq. (2.14), $r_c = mZ\alpha/a^2$, and noting Eq. (3.15) $a = mZ\alpha/n$, we see $ar_c = n$, which gives a semi-major axis of length $r_c = n^2 r_0$, where $r_0 = 1/mZ\alpha$ is the radius for the circular orbit of the ground state. For a circular orbit, the radius is the semi-major axis. Thus, r_c is the radius of a circular orbit for a state with principal quantum number n. For an orbit with eccentricity $e = \sin\nu$, the equations for the magnitude of $\boldsymbol{L}$ and $\boldsymbol{A}$ are

$$L = r_c a \cos\nu = n\cos\nu = \sqrt{l(l+1)} \tag{4.37}$$

$$A = r_c a \sin\nu = n\sin\nu = \sqrt{n^2 - l(l+1)} \tag{4.38}$$

This gives an eccentricity $\sin\nu$ equal to

$$e = \sin\nu = \sqrt{1 - \frac{l(l+1)}{n^2}} \tag{4.39}$$

and a semi-major axis equal to

$$b = r_c \sin\nu = n\sqrt{l(l+1)}. \tag{4.40}$$

Note that the expression for e is limited in its meaning. For an s state, it always gives $e = 1$, and for states with $l = n-1$ it gives $e = \sqrt{1/n}$, not the classically expected 0 for a circular orbit.

Orbits in U-Space

The corresponding great hypercircle orbits (ν, Θ) in U-space are described by giving the quantized angle ν, between the three-dimensional hyperplane of the orbit and the 4-axis, and the quantized angle Θ, between the

hyperplane of the orbit and the 3-axis:

$$\cos\nu = \sqrt{\frac{l(l+1)}{n^2}} \tag{4.41}$$

$$\cos\Theta = \sqrt{\frac{m^2}{l(l+1)}}. \tag{4.42}$$

Note the similarity in these two equations, suggesting that m relates to l the same way that l relates to n, suggesting a four-dimensional generalization of the usual vector model of the atom which only describes the precession of $\boldsymbol{L}$ about the z-axis.

The results for orbits in configuration and momentum space illustrate some interesting features:

(1) Equation $ar = n$ illustrates that the characteristic dimensions of an orbit in the configuration space and the corresponding orbit in momentum space are inversely proportional, as expected, since they are related by a Fourier transform, consistent with the Heisenberg Uncertainty Principle.
(2) If $l = 0$, then there is no classical state. The orbit in configuration space degenerates into a line passing through the origin, while the corresponding circular orbit in momentum space attains an infinite radius and an infinite displacement from the origin. Although this seems peculiar from the pure classical viewpoint, quantum mechanically it follows that for S states there is a non-vanishing probability of finding the electron within the nucleus. S states are very important in the quantum mechanics of the hydrogen atom.

In order to interpret these statements about quantized semiclassical elliptical orbits we observe that for the quantum mechanical state of the hydrogen-like atom with definite n, l, m, the probability density, which is the square of the absolute value of the wave function, is (1) independent of ϕ_r or ϕ_p and (2) it does not confine the electron to some orbital plane. Since the quantum mechanical distribution for such a state specifies no preferred direction in the 1–2 plane, we must imagine this distribution as corresponding in some way to an average over all possible orientations of the semiclassical elliptical orbit. This interpretation is supported by the fact that the region within which the quantum mechanical radial distribution function differs largely from zero is included between the values of r corresponding to the semiclassical turning points $r_c(1 \pm \sin\nu)$.

4.7 Four-Dimensional Vector Model of the Atom

In configuration space or momentum space, the angle between the classical plane of the orbit and the z-axis is Θ, which is usually interpreted in terms of the vector model of the atom, in which we imagine $\boldsymbol{L}$ to be a vector of magnitude $\sqrt{l(l+1)}$ precessing about the z-axis, with m as the component along the z-axis as shown in Fig. 4.2.

This precession may be linked to the ϕ_r independence of the probability and the absence of an orbital plane, as mentioned at the end of the preceding section. The precession constitutes a classical mechanism that yields the desired average over all possible orientations of the semi-classical elliptical orbit. Since the angle Θ is restricted to have only certain discrete values, one can say that there is a quantization of space.

The expression for $\cos\nu = \sqrt{l(l+1)/n^2}$ is quite analogous to that for Θ, Eq. (4.42), and so suggests a generalization of the vector model of the atom to four dimensions. The projection of the four-dimensional vector model onto the physical three-dimensional subspace must give the usual vector model. We can achieve this by imagining that a four-dimensional vector of length n, where n is the principal quantum number, is precessing in such a way that its third and fourth components are constants, while the first and second components vary periodically. The projection onto the 1–2–3 hyperplane is a vector of constant magnitude $\sqrt{l(l+1)}$ precessing about the 3-axis (Fig. 4.3). The component along the 3-axis is m. The component along the 4-axis is $A = \sqrt{n^2 - l(l+1)}$ the magnitude of the vector $\boldsymbol{A}$. The vectors $\boldsymbol{L}$ and $\boldsymbol{A}$ are perpendicular to each other. Thus, the precessing $\boldsymbol{n}$ vector makes a constant angle Θ with the 3-axis and a constant angle

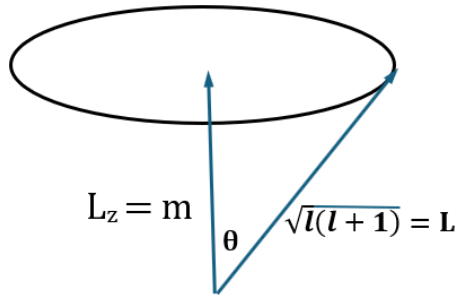

Fig. 4.2. Three-dimensional vector model of the atom. The angular momentum vector $\boldsymbol{L}$ precesses about the z-axis so the component in the z-direction is $L_z = m$.

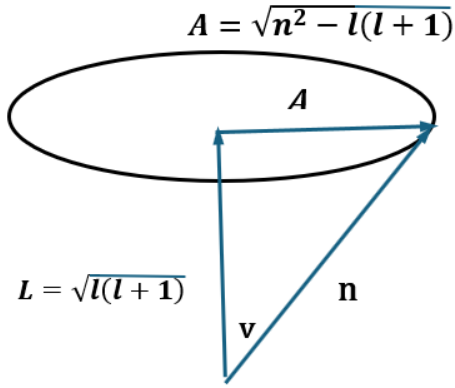

Fig. 4.3. Four-dimensional vector model of the atom. The vector representing the principal quantum number $\boldsymbol{n}$ precesses so that the vectors $\boldsymbol{L}$ and $\boldsymbol{A}$ are its components along the 3-axis and the 4-axis respectively.

$\pi/2 - \nu$ with the 4-axis. Since both angles are restricted to certain values, we may say that we have a quantization of four-dimensional space.

In the next chapter, we deal with the relativisitic Dirac hydrogen atom.

This page intentionally left blank

Chapter 5

The Dirac Hydrogen Atom: The Kepler Problem for a Relativistic Spinning Electron

We first discuss the conserved generalized parity operator introduced by Dirac and then derive and interpret the conserved pseudoscalar operator Λ, examining its non-relativistic limit. We present the symmetry group for the Dirac electron in a Coulomb potential.

5.1 Dirac's Generalized Parity Operator K_d

For a non-relativistic electron in a Coulomb field, the Pauli equation reduces to the Schrodinger equation

$$\left(\frac{p^2}{2m} - \frac{Z\alpha}{r} - E\right)\psi = 0 \tag{5.1}$$

and the scalar $\sigma \cdot \boldsymbol{L}$ is a constant on the motion. This suggests that there exists some conserved relativistic generalization of $\boldsymbol{\sigma} \cdot \boldsymbol{L}$ for the Dirac equation with the Hamiltonian[1]

$$H = \boldsymbol{\alpha} \cdot \boldsymbol{p} + \beta m - \frac{Z\alpha}{r}. \tag{5.2}$$

In order to investigate this possibility, we calculate the effect of $\boldsymbol{\sigma} \cdot \boldsymbol{L}$ on our four component Dirac spinors using the equation

$$\boldsymbol{J}^2 = \left(\boldsymbol{L} + \frac{\boldsymbol{\sigma}}{2}\right)^2 = j(j+1) = l(l+1) + \boldsymbol{\sigma} \cdot \boldsymbol{L} + \frac{3}{4}. \tag{5.3}$$

We know that either $j = l + 1/2$ or $j = l - 1/2$. Since the upper and lower components of the spinor have opposite parity, if $l = j - 1/2$ for

[1] We use the following conventions: $-i\gamma_5\boldsymbol{\sigma} = \boldsymbol{\alpha}$; $\gamma_\mu\gamma_\nu + \gamma_\nu\gamma_\mu = -2\delta_{\mu\nu}$; $\gamma^0 = \gamma_1\gamma_2\gamma_3\gamma_5$. It is convenient to use a direct product representation $\boldsymbol{\rho}\otimes\boldsymbol{\sigma}$ of the matrices. In the Dirac representation, we have $\gamma_5 = i\rho_1$, $\beta = \rho_3$, $\gamma_i = \rho_3\rho_1\rho_i$, where ρ_i and σ_i, $i = 1, 2, 3$ are two independent sets of Pauli spin matrices.

the upper component, then $l' = j + 1/2$ for the lower component and vice versa. Solving Eq. (5.3) for l equal to $j - 1/2$ and $j + 1/2$, we obtain the result

$$(\boldsymbol{\sigma} \cdot \boldsymbol{L} + l)\Psi(j,l) = \left(j + \frac{1}{2}\right) \begin{bmatrix} \psi_{j,l=j+\frac{1}{2}} \\ -\psi_{j,l=j-\frac{1}{2}} \end{bmatrix}$$
$$= \beta \left(j + \frac{1}{2}\right) \Psi(j,l), \tag{5.4}$$

where $\Psi(j,l)$ is a four-component Dirac spinor

$$\Psi(j,l) = \begin{bmatrix} \psi_{j,l=j+\frac{1}{2}} \\ \\ \psi_{j,l=j-\frac{1}{2}} \end{bmatrix}. \tag{5.5}$$

$\psi_{j,l}$ is a two-component spinor, and

$$\beta = \begin{pmatrix} 1 & 0 \\ 0 & -1 \end{pmatrix}. \tag{5.6}$$

If we multiply Eq. (5.4) by β and perform some simple manipulations, we obtain the following:

$$K_d \Psi(j,l) = (-1)^{l+j-1/2}(j + 1/2)\Psi(j,l) \tag{5.7}$$

with

$$K_d = \beta(\boldsymbol{\sigma} \cdot \boldsymbol{L} + 1). \tag{5.8}$$

In order to make the Dirac spinor an eigenspinor of K_d, which is the relativistic generalization of $\boldsymbol{\sigma} \cdot \boldsymbol{L}$, we had to insert a β because the upper and lower components have opposite parity. By an explicit calculation, we can show that

$$[K_d, H] = 0; \quad [K_d,\ \boldsymbol{J}] = 0, \tag{5.9}$$

so K_d is a conserved scalar. Another important feature of K_d is that its square is related to $\boldsymbol{J}^2$. If we operate on Eq. (5.7) with K_d or just square Eq. (5.8) and use the identity

$$\boldsymbol{\sigma} \cdot \boldsymbol{A}\boldsymbol{\sigma} \cdot \boldsymbol{B} = \boldsymbol{A} \cdot \boldsymbol{B} + i\boldsymbol{\sigma} \cdot \boldsymbol{A} \times \boldsymbol{B},$$

we find

$$K_d^2 = \boldsymbol{J}^2 + \frac{1}{4}. \tag{5.10}$$

It is useful to define a normalized operator

$$k = \frac{K_d}{j + 1/2}, \tag{5.11}$$

which obeys the equation

$$k\Psi(j,l) = (-1)^l(-1)^{j-1/2}\Psi(j,l) \equiv k'\Psi(j,l). \tag{5.12}$$

For fixed j, the operator k is proportional to the parity operator. The eigenvalues k' have been called the normality. The eigenstates are labeled k' and j (in addition to n and m). The two degenerate energy levels have the same n and j, but the eigenvalues k' are opposite in sign.

5.2 The Conserved Pseudoscalar Operator Λ

By definition, the operator Λ transforms one degenerate state into the other. Since the two states have opposite parities, Λ must have a parity equal to -1. In addition, since the two states have the same j, the operator must not change the angular momentum. Therefore, Λ is a pseudoscalar and obeys the following commutation relations

$$[\boldsymbol{J}, \Lambda] = 0; \;\; [H, \Lambda] = 0 \tag{5.13}$$

and the anticommutation relation

$$\{K_d, \boldsymbol{\Lambda}\} = 0. \tag{5.14}$$

Clearly, any conserved pseudoscalar constructed from the dynamical variables will be suitable. The pseudoscalar Λ will be unique up to a constant scalar function that commutes with Λ, namely, $f(H, \boldsymbol{J}^2)$. An essentially unique Λ is obtained if we require that

$$\Lambda^2 = 1.$$

This requirement means that Λ does not change the norm of the states and also specifies our phase convention. For $Z\alpha = 0$, there exists a conserved pseudoscalar, $\boldsymbol{\sigma} \cdot \boldsymbol{p}$, which, if normalized, would equal the helicity. Since K_d is a conserved scalar, it is possible to obtain another pseudoscalar constant by commutation:

$$[\boldsymbol{\sigma} \cdot \mathbf{p}, \; K_d] = \mathrm{i}\beta\boldsymbol{\sigma} \cdot (\boldsymbol{p} \times \mathbf{L} - \boldsymbol{L} \times \boldsymbol{p}). \tag{5.15}$$

By attempting to close the algebra of conserved quantities for $Z\boldsymbol{\alpha} = 0$, we have obtained a term equal to $(2ia)\beta\boldsymbol{\sigma} \cdot \boldsymbol{A}$, where $\boldsymbol{A}$ is the conserved

quantum mechanical Runge Lenz vector for $Z\alpha = 0$. This will be the first term in Λ. Since

$$\{\boldsymbol{\sigma} \cdot \boldsymbol{p}, K_d\} = 0,$$

we can write the left side of Eq. (5.15) as $2\boldsymbol{\sigma} \cdot \boldsymbol{p}\, K_d$. The term $\boldsymbol{\sigma} \cdot \boldsymbol{p}$ may be written in terms of the free Hamiltonian H_0:

$$H_0 = -i\gamma_5 \boldsymbol{\sigma} \cdot \boldsymbol{p} + \beta m. \tag{5.16}$$

Solving for $\boldsymbol{\sigma} \cdot \boldsymbol{p}$ gives

$$\boldsymbol{\sigma} \cdot \boldsymbol{p} = -i\gamma_5 (H_0 - \beta m). \tag{5.17}$$

If we follow the same procedure but use the Hamiltonian for $\mathrm{Z}\alpha \neq 0$ given in Eq. (5.2), we find

$$\boldsymbol{\sigma} \cdot \boldsymbol{p} + i\gamma_5 \frac{Z\alpha}{r} = -i\gamma_5 (H - \beta m). \tag{5.18}$$

Comparison of Eq. (5.17) and Eq. (5.18) suggests that when we turn on the electromagnetic interaction, we replace $\boldsymbol{\sigma} \cdot \boldsymbol{p}$ by $\boldsymbol{\sigma} \cdot \boldsymbol{p} + i\gamma_5 \frac{Z\alpha}{r}$. Thus, in analogy to Eq. (5.15), we compute the pseudoscalar

$$\left[\boldsymbol{\sigma} \cdot \boldsymbol{p} + i\gamma_5 \frac{Z\alpha}{r}, K_d\right] = 2\boldsymbol{\sigma} \cdot \boldsymbol{p} K + 2i\frac{2\alpha}{r}\gamma_5 K_d.$$

We find that the commutator of this pseudoscalar with H is a constant times $-im\ \frac{Z\alpha}{r}\gamma_5(\boldsymbol{\sigma} \cdot \boldsymbol{L} + 1)$. We must now find a term whose commuter with H will cancel this. From the quantum mechanical form of $\boldsymbol{A}$ (Eq. 2.2), we would expect Λ to contain a term similar to $2imZ\alpha\boldsymbol{\sigma} \cdot \frac{\boldsymbol{r}}{r}$ multiplied by 1 or β. Upon calculation, we find that the correct term does not contain the β. The final result for Λ is

$$\Lambda = \left[K_d, \boldsymbol{\sigma} \cdot \boldsymbol{p} + i\frac{Z\alpha}{r}\gamma_5\right] + 2imZ\alpha\boldsymbol{\sigma} \cdot \frac{\boldsymbol{r}}{r}$$

or, by using Eq. (5.18),

$$\Lambda = -2iK_d\gamma_5(H - \beta m) + 2imZ\alpha\boldsymbol{\sigma} \cdot \frac{\boldsymbol{r}}{r}.$$

To normalize Λ, we compute

$$\frac{\Lambda^2}{4} = -K_d^2\left(H^2 - m^2\right) - m^2(Z\alpha)^2. \tag{5.19}$$

Therefore, the normalized Δ is

$$\lambda = \frac{\Lambda}{|\Lambda|} = \frac{1}{\left[K_d^2\,(H^2 - m^2) + (mZ\alpha)^2\right]^{\frac{1}{2}}} \left[K_d\gamma_5(H - \beta m) - mZ\alpha\boldsymbol{\sigma}\cdot\frac{\boldsymbol{r}}{r}\right]. \tag{5.20}$$

This operator has been interpreted to be related to the conserved Runge–Lenz vector in the non-relativistic Schrodinger H atom [101].

5.3 The Symmetry Group of the Degenerate Levels

The normalized operators $\lambda = \Lambda/|\Lambda|$ and $k = K_d/|K_d|$ obey the following equations:

$$\lambda^2 = 1 \quad k^2 = 1 \quad \{k, \lambda\} = 0. \tag{5.21}$$

Therefore, the components of

$$\boldsymbol{\Sigma} = \frac{1}{2}(\lambda, -ik\lambda, k)$$

form an SU(2) algebra obeying the commutation relations

$$[\Sigma_i, \Sigma_j] = i\epsilon_{ijk}\Sigma_k.$$

Using our two degenerate levels as a basis, we may construct a matrix representation of the generators in terms of the Pauli matrices:

$$k = \begin{pmatrix} 1 & 0 \\ 0 & -1 \end{pmatrix} = \sigma_3, \quad k \text{ is like a parity operator in the subspace,}$$

$$\lambda = \begin{pmatrix} 0 & 1 \\ 1 & 0 \end{pmatrix} = \sigma_1, \quad \lambda \text{ interchanges the degenerate levels,}$$

$$-ik\lambda = \begin{pmatrix} 0 & -i \\ i & 0 \end{pmatrix} = \sigma_2, \quad \begin{matrix} -ik\lambda \text{ interchanges the levels} \\ \text{and multiplies by } -i \text{ times the parity.} \end{matrix}$$

Since the degree of degeneracy is always two for the Dirac hydrogen-like atom, we always have this two-dimensional representation of SU(2). The group structure here is the same as that of the isotopic spin group. Our two-dimensional representation of the group is equivalent to the two-dimensional representation of the isotopic spin group obtained by using a proton and a neutron as the basis states.[2]

[2]For the hydrogen-like atom degeneracy group, rotations for all angles have physical meaning. For the isotopic spin group, the same is not true. Although we may formally rotate from a neutron state to a proton state, no such intermediate states have been observed, nor are they allowed by superselection rules.

For the Dirac hydrogen-like atom, the conserved operators are $\boldsymbol{\Sigma}$ and $\boldsymbol{J}$. They are the elements of the complete degeneracy algebra

$$\begin{array}{ccccc} \mathrm{SU}(2) & & \bigotimes & & \mathrm{SU}(2) \\ \text{two-dimensional} & & & & (2j+1)\text{-dimensional} \\ \text{representation} & & & & \text{representation} \end{array} \tag{5.22}$$

This direct product representation SU(2)⊗SU(2) will be a subalgebra of the spectrum-generating algebra. If we label the representation by the Casimir operators of the two disjoint SU(2) groups, namely,

$$\begin{aligned} \boldsymbol{\Sigma}^2 &= \frac{1}{2}\left(1+\frac{1}{2}\right), \\ \boldsymbol{J}^2 &= j(j+1), \end{aligned}$$

then we have the $\left(\frac{1}{2}; j\right)$ representation. The degeneracy group corresponding to this is SO(4).

5.4 Calculation of Λ for the Pauli Hamiltonian with First-Order Relativistic Corrections

The expression for λ, Eq. (5.20), contains the Dirac Hamiltonian. We can approximate the Hamiltonian to obtain first-order corrections to λ. To obtain Λ to $O\left(m(Z\alpha)^4\right)$, we perform a Foldy–Wouthuysen transformation.[3] The Dirac Hamiltonian Eq. (5.2) may be transformed as follows:

$$\begin{aligned} H' &= UHU^{-1} \\ &= \beta m + \beta\frac{p^2}{2m} - \frac{Z\alpha}{r} + \frac{\pi Z\alpha}{2m^2}\delta(r) + \frac{Z\alpha}{4m^2}\frac{\boldsymbol{\sigma}\cdot\boldsymbol{L}}{r^3} + \frac{Z\alpha}{2m}\beta\gamma_5\boldsymbol{\sigma}\cdot\frac{\boldsymbol{r}}{r^3}, \end{aligned} \tag{5.23}$$

where

$$U = \exp\left(-\frac{i}{2m}\beta\gamma_5\boldsymbol{\sigma}\cdot\boldsymbol{p}\right).$$

[3] In order to determine the order of the terms, we note that in the non-relativistic domain $p \sim mcZ\alpha$, $r \sim 1/(mcZ\alpha)$.

A second unitary transformation eliminates the last term:

$$\begin{aligned} H'' &= VH'V^{-1} \\ &= \beta m + \beta\frac{p^2}{2m} + \beta\frac{p^4}{8m^3} - \frac{Z\alpha}{r} + \frac{Z\alpha}{4m^2}\frac{\boldsymbol{\sigma}\cdot\boldsymbol{L}}{r^3} + \frac{\pi Z\alpha}{2m^2}\delta(r) + 0\left(m(Z\alpha)^5\right), \end{aligned} \tag{5.24}$$

where

$$V = \exp\left(\gamma_5\boldsymbol{\sigma}\cdot\frac{\boldsymbol{r}}{r^3}\frac{Z\alpha}{4m^2}\right).$$

Executing the same transformation U on Λ yields[4]

$$\begin{aligned} \frac{\Lambda'}{2} &= U\frac{\Lambda}{2}U^{-1} \\ &= K_d\boldsymbol{\sigma}\cdot\boldsymbol{p} + imZ\alpha\boldsymbol{\sigma}\cdot\frac{\boldsymbol{r}}{r} + \frac{3}{4}\beta K_d\cdot\left\{\boldsymbol{\sigma}\cdot\boldsymbol{p}, \frac{Z\alpha}{r}\frac{1}{m}\right\} + 0\left(m(Z\alpha)^5\right). \end{aligned} \tag{5.25}$$

Transformation V changes Λ' by terms that are, at most, of order $m(Z\alpha)$.[5] Therefore,

$$\begin{aligned} \Lambda'' &= V\Lambda'V^{-1} \\ &= \Lambda' + 0\left(m(Z\alpha)^5\right). \end{aligned}$$

We may manipulate Eq. (5.25) into the form

$$\Lambda'' = \boldsymbol{\sigma}\cdot\boldsymbol{A}''(-2i),$$

where

$$\boldsymbol{A}'' = \beta\frac{(\boldsymbol{p}\times\boldsymbol{L} - \boldsymbol{L}\times\boldsymbol{p})}{2}\left(1 + \frac{3}{2}\frac{Z\alpha}{r}\frac{1}{m}\right) - mZ\alpha\frac{\boldsymbol{r}}{r}\left(1 + \frac{3}{4}\frac{1}{m^2}\beta K\frac{1}{r^2}\right). \tag{5.26}$$

To the order $m(Z\alpha)^2$, we see that $\boldsymbol{A}''$ is $\sqrt{-2mE}$ times the nonrelativistic quantum mechanical Runge–Lenz vector (Eq. 3.2). In the nonrelativistic limit, we might interpret this result in terms of the vector model of the atom. The vectors $\boldsymbol{L}$ and $\boldsymbol{S}$ precess about $\boldsymbol{J} = \boldsymbol{L} + \boldsymbol{S}$. If we visualize $\boldsymbol{A}$ as precessing about $\boldsymbol{J}$ with the same rotational frequency as $\boldsymbol{L}$ (and $\boldsymbol{S}$) and recall $\boldsymbol{L}\cdot\boldsymbol{A} = 0$, then we see that $\boldsymbol{J}\cdot\boldsymbol{A} = \frac{1}{2}\boldsymbol{\sigma}\cdot\boldsymbol{A}$ may be constant despite the fact that neither $\boldsymbol{A}$ nor $\boldsymbol{\sigma}$ are conserved separately (see Fig. 5.1).

[4]Note that K is unchanged by the transformations U and V.

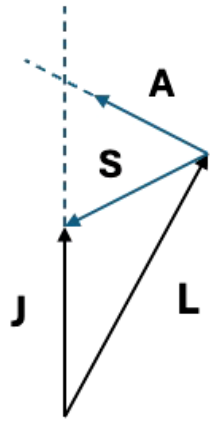

Fig. 5.1. Precession of $\boldsymbol{A}$, $\boldsymbol{S}$, and $\boldsymbol{L}$ about $\boldsymbol{J}$. Note that $\boldsymbol{L} \cdot \boldsymbol{A} = 0$.

In the next chapter, we introduce the non-invariance group SO(4,1), which is a representation of all the energy states of the non-relativistic H atom.

PART 2

The Coulomb Potential and Non-invariance Groups

Vast worlds lie within the
hollows of each atom
multifarious as the motes
in a sunbeam.
Yoga Vasistha
Ancient Indian Vaisesika treatise

In Part 1, we discussed the classical features and the symmetry operators of the hydrogen-like atom. We discussed the groups formed by these operators and the representations of the groups realized by the hydrogen-like atom. A summary of the results is given in Table 1.1 on page 21.

In Part 2, we consider the Schrodinger hydrogen-like atom and its unitary "non-invariance" operators $e^{iG_i\beta_i}$, where G_i is a generator and β_i is a real parameter, using eigenstates of $(Z\alpha)^{-1}$ for our basis. These operators transform an eigenstate of the Schrodinger kernel K (Eq. 3.25) with a definite value of the coupling constant (or principal quantum number) into a linear combination of eigenstates with different values of the coupling constant (or different principal quantum numbers).[1] Unlike the invariance operators $\boldsymbol{a}$ and $\boldsymbol{L}$, the non-invariance operators clearly do not commute with the kernel K:

$$[G_i, K] \neq 0.$$

The set of all invariance and non-invariance operators forms a group with which we may generate all eigenstates in our complete set from a given eigenstate. We show that this group, called the spectrum generating group of the hydrogen-like atom, is $\mathrm{SO}(4,1)$, the group of orthogonal transformations in a five-dimensional space with a metric $g_{AB} = (-1,1,1,1,1)$, $A, B = 0,1,2,3,4$.[2]

The complete set of eigenstates of $(Z\alpha)^{-1}$ for the hydrogen-like atom forms an irreducible infinite-dimensional representation of $\mathrm{SO}(4,1)$ which,

[1] Yossef Dothan, *Phys. Rev. D*, 2, 2944 (1970) has hypothesized that such operators may have explicit time dependence but are constant in time $\left(\frac{dG}{dt} i = 0\right)$. This hypothesis is equivalent to saying that G_i is a generator of a symmetry transformation of the time-dependent Schrodinger equation.

[2] $\mathrm{SO}(p,q)$ is the group of 'orthogonal' transformations that preserve the quantity

$$x = x_1^2 + x_2^2 + \cdots + x_p^2 - x_{p+1}^2 - \cdots - x_{p+q}^2.$$

The quantity x may be viewed as the norm of a $p+q$-dimensional vector in a space that has a metric with p plus signs and q minus signs. The letters SO stand for special orthogonal, meaning the orthogonal transformations have determinant equal to $+1$.

we shall find, is reducible into an infinite sum of irreducible representations of SO(4), each corresponding to the degeneracy group for a particular principal quantum number n.

In Chapter 6, the first chapter of Part 2, we introduce the non-invariance or spectrum generating group of the hydrogen atom SO(4,1), and discuss the generators of group transformations and relate them to the group of conformal transformations in momentum space. We evaluate the Casimir operators for SO(4,1).

In Chapter 7, the spectrum generating group SO(4,1) is expanded to SO(4,2) in order to be able to write Schrodinger's equation as an algebraic equation in terms of the group generators. All physical states together form a basis for a unitary irreducible representation of this non-invariance groups. We derive manifestly Hermitian expressions in terms of the momentum and position canonical variables for the additional generators of the group transformations and discuss the meaning of the generators. The values of the Casimir operators that characterize the group representation are calculated by considering the dynamical structure of the hydrogen-like atom. Some important group theory results are derived that will be used in the calculations of radiative shifts. We discuss the important subgroups of SO(4,2).

This page intentionally left blank

Chapter 6

The Spectrum Generating Group SO(4,1) for the Hydrogen-like Atom

We consider the Schrodinger hydrogen atom and its unitary "non-invariance" or spectrum generating operators $e^{iG_i\beta_i}$, where G_i is a generator and β_i is a real parameter, using eigenstates of $(Z\alpha)^{-1}$ for the basis of our representation. These operators transform an eigenstate of the kernel K (Eqs. 3.25, 3.34) with a definite value of the coupling constant (or principal quantum number) into a linear combination of eigenstates with different values of the coupling constant (or different principal quantum numbers) and different l and m. Unlike the invariance generators $\boldsymbol{L}$ and $\boldsymbol{A}$, the non-invariance generators clearly do not generally commute with the kernel K, $[G_i, K] \neq 0$, so they change the principal quantum number.

The set of all invariance and non-invariance operators forms a group with which we may generate all eigenstates in our complete set from a given eigenstate. We show that this group, called the spectrum generating group of the hydrogen-like atom, is SO(4,1), the group of orthogonal transformations in a five-dimensional space with a metric $g_{AB} = (-1, 1, 1, 1, 1)$, where $A, B = 0, 1, 2, 3, 4$. The complete set of eigenstates of $(Z\alpha)^{-1}$ for the hydrogen-like atom forms a unitary, irreducible, infinite-dimensional representation of SO(4,1) which, we shall find, can be decomposed into an infinite sum of irreducible representations of SO(4), each corresponding to the degeneracy group for a particular principal quantum number. A unitary representation means that all generators are unitary operators. An irreducible representation does not contain lower dimensional representations of the same group. In Section 6.3, we discuss the isomorphism between the spectrum generating group SO(4,l) and the group of conformal transformations in momentum space. An isomorphism means that the groups have the same structure and can be mapped to each other.

6.1 Motivation for Introducing the Spectrum Generating Group SO(4,1)

We examined the group structure for the degenerate eigenstates of $(Z\alpha)^{-1}$ for the Schrodinger hydrogen-like atom: the degenerate states n^2 form an irreducible representation of SO(4). The next question we might ask is: Do all or some of the states with different principal quantum numbers form an irreducible representation of some larger group which is reducible into SO(4) subgroups? If such a group exists, then it clearly is not an invariance group of the kernel K, as shown in Eq. (3.34):

$$\left(\frac{1}{n} - K(a)\right) \quad |nlm; a) = 0.$$

If we want our non-invariance group to include just some of the states then it can be a compact group, since unitary representations of compact groups can be finite dimensional. If we want to include all states, then it will be a non-compact group since there are an infinite number of eigenstates of $(Z\alpha)^{-1}$ and all unitary representations of non-compact groups are infinite dimensional [22].

We can find a compact non-invariance group for the first N levels of the coupling constant, $n = 1, 2, \ldots, N$. The dimensionality of our representation is

$$\sum_{n=1}^{N} n^2 = \frac{N(N+1)(2N+1)}{6}. \tag{6.1}$$

Mathematical analysis of the group SO(5) shows that this is the dimensionality of the irreducible symmetrical tensor representation of SO(5) given by the tensor with five upper indices $T^{abc\cdots}$, where $a, b, .. = 1, 2, 3, 4$ or 5 [24]. Reducing this representation of SO(5) into its SO(4) components gives

$$\begin{aligned}(\text{symm} \cdot \text{tensor} N)_{SO(5)} &= (0,0) \oplus \left(\frac{1}{2}, \frac{1}{2}\right) \oplus \ldots \quad \oplus \left(\frac{N-1}{2}, \frac{N-1}{2}\right) \\ &= (\text{symm} \ \cdot \ \text{tensor} \ n = 1)_{SO(4)} \oplus \\ &\quad (\text{symm} \ \cdot \text{tensor} \ n = 2)_{SO(4)} \oplus \\ &\quad \ldots \oplus \quad (\text{symm} \cdot \text{tensor} n = N)_{SO(4)},\end{aligned} \tag{6.2}$$

which is precisely the structure of the first N levels of a hydrogen-like atom. If we want to include all levels then we guess that the appropriate non-compact group is SO(4,1), whose maximal compact subgroup is SO(4). Thus, we conjecture that all states form a representation of SO(4,1).

Consider the Lie algebra of O(4,1) and the general structure of its generators in terms of the canonical variables. The matrices representing the rotations of O(n) are antisymmetric n × n matrices, with n(n − 1)/2 independent off-diagonal elements. Thus, the algebra of O(n) has n(n−1)/2 generators, and to extend the algebra of O(n) to O(n + 1), n additional generators are required, which can be taken as components of an n-vector. To extend the Lie algebra from O(4) to O(5) or O(4,1) we can choose the additional generators G_a to be components of a four-vector G under O(4). Assuming the generators of O(4) are S_{ab} then:

$$[S_{ab}, G_{\mathrm{c}}] = i(G_b\delta_{ac} - G_a\delta_{bc}) \quad a, b, c = 1, 2, 3, 4. \tag{6.3}$$

If we apply Jacobi's identity Eq. (1.7) to S_{ab}, G_a, and G_b and use Eq. (6.3) we find

$$[S_{ab}, [G_a, G_b]] = 0. \tag{6.4}$$

We require that the Lie algebra closes, so $[G_a, G_b]$ must be a linear combination of the generators, clearly proportional to S_{ab} and we choose the normalization such that

$$[G_a, G_b] = -iS_{ab}. \tag{6.5}$$

If we define

$$G_4 = S_{40} = S; \quad G_i = S_{i0} = B_i \tag{6.6}$$

and recall Eq. (3.4)

$$L_i = e_{ijk}S_{jk} \quad A_i = S_{i4}$$

then the additional commutation relations that realize SO(4,1) may be written in terms of $\boldsymbol{L}, \boldsymbol{A}, \boldsymbol{B}$, and S:

$$\begin{aligned} [L_i, B_j] &= i\epsilon_{ijk}B_{\mathrm{k}} & [L_i, S] &= 0, \\ [S, A_j] &= iB_j & [S, B_j] &= iA_j, \\ [A_j, B_k] &= i\delta_{jk}S & [B_i, B_j]. &= -i\epsilon_{ijk}L_k. \end{aligned} \tag{6.7}$$

The top two commutators show that $\boldsymbol{B}$ transforms as a three-vector under O(3) rotations and that S is a scalar under rotations. Alternatively we can write the commutation relations in terms of the generators S_{AB}, $A, B = 0, 1, 2, 3, 4$:

$$[S_{AB}, S_{CD}] = i(g_{AC}S_{BD} + g_{BD}S_{AC} - g_{AD}S_{BC} - g_{BC}S_{AD}), \tag{6.8}$$

where $g_{00} = -1, g_{aa} = 1$, where $a = 1, 2, 3, 4$.

The commutators above follow directly from the mathematical theory of SO(4,1), but the theory does not tell us what these generators represent, just their commutation properties. We now investigate the general features of the SO(4,1) representations provided by the hydrogen-like atom and how to represent the generators in terms of the canonical variables.

6.2 Casimir Operators

The two Casimir operators of SO(4,1) are [94, Chap. 11; 124]

$$Q_2 = -\frac{1}{2}S_{AB}S^{AB} = S^2 + \boldsymbol{B}^2 - \boldsymbol{A}^2 - \boldsymbol{L}^2, \tag{6.9}$$

and

$$Q_4 = -w_A w^A = (S\boldsymbol{L} - \boldsymbol{A}\times\boldsymbol{B})^2 - \frac{1}{4}[\boldsymbol{L}\cdot(\boldsymbol{A}+\boldsymbol{B}) - (\boldsymbol{A}+\boldsymbol{B})\cdot\boldsymbol{L}]^2, \tag{6.10}$$

where[3] $w_A = \frac{1}{8}\epsilon_{ABCDE}S^{BC}S^{DE}$

For SO(4), we recall that for the SO(4) representations the structure of the generators in terms of the canonical variables led to the vanishing of one Casimir operator $C_1 = \boldsymbol{L}\cdot\boldsymbol{A}$ and consequently to the appearance of only symmetrical tensor representations. We will find Q_4 vanishes for analogous reasons.

If $\boldsymbol{B}$ is a pseudovector, it is proportional to $\boldsymbol{L}$, which is the only independent pseudovector that can be constructed from the dynamical variables. The coefficient of proportionality, a scalar, X need not commute with H:

$$\boldsymbol{B} = X\boldsymbol{L} \quad [X,\boldsymbol{L}] = 0 \quad [X,H] \neq 0. \tag{6.11}$$

Since $[B_i, B_j] = -ie_{ijk}L_k$ it follows that $X^2 = -1$ and $\boldsymbol{B}$ would therefore be a constant multiple of $\boldsymbol{L}$ and not an independent generator. Thus, $\boldsymbol{B}$ must be a vector and expressible as a linear combination of the dynamical variables

$$\boldsymbol{B} = f\boldsymbol{r} + h\boldsymbol{p}, \tag{6.12}$$

where f and h are scalar functions of r, p^2, and $\boldsymbol{r}\cdot\boldsymbol{p}$. Accordingly, we find

$$\boldsymbol{B}\cdot\boldsymbol{L} = \boldsymbol{L}\cdot\boldsymbol{B} = 0. \tag{6.13}$$

[3]Here, ϵ is the anti-symmetric Levi-Civita tensor which has the value $+1 = \epsilon_{12345}$ and $+1$ for an even number of permutations and -1 for an odd number of permutations of the indices, and vanishes if any two indices are equal.

Further since $\boldsymbol{B}$ is a vector and $\boldsymbol{A}$ is a vector, $\boldsymbol{A} \times \boldsymbol{B}$ is a pseudovector and therefore is proportional to $\boldsymbol{L}$, the only independent pseudovector that can be constructed from the dynamical variables:

$$\boldsymbol{A} \times \boldsymbol{B} = Y\boldsymbol{L}, \quad [Y, \boldsymbol{L}] = 0, \tag{6.14}$$

where Y is scalar. For this equation to be consistent with the SO(4,1) commutation relations, we find $Y = S$ and therefore

$$\boldsymbol{A} \times \boldsymbol{B} = S\boldsymbol{L}. \tag{6.15}$$

It follows from $\boldsymbol{L} \cdot \boldsymbol{A} = 0$ and from Eqs. (6.13) and (6.15) that for the SO(4,1) representations realized by the hydrogen-like atom

$$Q_4 = 0. \tag{6.16}$$

As with the SO(4) symmetry, the dynamics of the hydrogen atom require that only certain representations of SO(4,1) appear. From the mathematical theory of irreducible infinite dimensional unitary representations of SO(4,1) we have the following results:

$$\begin{aligned} &\text{Class I:} \quad Q_4 = 0; \quad Q_2 \text{ real, } > 0 \\ &\qquad\qquad \text{SU(2) } \times \text{SU(2) content:} \qquad] \\ &(Q)^I = (0,0) \oplus \left(\frac{1}{2}, \frac{1}{2}\right) \oplus (1,1) \oplus \dots \end{aligned} \tag{6.17}$$

$$\begin{aligned} &\text{Class II: } Q_4 = 0, Q_2 = -(s-1)(s+2), s = \text{ integer } > 0 \\ &\qquad\qquad \text{SU(2)} \times \text{SU(2) content:} \\ &(Q)^{II} = \left(\frac{s}{2}, \frac{s}{2}\right) \oplus \left(\frac{s+1}{2}, \frac{s+1}{2}\right) \oplus \cdots \end{aligned} \tag{6.18}$$

The class I representations are realized by the complete set of eigenstates of $(Z\alpha)^{-1}$ for the hydrogen-like atom. Note, however, that we have an infinite number of such class I representations since Q_2 may have any positive real value. We shall find that for $Q_2 = 2$ we may extend our group from SO(4,l) to SO(4,2). The class II representations are realized by the eigenstates of $(Z\alpha)^{-1}$ with the principal quantum numbers from $n = s + 1$ to n becoming infinite. The first s levels could, if we choose, be described by SO(5).

In this section, we have analyzed the group structure and the representations using the complete set of eigenstates of $(Z\alpha)^{-1}$ for our basis. We might ask: What if we used energy eigenstates instead as a basis for the representations? From Section 3.4, we know that the quantum numbers

and multiplicities of the $(Z\alpha)^{-1}$ eigenstates are precisely the same as those of the bound energy eigenstates. Thus, with the energy eigenstates as our basis, we would reach the same conclusions about the group structure as before, but we would include only the bound states in our representations and we would be ignoring all scattering states.

6.3 Relationship of the Dynamical Group SO(4,1) to the Conformal Group in Momentum Space

We can give a more complete analysis of the hydrogen-like atom in terms of SO(4,1) by considering the relationship between the four-dimensional rotations of the four-vector U'_a with $a = 1, 2, 3, 4$, which we discussed in Section 3.5.1, and the group of conformal transformations in momentum space. Conformal transformations preserve the angles between directed curves, but not necessarily the lengths. The rotations generated by the Runge–Lenz vector $\boldsymbol{a}$ and the angular momentum $\boldsymbol{L}$ leave the scalar product $U_a V^a$ of four-vectors invariant and therefore are conformal transformations. The stereographic projection that we used is also a conformal transformation. Since the product of two conformal transformations is itself a conformal transformation, we must conclude that $\boldsymbol{a}$ generates a conformal transformation of the momentum three-vector $\boldsymbol{p}$.

In order to express the most general conformal transformation, we must introduce two additional operators that correspond to the operators $\boldsymbol{B}$ and S introduced in Section 6.1. Using the isomorphism between the generators $\boldsymbol{L}$, $\boldsymbol{a}$, $\boldsymbol{B}$, and S of SO(4,1) and the generators of conformal transformations in momentum space, we can immediately obtain expressions for the additional generators $\boldsymbol{B}$ and S in terms of the canonical variables, which is our objective. We need these additional generators to complete our SO(4,1) group for the hydrogen atom.

To derive the isomorphism we use the most convenient representation, namely that based on eigenstates of $(Z\alpha)^{-1}$ convenient for momentum space calculations $\left(\rho = \frac{(p^2+a^2)}{2a^2}\right)$. Once established, the isomorphism becomes a group theoretical statement and is independent of the particular representation.

The conformal group in momentum space

An arbitrary infinitesimal conformal transformation in momentum three-space may be written as

$$\delta p_j = \delta a_j + \delta\omega_{jk} p_k + \delta\rho p_j + \left(p^2 \delta c_j - 2p_j \boldsymbol{p}\cdot\delta\boldsymbol{c}\right) \tag{6.19}$$

where $\delta\omega_{jk} = -\delta\omega_{kj}$.

The terms in δp_j arise as follows:

$$\begin{array}{l} \delta a_j \text{ translation generated by} \boldsymbol{R}\cdot\delta\boldsymbol{a} \\ \delta\omega_{jk} \text{ rotation generated by } \boldsymbol{J}\cdot\delta\boldsymbol{\omega}, J_{ij} = \epsilon_{ijk}J_k \\ \delta\rho \text{ dilation generated by} D\delta\rho \\ \delta c_j \text{ special conformal transformation generated by } \boldsymbol{K}\cdot\delta\boldsymbol{c}. \end{array} \tag{6.20}$$

This is a 10 parameter group with the generators $(\boldsymbol{R}, \boldsymbol{J}, D, \boldsymbol{K})$ which obey the following commutation relations:

$$\begin{array}{ll} [D, R_j]\cdot = iR_j & [D, J_i] = 0 \\ [D, K_j] = -iK_j & [R_i, J_k] = i\epsilon_{ijk}R_k \\ [K_n, R_m] = 2i\epsilon_{nmr}J_r - 2i\delta_{mn}D & [J_i, J_k] = i\epsilon_{ikm}J_m \quad . \\ [R_i, R_j] = 0 & [K_i, J_k] = i\epsilon_{ikm}K_m \\ [K_j, K_j] = 0 & \end{array} \tag{6.21}$$

There is an isomorphism between the algebra of the generators of conformal transformations and the dynamical non-invariance algebra of SO(4,1) of the hydrogen atom. Since J_i is the generator of spatial rotations, we make the association $L_i = J_i$. Comparing the differential change in p_i from a transformation generated by $\boldsymbol{A}\cdot\delta\boldsymbol{\nu}$ (in the representation with $\rho = \frac{p^2+a^2}{2a^2}$, Eq. (3.49)

$$\begin{aligned} \delta p_i &= i\left[\boldsymbol{a}\cdot\delta\boldsymbol{\nu}, p_i\right] \\ &= -\frac{1}{2a}\left[\left(p^2 - a^2\right)\delta\nu_i - 2\boldsymbol{p}\cdot\delta\boldsymbol{\nu}p_i\right]. \end{aligned} \tag{6.22}$$

to the differential change in p_i from a special conformal transformation Eq. 6.19 leads to the association

$$a_i = \frac{1}{2}\left(\frac{K_i}{a} - aR_i\right). \tag{6.23}$$

To confirm the identification, we can use the commutation relations of the conformal group to show that the O(4) algebra of $\boldsymbol{L}$ and $\boldsymbol{a}$ corresponds precisely to that of $\boldsymbol{J}$ and $\frac{1}{2}(\frac{\boldsymbol{K}}{a} - a\boldsymbol{R})$. This correspondence in commutators indicates that the representation of $\boldsymbol{a}$ is valid whether we use $\rho = (p^2 + a^2)/2a^2$ or $\rho = n/(ar)$. The correspondence in commutators alone suggests that our SO(4) degeneracy group should be considered as a subgroup of the larger group SO(4,1). It suggests introducing the operators

$$\boldsymbol{B}(a) \equiv \boldsymbol{B} = \frac{1}{2}\left(\frac{\boldsymbol{K}}{a} + a\boldsymbol{R}\right) \qquad S = D. \tag{6.24}$$

The commutation relations of S and $\boldsymbol{B}$ which follow from Eq. (6.24) and from the commutation relations Eq. (6.21) are identical to the commutation relations given for S and $\boldsymbol{B}$ in Section 6.1. Thus, considering the $\boldsymbol{a}$ and $\boldsymbol{L}$ transformations in momentum space as conformal transformations, we were led to introduce the generators $\boldsymbol{B}$ and S and obtain the dynamical algebra SO(4,l). Further, we are led to the expressions for these generators in terms of the canonical variables.

By comparing the expression for $\boldsymbol{a}$ in terms of the conformal generators Eq. (6.23) with our known expressions for $\boldsymbol{a}$, Eq. (3.49) or Eq. (3.50), we obtain expressions for K_i and R_i in terms of the canonical variables. If we use the eigenstates convenient for configuration space calculations ($\rho = n/ar$) we make the identifications

$$\begin{aligned} \boldsymbol{K} &= \frac{1}{2}(\boldsymbol{r}p^2 + p^2\boldsymbol{r}) - \boldsymbol{r}\cdot\boldsymbol{p}\boldsymbol{p} - \boldsymbol{p}\boldsymbol{p}\cdot\boldsymbol{r} - \tfrac{\boldsymbol{r}}{4r^2}. \\ \boldsymbol{R} &= \boldsymbol{r}. \end{aligned} \tag{6.25}$$

Substituting these results in the equation for $\boldsymbol{B}$ we find

$$\boldsymbol{B} = \frac{1}{2a}\left(\frac{p^2\boldsymbol{r} + \boldsymbol{r}p^2}{2} - \boldsymbol{r}\cdot\boldsymbol{p}\boldsymbol{p} - \boldsymbol{p}\boldsymbol{p}\cdot\boldsymbol{r} - \frac{\boldsymbol{r}}{4r^2}\right) + \frac{a\boldsymbol{r}}{2}, \tag{6.26}$$

which is a manifestly Hermitean operator valid throughout Hilbert space. From Eqs. (6.23) and (6.24) we can show that

$$\boldsymbol{B} - \boldsymbol{a} = a\boldsymbol{r}. \tag{6.27}$$

To compute D we substitute the expressions for $\boldsymbol{K}$ and $\boldsymbol{R}$ into the commutation relation from Eq. (6.21)

$$D = \frac{i}{2}[K_i, R_i]$$

obtaining the result

$$D = \frac{1}{2}(\boldsymbol{p}\cdot\boldsymbol{r} + \boldsymbol{r}\cdot\boldsymbol{p}) = S, \tag{6.28}$$

which is identical to the generator of the scale change transformation $D(\lambda)$ defined in Eq. (3.37) in Section 3.4. S is defined in Eq. (6.6).

The significance of the generator $D = S$ of the scale change in terms of SO(4,1) is apparent if we compute

$$e^{i\lambda D}\left(a\boldsymbol{R} \pm \frac{\boldsymbol{K}}{a}\right)e^{-i\lambda D} = a'\boldsymbol{R} \pm \frac{\boldsymbol{K}}{a'}, \tag{6.29}$$

where $a' = e^{\lambda}a$.

The unitary transformation $e^{i\lambda D}$ can be viewed as generating an inner automorphism of SO(4,1) which is an equivalent representation of SO(4) characterized by a different value of the quantity a or the energy. In other words, under scale change $e^{i\lambda D}$, the basis states for our representation of SO(4,1), $|nlm;a)$, transform to a new set $|nlm;e^{\lambda}a)$ in agreement with our discussion in Section 3.3. The scale change also changes the operators; for example, the operator $B(a)$ changes in a corresponding manner

$$e^{i\lambda D}B(a)e^{-i\lambda D} = B(e^{\lambda}a). \tag{6.30}$$

Since the algebra of our generators closes, we may also view $e^{i\lambda D}$ as transforming a given generator into a linear combination of the generators. With the definitions of $\boldsymbol{a}$ and $\boldsymbol{B}$ (Eqs. (6.23) and (6.24)) we can easily show that (6.29), with the upper sign, can also be written

$$e^{i\lambda D}\boldsymbol{B}e^{-i\lambda D} = \boldsymbol{B}\,\cosh\lambda + \boldsymbol{a}\,\sinh\lambda. \tag{6.31}$$

Similarly, we have

$$e^{i\lambda D}\boldsymbol{a}e^{-i\lambda D} = \boldsymbol{B}\,\sinh\lambda + \boldsymbol{a}\,\cosh\lambda. \tag{6.32}$$

In Chapter 7, we will expand the group SO(4,1) to SO(4,2) to allow us to express Schrodinger's equation in terms of the generators of SO(4,2).

This page intentionally left blank

Chapter 7

The Group SO(4,2)

7.1 Motivation for Introducing SO(4,2)

We would like to express Schrodinger's equation as an algebraic equation in the generators of some group [50, 51]. As we cannot do this with our SO(4,l) generators S_{AB}, we expand the group again. To guide us, we recall that to expand SO(3) to SO(4) we added a three-vector of generators $\boldsymbol{A}$, and to expand SO(4) to SO(4,1) we added a four-vector of generators $(S, \boldsymbol{B})$. In both cases, this type of expansion produced a set of generators that were convenient for the study of the hydrogen-like atom. We guess that the appropriate expansion of SO(4,1) is obtained by adding a five-vector (under SO(4,1)) of generators Γ_A, $A = 0, 1, 2, 3, 4$, to obtain SO(4,2) [50, 51]. We can provide additional motivation for this choice by considering Schrodinger's equation. The generators in terms of which we want to express this equation must be scalars under L_i rotations since the energy levels do not depend on the orientation in space. Also we know $S = S_{40}$ (Eqs. (6.6) and (6.29)) generates scale changes of Schrodinger's equation. Since Γ_A is a five-vector under SO(4,1), it must satisfy the equation

$$[S_{AB}, \Gamma_C] = i(\Gamma_B g_{AC} - \Gamma_A g_{BC}). \tag{7.1}$$

The spatial components of Γ_A, which are $(\Gamma_1, \Gamma_2, \Gamma_3) = \boldsymbol{\Gamma}$, transform as a vector under rotations generated by $\boldsymbol{L}$.

To construct the Lie algebra of SO(4,2), we require that the set of operators $\{\Gamma_A, S_{AB}; A, B = 0, 1, 2, 3, 4\}$ must close under the operations of commutation. By applying Jacobi's identity, Eq. (1.7), to Γ_A, Γ_B, and S_{AB}, and requiring that Γ_A and Γ_B do not commute, we find

$$[S_{AB}, [\Gamma_A, \Gamma_B]] = 0 \quad A, B = 0, 1, 2, 3, 4.$$

Since we require our Lie algebra to close, the commutator of Γ_A and Γ_B must be proportional to S_{AB}. We normalize Γ so

$$[\Gamma_A, \Gamma_B] = -iS_{AB} \quad A, B = 0, 1, 2, 3, 4. \tag{7.2}$$

If we define

$$S_{A5} = \Gamma_A = -S_{5A} \quad A = 0, 1, 2, 3, 4. \tag{7.3}$$

and recall

$$A_i = S_{i4} \quad B_i = S_{io} \quad L_i = e_{ijk}S_{jk} \quad S = S_{40}$$

then we may unite all the commutation relations of Γ_A and S_{AB} in the single equation:

$$[S_{\mathcal{AB}}, S_{\mathcal{CD}}] = i(g_{\mathcal{AC}}S_{\mathcal{BD}} + g_{\mathcal{BD}}S_{\mathcal{AC}} - g_{\mathcal{AD}}S_{\mathcal{BC}} - g_{\mathcal{BC}}S_{\mathcal{AD}}), \tag{7.4}$$

where $\mathcal{A}, \mathcal{B}, \ldots, = 0, 1, 2, 3, 4, 5$ and $g_{00} = g_{55} = -1$; $g_{aa} = 1, a = 1, 2, 3, 4$.

These are the commutation relations for the Lie algebra of SO(4,2). In terms of $\boldsymbol{A}, \boldsymbol{B}, \boldsymbol{L}, S$ and Γ_A the additional commutation relations for the non-commuting generators are [66]:

$$\begin{array}{ll}
[B_i, \Gamma_j] = i\Gamma_0\delta_{ij} & [\Gamma_i, \Gamma_j] = -i\epsilon_{ijk}L_k \\
[A_i, \Gamma_j] = i\Gamma_4\delta_{ij} & [\Gamma_i, \Gamma_0] = -iB_i \\
[L_i,\ \Gamma_j] = i\epsilon_{ijk}\Gamma_k & [\Gamma_i, \Gamma_4] = -iA_i \\
 & [\Gamma_4, \Gamma_0] = -iS \\
[B_i, \Gamma_0] = i\Gamma_i & [A_i, \Gamma_4] = -i\Gamma_i \\
[S, \Gamma_0] = i\Gamma_4 & [S, \Gamma_4] = \ i\Gamma_0.
\end{array} \tag{7.5}$$

The fact that $S = S_{40}$ mixes the zero and four components of a five-vector suggests that Schrodinger's equation may be expressed in terms of the components Γ_0 and Γ_4, which are scalars under L_i, of the five-vector Γ_A.

7.2 Casimir Operators

The Lie algebra of SO(4,2) is rank three so it has three Casimir operators [56] W_2, W_3, and W_4:

$$W_2 = -\frac{1}{2}S_{\mathcal{AB}}S^{\mathcal{AB}} = Q_2 + \Gamma_A\Gamma^A, \tag{7.6}$$

where Q_2 is the non-vanishing SO(4,1) Casimir operator Eq. (6.9), and

$$W_3 = \epsilon^{\mathcal{ABCDEF}}S_{\mathcal{AB}}S_{\mathcal{CD}}S_{\mathcal{EF}} \tag{7.7}$$

$$W_4 = S_{\mathcal{AB}} S^{\mathcal{BC}} S_{\mathcal{CD}} S^{\mathcal{DA}}, \tag{7.8}$$

where $\mathcal{A}, \mathcal{B}, \mathcal{C}, \mathcal{D}, \mathcal{E}, \mathcal{F} = 0, 1, 2, 3, 4, 5$.

Computation of W_3

We can show that $W_3 = 0$ from dynamical considerations similar to those used in the discussion of SO(4,1) Casimir operators. The only terms that can be included in W_3 are scalars formed from products of three generators with different indices

$$\boldsymbol{B} \cdot \boldsymbol{A} \times \boldsymbol{\Gamma}, \quad \boldsymbol{A} \cdot \boldsymbol{\Gamma} \times \boldsymbol{B}, \quad \boldsymbol{\Gamma} \cdot \boldsymbol{B} \times \boldsymbol{A} \tag{7.9}$$

$$\Gamma_4 \boldsymbol{L} \cdot \boldsymbol{B}, \qquad \Gamma_0 \boldsymbol{L} \cdot \boldsymbol{A}, \qquad S\boldsymbol{\Gamma} \cdot \boldsymbol{L}. \tag{7.10}$$

It is interesting that these terms are actually all pseudoscalars. Terms such as $\boldsymbol{B} \cdot \boldsymbol{A} \times \boldsymbol{L}$ are simply not possible due to the structure of W_3, which requires that all terms contain $\boldsymbol{\Gamma}$ or a component of Γ. We know that $\boldsymbol{\Gamma} = (\Gamma_1, \Gamma_2, \Gamma_3)$ must not be a pseudovector, otherwise it would be proportional to $\boldsymbol{L}$ and therefore not an independent generator. Since it is a vector, it must be equal to a linear combination of $\boldsymbol{r}$ and $\boldsymbol{p}$. Therefore, we conclude

$$\boldsymbol{\Gamma} \cdot \boldsymbol{L} = \boldsymbol{L} \cdot \boldsymbol{\Gamma} = 0. \tag{7.11}$$

Since $\boldsymbol{\Gamma}$ and $\boldsymbol{B}$ are both vectors and $\boldsymbol{L}$ is the only pseudovector we have, we conclude $\boldsymbol{\Gamma} \times \boldsymbol{B} = \lambda \boldsymbol{L}$. In order to determine the scalar λ we evaluate the commutators

$$[B_k, (\boldsymbol{\Gamma} \times \boldsymbol{B})_k], \quad \text{and} \quad [\Gamma_k, (\boldsymbol{\Gamma} \times \boldsymbol{B})_k] \tag{7.12}$$

and find

$$\boldsymbol{\Gamma} \times \boldsymbol{B} = \Gamma_0 \boldsymbol{L} = -\boldsymbol{B} \times \boldsymbol{\Gamma}. \tag{7.13}$$

The analogous equations for $\boldsymbol{A}$ and $\boldsymbol{\Gamma}$, and for $\boldsymbol{A}$ and $\boldsymbol{B}$ are

$$\boldsymbol{\Gamma} \times \boldsymbol{A} = -\Gamma_4 \boldsymbol{L} = -\boldsymbol{A} \times \boldsymbol{\Gamma} \tag{7.14}$$

$$\boldsymbol{A} \times \boldsymbol{B} = S\boldsymbol{L} = -\boldsymbol{B} \times \boldsymbol{A}. \tag{7.15}$$

From Eqs. (7.14) and (7.15), we see that because of the dynamical structure of the generators, each of the quantities in Eq. (7.9) is proportional to the quantity directly below in Eq. (7.10). We have also shown that (Eqs. (3.2), (7.11), (6.13))

$$\boldsymbol{L} \cdot \boldsymbol{B} = \boldsymbol{L} \cdot \boldsymbol{A} = \boldsymbol{\Gamma} \cdot \boldsymbol{L} = 0. \tag{7.16}$$

Accordingly each scalar in our list vanishes and

$$W_3 = 0. \tag{7.17}$$

Computation of W_2

To compute W_2 we need to evaluate

$$\Gamma^2 \equiv \Gamma_A \Gamma^A = \Gamma_4^2 + \Gamma_i \Gamma^i - \Gamma_0^2. \tag{7.18}$$

From the structure of W_2 as shown in Eq. (7.6), we see that Γ^2 must be a number since W_2 and Q_2 are both Casimir operators and, therefore, numbers for a particular representation. Accordingly, we have

$$[\Gamma^2, \Gamma_A] = 0. \tag{7.19}$$

From this equation, we can deduce a lemma that allows us to easily evaluate W_2 and W_4 in terms of the number Γ^2. Using Eq. (7.19) and the definition of S_{AB} Eq. (7.2) we find

$$\Gamma^A S_{AB} + S_{AB} \Gamma^A = 0,$$

where, as usual, we are summing over repeated indices.

Contracting Eq. (7.1) with g_{AC} gives

$$S_{AB}\Gamma^A - \Gamma^A S_{AB} = 4i\Gamma_B.$$

Consequently, it must follow that

$$S_{AB}\Gamma^A = 2i\Gamma_B = -\Gamma^A S_{AB}. \tag{7.20}$$

We are now able to evaluate the quantity

$$S_{AB}S^B_{\ C} = iS_{AB}[\Gamma^B, \Gamma_C] = i(S_{AB}\Gamma^B\Gamma_C - S_{AB}\Gamma_C\Gamma^B).$$

Using Eq. (7.1) for the commutator of S_{AB} with Γ_C and Eq. (7.20) for the contraction $S_{AB}\Gamma^B$ we prove the lemma

$$S_{AB}S^B_{\ C} = 2iS_{CA} - \Gamma_A\Gamma_C + \Gamma^2 g_{AC}. \tag{7.21}$$

The value of the SO(4,1) Casimir operator $Q_2 = \frac{1}{2}g^{AC}S_{AB}S^B_{\ C}$ follows directly from the lemma:

$$Q_2 = 2\Gamma^2. \tag{7.22}$$

So, we have from Eq. (7.6)

$$W_2 = 3\Gamma^2. \tag{7.23}$$

Computation of W_4

The Casimir operator W_4 can be written as

$$W_4 = S_{\mathrm{A}\mathcal{B}}S^{\mathcal{B}\mathrm{C}}S_{C\mathcal{D}}S^{\mathcal{D}\mathrm{A}} + S_{\mathrm{A}\mathcal{B}}S^{\mathcal{B}5}S_{5\mathcal{D}}S^{\mathcal{D}\mathrm{A}} + S_{5\mathcal{B}}S^{\mathcal{B}\mathrm{C}}S_{\mathrm{C}\mathcal{D}}S^{\mathcal{D}5} + S_{5\mathcal{B}}S^{\mathcal{B}5}S_{5\mathcal{D}}S^{\mathcal{D}5}, \tag{7.24}$$

where we have two different fonts $\mathcal{B},\mathcal{D} = 0,1,2,3,4,5$ and $\mathrm{A},\mathrm{C} = 0,1,2,3,4$.

In order to evaluate W_4 in terms of Γ^2 we compute $S_{\mathrm{A}\mathcal{B}}S^{\mathcal{B}\mathrm{C}}$. Recalling $\Gamma_{\mathrm{A}} = S_{\mathrm{A}5}$ we see

$$S_{\mathrm{A}\mathcal{B}}S^{\mathcal{B}\mathrm{C}} = \Gamma_{\mathrm{A}}\Gamma^{\mathrm{C}} + S_{\mathrm{A}B}S^{B\mathrm{C}}. \tag{7.25}$$

Substituting the lemma Eq. (7.21), we find

$$S_{\mathrm{A}\mathcal{B}}S^{\mathcal{B}\mathrm{C}} = 2iS^{C}_{\ \mathrm{A}} - \Gamma^2 g_{A}^{\ \mathrm{C}}. \tag{7.26}$$

From Eq. (7.20), it follows that

$$S_{5\mathcal{B}}S^{\mathcal{B}\mathrm{C}} = 2i\Gamma^{\mathrm{C}}. \tag{7.27}$$

Substituting Eqs. (7.22), (7.25–7.27) into Eq. (7.24) for W_4 we find

$$W_4 = 6(\Gamma^2)^2 - 24\Gamma^2. \tag{7.28}$$

The fact that the non-vanishing Casimir operators (Q_2, W_2, and W_4) for SO(4,1) and SO(4,2) are given in terms of Γ^2 implies that the representation of SO(4,2) determines the particular representation of SO(4,l) appropriate to the hydrogen-like atom. In turn, the value of Γ^2 is determined by the structure of the Γs in terms of the canonical variables. In Section 7.4, we derive these structures and find that

$$\Gamma^2 = 1.$$

Therefore, the quadratic SO(4,1) Casimir operator Q_2 has the value

$$Q_2 = 2$$

and the SO(4,2) Casimir operators have the values:

$$W_2 = 3 \quad W_3 = 0 \quad W_4 = -18.$$

Researchers who have published different representations of SO(4,2) based on the hydrogen atom and that give their Casimir operators all have $W_2 = 3$ (or their equivalent) and $W_3 = 0$ [47, 91, 94], however, two authors have representations with $W_4 = 0$ [47, 94] and one [91] has $W_4 = -12$, compared to our value of -18.

From the mathematical theory of representations it follows that our representations of SO(4,1) and SO(4,2) are both unitary and irreducible.

This means that there is no subset of basis vectors that transform among themselves as SO(4,1) or as SO(4,2).

7.3 Some Group Theoretical Results

In this section, we derive the transformation properties of the SO(4,2) generators and then a novel contraction formula that will prove useful for situations in which we want to express the Schrodinger Hamiltonian, for example, in our calculation of the radiative shift for the hydrogen atom in Chapter 12. We will work primarily with the SO(4,2) generators expressed as the combination of the SO(4,1) generators S_{AB} and the five-vector Γ, with $g_{AB} = (-1, 1, 1, 1, 1)$, where $A, B = 0, 1, 2, 3, 4$.

Transformation properties of the generators

We can evaluate quantities like

$$^{AB}\Gamma_B(\theta) \equiv e^{iS_{AB}\theta}\Gamma_B e^{-iS_{AB}\theta} \quad \text{(no sum over A or B)} \tag{7.29}$$

by expanding the exponentials in an infinite series, and then using the commutation relations of the generators S_{AB} and Γ_A (Eq. 7.1), and the Γ_B (Eq. 7.2), repeatedly. However, it is easier to solve the differential equations satisfied by $^{AB}\Gamma_B$ and to use the appropriate boundary conditions. Differentiating Eq. (7.29) and using the commutation relations, we obtain the equations

$$\frac{d}{d\theta}\,{}^{AB}\Gamma_B = -g_{BB}\,{}^{AB}\Gamma_A \qquad \frac{d^2}{d\theta^2}\,{}^{AB}\Gamma_B = -g_{AA}g_{BB}\,{}^{AB}\Gamma_B, \tag{7.30}$$

which have the solution

$$^{AB}\Gamma_B = \Gamma_B \cos\sqrt{g_{AA}g_{BB}}\theta + \frac{g_{BB}}{\sqrt{g_{AA}g_{BB}}}\Gamma_A \sin\sqrt{g_{AA}g_{BB}}\theta. \tag{7.31}$$

Using a similar procedure we find

$$e^{i\Gamma_A\theta}S_{AB}e^{-i\Gamma_A\theta} = S_{AB}\cosh\sqrt{g_{AA}}\theta + \sqrt{g_{AA}}\Gamma_B \sinh\sqrt{g_{AA}}\theta \tag{7.32}$$

$$e^{i\Gamma_A\theta}\Gamma_B e^{-i\Gamma_A\theta} = \Gamma_B\cosh\sqrt{g_{AA}}\theta + \frac{1}{\sqrt{g_{AA}}}S_{AB}\sinh\sqrt{g_{AA}}\theta, \tag{7.33}$$

where no summation over A or B is implied.

These formulae, Eqs. (7.31–7.33), give the SO(4,2) transformation properties of the SO(4,2) generators.

The contraction formula

If we multiply Eq. (7.33) from the right by $e^{i\Gamma_A\theta}$ and then contract from the left with Γ_B, we obtain

$$\sum_B \Gamma^B e^{i\Gamma_A\theta}\Gamma_B = \left[(1-g_{AA}\Gamma_A^2)\cosh\sqrt{g_{AA}}\theta + \frac{2i\Gamma_A}{\sqrt{g_{AA}}}\sinh\sqrt{g_{AA}}\theta\right] e^{i\Gamma_A\theta} + g_{AA}\Gamma_A^2 e^{i\Gamma_A\theta}, \tag{7.34}$$

where we have used $\Gamma^2 = 1$ and Eq. 7.20. Expanding the hyperbolic functions in terms of exponentials and collecting terms gives

$$\sum_B \Gamma^B e^{i\Gamma_A\theta}\Gamma_B = \frac{1}{2}\left(1+\frac{i\Gamma_A}{\sqrt{g_{AA}}}\right)^2 e^{i(\Gamma_A - i\sqrt{g_{AA}})\theta} + \frac{1}{2}\left(1-\frac{i\Gamma_A}{\sqrt{g_{AA}}}\right)^2 e^{i(\Gamma_A + i\sqrt{g_{AA}})\theta} + g_{AA}\Gamma_A^2 e^{i\Gamma_A\theta}. \tag{7.35}$$

A Fourier decomposition of a function of Γ_A may be written

$$f(\Gamma_A) = \frac{1}{2\pi}\int d\theta h(\theta) e^{i\Gamma_A\theta}. \tag{7.36}$$

Consequently, we have

$$\sum_B \Gamma^B f(\Gamma_A)\Gamma_B = \frac{1}{2}\left(1+\frac{i\Gamma_A}{\sqrt{g_{AA}}}\right)^2 f(\Gamma_A - i\sqrt{g_{AA}}) + \frac{1}{2}\left(1-\frac{i\Gamma_A}{\sqrt{g_{AA}}}\right)^2 f(\Gamma_A + i\sqrt{g_{AA}}) + g_{AA}\Gamma_A^2 f(\Gamma_A). \tag{7.37}$$

By performing a suitable rotation, we can generalize this formula from functions of Γ_A to functions of $\Gamma_A n^A$ where $n_A n^A = \pm 1$. For $n^2 = -1$, we start with $\Gamma_A = \Gamma_0$ and rotate to obtain a very general result

$$\sum_B \Gamma_B f(n\Gamma)\Gamma^B = \frac{1}{2}(n\Gamma+1)^2 f(n\Gamma+1) + \frac{1}{2}(n\Gamma-1)^2 f(n\Gamma-1) - (n\Gamma)^2 f(n\Gamma), \tag{7.38}$$

where $n\Gamma = -n_0\Gamma_0 + n_i\Gamma_i + n_4\Gamma_4$.

We will have occasion to apply this formula for the special case

$$f(n\Gamma) = \frac{1}{\Gamma n - \nu}. \tag{7.39}$$

Using the representation

$$\frac{1}{\Gamma n - \nu} = \int_0^\infty ds e^{\nu s} e^{-\Gamma n s}, \tag{7.40}$$

we obtain the important result

$$\Gamma_A \frac{1}{\Gamma n - \nu} \Gamma^A = -2\nu \int_0^\infty ds\ e^{\nu s} \frac{d}{ds} \left(\sinh^2 \frac{s}{2} e^{-\Gamma n s} \right) \tag{7.41}$$

which is in a form convenient for calculations of radiative shifts.

Derivation of the Γ_A in terms of canonical variables

For our basis states we shall use eigenstates of $(Z\alpha)^{-1}$ convenient for configuration space calculations ($\rho = na/r$, Section 3.4.1). We choose these states rather than those convenient for momentum space calculations because they lead to simpler expressions for the Γ_A in terms of the canonical variables, although the expression for $\boldsymbol{a}$ is slightly more complicated. Our basis states must obey the equation of the energy eigenvalues or coupling constant Eq. 3.34

$$\left[\frac{1}{K_1(a)} - n \right] |nlm) = 0. \tag{7.42}$$

We know that K_1^{-1} must commute with the generators of the SO(4) symmetry group $\boldsymbol{a}_i = S_{i4}$ and $S_{ij} = \epsilon_{ijk} L_k$ because the kernel K_1 is a scalar that determines degenerate energy eigenstates. We expect that it is related to the five-vector $\boldsymbol{\Gamma}$ of generators that we added to go from SO(4,1) to SO(4,2). The only components of $\boldsymbol{\Gamma}$ that are scalars are Γ_0 and Γ_4. We choose

$$\Gamma_0 = [K_1(a)]^{-1} = \sqrt{ar} \frac{p^2 + a^2}{2a^2} \sqrt{ar} = \frac{1}{2} \left(\frac{\sqrt{r} p^2 \sqrt{r}}{a} + ar \right), \tag{7.43}$$

so that

$$(\Gamma_0 - n)|nlm) = 0. \tag{7.44}$$

This last equation is the Schrodinger equation expressed in our language of SO(4,2): our states $|nlm)$ are eigenstates of Γ_0 with eigenvalue n.

To find Γ_4, we calculate $\Gamma_4 = -i[S, \Gamma_0]$, using Eq. (6.28) for S, we find

$$\Gamma_4 = \sqrt{ar}\frac{p^2 - a^2}{2a^2}\sqrt{ar} = \frac{1}{2}\left(\frac{\sqrt{r}p^2\sqrt{r}}{a} - ar\right). \tag{7.45}$$

Sometimes it is convenient to use the linear combinations

$$\Gamma_0 - \Gamma_4 = ar \quad \Gamma_0 + \Gamma_4 = \frac{\sqrt{r}p^2\sqrt{r}}{a}, \tag{7.46}$$

which can be used to express the dipole transition operator [46].

We can find Γ_i from Eq. (7.5), $\Gamma_i = -i[B_i, \Gamma_0]$, where B_i is from Eq. (6.26):

$$\Gamma_i = \sqrt{r}p_i\sqrt{r}, \tag{7.47}$$

which we might initially have guessed since $[\Gamma_i, \Gamma_j] = -i\epsilon_{ijk}L_k$ and $[rp_i, rp_j] \sim L_k$. Every component of Γ_A is Hermitean; consequently, the generators S_{AB} that are given by the commutators Eq. (7.2) are also Hermitian. We may explicitly verify that these expressions for Γ_A lead to a consistent representation of all generators in the SO(4,2) Lie algebra.

Under a scale change generated by S, Γ_i is invariant and Γ_4 and Γ_0 transform in the same manner as $\boldsymbol{a}$ and $\boldsymbol{B}$ (Eq. 6.29): they retain their form but a is transformed into $e^{\lambda}a$:

$$e^{i\lambda S}\left\{\begin{matrix}\Gamma_0\\ \Gamma_4\end{matrix}\right\}e^{-i\lambda S} = \frac{1}{2}\left(\frac{\sqrt{r}p^2\sqrt{r}}{e^{\lambda}a} \pm e^{\lambda}ar\right). \tag{7.48}$$

The scale change generates an inner automorphism of SO(4,2) characterized by a different value of the parameter a.

7.4 Subgroups of SO(4,2)

The two most significant subgroups are generated by [66]:

1. L_i, a_i or S_{jk}, S_{i4}, forming an SO(4) subgroup. These generators commute with Γ_0 and therefore constitute the degeneracy group for states of energy $-a^2/(2m)$ and fixed principal quantum number n (or fixed coupling constant na/m). The Casimir operator for this subgroup is

$$\boldsymbol{a}^2 + \boldsymbol{L}^2 = n^2 - 1 = \Gamma_0^2 - 1. \tag{7.49}$$

We discussed this subgroup in Section 3.2 in terms of $\boldsymbol{L}$ and $\boldsymbol{A}$ and the states $|nlm\rangle$. The same results are obtained with the generators $\boldsymbol{L}$ and

$\boldsymbol{a}$ with the states $|nlm)$. For example, we have the raising and lowering operators for m and l (Eqs. 3.21, 3.22). With the definition

$$L_\pm = L_1 \pm iL_2, \tag{7.50}$$

it follows that

$$[L_3, L_\pm] = \pm L_\pm, \tag{7.51}$$

which gives

$$L_\pm|nlm) = \sqrt{(l(l+1) - m(m\pm 1)}|nl\ m\pm 1) \qquad L_3|nlm) = m|nlm). \tag{7.52}$$

for $l \geq 1$. In analogy to $L_\pm$ one can define

$$a_\pm = a_1 \pm ia_2, \tag{7.53}$$

which obey the relations

$$[a_3, a_\pm] = \pm L_3 \qquad [L_3, a_\pm] = \pm a_\pm \tag{7.54}$$

and

$$a_\pm|nlm) = \mp \left(\frac{(n^2-(l+1)^2)(l+2\pm m)(l+1\pm m)}{4(l+1)^2-1}\right)^{\frac{1}{2}} |nl+1m\pm 1) \tag{7.55}$$

$$\pm \left(\frac{(n^2-l^2)(l\mp m)(l-1\mp m)}{4l^2-1}\right)^{\frac{1}{2}} |nl-1m\pm 1) \tag{7.56}$$

for $l \geq 1$. The action of $a_\pm$ is not directly analogous to that of $L_\pm$ in Eq. (3.21) because we are using $|nlm)$ as basis states. If we used $|na_3l_3 = m)$ as basis states, the action would be similar. An operator that changes only the angular momentum is a_3

$$a_3|nlm) = \left(\frac{(n^2-(l+1)^2)((l+1)^2-m^2)}{4(l+1)^2-1}\right)^{\frac{1}{2}} |nl+1m)$$

$$+ \left(\frac{(n^2-l^2)(l^2-m^2)}{4l^2-1}\right)^{\frac{1}{2}} |nl-1m) \tag{7.57}$$

for $l \geq 1$. Since a_3 commutes with L_3 and Γ_0, it does not change n or m.

2. Γ_4, $S = S_{40}$, Γ_0, forming a SO(2,1) subgroup. These operators commute with $\boldsymbol{L}$ but not with Γ_0, hence then can change n but not $\boldsymbol{L}$

or m. The Casimir operator for this subgroup is[1]

$$\Gamma_0^2 - \Gamma_4^2 - S^2 = \boldsymbol{L}^2 = l(l+1). \tag{7.58}$$

We can define the operators [66]

$$j_1 = \Gamma_4 \qquad j_2 = S \qquad j_3 = \Gamma_0 \tag{7.59}$$

with commutators

$$[j_1, j_2] = -ij_3 \quad [j_2, j_3] = ij_1 \quad [j_3, j_1] = ij_2. \tag{7.60}$$

We can define the raising and lowering operators

$$j_\pm = j_1 \pm ij_2 = \Gamma_4 \pm iS, \tag{7.61}$$

which obey the commutation relations

$$[j_\pm, j_3] = \mp j_\pm. \tag{7.62}$$

We find (in analogy to Eq. 7.52)

$$\Gamma_0|nlm) = n|nlm) \quad (\Gamma_4 \pm iS)|nlm) = \sqrt{n(n\pm 1) - l(l+1)}|n \pm 1\ lm) \tag{7.63}$$

We can express the action of $\Gamma_0 - \Gamma_4 = ar$ on our states

$$\begin{aligned} ar|nlm) = \frac{1}{2}((n)(n-l) - l(l+1))^{\frac{1}{2}}|n-1\ lm) \ + n|n\, lm) \\ + \frac{1}{2}((n)(n+l) - l(l+1))^{\frac{1}{2}}|n+1\ lm). \end{aligned} \tag{7.64}$$

As mentioned previously, the operator S generates scale changes as shown in Eq. (6.29), where the value of a is changed. We can also express the action of S equivalently as transforming Γ_0 into Γ_4, as suggested by Eq. (6.31):

$$e^{iS\lambda}\Gamma_0 e^{-iS\lambda} = \Gamma_0 \cosh\lambda - \Gamma_4 \sinh\lambda, \tag{7.65}$$

$$e^{iS\lambda}\Gamma_4 e^{-iS\lambda} = \Gamma_4 \cosh\lambda - \Gamma_0 \sinh\lambda. \tag{7.66}$$

[1] To prove this note that $\boldsymbol{L}^2 = (\boldsymbol{r}\times\boldsymbol{p})^2 = r^2p^2 - r^2p_r^2$ where $p_r = (1/2)(\frac{\boldsymbol{r}}{r}\cdot\boldsymbol{p} + \boldsymbol{p}\cdot\frac{\boldsymbol{r}}{r})$ and $[r, p_r] = i$. Thus $\boldsymbol{L}^2 = r^2p^2 - rp_rrp_r - irp_r$. But $\boldsymbol{L}^2 = (1/\sqrt{r})\boldsymbol{L}^2\sqrt{r}$ and $S_{04} = -\sqrt{r}p_r\sqrt{r}$ so it follows that $\boldsymbol{L}^2 = (\Gamma_0 - \Gamma_4)(\Gamma_0 + \Gamma_4) - SO_{04}^2 - iS_{04}$ which gives the result quoted.

7.5 Time Dependence of SO(4,2) Generators

For a generator to be constant it must commute with the Hamiltonian as discussed in Section 2.1. Since the SO(4,2) group is the non-invariance or spectrum generating group, the additional generators do not all commute with the Hamiltonian. It is notable that as far as we know only one paper considers the time dependence of the generators of non-invariance groups in general and one briefly considers SO(4,2) specifically [107, 139]. Our results certainly clarify and make explicit the time dependence and show that it is just a particular aspect of the SO(4,2) transformations. In our representation $|nlm;a)$, the Hamiltonian has been transformed into Γ_0 and the Schrodinger energy eigenvalue equation has become $\Gamma_0|nlm) = n|nlm)$. Accordingly, all generators that commute with Γ_0 are constants of motion, including $\boldsymbol{a}$, $\boldsymbol{L}$. The other operators $\boldsymbol{B}, \boldsymbol{\Gamma}, S, \Gamma_4$ have a time dependence given by Eqs. (7.32) and (7.33), for example

$$S(t) = e^{iHt}S(0)E^{-iHt} = e^{i\Gamma_0 t}Se^{-i\Gamma_0 t} = S\cos t + \Gamma_4 \sin t \tag{7.67}$$

$$\Gamma_4(t) = e^{iHt}\Gamma_4(0)E^{-iHt} = e^{i\Gamma_0 t}\Gamma_4 e^{-i\Gamma_0 t} = \Gamma_4 \cos t - S\sin t. \tag{7.68}$$

Consequently, terms like $j_\pm$ (Eq. 7.61) have a simple exponential time dependence

$$j_\pm(t) = j_\pm(0)e^{\pm it}. \tag{7.69}$$

Similarly, $\boldsymbol{\Gamma} \pm i\boldsymbol{B}$ has an exponential time dependence.

7.6 Expressing the Schrodinger Equation in Terms of the Generators of SO(4,2)

We can write the Schrodinger equation for the usual energy eigenstate $|nlm\rangle$ with energy $E_n = -a_n^2/2m$ of a particle in a Coulomb potential in terms of SO(4,2) generators. Since the generators are in terms of energy $-a^2/2m$, we need to make a scale change. From Section 3.4, Eq. (3.42), the relationship between the Schrodinger energy eigenstate $|nlm\rangle$ and the eigenstate $|nlm)$ of $(Z\alpha)^{-1}$ is

$$|nlm;a) = e^{-iS\lambda_n}\sqrt{\rho(a_n)}|nlm\rangle, \tag{7.70}$$

where

$$e^{\lambda_n} = \frac{a_n}{a} \quad \rho(a_n) = \frac{n}{a_n r}. \tag{7.71}$$

Substituting Eq. (7.70) in the eigenvalue equation Eq. (7.44) for $|nlm;a)$ and employing the transformation Eqs. (7.65) and (7.66), we find the usual

Schrodinger equation can be expressed in SO(4,2) terms as

$$(\Gamma n - n)\sqrt{\rho(a_n)}|nlm\rangle = 0, \tag{7.72}$$

where

$$\Gamma n \equiv \Gamma_A n^A = \Gamma_0 n^0 + \Gamma_i n^i + \Gamma_4 n^4 \tag{7.73}$$

$$n^o = \cosh\lambda_n = \frac{a^2 + a_n^2}{2aa_n}\,, \quad n^i = 0, \quad n^4 = -\sinh\lambda_n = \frac{a^2 - a_n^2}{2aa_n} \tag{7.74}$$

and $n_A n^A = n_4^2 - n_0^2 = -1$.

Equation (7.72) expresses Schrodinger's equation for an ordinary energy eigenstate $|nlm\rangle$ with energy $E_N = -a_n^2/2m$ in the language of SO(4,2). It shows the relationship between these energy eigenstates and the basis states of $(Z\alpha)^{-1}$ that are used for the SO(4,2) representation.

The next chapter, the first in Part 3, deals with radiative shifts in classical and quantum systems.

This page intentionally left blank

PART 3

Radiative Level Shifts

The hydrogen atom is the
fundamental two-body system
and perhaps the most important
tool of physics; years after the Bohr theory
the challenge is still there to calculate
its properties to the highest accuracy possible.
Stanley Brodsky

Radiation is a process common to classical and quantum systems with very different effects in each regime. In a quantum system, the interaction of a bound electron with its own radiation field leads to complex shifts in the energy levels of the electron, with the real part of the shift corresponding to a shift in the energy level and the imaginary part to the width of the energy level. The most celebrated radiative shift is the Lamb shift between the $2s_{1/2}$ and the $2p_{1/2}$ levels of the hydrogen atom. The measurement of this shift in 1947 by Willis Lamb Jr. and his graduate student Robert Rutherford proved that the prediction by Dirac theory that the energy levels were degenerate was incorrect.

Hans Bethe's calculation of the shift demonstrated that the renormalization process, suggested by Kramers, was required to deal with the divergences plaguing the existing theories and led to the understanding that interactions of the electron with its own radiation field needed to be considered. it was also becoming clear that interactions with the zero-point vacuum field, the lowest energy state of the quantized electromagnetic field, needed to be considered since it has measurable effects, for example, the Lamb shift and the Casimir force, not just resetting the zero of energy. Understanding the calculation of these effects led to the birth of modern quantum electrodynamics (QED). Other calculations of the Lamb shift followed by Welton and Power in an effort to clarify the physical mechanisms leading to the shift.

We explore the history of Bethe's calculation and its significance. We discuss radiative effects in classical and quantum systems from different perspectives, with the emphasis on understanding the fundamental physical phenomena. Illustrations are drawn from systems with central forces: the H atom, and the three-dimensional harmonic oscillator.

A first-order QED calculation of the complex radiative shift for a spinless electron is presented based on the $mass^2$ operator and the non-relativistic approximation of the Klein–Gordon equation. No other assumptions are made. We employ a SO(4,2) group theoretical approach, which gives the

shift as an integral over frequency of a function, which we call a shift spectral density. The shift spectral density reveals how different frequencies contribute to the total energy shift. We find, for example, that half the radiative shift for $N = 1$ level in H comes from photon energies below 9700 eV, and that the expressions by Power and Welton do not have the correct low frequency behavior, although they do give the correct value for the total shift.

The shift of atomic energy levels from the levels given by the Dirac or Klein–Gordon equations with the appropriate potentials results from effects radiative shift that can be classified into four groups [2, 95, 128, 149–158]:

(1) The interaction of the bound particle with its own radiation field.
(2) Vacuum polarization effects.
(3) Finite nuclear mass effects, including relativistic recoil corrections.
(4) Nuclear structure effects, including finite size and polarization corrections, and the interaction of the nuclear magnetic moment with the magnetic field of the electron.

The most frequently discussed and measured shift in energy levels is the celebrated Lamb shift between the $2s_{1/2}$ and $2p_{1/2}$ levels in the hydrogen atom. Although measurements of the shift were attempted in the 1930s, it was not measured accurately until 1947 when Lamb and Retherford employed rf spectroscopy and exploited the metastability of the $2s_{1/2}$ level and determined that the shift was approximately 1050 MHz, or 1 part in 10^6 of the $2s_{1/2}$ level [18, 159–162]. Shortly thereafter Bethe [19] published a non-relativistic quantum theoretical calculation of the shift assuming that it was due to the interaction of the electron with a radiation field. Bethe did not state in his paper whether the source of the radiation field leading to the radiative shift was the quantum fluctuations of the vacuum field or the radiation field of the atom. Both fields had been proposed as leading to the shift in the self energy of the electron. For example Weisskopf had proposed that the vacuum field contributed to the self energy of the electron in the H atom. Indeed, to first order the fields are equivalent. Several researchers tend to believe Bethe meant the radiation fields of the atom. Welton and Feynman provided explanations of the Lamb shift in terms of interactions with the quantum vacuum field.

This lowest order radiative shift (to $\alpha(Z\alpha)^4$) accounts for about 96% of the measured shift. As the years passed, the calculation was refined and the effects (2), (3), and (4) were included. New measurements were made and old data were reanalyzed. There are many articles on these

TABLE 1

VARIOUS CONTRIBUTIONS TO THE LAMB SHIFT IN H – $2S_{\frac{1}{2}} - 2P_{\frac{1}{2}}$

	DESCRIPTION	ORDER	MAGNITUDE (MHz)
1.	Radiative shift		
	2^{nd} ORDER	$\alpha(Z\alpha)^4 m\{\log Z\alpha, 1\}$	$1079.32 \pm .02$
	$(\alpha^{-1} = 137.0361)$	$\alpha(Z\alpha)^5 m$	7.14
		$\alpha(Z\alpha)^6 m\{\log^2 Z\alpha, \log Z\alpha, 1\}$	$-\ 0.38 \pm .04$
	4^{th} ORDER	$\alpha^2(Z\alpha)^4 m \begin{cases} F_1(0) \\ F_2(0) \end{cases}$	$.45 \pm .07$ $-\ 0.10$
		$\alpha^2(Z\alpha)^5 m$	$\pm .02$
2.	Vacuum polarization		
	2^{nd} ORDER	$\alpha(Z\alpha)^4 m$	$-\ 27.13$
	4^{th} ORDER	$\alpha^2(Z\alpha)^4 m$	$-\ 0.24$
3.	Finite nuclear mass		
	REDUCED MASS CORRECTIONS	$\alpha(Z\alpha)^4 \frac{m}{M} m \log\{Z\alpha, 1\}$	$-\ 1.64$
	RECOIL	$(Z\alpha)^5 \frac{m}{M} m \log\{Z\alpha, 1\}$	$0.36 \pm .01$
4.	Nuclear structure		
	PROTON SIZE	$(Z\alpha)^4 (mR_N)^2 m$	0.13
		total	$1057.91 \pm .16$

Fig. 1. Approximate Contributions to the Lamb Shift.

calculations, so we limit ourselves to giving a few general references and a few recent references [2, 157, 158, 163–168]. In this text, we deal with only the dominant radiative component of the shift.

Table 1 gives a summary of the approximate theoretical values for the contribution to the Lamb shift from the different effects.

The agreement between theory and experiment has varied over the last 70 years, indicating the complexity of the theoretical calculation and the difficulties in the experimental measurements. The difference in the values for the Lamb shift obtained from theory and experiment has reflected many things: that not all physical effects were accounted for, that higher order terms had to be included, that errors were made in the calculations, that the accepted value of the fine structure constant changed, that experimental results were reinterpreted, that the radius of the proton was needed. Today, after decades of concerted effort, the agreement is phenomenal, one of the most precise of any in the physical sciences, to 13 decimal places [1].

We discuss the radiative shift of a particle that is in a bound energy eigenstate from various viewpoints.

In Chapter 8, we review some of the history of the Lamb shift and discuss radiative effects in classical physics. We discuss Bethe's calculation, and its significance for QED. We clarify the physical meaning of the radiative shifts that appear in field theory by explaining the effects of the zero-point vibrations of the electromagnetic field in a semiclassical analysis. We express the radiative shift as the difference in the energy of the particle when freely oscillating in the zero-point field and when oscillating in the zero-point field while bound in a potential. We consider the radiative shift in the language of field theory: the shift equals the change in the mass renormalization of the particle that occurs when it becomes bound.

In Chapter 9, we discuss radiative effects in classical physics and quantum physics for central force potentials, and illustrate with two examples, the Coulomb potential and the 3D isotropic harmonic potential. We try to provide an intuitive sense of radiative shifts that appear in field theory by considering the effects of the zero-point fluctuations of the electromagnetic field in a semiclassical analysis of the motion of a bound particle. We discuss the general nature of radiative shifts, for example, that the presence of a boundary can lead to a radiative shift.

In Chapter 10, we consider the radiative shift in the language of field theory: the shift equals the change in the mass renormalization of the particle that occurs when it becomes bound. The approach reflects Bethe's interpretation of the divergences he encountered. We derive an expression for the complex shift in terms of matrix elements of the $mass^2$ operator M^2, which corresponds to the total self-energy squared of the bound particle. Using the equations of motion for a relativistic scalar particle in a potential, we derive an expression for M^2 to order α in the radiation field, i.e. assuming that only one radiation field photon is exchanged. We also consider the requirements for gauge invariance in our expressions for a physical shift.

In Chapter 11, we consider the radiative level shifts in the non-relativistic dipole approximation, demonstrating that the shift is complex: the imaginary part corresponds to the width for decay by dipole emission and the real part corresponds to the displacement of the energy level.

We show that the real and imaginary parts satisfy a dispersion relation, which is fundamentally just an expression of causality [169]. We interpret the radiative shift as due to the virtual transitions induced by the interaction of the particle with its own radiation field. This interaction means that a given energy level has a finite width and that the mean energy of the initial state of the system, averaged over time, is shifted.

In Chapters 11 and 12, we derive integral expressions for the complete radiative shifts for semi-relativistic spinless mesons in our two potentials as functions of the coupling constants, rather than developing a perturbation expansion as is customary. Our semi-relativistic approximation is to drop the V^2 term in the Klein–Gordon equation, thereby ensuring that we have the same group structure as in the non-relativistic problem (Chapter 7).

In Chapter 12, we use the group theory of SO(4,2) to determine the radiative shifts in energy levels for a spinless electron in a Coulomb potential due to its interaction with its own radiation field, or equivalently with the quantum vacuum. In the non-relativistic or dipole approximation the level shift contains a matrix element of a rotation operator of an O(1,2) subgroup of the group SO(4,2). We can sum this over all states, obtaining the character of the representation, yielding a single integral which is a generating function for the radiative shift for any level in the non-relativistic or dipole approximation. The integral is an analytic expression for the level shift. A brief conclusion follows.

In Chapter 13, we compute the radiative shift for a spinless relativistic electron bound in a harmonic potential.

In Chapter 14, we introduce the concept of the spectral shift density, the quantity that has to be integrated over frequency to obtain the radiative shift. The spectral shift density indicates the relative contribution to the radiative shift from different frequencies. This allows us to compare the various methods that have been used to compute the Lamb shift, examining their high and low frequency behavior.

In Chapter 15, we discuss the cloud of virtual electromagnetic energy that surrounds the H atom and is responsible for the Lamb shift and van der Waals and Casimir forces.

Chapter 8

History and Some Aspects of the Lamb Shift

8.1 Background

We discuss aspects of Bethe's pivotal calculation, including its history, its significance, and its impact on the development of quantum electrodynamics. We then consider radiative shifts from different perspectives, classical and QED, with the objective of highlighting the connections between different aspects of the Lamb shift and clarifying the physical processes involved.

Our QED calculations are limited to the lowest-order shift for spinless electrons, the same as in Bethe's calculation. To explore the connections between physical phenomena and mathematics, we derive the complex first-order radiative shift in terms of the $mass^2$ operator using the fundamental equations of motion and then relate the results to Feynman diagrams. This is a more difficult derivation than simply using second-order perturbation theory or Feynman diagrams. Generally, textbook derivations only consider the real part of the shift. The radiative shifts are interpreted as the difference in energy or mass renormalization between a free electron and a bound electron, precisely as Bethe described it. The real part of the shift is the level shift and the imaginary part the level width, and we derive a dispersion relation between these parts. Atomic level shifts can be approximately modeled as arising from transitions with the absorption and emission of virtual photons that cause the atom to be in different energy states some of the time. To offer two perspectives, we discuss results for two central force systems, the H atom and the three-dimensional isotropic simple harmonic oscillator.

As we noted in Chapter 1, the hydrogen atom is the fundamental two-body system and perhaps the most important tool of atomic physics, and the continual challenge is to calculate its properties to the highest accuracy possible. The current QED theory is the most precise of any physical theory[1]: This remarkable precision began with the measurement and calculation of the first-order radiative Lamb shift, and that is why we are presenting a historical discussion of it. The derivation of this shift is present, in one form or another, in virtually every book on quantum field theory [3, 172–175]. The derivation is often based on the Schrodinger equation, using second-order perturbation theory to include the minimal coupling to the radiation field of the electron or to the electromagnetic field of the quantum vacuum.

There are many excellent and comprehensive reviews of the Lamb shift and the computation of energy levels to high precision in hydrogen-like atoms, including all the different effects [2, 95, 128, 149–158]. As noted above, the purpose of our discussion is quite different. We offer new perspectives on the physics that began the new age of QED.

8.2 History and Significance of Bethe's Calculation

8.2.1 *Brief history before Bethe's calculation*

Physicists had considered the need to account for an interaction of the electron with it own radiation field or with the vacuum field but did not have a suitable theory. Oppenheimer in 1930 had computed that the interaction with the atom's radiation field would lead to an infinite shift in energy, and therefore he rejected the notion as unphysical and thought that major changes in the theory were needed [176]:

> The theory thus leads to the false prediction that spectral lines will be infinitely displaced from the values predicted by the Bohr frequency condition... As it stands the integral over ν diverges absolutely.. We have treated these difficulties in some detail because they show that the present theory will not be applicable to any problem where relativistic effects are important, where that is, we cannot be guided by the limiting case $c \to \infty$... It appears improbable that the difficulties discussed in this work will be soluble without an adequate theory of the masses of the electron and the proton; nor is it certain that such a theory will be possible on the basis of the special theory of relativity.

In 1939, Weisskopf computed the self-energy of the electron "due to forced vibrations under the influence of the zero-point fluctuations of the

radiation field." He obtained a divergent result. This was one of the first attempts to integrate the effects of the quantum vacuum fluctuations into the explanations of self energy. Also note that he referred to the quantum vacuum as a radiation field [181].

Indeed, Bethe, in his landmark paper also used the phrase "radiation field" so it not absolutely certain, in my mind, precisely what he meant. To the lowest order, the calculation would be the same for the radiation field or the field of the vacuum fluctuations. Bethe used the expression for the free field vector potential in his calculation, consistent with a vacuum field or a first order radiaion field calculation

In 1938, Kramers had suggested the idea of renormalization of the mass due to interactions with the vacuum field and its necessity in classical as well as in quantum theories, but had no clear idea how to do it in practice [177]. As Bethe said in an interview in 1996 [178, 179]:

> Kramers had said [at the Shelter Island Conference] that we misunderstood the self energy of the electron. The divergent self energy of the electron was already included in the physical mass. We need to consider the difference in the self energy between a free electron and one bound in an atom.

It was believed that the divergence in the self energy of a electron due to its interaction with the radiation field was linear in the cutoff frequency until, in 1939, at Fermi's suggestion, Weisskopf used the relativistic Dirac theory and showed (after correcting a critical error in sign pointed out by Furry [180]) that the electron self energy divergence was logarithmic [181]. He computed that the electron charge distribution was spread over a Compton wavelength with a shape described by a Hankel function because of its interaction with the vacuum field, a calculation that remains valid today [3].

The Dirac theory predicted that the $2s_{1/2}$ and $2p_{1/2}$ levels in the H atom were degenerate. Measurements of the energy difference had been done but with mixed results. Then, in 1947, Willis Lamb Jr.[1] applied the expertise

[1]Willis Eugene Lamb Jr. was an American physicist, born in Los Angeles in 1913, who won the Nobel Prize in Physics in 1955 "for his discoveries concerning the fine structure of the hydrogen spectrum." He went to the University of California at Berkeley where he received an undergraduate degree in chemistry, and then a PhD in theoretical physics in 1938, working with J. Robert Oppenheimer as his advisor. David Bohm received his PhD with Oppenheimer a few years later. At one point as a young man, Lamb considered becoming a professional chess player instead of a physicist [182]! After receiving his PhD, he then joined the faculty at Columbia University, where he did research at the Columbia

in microwave technology that he developed working with Prof. Isador Rabi at Columbia on radar research during WWII to the precise determination of the $2s_{1/2} - 2p_{1/2}$ energy difference of 1050 MHz or 4.3×10^{-6} eV. Dyson who, as a graduate student working with Bethe at Cornell, recalled [184]:

> And of course the people at Cornell were very closely in touch with the people in Columbia, and in particular Willis Lamb talked to Hans Bethe, who was the professor at Cornell, and Bethe then sat down and gave the first more or less adequate theory of the Lamb shift, just from a physical point of view. He understood that the reason why you had the Lamb shift was that the electron in the hydrogen atom was interacting with the Maxwell electromagnetic field, in addition to interacting with the proton, so that the effect of the fluctuations in the Maxwell field was disturbing the electron while it was revolving around the proton, causing a slight change in the position of the orbits. And so it was the back reaction of the electromagnetic field on the electron that Lamb had been measuring. And so Bethe understood that from a physical point of view. The problem was then, could you actually calculate it? And with the quantum electrodynamics as it was then, it turned out you couldn't; that if you just applied the rules of the game as they were then understood and tried to calculate the Lamb shift, the answer came out infinity, not a number of megacycles but an infinite number of megacycles. So that wasn't very useful and so it was clearly a real defect of the theory that it couldn't grapple with this problem.

Lamb presented his results at the Conference on the Foundations of Quantum Mechanics held at Shelter Island 1–3 June 1947, and published them 18 June 1947 in a three-page paper in Physical Review [18]. Dyson later commented on the reaction to Lamb presenting his results at the conference [184]:

> The hydrogen atom being the simplest and most deeply explored object in the whole universe, in a way—I mean if you don't understand the hydrogen atom, you don't understand anything, and to find that things were wrong even with a hydrogen atom was a big shock. So it became the ambition of every theoretical physicist to understand this.

Radiation Laboratory from 1943 to 1951 with Prof. Isador Rabi, who won the Nobel Prize in physics in 1944. Lamb taught at Stanford, Oxford, Columbia, Yale, and University of Arizona. Norman Kroll was one of his students. For the last three decades of his life, he was critical of the standard interpretation of quantum mechanics, particularly the quantum theory of measurement and did not believe in the idea of a photon [183]. He died in 2008 at age 94.

At the conference, many people, including Schwinger, Weisskopf, and Oppenheimer, suggested that the deviation resulted from quantum fluctuations acting on the electron in the atom. However, the shift from this interaction was infinite in all existing theories and therefore had been ignored. The consensus was that the current theory was fundamentally flawed and that a radically new idea was needed to deal with this. On the 75-mile train ride home to Schenectady, NY, Bethe did a non-relativistic calculation using second-order perturbation theory, assuming minimal coupling with a quantized electromagnetic field. The calculation predicted that the interaction of the electron with the radiation field would lead to a shift of 1040 MHz [19]. Bethe wrote a paper that was three pages long and sent it to the participants on 9 June. The paper was received by the Physical Review and published on 15 August. As Bethe later recalled in an interview [178, 179]:

> The combination of these two talks of Kramers and Lamb stimulated me greatly and I said to myself: let's try to calculate that Lamb shift, let's try to calculate the difference between the self energy of a free electron and that of an electron bound in the hydrogen in the N = 2 state. At the conference I said to myself: I can do that. And indeed once the conference was over I traveled to Schenectady to General Electric Research Labs. On the train I figured out how much that difference might be. I had to remember the interaction of the electromagnetic quanta with the electron. I wasn't sure about a factor of two. So if I remembered correctly, I seem to get just about the right energy separation of 1000 MHz, but I might be wrong by a factor of two. So the first thing I did when I came to the library at General Electric was to look up Heitler's book on radiation theory. I found that indeed I had remembered the number correctly and that I got 1000 MHz. ...I was helped very much by a previous paper by Weisskopf who had shown that in Dirac pair theory that the energy of an electron only diverged logarithmically when you get to high energy. So I said to myself once I take the difference between the bound electron and free electron the logarithmic divergence will probably disappear and it will converge. So let's just calculate the effect of quanta up to the energy of the electron mass times c squared and let's hope the relativistic correction won't make any difference.

Dirac has called this result the "most important calculation in physics for decades." Freeman Dyson described it as "a turning point in the history of physics.... It broke through a thicket of skepticism and opened the way to the modern era of particle physics. It showed us all how to connect QED with the real world" [184, 185]. In his Nobel lecture, Feynman called Bethe's calculation "the most important discovery in the

Fig. 8.1. Hans Bethe, holding the pocket computer of his times. (Thanks to the APS archives for the photo).

history of quantum electrodynamics" [186, 187]. In a major 2001 review article, Eides states: "Discovery of the Lamb shift, a subtle discrepancy between the predictions of the Dirac equation and the experimental data, triggered development of modern relativistic quantum electrodynamics and subsequently the Standard Model of physics" [152]. We discuss Bethe's approach in detail in Sec. 9.3.1.

The key to Bethe's success was his interpretation of the infinities that arise in the calculation. He saw that one infinite energy shift was independent of the Coulomb potential, and therefore, he reasoned, should correspond to a mass renormalization of the free electron. He interpreted the infinity as a renormalization of a bare electron resulting in an electron with the observed physical mass. This insight allowed him to continue with the calculation and compute the finite energy shift due to the interaction of the electron with the vacuum field for a specific atomic state. The resulting frequency integration led to another divergence, but only logarithmic, thus he used an energy cutoff of mc^2 to ensure a finite result, reasoning that since the calculation was non-relativistic a cutoff was justified. His insightful assumptions led to a result of surprising accuracy.[2]

[2]Hans Bethe was born in Germany in 1906. As a child, his father, a physician, told of Hans at age four sitting on the stoop of their house, a piece of chalk in each hand, taking square roots of numbers. By the age of five, he had fully understood fractions and could add, subtract, multiply, and divide any two of them. At age seven, he was finding ever-larger prime numbers and had made a table of the powers of two and three, up to

To obtain the final numerical result required a calculation of the so-called Bethe log (which he credited to GE workers Dr. Stehn and Miss Steward), which can be interpreted as the average excitation energy for the radiative interaction. It equals the average energy difference between the level whose shift is being computed and the other levels which are reached by virtual transitions due to interaction with the quantized radiation field. The calculations showed that the average excitation energy for the $N = 2$ state was about 17.8 Rydbergs or 240 eV (1 Rydberg = 13.6 eV, corresponding to the energy of the ground state of the H atom), which Bethe thought was "an amazingly high value" that indicated scattering states dominated the Bethe log, but the result was still clearly in the non-relativistic energy range since $240\,\text{eV} \ll mc^2 = 0.5\,\text{MeV}$. (More amazing, we show in Chapter 14 that over 95% of the ground state shift arises from excitation energies that are greater than the ionization potential, that is scattering states.) The value of the Bethe log computed was slightly in error, and the currently accepted value for the $2s$ state is 16.6392 [152], which changes the calculated $2s_{1/2} - 2p_{1/2}$ shift from 1040 MHz, the value Bethe gave in his paper, to 1052 MHz, compared to the currently accepted value of about 1057.845 MHz.

Some reflections of Freeman Dyson shed some light on Bethe's personality and his work style, which may have led to his success [178]:

2^{14} and 3^{10}, and had memorized them [188]. After two years at Frankfort University, he transferred to Munich in 1926, joining Arnold Sommerfeld's group, where he learned the need to work hard and built his confidence. He received his doctorate summa cum laude a few years later. On a fellowship, he went to Rome and worked with Fermi. From Fermi, Bethe learned to reason qualitatively, to obtain insights from back-of-envelope calculations, and to think of physics as easy and fun, as challenging problems to be solved. Bethe's craftsmanship was an amalgam of what he learned from Fermi and Sommerfeld, two great physicists and teachers, and combined the best of both: the thoroughness and rigor of Sommerfeld with the clarity and simplicity of Fermi. This craftsmanship is displayed in full force in the many reviews that Bethe wrote [158], which remains a classic even today. In 1932, Bethe began an appointment at Tubingen, but Hitler's rise to power and the enactment of racial laws in 1933 prohibiting any Jew from state or federal position forced Bethe to leave. In 1935, he joined the physics faculty at Cornell, and enjoyed the atmosphere very much, and remained there for most of his career. During WWII, he served as head of the Theoretical Division at Los Alamos, under Oppenheimer. Bethe won the Nobel Prize in physics in 1967 for "for his contributions to the theory of nuclear reactions, especially his discoveries concerning the energy production in stars." He explained why the sun keeps shining, and did not win it for his contributions to QED. In later years, he advocated for peaceful use of nuclear energy and nuclear disarmament. He died in 2005 at age 98.

> He had this intense love of doing physics collectively. I mean that it wasn't really physics if you did by yourself, it was something you did with a group of people. And so I just loved it from the beginning and became very much a part of it right away. And then, of course, his way of work was actually quite unique, I mean if you compare Bethe with anybody else I knew. First of all, he had total command of the facts, that he absolutely just - you never needed to look up a number in a table because he knew them all. He knew all the energy levels of hydrogen and he knew the atomic weights of the different elements and the density of lead and gold and uranium, all these just physical quantities, he knew them all. In addition, of course, he had an extraordinary ability to sit down and calculate and just simply go at it. . .And he was, of course, also just extraordinarily reliable: if he said something, you could believe it. He was very careful about everything he said. So just a thoroughly solid person. Very different from Feynman, because Feynman was far more imaginative. I mean, one thing Bethe did not have was imagination; he never really invented anything, he just used the theories that were there to explain the facts, and he knew the facts and he knew the theories, so he just put them together; whereas Feynman was always inventing things and he didn't believe the theories that were taught in the textbooks, he had to make them up for himself, so he had a much harder time; but still, of course, in the end you need imagination too; I mean, both kinds of physicists are needed.

The lowest order radiative shift of magnitude $(4/3\pi)mc^2\alpha(Z\alpha)^4$ that Bethe computed involves the emission and absorption of one virtual photon, the so-called one-loop correction, so that in the expression for the shift the α arising from the coupling is raised to the first power. This first-order radiative shift accounts for about 96% of the energy difference between the $2s_{1/2}$ and $2p_{1/2}$ states.

The other major effect of the same order that contributes to the classic Lamb shift is vacuum polarization, often called the Uehling contribution, which had been computed successfully before the Lamb shift measurement and gives a shift of about -27 MHz [158, 189, 190]. Vacuum polarization arises from the presence of a virtual electron-positron cloud, approximately a Compton wavelength in radius, surrounding a charge, essentially producing a dielectric constant in the vacuum region near a charge. For S states, the electron goes very close to the proton, penetrating this cloud around the proton, and therefore effectively sees a larger charge and experiences a stronger binding force, which lowers the energy level by approximately 2.4% or 25 MHz [152, 180]. The fact that including the effect of the vacuum polarization ensured greater agreement with the experiment convinced physicists that the vacuum polarization contribution was real and correct.

8.2.2 *The effect of Bethe's calculation on the development of quantum theory*

Bethe commented on his 1947 paper in a videotaped interview in 1998 [178]:

> And as far as I know, this paper both disappointed and stimulated other people who were more versed in relativistic theory, namely Schwinger and Feynman... and also Weisskopf. Weisskopf pursued the theory in an old-fashioned way and calculated the relativistic part, together with some of his collaborators. And Schwinger was stimulated to produce a completely new theory, a relativistically invariant theory of quantum electrodynamics. But essentially extending the old quantum electrodynamics, making it relativistically invariant. Feynman at Cornell used the completely novel and independent way of getting at the same problem. He had his own way of doing quantum mechanics, his own way of putting in the electric field. And it turned out that in the end that Feynman's new way was very much easier than Schwinger's way.

Shortly after Bethe's calculation, Dyson published, as a problem assigned by Bethe, a calculation of the Lamb shift for a spinless electron [191]. Formal and rigorous relativistic calculations using perturbation theory and including spin were performed in 1949 by J. French and V. Weisskopf [192] and N. Kroll and W. Lamb [193]. Weisskopf later commented about these calculations that they "resulted in good agreement with the experiment. However, the methods used by those authors of subtracting two infinities were clumsy and unreliable [180]." However, history has been kind to these calculations that were not dependent on cut-off points, which were perhaps clumsy and difficult, but produced excellent results that have stood the test of time [3, 173].

Bethe's breakthrough in understanding the role of the vacuum electromagnetic field and how to deal with divergences led to intense theoretical work in quantum electrodynamics. It is most remarkable that within a year, three different approaches to quantum electrodynamics were independently developed that were relativistic and could deal with divergences with some success. Schwinger, Tomonaga, and Feynman each had proposed a manifestly covariant method, and shown its capability to address a broader range of QED problems than just the energy levels of the H atom [186, 194]. Although all of these methods appeared to be different, with his characteristic insight, Freeman Dyson showed that they had essential similarities and were mutually consistent [195]. He summarized: "The advantages of the Feynman theory are simplicity and ease of application, while those of Tomonaga-Schwinger are generality and theoretical

completeness." These new methods could be used to treat the radiative interaction as a perturbation to any desired order of approximation. Dyson also compared the results to those from the S matrix theory [196]. Dyson observed that Oppenheimer was particularly reluctant to accept Feynman's approach [197].

Welton provided some physical insight into the radiative shift with an approximate calculation based on a semi-classical model of the vacuum field which caused the oscillation of the electron bound in the Coulomb field, effectively increasing its size [198]. This motion meant that the electron saw a modified Coulomb potential. Only for S states was the spread of the electron sufficient to modify the energy level, in rough agreement with Bethe's result. This calculation is discussed in more detail in Section 9.3.2.

In their comprehensive 2001 review [152], Eides *et al.* give a different perspective on the spread of the electron: "According to QED an electron continuously emits and absorbs virtual photons and as a result its electric charge is spread over a finite volume instead of being pointlike," and then they use the expression for the form factor, $F(-\mathbf{k}^2) = 1 - (1/6)\langle r^2\rangle \mathbf{k}^2$, to obtain the rms radius, obtaining a value of 1330 MHz for the Lamb shift. Their calculation differs from that of most authors [3, 175], in that they assume the bound electron is slightly off mass shell so the cutoff term becomes $ln(1/Z\alpha)^2$ rather than $ln(1/Z\alpha)$.

A period of intense theoretical development followed Bethe's calculation, characterized by calculations of the energy levels of the H atom and QED in general, performed with increasing precision and complexity. Some of the key developments from 1950 to about 1970 are in the papers [157, 199–204]; from 1980 to 2000 are in [166, 205–221]; and from 2000 to the present are in [9, 11, 167, 168, 222–232]. Theorists applied themselves to compute the numerous other effects leading to the total shift between the $2s_{1/2}$ and $2p_{1/2}$ levels, as well as for other levels, including relativistic corrections, center of mass effects, recoil corrections, radiative recoil corrections, nuclear size and spin effects, and more rigorous, more precise, and higher order calculations of the radiative shifts (for reviews, see [2, 95, 128, 149–155]).

One of the biggest challenges in the precise computation of the radiative shifts is the necessity to deal with frequencies from the IR to relativistic values. For the low frequencies, the starting point is the non-relativistic dipole approximation, and the Coulomb gauge is the most convenient. On the other hand, for the high frequencies, relativistic dynamics is needed, the binding energy can be neglected, and the most convenient gauge is the

covariant Feynman gauge. Matching the contributions from both regions is a challenging procedure. Commenting on these perennial matching issues in a 2001 review, Eides *et al.* observe [152].

> It is a strange irony of history that due to these difficulties it became common wisdom in the sixties that it was better to avoid separation of the contributions coming from different momenta regions than to try to invent an accurate matching procedure... Bjorken and Drell wrote, having in mind the separation procedure: The reader may understandably be unhappy with this procedure... we recommend the recent treatment of Erickson and Yennie which avoids the division into soft and hard photons. Schwinger wrote "...there is a moral here for us. The artificial separation of high and low frequencies, which are handled in different ways, must be avoided." All this advice was written even though it was understood that the separation of the large and small distances was physically quite natural and the contributions coming from large and small distances have a different physical nature.

Davies concluded in a 1982 paper:

> ...the explanation of the Lamb shift is a far more orderly affair if it is consistently carried through within the framework of old fashioned perturbation theory...the joining up of the low and high energy contributions does not involve any new physics: it is a simple mathematical device to enable the use of two distinct approximation schemes [221].

In actual fact, the attitude has changed in the last decade, and theorists have developed more elaborate methods to deal with matching contributions from high and low frequency regions and are now trying to embrace the split to clarify the physical nature of corrections and improve the results of computations [152, 231].

In Steven Weinberg's 1995 classic "The Quantum Theory of Fields," he uses an elegant method of computing radiative shifts in which he introduces a photon mass in the photon propagators that ultimately cancels when the low and high momenta regions are combined. As he says, his result is 1052.19 MHz, "just the same as the old result of Kroll and Lamb [193] and French and Weisskopf [192] which they obtained using the techniques of old-fashioned perturbation theory [173]." Lowell Brown in his book *Quantum Field Theory* advocates using analytical continuation in the spatial dimensionality of the field [174]. He notes that in $n > 4$ dimensions there is no IR divergence and, in $n < 4$, there is no UV divergence; thus, in the limit of $n \to 4$, one can obtain the correct results.

8.2.3 *Current focus in precision QED for light atoms*

New developments in calculations include simplifications of the Bethe-Salpeter equation for a system with masses that are very different, such as the proton and electron [9, 205, 212, 231–233]. The simplifications are described as effective potential methods, and the "on the mass shell" approach [151]. Computers are used heavily for numerical computations. Higher and higher order corrections are being computed [9, 11, 167, 168, 208, 212, 214, 219, 222–224, 231, 232], using numerical as well as analytical methods [225–230]. In Lamb shift calculations for the classic $2s_{1/2} - 2p_{1/2}$ shift, there are hundreds of separate terms that are computed to secure a precision of 1 part in 10^{13}.

The interest in the Lamb Shift in hydrogen has moved to a more general interest in the QED analysis of two-particle bound states in systems generally with low Z and one or two electrons [2, 95, 128, 149–152, 196, 199–202, 205]. This includes bound states of an electron and a positron (positronium), bound states of a muon and a proton (muonium), and even antihydrogen. Systems with high $Z\alpha$ coupling are of interest for the study of nuclear effects or the study of perturbations as a function of $Z\alpha$. Precision QED analysis has also been applied to deuterium and ionized tritium and systems with two electrons, like He. There have been incredible advances in experimental methods that now include atom interferometry, laser spectroscopy, and two-photon spectroscopy, which can be used to study transitions such as $1S \rightarrow 2S$ and $1S \rightarrow 3S$ that do not have a change in the angular momentum. The $1S \rightarrow 2S$ transition has a natural line width of only 1.3 Hz, so experimental determinations are a thousand times more accurate than for any other transition in H, where typical line widths are about 1 MHz or more. For this transition, precision up to 15 decimal places is possible [1]. This means the determination of the $2s_{1/2} - 2p_{1/2}$ Lamb shift is not limited by the $2s$ line which is very broad. Many different transitions in these systems are studied, and the results are correlated to secure more precision and to determine likely values of the fine structure constant and the Rydberg constant and, hopefully, the radius of the proton. The radius obtained from the measurements of hydrogen and muonic hydrogen differs by four standard deviations, a puzzle that is currently being addressed [234, 235].

There are physicists, including notables Dirac, Schrödinger, Einstein, Pauli, Lamb, Bohm, Feynman, and others who are not satisfied with the present version of quantum electrodynamics, in which perturbation theory,

which should rightfully deal with small perturbations, is dealing with infinite terms. Three years before he died, Feynman wrote:

> The shell game that we play..is technically called renormalization. But no matter how clever the word is, it is what I would call a dippy process! Having to resort to such hocus-pocus has prevented us from proving that the theory of quantum electrodynamics is mathematically self-consistent [236].

It is ironic that Bethe's original calculation appears to have set this direction for the development of QED. Had he not had such success with his original calculation, perhaps we would have a theory without infinities today that provided a more satisfying intellectual and philosophical viewpoint. However, it is hard to argue with success.

In Chapter 9 we discuss radiative shifts in classical and quantum systems, including the role of the quantum vacuum.

This page intentionally left blank

Chapter 9

Radiative Shifts, Classical Physics, and the Zero-Point Fluctuations of the Electromagnetic Field

9.1 Background on QED Radiative Shift Calculations

The zero-point vacuum fluctuations have a spectral energy density of $\rho(\omega) = \hbar\omega^3/2\pi^2c^3$. In QED, the vacuum field is typically expressed as a sum over an infinite number of plane waves with all possible momenta $\hbar\mathbf{k}$ and directions $\mathbf{k}/k$ with the restriction that the energy E_k in each mode is $\hbar\omega_k/2 = \hbar k/2c$. The vector potential is [3][1]

$$\mathbf{A}(\mathbf{r},t) = \sum_{\mathbf{k},\lambda} \sqrt{\frac{2\pi\hbar c^2}{\omega_k V}} (a_{\mathbf{k}\lambda} e^{i(\mathbf{k}\cdot\mathbf{r}-\omega_k t)} + a^\dagger_{\mathbf{k}\lambda} e^{-i(\mathbf{k}\cdot\mathbf{r}-\omega_k t)})\ \mathbf{e}_{\mathbf{k},\lambda}, \tag{9.1}$$

where the raising and lowering operators obey the commutation rules

$$[a_{\mathbf{k}\lambda}, a^\dagger_{\mathbf{k}'\lambda'}] = \delta_{\mathbf{k}\mathbf{k}'}\delta_{\lambda\lambda'} \tag{9.2}$$

and $\boldsymbol{\epsilon}_{\boldsymbol{k},\lambda}$ are the two normalized polarization vectors ($\lambda = 1, 2$) that are orthogonal to $\mathbf{k}$, thus $\mathbf{k}\cdot\mathbf{e}_{\mathbf{k},\lambda} = 0$, and

$$\mathbf{e}_{\mathbf{k},\lambda}\cdot\mathbf{e}_{\mathbf{k},\lambda'} = \delta_{\lambda\lambda'}. \tag{9.3}$$

The electric field is $\mathbf{E}(\mathbf{r},\mathbf{t}) = -\partial\mathbf{A}(\mathbf{r},t)/\partial t$ and $\mathbf{B}(\mathbf{r},t) = \nabla\times\mathbf{A}(\mathbf{r},t)$. The interaction Hamiltonian for a particle of charge e and mass m in the

[1]The quantization volume V is an artifice to avoid infinite volumes. In this box normalization $k_x = 2\pi n_x/L_x$, $k_y = 2\pi n_y/L_y$, and $k_z = 2\pi n_z/L_z$, with $V = L_xL_yL_z$. The integers n_x, n_y, and n_z go from $-\infty$ to $+\infty$.

vacuum field is

$$H_I = \frac{1}{2m}(\boldsymbol{p} - e\boldsymbol{A})^2, \tag{9.4}$$

where $\boldsymbol{A}$ is the vector potential for the vacuum field. The radiative shift in energy levels, such as the Lamb shift, arises from the $\boldsymbol{p} \cdot \boldsymbol{A}$ term. The contribution to the energy shift due to the $\boldsymbol{A}^2$ term does not depend on the state of the atom and so is ignored in calculations of the radiative shifts between levels.

To summarize the properties of the vacuum field in QED: no real photons are present, only random virtual photons of energy $\hbar\omega_k/2$ and momentum $h\mathbf{k}/2c$, with all possible values of momentum, are present, consistent with Eq. (9.1). The expectation values of the electromagnetic fields vanish: $\langle \boldsymbol{E} \rangle = 0$, $\langle \boldsymbol{B} \rangle = 0$, but the variances do not: $\langle \boldsymbol{E}^2 \rangle \neq 0$, $\langle \boldsymbol{B}^2 \rangle \neq 0$. The fields are isotropic (invariant under rotations), invariant under space–time translations (homogeneous), and under boosts (Lorentz invariant). The energy density spectrum is proportional to ω^3, which is the only spectral density that is Lorentz invariant [3]. This means that if you are traveling through space at some velocity, the vacuum field will always look the same, with the same spectral density. For temperatures above 0 K, there is an additional black body component to the vacuum field, which we do not consider here.

In QED, we can model mass or charge renormalization with the process:

bare point electron + vacuum fluctuations + radiative reaction →
electron with physical mass, charge, and effective size of a Compton wavelength

A bare, free, charged, point particle is constantly being accelerated in the field, acquiring a mean kinetic energy that increases its effective mass. Since the particle is oscillating, the effective volume occupied by the particle increases and it can no longer be usefully regarded as a point particle, but as a particle with an effective dimension of a Compton wavelength. The interaction of the free electron with the vacuum field results in the renormalization of the ideal point electron, so it has the physical properties of a real electron. It cannot radiate because the zero point vibrations represent the lowest energy state of the vacuum.

A similar process occurs for an atom, in which the atom undergoes allowed virtual transitions due to the vacuum field. These transitions can

be seen as shifting the energy corresponding to a given state of the atom. A QED based model for this mechanism responsible for the radiative part of the Lamb shift is discussed in Section 11.4.1.

In QED, radiative shifts are often calculated using Feynman diagrams, in which the atom is depicted as propagating in time, and it emits or absorbs a virtual photon changing its state correspondingly; then a short time later (consistent with the time-energy uncertainty principle) absorbs or emits the same virtual photon and returns to the initial state. The free vacuum field is generally interpreted as the cause of these transitions. On the other hand, the transitions can be interpreted as due to the interaction of the electron with its own radiation field. To first order, the radiation field of the electron is the same as the free field of the quantum vacuum. Hence, QED radiative shifts are the same to the first order whether we compute them as arising from self-interaction with the radiation field or as arising from interaction with the ubiquitous virtual fluctuating zero-point vacuum field. Although these interpretations fit the equations and appear reasonable, it should be pointed out that no experiments could verify that these virtual transitions actually occur since the times are so short; it is a matter of preference how one views these phenomena.

Milonni has clarified the role of vacuum fluctuations and the radiative reaction in QED calculations of the Lamb shift and the Casimir force [3, Section 4.13] or [172, Section 7.4]. If the annihilation and creation operators in the vector potential are made to be symmetric in the calculations, then the level shift is determined to be due solely to the free vacuum field. This is how Welton and Feynman did their calculations, and how the Stark effect is typically computed. However, if the operators are normally ordered, then the level shift is found to be due to the radiation field of the electron, which Milonni also refers to as a source field. Thus, the preference of the person doing the calculation determines which field appears to be responsible for the Lamb shift.

9.2 Radiative Effects in Classical Physics

Classically, any charge radiates when it is accelerated, and this emission of radiation, which carries away momentum, angular momentum, and energy, alters the unperturbed motion of the particle. To account for this radiation classically, we include in the equations of motion a resistive or damping force proportional to the third derivative with respect to time of the position.

For a classical radiating electron in a Coulomb potential, Newton's second law becomes the Abraham–Lorentz equation of motion

$$m\frac{d^2\mathbf{r}}{dt^2} = -\frac{Ze^2\mathbf{r}}{r^3} + \frac{2e^2}{3c^2}\frac{d^3\mathbf{r}}{dt^3}. \tag{9.5}$$

The second term on the right is the Abraham–Lorentz force, the non-relativistic radiative reaction force for an accelerating charged particle. The radiation field of the particle essentially exerts a force on itself, sometimes called a "self-field", a phenomenon that leads to renormalization and radiative shifts in QED. The classical equations of motion become sufficiently complicated, so that they are usually solved only in an approximation [237]. We illustrate the effects by considering the non-relativistic classical hydrogen atom and the non-relativistic classical simple harmonic oscillator.

9.2.1 *The classical hydrogenike atom*

Without radiative damping, a classical electron in a Coulomb potential would travel in elliptical or circular orbits in a periodic way. Including the damping means that the orbits decay with the emission of radiation. As time passes elliptical orbits tend to become circular and the mean radius decreases leading to collapse of the atom. The electron in a classical H atom, starting at a radius of 0.53A (given by quantum mechanics), would collapse in about 1.3×10^{-11} s [238–240]. Consideration of the rate of decay of the energy and the angular momentum for an atom with charge Ze leads to the equation for the radius $r_{cl}(t)$ of a circular orbit for a mass m and charge e as a function of time

$$r_{cl}^3(t) = r_{cl}^3(0) - 4\frac{\alpha(Z\alpha)}{m^2}t \tag{9.6}$$

with classical orbital frequency

$$\omega_{cl} = \sqrt{\frac{Z\alpha}{mr_{cl}^3}}. \tag{9.7}$$

The Lamor equation $P = (2/3)(\alpha\dot{v}^2)$ gives the radiated power. The acceleration $\dot{v}$ can be obtained from the Coulomb force $F = m\dot{v} = Z\alpha/r_{cl}^2$, giving the radiated power

$$\mathrm{P}(t) = \frac{2}{3}\frac{\alpha(Z\alpha)^2}{m^2}\frac{1}{r_{cl}^4}. \tag{9.8}$$

Applying the Correspondence Principle we obtain the transition probability

$$\Gamma = \frac{P(t)}{\omega_{cl}} = \frac{2}{3} m\alpha \frac{(Z\alpha)^{3/2}}{(mr_{cl})^{5/2}}. \tag{9.9}$$

Substituting the quantum mechanical result for the radius of the H atom for large principal quantum number N

$$r_c = \frac{N^2}{mZ\alpha} \tag{9.10}$$

gives the transition rate or width for state N

$$\Gamma_{\mathrm{N}} = \frac{2}{3} m \frac{\alpha(Z\alpha)^4}{\mathrm{N}^5}. \tag{9.11}$$

This width is 2π times the energy lost classically by radiation in one revolution (about 2π 48 MHz = 301 MHz, assuming $N = 2$). We show that for large N this width equals the imaginary part of the radiative shift calculated from quantum field theory.

Efforts have been made to stabilize the ground state of the hydrogen atom using stochastic electrodynamics (SED), which is classical electrodynamics with an additional field, a classical version of the zero-point electromagnetic field that is included with the objective of obtaining the same results as quantum theory [238–241]. Stochastic electrodynamics (SED) includes a classical stochastic field that has the same energy density as the quantum vacuum field. In the SED modeling efforts of the hydrogen atom to date, the classical field supplies the energy lost by radiation from the classical electron that orbits the proton, thus stabilizing the orbit for a short time, but then results in the ionization of the atom.

9.2.2 *Radiative shifts to lowest order in the classical simple harmonic oscillator*

In a real harmonic oscillator, damping is present due to internal friction, environmental interactions, and radiation. The damping shifts the resonant frequency and causes the oscillations to decay in time. Consequently, the emitted radiation is no longer monochromatic, but has a frequency spectrum with a finite width. For an undamped one-dimensional oscillator with charge e, mass m, and resonant frequency ω_0, the displacement from equilibrium is

$$X(t) = Re(X_0 e^{-i\omega_0 t}). \tag{9.12}$$

Including a radiative damping force in the equations of motion produces a complex shift in the resonant frequency [237]

$$\omega_0 \to \omega_0 + \Delta\omega_0 + \frac{i}{2}\Gamma, \tag{9.13}$$

where

$$\Delta\omega_0 = -\frac{5}{18}\left(\frac{\alpha\hbar}{mc^2}\right)^2 \omega_0^3 \quad \Gamma = \frac{2}{3}\frac{\alpha\hbar}{mc^2}\omega_0^2. \tag{9.14}$$

The factors of c and $\hbar$ arise for the classical oscillator since radiation is emitted. The term $\alpha\hbar/mc^2$ is the time it takes for light to travel a distance equal to α times the reduced Compton wavelength, 9.6×10^{-24} sec, which also equals the time it takes for light to travel a distance equal to the classical electron radius.[2] Radiative effects are only important for accelerations that result in changes in velocity for times less than $\alpha\hbar/mc^2$. For the classical harmonic oscillator, the shift $\Delta\omega_0$ is a higher order effect than the width Γ.

When we recall that in quantum mechanics the energy is proportional to the frequency $E = \hbar\omega$ and that the time dependence of an eigenstate of energy E is e^{-itE}, it is no surprise that in quantum electrodynamics radiative effects produce a complex shift in the bound state energies of a system, the real part being the shift in the energy level and the imaginary part being the width of the state that determines its lifetime.

We can verify the Bohr Correspondence Principle for the three-dimensional isotropic harmonic oscillator. This principle states that in the limit of large quantum numbers the classical power radiated in the fundamental band is equal to the product of the photon energy and the quantum mechanical transition probability (or the reciprocal of the lifetime). The power radiated from the classical isotropic oscillator is all in the fundamental band and has the value

$$\mathrm{P} = \frac{2}{3}\alpha\omega_0^4\overline{A^2}, \tag{9.15}$$

where $\overline{A^2}$ is the mean square amplitude of oscillation. The corresponding transition rate or line width Γ is

$$\Gamma = \frac{\mathrm{P}}{\omega_0} = \frac{2}{3}\alpha\omega_0^3\overline{A^2}. \tag{9.16}$$

[2]The classical radius of the electron is $r_{cl} = e^2/(mc^2) = 2.8 \times 10^{-13}$ cm, which can be written at $\alpha\hbar/mc = \alpha\lambda\!\!\!^{-}$, where $\lambda\!\!\!^{-}$ is the reduced Compton wavelength of the electron 3.8×10^{-11} cm (Compton wavelength divided by 2π).

For a quantum mechanical three-dimensional oscillator, the energy for a state N is $E_N = (N + \frac{3}{2})\omega_0 \approx m\omega_0^2\overline{A^2}$ and we find

$$\overline{A^2} = \left(N + \frac{3}{2}\right)\frac{1}{m\omega_0}. \tag{9.17}$$

Accordingly, in the limit of large quantum numbers, it follows from the Bohr Correspondence Principle that

$$\Gamma_{\mathrm{N}} = \frac{2}{3}\left(\frac{\alpha}{m}\right)\omega_0^2 N. \tag{9.18}$$

We show in Section 11.5 that this width Γ_{N} equals the radiative level width computed in quantum mechanics. The Correspondence Principle makes no statement about the level shift, which is the real part of the radiative shift, and indeed the classical calculation yields a level shift of order $(\alpha)^2$ while the quantum mechanical result is of order α.

9.2.3 *Comparison of results for harmonic oscillator and Coulomb potential*

The level width (Eq. 9.18) of the harmonic oscillator increases with the principal quantum number N, while for the hydrogen atom, the level width (Eq. 9.11) decreases with N. There is a similar inverse relationship of the level width with the mass. These results follow because the force on the particle increases with distance for the harmonic oscillator, while it decreases with distance for the H atom. For the harmonic oscillator the force center is at the center of the ellipse; for the Coulomb potential the force center is at a focus. The classical radiative damping in the harmonic oscillator gives a complex shift that illustrates the close relationship between radiative level shifts, as in the Lamb shift, and radiative widths. The level widths for both systems are related by the Bohr Correspondence Principle to the classical power radiated.

9.3 The Relationship Between Radiative Shift and the Zero-Point Field: The Radiative Shift Calculations of Bethe, Welton, and Power

In classical physics, the electromagnetic field in the vacuum vanishes (unless we are dealing with SED, stochastic electrodynamics). However, from quantum electrodynamics, we know that we must consider the effects of

the zero-point fluctuations of the electromagnetic field.[3] Three different approaches have been used to explain the Lamb shift.

9.3.1 *Bethe's approach*

The first calculation of the Lamb shift of a hydrogen atom was done by Bethe in 1947, who assumed that the shift was due to the interaction of the atom with a quantized electromagnetic field, which we assume is the zero-point field. He calculated the shift using second order perturbation theory, assuming that there was minimal coupling in the Hamiltonian:

$$H_{int} = -\frac{e}{mc}\mathbf{A}\cdot\mathbf{p} + \frac{e^2}{2mc^2}\mathbf{A}^2, \tag{9.19}$$

where m is the mass of the electron and $\mathbf{A}$ is the vector potential for the vacuum field given by Eq. 9.1.

As we have explained, the shift arises from the perturbation $-(e/mc)\boldsymbol{A}\cdot\boldsymbol{p}$. The shift from the $\mathbf{A}^2$ term is independent of the state of the atom and is therefore neglected. In the non-relativistic dipole approximation, the vector potential is evaluated as $\boldsymbol{A}(0,t)$.

$$\mathbf{A}(0,t) = \sum_{\mathbf{k},\lambda}\left(\frac{2\pi\hbar c^2}{\omega_k V}\right)^{1/2}(a_{\mathbf{k},\lambda}e^{-i\omega_k t} + a^\dagger_{\mathbf{k},\lambda}e^{i\omega_k t})\boldsymbol{\epsilon}_{\boldsymbol{k},\lambda} \tag{9.20}$$

The total shift for level N from second order perturbation theory is [3]

$$\Delta E_{NTot} = \sum_n \sum_{\boldsymbol{k},\lambda} \frac{|\langle n, 1_{\boldsymbol{k}\lambda}|h_{\boldsymbol{k}\lambda}|N, vac\rangle|^2}{E_N - E_m - \hbar\omega_k}, \tag{9.21}$$

where

$$h_{\boldsymbol{k}\lambda} = -\frac{e}{mc}\left(\frac{2\pi\hbar c^2}{\omega_k V}\right)a^\dagger_{\boldsymbol{k}\lambda}(\boldsymbol{\epsilon}_{\boldsymbol{k}\lambda}\cdot\boldsymbol{p}). \tag{9.22}$$

The vacuum field induces a transition from the initial state $|N, vac\rangle$ to an intermediate state with one photon $|n, 1_{\boldsymbol{k}\lambda}\rangle$ and energy $E_n + \hbar\omega_k$. The

[3] We also mention the vacuum fluctuations of the charge density, characterized by virtual electron–positron pairs, which leads to the renormalization of the electron charge. Since this charge renormalization contributes much less to the shift between states than the mass renormalization from the zero-point vibrations of the EM field, we shall not consider it here. In mesic atoms, in which the meson orbit is largely within the nucleus, the opposite situation occurs.

matrix element of the operator inducing the transition is

$$\langle n, 1_{\boldsymbol{k}\lambda}|h_{\boldsymbol{k}\lambda}|N, vac\rangle = -\frac{e}{mc}\left(\frac{2\pi\hbar c^2}{\omega_k V}\right)\boldsymbol{p}_{nN}\cdot\epsilon_{\boldsymbol{k}\lambda}, \tag{9.23}$$

which means the energy shift equals

$$\Delta E_{NTot} = -\frac{2}{3\pi}\frac{\alpha}{m^2c^2}\sum_n \int dE E\frac{\langle NL|p_i|n\rangle\langle n|p_i|NL\rangle}{E_n - E_N + E}, \tag{9.24}$$

where the quantum vacuum field energy is $E = \hbar\omega$, $\alpha = e^2/\hbar c$ is the fine structure constant, and the momentum matrix elements are $|\boldsymbol{p}_{nN}| = |\langle n|\boldsymbol{p}|N\rangle|$. The sum is over all intermediate states $|n\rangle$, scattering and bound, where $n \neq N$. This shift has a linear divergence. Bethe's insight was to tame this divergence by removing the contribution to the shift from the free electron in the H atom. He therefore subtracted the shift ΔE_{free} obtained by letting the binding energy vanish in Eq. (9.24) $(E_n - E_N) \to 0$:

$$\Delta E_{free} = -\frac{2}{3\pi}\frac{\alpha}{m^2c^2}\sum_n |\mathbf{p}_{nN}|^2 \int dE. \tag{9.25}$$

The observable shift is therefore

$$\Delta E_{NL} = \Delta E_{NTot} - \Delta E_{free}. \tag{9.26}$$

This yields Bethe's final result

$$\Delta E_{NL} = \frac{2\alpha}{3\pi(mc)^2}\sum_n^s \int_0^{\hbar\omega_C} dE\frac{(E_n - E_N)\langle NL|p_i|n\rangle\langle n|p_i|NL\rangle}{E_n - E_N + E - i\epsilon}, \tag{9.27}$$

where ω_C is a cutoff frequency for the integration that we will take as $\hbar\omega_C = mc^2$.

Using an idea from Kramers, Bethe did this renormalization, taking the difference between the terms with a potential present and without a potential present, essentially performing the free electron mass renormalization. He reasoned that relativistic retardation could be neglected and the radiative shift could be reasonably approximated using a non-relativistic approach, and he cut the integration off at an energy corresponding to the mass of the electron. He obtained a finite result that required a numerical calculation over all states, bound and scattering, that gave good agreement with measurements [18, 19, 158].

The spectral density in the Bethe formalism, which we will analyze in Chapter 14, is the quantity in Eq. (9.27) being integrated over E which gives the contribution to the shift as a function of the frequency of the

vacuum field. It includes the sum over states n. The term for n represents the contribution to the Lamb shift for the virtual transition from state N to state n. Note since the ground state is the lowest state, all intermediate states have higher energies, so the ground state shift has to be positive.

For comparison with the other calculations of the Lamb shift, it is helpful to show the next steps Bethe took to evaluate the shift ΔE_n for the S states, which have the largest shifts. Note that the spectral density in Eq. (9.27), that we will discuss in Section 14.2, is not affected by the subsequent approximations Bethe made to evaluate the integral. First the E integration is done:

$$\Delta E_N^{Bethe} = \frac{2\alpha}{3\pi}\left(\frac{1}{mc}\right)^2 \sum_n |\mathbf{p}_{Nn}|^2 (E_n - E_N) \ln \frac{(mc^2 + E_n - E_N)}{|E_n - E_N|}. \quad (9.28)$$

To simplify the evaluation Bethe assumed $|E_n - E_N| \ll mc^2$ in the logarithm and that the logarithm would vary slowly with n so it could be replaced by an average value

$$\widehat{\Delta E}_n^{Bethe} = \frac{2\alpha}{3\pi}\left(\frac{1}{mc}\right)^2 \ln \frac{mc^2}{|E_n - E_N|_{Ave}} \sum_n |\mathbf{p}_{Nn}|^2 (E_n - E_N), \quad (9.29)$$

where the hat over the ΔE indicates this is an approximation to Eq. (9.27). The summation can be evaluated using the dipole sum rule

$$2\sum_n^s |\mathbf{p}_{Nn}|^2 (E_n - E_N) = \hbar^2 \langle N|\nabla^2 V|N\rangle. \quad (9.30)$$

The value of the Laplacian with a Coulomb potential $V = -Ze^2/r$ is $\nabla^2 V(r) = 4\pi Ze^2\delta(\mathbf{r})$, so we have

$$\left\langle N \left| \nabla^2 V \right| N \right\rangle = 4\pi Ze^2 |\psi_N(0)|^2, \quad (9.31)$$

where $\psi(r)$ is the wave function for a Coulomb potential. $|\psi_N(0)|^2$ is zero except for S states

$$|\psi_N(0)|^2 = \frac{1}{\pi}\left(\frac{Z\alpha mc}{N\hbar}\right)^3. \quad (9.32)$$

For S states, this gives an energy shift equal to [3]:

$$\widehat{\Delta E}_N^{Bethe} = \frac{4mc^2}{3\pi}\alpha(Z\alpha)^4 \frac{1}{N^3} \ln \frac{mc^2}{|E_n - E_N|_{Ave}}. \quad (9.33)$$

The average $\ln(mc^2/|E_n - E_N|)_{Ave}$ in this expression, which Bethe computed numerically by summing over states, can be given in terms of the so

called Bethe log $\gamma(N, L)$:

$$\ln \frac{mc^2}{|E_n - E_N|_{Ave}} = -\gamma(N, L) + \delta_{L0} \ln \frac{2}{(Z\alpha)^2}.$$

For an S states with principal quantum number N, $\gamma(N, 0)$ is

$$\gamma(N, 0) = \frac{\sum_m |\mathbf{p}_{Nn}|^2 (E_n - E_N) \ln \frac{(1/2)(Z\alpha)^2 mc^2}{|E_n - E_N|}}{\sum_m |\mathbf{p}_{Nn}|^2 (E_n - E_N)}. \tag{9.34}$$

The sum is over all states, bound and scattering. Comparison of Eq. (9.33) to the definition of $\gamma(N, 0)$ Eq. (9.34), we see there is a difference in the argument of the ln function. This difference causes the appearance of the term $\ln(2/Z\alpha)^2$. Bethe also has extended the formalism to shifts for states that are not S states [158]. To determine the shift, it is necessary to evaluate the Bethe log by performing a numerical calculation over all states, bound and scattering. The final result gave good agreement with measurements [18, 19, 158].

Regarding the approximations Bethe made to obtain Eq. (9.28) from Eq. (9.29) and the use of the Bethe log Eq. (9.34), he commented: "The important values of $|E_n - E_N|$ will be of order of the ground state binding energy for a hydrogenic atom. This energy is very small compared to mc^2 so the log [in our Eq. (9.28)] is very large and not sensitive to the exact value of $(E_n - E_N)$. In the numerator, we neglect $(E_n - E_N)$ altogether and replace it by an average energy [158]."

Our work shows that Bethe was correct that the relative contribution from energies of the order of the ground state is very important, but we find in Chapter 14, when we analyze the contribution to the Lamb shift from different frequencies, that the contribution from higher energy scattering states is very significant, and therefore that the approximation $|E_n - E_N| \ll mc^2$ is not valid for scattering states for which E_n increases to the value mc^2. We are not aware of any quantitative estimates of the error in the approximation. The difference, 0.3%, between our value for the total 1S shift and that of Bethe may be due to this approximation, although we have not verified this. On the other hand, Bethe's approximation may have made his non-relativistic approach viable.

9.3.2 *Welton's approach*

To provide a more intuitive physical picture of the shift, Welton and Weisskopf considered the effect of a zero-point vacuum field on the motion

of an electron bound in a Coulomb potential [198, 242]. The fluctuation in the position of the electron ξ due to the random zero-point vacuum field $\mathbf{E}_0$ causes a variation in the potential energy. If $\boldsymbol{r}$ is the location of the particle when it is unperturbed by the zero point field, then when perturbed, the particle effectively sees a potential $V(\boldsymbol{r}+\boldsymbol{\xi})$. For weak binding, $\xi \ll r$, and we make the expansion[4]

$$V(\mathbf{r}+\boldsymbol{\xi}) = V(\mathbf{r}) + \boldsymbol{\xi}\cdot\boldsymbol{\nabla}V(\mathbf{r}) + \frac{1}{2}\left(\boldsymbol{\xi}\cdot\boldsymbol{\nabla}\right)^2 V(\mathbf{r}) + \cdots . \tag{9.35}$$

Because of the harmonic time dependence of the vacuum field, $\langle\boldsymbol{\xi}\rangle$ vanishes and the radiative shift is given approximately by the vacuum expectation value of the last term:

$$\Delta \mathrm{E}_{\mathrm{N}}^{\mathrm{Welton}} = \frac{\langle\xi^2\rangle}{6}\left\langle\nabla^2 \mathrm{V}(\mathbf{r})\right\rangle_N , \tag{9.36}$$

where we assume the potential has spherical symmetry, thus $\langle\xi_1^2\rangle = \langle\xi_2^2\rangle = \langle\xi_3^2\rangle = \langle\xi^2/3\rangle$. Eq. (9.36), which is valid for any central force, gives ΔE_N^{Welton} as the product of two factors, one depending on the nature of the fluctuations of the radiation field and the other depending on the structure of the system. To estimate $\langle\boldsymbol{\xi}^2\rangle$ for the vacuum field we consider the Hamiltonian for a particle of mass m and charge e in the vacuum field using the radiation gauge ($V = 0, \nabla\cdot\boldsymbol{A} = 0$):

$$H = \frac{1}{2m}(\boldsymbol{p} - e\boldsymbol{A}(t,0))^2. \tag{9.37}$$

We use the value of the vector potential for the free vacuum field at the origin, $\boldsymbol{A}(t,0)$, which is equivalent to the dipole approximation. The proton and the electron can be considered to become a point dipole. Hamilton's equations give the result

$$\mathrm{m}d^2\boldsymbol{\xi}/dt^2 = \mathrm{e}\ d\boldsymbol{A}/dt. \tag{9.38}$$

Integrating gives

$$\boldsymbol{\xi(t)} = \frac{\mathrm{e}}{\mathrm{m}}\int_{-\infty}^{\mathrm{t}} \mathrm{d}t\boldsymbol{A}\left(t',0\right). \tag{9.39}$$

Squaring this and taking the vacuum expectation value gives:

$$\langle\boldsymbol{\xi}\cdot\boldsymbol{\xi}\rangle = \left(\frac{e}{m}\right)^2 \int_{-\infty}^{t} dt' e^{+\epsilon t'} \int_{-\infty}^{t} dt'' e^{+\epsilon t''} \langle(\boldsymbol{A}(t',0)\cdot\boldsymbol{A}(t'',0))_+\rangle. \tag{9.40}$$

[4]This expansion is essentially the dipole approximation.

The vacuum expectation value on the right side is simply $-ig_{ij}D^{ij}$, where D^{ij} is the radiation gauge propagator in configuration space[5]:

$$\mathrm{D}_{ij}\left(\mathrm{t}'-\mathrm{t}''\right)=\frac{1}{(2\pi)^4}\int \mathrm{d}^4\mathrm{k}\left(\delta_{ij}-k_{\mathrm{i}}k_{\mathrm{j}}\cdot\frac{1}{\boldsymbol{k}^2}\right)\frac{1}{k^2}e^{-i\omega(t'-t'')}. \tag{9.41}$$

Accordingly, we find

$$\left\langle \boldsymbol{\xi}^2\right\rangle=\frac{2\alpha}{\pi}\left(\frac{\hbar}{mc}\right)^2\int_{E_0}^{\hbar\omega_C}\frac{dE}{E}, \tag{9.42}$$

where we show the factors of $\hbar$ and c to stress that the term in parentheses $(\hbar/mc)$ is $\lambda\!\!\!^{-}_c$, the reduced Compton wavelength of the particle, which we take to be the electron; thus $\lambda\!\!\!^{-}_c$ is 3.86×10^{-11} cm.[6]

We take the upper limit $\hbar\omega_C$ to be mc^2 to correspond to the mass of the electron, the same limit used by Bethe. For greater frequencies, it is clear that our semiclassical calculation is invalid because of relativistic kinematical effects and particle–antiparticle pair creation, which will become possible. (Another justification for taking this limit is given when we discuss this process from the point of view of the uncertainty principle). For the lower limit, we take some characteristic energy E_0 of the bound state system, for example the magnitude of the ground state energy. This gives a value of 8.4×10^{-12} cm $= 0.22\lambda\!\!\!^{-}_c = \sqrt{\langle\boldsymbol{\xi}^2\rangle}$ for the RMS displacement of the electron due to the vacuum fluctuations.

The final expression for the shift in the energy of a particle bound in a central potential V(r) is

$$\Delta E^{Welton}=\frac{\alpha}{3\pi}\left(\frac{\hbar}{mc}\right)^2\ln\left(\frac{mc^2}{E_0}\right)\langle\nabla^2V(\boldsymbol{r})\rangle. \tag{9.43}$$

This equation is valid for all central forces, including the Coulomb potential or the simple harmonic oscillator. Because of our simplifications in the treatment, the shift is not complex, but just represents the real portion of the complex level shift. This equation is the first term in Eq. (11.50), which gives the complex shift derived by field theory for a central potential.

The Welton model is a simple, physically appealing semi-classical model. A modified version of Welton's model has been published by Passante and Rizzuto, in which they perform a rigorous quantum mechanical derivation

[5]The metric is $(-1,1,1,1)$ for $\mu=0,1,2,3$; $i,j=1,2,3$.

[6]We can also derive Eq. (9.42) using a Fourier decomposition of $md^2\boldsymbol{\xi}/dt^2$ and integrating over the frequency distribution of the vacuum field [3].

of the change in the electron orbitals based on the virtual transitions that lead to the radiative shift [243]. This new version does not suffer from some of the drawbacks of Welton's original version.

Welton's model for Coulomb potential

For the Coulomb potential, the Laplacian is given by Eq. (9.31) and (9.32). If we use a quantum mechanical average of the Laplacian, then the expression for the shift for an S state with principal quantum number N is

$$\Delta_N^{Welton} = \frac{4\alpha(Z\alpha)^4 mc^2}{3\pi}\frac{1}{N^3}\int_{E_0}^{mc^2}\frac{dE}{E} \tag{9.44}$$

which can be integrated to give

$$\Delta_N^{Welton} = \frac{4\alpha(Z\alpha)^4 mc^2}{3\pi}\frac{1}{N^3}\ln\frac{mc^2}{E_0} \tag{9.45}$$

where E_0 is a characteristic low energy, which we might choose as the energy of the ground state. For the Coulomb potential, the Laplacian is proportional to $\delta^3(r)$, so classically the shift vanishes since the classical electron is never at the center, whereas quantum mechanically the shift is only for S states. On the other hand, if we happen to compare Eq. (9.45) to Eq. (9.33), we see that if we take the same lower limit $|E_n - E_N|_{Ave}$ as in the Bethe log Eq. (9.34), we get exactly the same total S state shift as in the approximate Bethe formalism Eq. (9.29). With these limits, the RMS amplitude of oscillation of the electron bound in the Coulomb potential $\sqrt{\langle(\vec{\xi})^2\rangle}$ is about 72 fermis, about 1/740 of the mean radius of the 1S electron orbit.

Welton's model for simple harmonic oscillator

For the 3D harmonic oscillator $V = (1/2)m\omega_o^2(x^2+y^2+z^2)$, the Laplacian is a constant $\nabla^2 V = 3m\omega_o^2$, and for the characteristic low energy we take $E_0 = \hbar\omega$, so the shift for every level is a constant equal to

$$\Delta_{SHO}^{Welton} = \frac{\alpha}{\pi}\frac{(\hbar\omega_0)^2}{mc^2}\ln\frac{\hbar\omega_C}{\hbar\omega_0}. \tag{9.46}$$

This level shift is the same as the real part of the complex level shift Eq. (11.57), derived by QED in Chapter 11. For the harmonic oscillator, we get the same constant shift whether we take a classical or a quantum mechanical average. For an oscillator with a ground state energy of 2 eV,

the ln term is about 12.4 and the shift is about 2.3×10^{-7} eV, which is comparable to the $2s_{1/2} - 2p_{1/2}$ lamb shift value of 4.3×10^{-6} eV.

9.3.3 *Feynman's approach (implemented by Power)*

Feynman proposed another approach to compute the Lamb shift: he maintained that the change in the energy in the quantum vacuum due to the presence of the H atoms would exactly equal the Lamb shift. Feynman's approach highlights the changes in the vacuum field energy due to the interactions with the H atoms. Power, based on the suggestion by Feynman, considered the change in vacuum energy when N hydrogen atoms are placed in a volume V, using the expression for the index of refraction $n(\omega_k)$ [3, 203, 244]. The H atoms cause a change in the index of refraction and therefore a change in the frequencies of the vacuum fluctuations present. The corresponding change in vacuum energy ΔE is

$$\Delta E^{Power} = \sum_k \frac{1}{n(\omega_k)} \frac{1}{2} \hbar \omega_k - \frac{1}{2} \hbar \omega_k. \tag{9.47}$$

For a dilute gas of atoms in a level N, the index of refraction is

$$n(\omega_k) = 1 + \frac{4\pi N_d}{3\hbar} \sum_n \frac{\omega_{nN} |\mathbf{d}|^2_{nN}}{\omega^2_{nN} - \omega^2_k}, \tag{9.48}$$

where N_d is the number density, $\omega_{nN} = (E_n - E_N)/\hbar$ and $\mathbf{d}_{nN} = e\mathbf{x}_{nN}$, the transition dipole moment. After substituting $n(\omega_k)$ into Eq. (9.47), we get a divergent result for the energy shift. Following Bethe's approach, we need to subtract from ΔE the energy shift for the N free electrons, which equals the shift when $\omega_{nN} \to 0$, with no binding energy. After making this subtraction and converting the sum over k to an integral over ω, and letting $NV \to 1$, the observable shift in energy is obtained [3]:

$$\Delta E^{Power}_N = -\frac{2}{3\pi c^3} \sum_n \omega^3_{nN} |\mathbf{d}_{nN}|^2 \int_0^{mc^2/\hbar} \frac{d\omega \omega}{\omega^2_{nN} - \omega^2}. \tag{9.49}$$

Noting that

$$\langle n|\mathbf{p}|N\rangle = \frac{i}{\hbar} m \langle n|[H, \mathbf{x}]|N\rangle = \frac{i}{\hbar} m (E_n - E_N) \langle n|\mathbf{x}|N\rangle, \tag{9.50}$$

we can show

$$|\mathbf{p}_{nN}|^2 = m^2 \omega^2_{nN} |\mathbf{x}_{nN}|^2 = \frac{m^2 \omega^2_{nN}}{e^2} |\mathbf{d}_{nN}|^2. \tag{9.51}$$

This allows us to write Power's result Eq. (9.49) as

$$\Delta E_N^{Power} = -\frac{2e^2}{3\pi m^2 c^3} \sum_n \omega_{nN} |\mathbf{p}_{nN}|^2 \int_0^{mc^2/\hbar} \frac{d\omega\omega}{\omega_{nN}^2 - \omega^2}. \tag{9.52}$$

Writing this equation in terms of $E = \hbar\omega$ instead of ω yields

$$\Delta E_N^{Power} = -\frac{2\alpha}{3\pi} \left(\frac{1}{mc}\right)^2 \sum_n |\mathbf{p}_{nN}|^2 (E_n - E_N) \int_0^{mc^2} \frac{EdE}{(E_n - E_N)^2 - E^2} \tag{9.53}$$

In Chapter 14, we will use this equation to analyze the spectral density for Power's method, showing the spectral density is different from Bethe's at low frequencies but the same at high frequencies. When Eq. (9.53) is integrated with respect to E, taking the principal value, we obtain

$$\Delta E_N^{Power} = \frac{2\alpha}{3\pi} \left(\frac{1}{mc}\right)^2 \sum_n |\mathbf{p}_{nN}|^2 (E_n - E_N) \times \ln\left[\frac{mc^2 + (E_n - E_N)}{E_n - E_N} \times \frac{mc^2 - (E_n - E_N)}{E_n - E_N}\right]^{1/2}. \tag{9.54}$$

Except for the argument in the ln function, which corresponds to the upper limit of integration, this is the same as Bethe's expression Eq. (9.33) for the shift. If we assume $mc^2 \gg E_n - E_N$, as Bethe did, then both expressions for the total shift are identical. We know, however, that there are significant contributions to the shift from scattering states E_n that have energies near mc^2. Thus, this approximation is not valid at very high energies of E_n because the second factor in the ln function in Eq. (9.54) may even become less than one since E_N is negative, making the ln term negative.

Milonni and his collaborators have modified the derivation of the Lamb shift that is based on Feynman's approach so that the result is identical to Bethe's result [244]. They note the expression for the index of refraction assumes the presence of a real photon, which leads to an unphysical contribution that is usually eliminated by the choice of the cutoff frequency ω_C. To correct for this problem without relying on the cutoff frequency, they include in the shift the contribution from the self interaction of the atom as well as the contribution from the vacuum fluctuations. When both contributions are included, the total shift is the same as Bethe's result. Their approach would likely eliminate the problematical ln term in Eq. (9.54) that may become negative for very large E_n.

One assumption in the computation by Power is that the index of refraction in the box containing the atoms is spatially uniform. We will return to this assumption and suggest in Chapter 15 a model that predicts, for a single atom, the changes in the vacuum field energy as a function of position for each spectral component of the radiative shift.

9.3.4 *Observing zero-point vibrations of the electron*

We might ask: Why do we not observe point particles with their unrenormalized masses oscillating in the zero point field? The answer is an observation of distances of the order of $\sqrt{\langle \boldsymbol{\xi}^2 \rangle} \approx \sqrt{\alpha}(\hbar/mc)$ (Eq. 9.42), about one tenth of the Compton wavelength, would, by the uncertainty principle, involve momenta of the order of $mc/\sqrt{\alpha}$ and energies of the order of mc^2/α, causing violent uncontrollable perturbations in the zero-point motion and leading to the creation of particle–antiparticle pairs in the vicinity of the particle we were attempting to observe.

To illuminate the nature of the free particle renormalization by analogy, consider an impenetrable massless black box containing a gas. Since $E = mc^2$, the kinetic energy of the gas molecules contributes to inertial mass, and the observable mass depends not only on the mass of the gas molecules but also on their temperature, which indicates their mean kinetic energy. The separate contributions to the observable mass of the box cannot be measured directly, but if we know the temperature, we can compute them. The analogy of this hypothetical situation is quite close to the free particle renormalization since we can regard the zero-point vibration as causing infinite or very large virtual temperature fluctuations. In renormalization, the initial mass of the particle is chosen so that the renormalized mass is equal to the known physical mass.

9.4 General Nature of Radiative Shifts

Before ending this section, it seems important conceptually to stress the general nature of radiative shifts [3, 245–248]. First, we note that a shift in the particle mass from the infinite free space (renormalized) value occurs whenever the particle is not in infinite free space. Not only an external potential, but any object altering the zero-point field of infinite free space will produce a shift in the energy levels of an atom.[7] For example, there

[7] The shift is also dependent on temperature since the vacuum field has a temperature dependent component due to the presence of black body radiation.

is a change in the mass, charge, and magnetic moment of an electron or a change in the Lamb shift of an atom when we put it near a surface or between two surfaces or in a dielectric medium [245, 246, 249, 250].

A second observation we would like to mention is that radiative shifts can occur whenever we have an interaction between a particle and a field, not necessarily just the electromagnetic field. For example, there are shifts for the gravitational field or for the meson field of a nucleus [247].

In the next chapter, we use quantum field theory to derive an expression for the radiative shift of an hydrogen atom.

Chapter 10

The Radiative Shift in Field Theory

There are numerous ways to compute first-order radiative shifts, as explained in detail in excellent texts, for example [3, 172, 173, 175]. We employ a different approach, calculating the shift in terms of the $mass^2$ operator, in hopes that this clarifies the physical significance of renormalization and the shift more clearly than some other methods [251]. We give comments on the various approaches, including the traditional methods. We do not include the effects of electron spin in our first-order non-relativistic calculations. The only assumptions made are the equations of motion and the minimal coupling of the vector potential to the momentum.

10.1 The $Mass^2$ Operator

The radiative shift of a particle can be understood as the difference between the mass renormalization for a bound particle and the mass renormalization for a free particle, which we consider to be a spinless electron or meson. Therefore, we briefly review the mass renormalization of a free electron (assuming that all other quantities except the mass have been renormalized). The equation of motion for a free bare meson field is

$$-\partial'^2\phi_0(x') + m_0^2\phi_0\,(x') = 0, \tag{10.1}$$

where m_0 is the unrenormalized mass[1]. The propagator for the bare meson $G_0(x', x'')$ satisfies the equation

$$(-\partial'^2 + m_0^2)G_0\,(x', x'') = \delta(x' - x''). \tag{10.2}$$

[1]The primes indicate eigenvalues of operators, and unprimed quantities indicate abstract operators. The quantity x' means the four-vector $(t', \boldsymbol{r'})$.

We can rewrite this equation as

$$G_0\left(x', x''\right) = \frac{1}{-\partial'^2 + m_0^2}\delta\left(x' - x''\right) \tag{10.3}$$

or in momentum space

$$G_0(p) = \frac{1}{p^2 + m_0^2}. \tag{10.4}$$

The meson has a charge distribution and therefore interacts with its own electromagnetic field, producing a change in mass. The propagator for a free self-interacting meson becomes

$$G_F(p) = \frac{1}{p^2 + m_{\mathrm{o}}^2 + M_{\mathrm{F}}^2(p)}, \tag{10.5}$$

where $M_F^2(p)$ is the $mass^2$ operator for a free, self-interacting or dressed meson. If m^2 is the observed (renormalized) physical mass, then the propagator $G_F(p)$ must have a pole at $p^2 = -m^2$. Thus,

$$m^2 = m_o^2 + M_F^2(p^2 = -m^2). \tag{10.6}$$

The space-time methods of Feynman, which were developed right after Bethe's calculation, were helpful in providing a physical picture of the phenomena and in facilitating calculations [186]. In that spirit, we consider the diagrams in Fig. 10.1 that show the processes that represent the $mass^2$ operator M_F^2 to order e^2 or α in the radiation field of the meson (one photon of the radiation field is present). By analyzing the $mass^2$ operator in Section 10.5, we show that these are indeed appropriate Feynman diagrams.

In configuration space, the equation of motion for the free self-interacting meson is

$$(p^2 + m_0^2)G_F(x', x'') + \int d^4x''' M_F^2(x' - x''')G_F(x''', x'') = \delta(x' - x''). \tag{10.7}$$

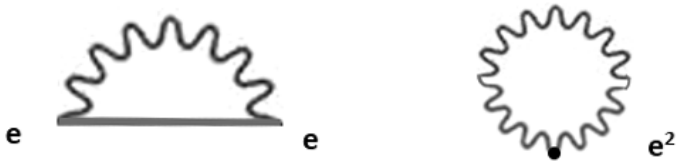

Fig. 10.1. Feynman diagrams for mass renormalization. Time axis is horizontal. The diagram on the left corresponds to the $\boldsymbol{p} \cdot \boldsymbol{A}$ term and shows an electron emitting a virtual photon and then at a later time reabsorbing the photon. The diagram on the right corresponds to the $\boldsymbol{A}^2$ term.

The presence of the convolution integral indicates that we can view the meson as having a finite extent. The shape of the meson centered at r' is proportional to the Fourier transform of $m_0^2 + M_F^2(p)$, namely

$$\delta(r' - r'') + \frac{1}{m^2}(M_F^2(r' - r'') + m_0^2 - m^2). \tag{10.8}$$

The effective finite extent of the meson in the vacuum field is central to the interpretation of the Lamb shift. Alternatively, we can say that we have a point particle, but now it is in a non-local potential. Although we need never explicitly mention the zero-point vibrations in our field-theoretic calculation, we could interpret the Feynman diagrams as corresponding to the zero-point fluctuations or to the interaction of the electron with its own radiation field [172, p. 240].

We can estimate the amplitude $\langle \boldsymbol{\xi}^2 \rangle$ of the zero-point oscillations of the meson (or equivalently, the emission and absorption of virtual photons) by applying the uncertainty relations to the process depicted in Fig. 10.1. When the photon is emitted, the particle receives a momentum k_i with uncertainty Δk_i. Consequently, the uncertainties in the position $\boldsymbol{\xi}$ and velocity $\boldsymbol{v}$ of the particle satisfy the relations $\Delta\xi > 1/\Delta k_i$ and $\Delta v_i \approx \Delta k_i/m$. Requiring that $\Delta v_i \approx 1$ implies that $\Delta k_i \approx m$ and $\Delta\xi_i > 1/m =$ Compton wavelength. To get the effective $\langle \boldsymbol{\xi}^2 \rangle$, we must multiply by the probability that the photon has been emitted. The diagram has two vertices so the probability is proportional to α, which leads to the result $\alpha(\Delta\xi)^2 = \langle \boldsymbol{\xi}^2 \rangle \approx 3\alpha/m^2 = 3\alpha(\hbar/mc)^2$ the mean amplitude squared of the zero-point vibrations, which is comparable to the result (Eq. 9.42) obtained using the equations of motion for the vector potential.

When we place a bare meson (or spinless electron) in an external potential, we assume that it forms a bound state. The propagator and therefore the equations of motion are as before except that: (1) the free $mass^2$ operator M_F^2 is replaced by a bound state mass operator M^2; (2) the propagator G_F for a free particle with radiative interaction is replaced by the corresponding propagator G for a bound particle; and (3) p_μ is replaced by the four-vector by $\Pi_\mu = p_\mu - V_\mu$, where V_μ is the external four-potential in accordance with minimal coupling [3]. The energy of the bound state is shifted by a mechanism similar to that for a free bare meson. The Feynman diagrams are shown in Fig. 10.2.

The double line represents a meson propagating in the external potential. The difference between the diagrams for the bound meson and the free meson corresponds to the radiative level shift (Fig. 10.3). In other words, the radiative shift in a bound state level is the change in the self-energy of

Fig. 10.2. Feynman diagrams for the bound state mass renormalization. The double line represents a meson bound in an external potential.

Fig. 10.3. Feynman diagrams showing the level shift is the difference between the bound state mass renormalization and the free particle mass renormalization. The double line represents a meson bound in an external potential.

a particle that occurs when it becomes bound. As discussed in Section 8.2, this is exactly the way Bethe framed the problem of computing the Lamb shift. The intermediate state of the atom, i.e., while the virtual radiation field photon has been exchanged, is unknown. In his historic approach, the cumulative effect of these virtual transitions is given by the Bethe log term.

To indicate in more detail the process involved in the radiative shift for a Coulomb potential, we expand the double line representation of the bound meson, indicating separate meson and proton lines and the photons exchanged that represent the Coulomb force (Fig. 10.4). The graphs that give the radiative changes are of the form shown in Fig. 10.5. The lowest order shift, to order α (first order) in the radiation field and $(Z\alpha)^4$ (second order) in the Coulomb field, is given simply by the vertex correction (Fig. 10.6).

Rather than consider separately all the various graphs in the Coulomb field and obtain an answer in a series with powers of $Z\alpha$ or $ln(Z\alpha)$ as is done with higher order calculations [152, 199, 214, 219], we calculate the radiative correction using the equations of motion for a meson (spinless electron) in a Coulomb field and then make approximations to first order assuming that the proton or Coulomb source is an infinitely heavy point charge. We are neglecting relativistic effects, recoil effects, center of mass corrections, radiative corrections and size effects for the proton. To include these effects,

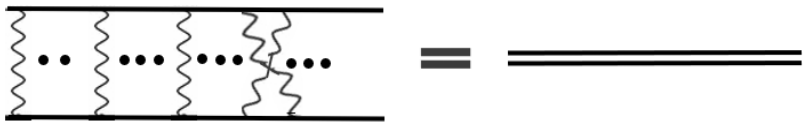

Fig. 10.4. Feynman diagrams for the meson (top line) bound to the Coulomb field of a proton (bottom line). The dots indicate that all possible configurations of Coulomb photons, including crossed photon lines, are to be included.

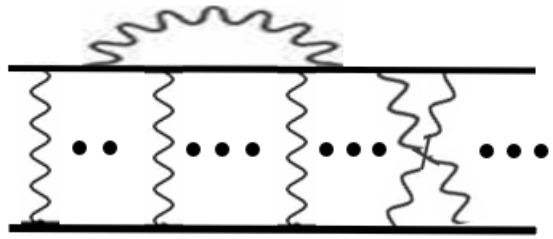

Fig. 10.5. Feynman diagrams for the meson (top line) bound to the Coulomb field of a proton (bottom line), with the exchange of Coulomb photons and one radiative photon emitted and reabsorbed by the meson.

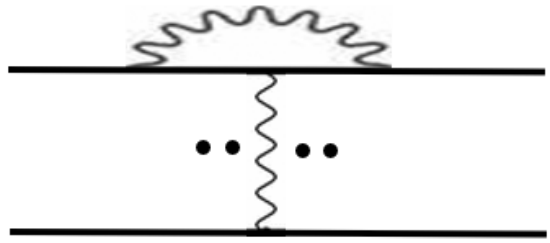

Fig. 10.6. Feynman diagram for lowest order radiative correction to the bound meson.

we would need to use the Bethe–Salpeter equation [95, 158, 223]. On the other hand, Weinberg (in 1995) did not think the Bethe–Salpeter equation was the correct equation for relativistic interactions (it includes no crossed photon diagrams), and he concluded: "It must be said that the theory of relativistic effects and radiative corrections in bound states is not yet in entirely satisfactory shape" [173].

In general, we are concerned with directly measurable quantities, namely the shift in the energy difference between two states of a bound meson. For example, we calculate the change in the $2s$-$2p$ separation. Clearly, this shift

is given by the difference in renormalization between a meson bound in a $2s$ state and one bound in a $2p$ state. Thus, the renormalization of a free meson is never actually used.

10.2 Expressing the Radiative Shift in Terms of the Matrix Elements of the $Mass^2$ Operator

From the equation for the propagator of a self-interacting meson in a potential $V^\mu(x)$, we can find the equation obeyed by the corresponding meson wave functions. Taking mass-renormalized wave functions of the meson in the potential field as our unperturbed states, we apply first-order perturbation theory to find the expression for the radiative shift in terms of matrix elements of the perturbation $\overline{M}^2$. The Green function or propagator for a meson field $\phi(x')$ that interacts with its own radiation field and the external potential V_μ satisfies the equation:

$$(\Pi'^2 + m^2 + \overline{M}^2)G(x', x'') = \delta(x' - x''), \tag{10.9}$$

where

$$\Pi'_\mu = \frac{1}{i}\partial'_\mu - V_\mu(x'), \tag{10.10}$$

m is the physical mass, M^2 is the $(mass)^2$ operator and $\overline{M}^2$ is the renormalized $mass^2$ operator for a meson in a Coulomb potential

$$\overline{M}^2 = M^2 + m_0^2 - m^2. \tag{10.11}$$

Equation (10.9) is similar in form to Eq. (10.7). However, in Eq. (10.7) we explicitly indicate the integration over x''', whereas in Eq. (10.9) we use a shorthand notation for integration. We assume that our four-potential is such that we can work in a gauge with $V_i = 0, V^0 = V(r)$. Since we want an energy shift, we take the Fourier transform of Eq. (10.9) with respect to time

$$(p'^2 - (\widetilde{E} - V')^2 + m^2 + \overline{M}^2(\widetilde{E}))G(\widetilde{E}, \boldsymbol{r}', \boldsymbol{r}'') = \delta(\boldsymbol{r}' - \boldsymbol{r}''), \tag{10.12}$$

where we define

$$\overline{M}^2(\widetilde{E})\mathrm{G}(\widetilde{\mathrm{E}}, \mathbf{r}', \mathbf{r}'') \equiv \int \mathrm{d}^3\mathrm{r}'''\overline{M}^2(\widetilde{\mathrm{E}}, \mathbf{r}', \mathbf{r}''')\mathrm{G}(\widetilde{\mathrm{E}}, \mathbf{r}''', \mathbf{r}'') \tag{10.13}$$

and $\widetilde{E}$ is the relativistic total energy. We can convert Eq. (10.12) to an equation for the wave functions by expressing the Green function as the

vacuum expectation value of the time ordered product of the meson field $\phi(x')$:

$$G(x', x'') = i\langle(\phi(x')\phi^\dagger(x''))_+\rangle. \tag{10.14}$$

If we insert a complete set of eigenstates of the Hamiltonian (particle, antiparticle, bound, and scattering) in this equation for G and use the equation of motion for $\phi(x)$:

$$\phi(\boldsymbol{r}, t) = e^{iHt}\phi(\boldsymbol{r}, 0)e^{-iHt}, \tag{10.15}$$

we find

$$\mathrm{G}(\widetilde{\mathrm{E}}, \mathbf{r}', \mathbf{r}'') = \sum_{\mathrm{k}} \frac{\Phi_{\mathrm{k}}(\boldsymbol{r}')\,\Phi_{\mathrm{k}}(\boldsymbol{r}'')}{\widetilde{E} - \widetilde{E}_{\mathrm{k}}} + \text{contribution of scattering states.} \tag{10.16}$$

The $\Phi_k(\boldsymbol{r})$ are the relativistic bound state particle wave functions $\langle 0|\phi(\boldsymbol{r}, 0)|\widetilde{E}_k\rangle$ with the renormalized mass and a relativistic total energy $\widetilde{E}_k$. If Eq. (10.12) is to be satisfied when we substitute this form for G and let $k = n, \widetilde{E} = \widetilde{E}_n$, and $r' \neq r''$, then it follows that

$$(p'^2 + m^2 - (\widetilde{E}_n - V')^2 + \overline{M}^2(\widetilde{E}_n))\Phi_n(\boldsymbol{r}') = 0. \tag{10.17}$$

We now use first-order perturbation theory to calculate the radiative shift due to $\overline{M}^2(\widetilde{E}_n)$. The unperturbed wave functions are the renormalized relativistic wave functions $\widetilde{\psi}_n(\boldsymbol{r}')$ for a meson which satisfy the equation

$$[p'^2 - (\widetilde{E}_n^0 - V')^2 + m^2]\widetilde{\psi}_n(\boldsymbol{r}') = 0, \tag{10.18}$$

where $\widetilde{E}_n^0$ is the unperturbed relativistic energy eigenvalue. For our normalization, we choose

$$(\widetilde{\psi}_n, (\widetilde{E}_n^\circ - \mathrm{V}')\widetilde{\psi}_n) = m, \tag{10.19}$$

where the scalar product is defined as follows:

$$(\phi, A\psi) = \int d^3r'\, \phi^*(\boldsymbol{r}')(A\psi(\boldsymbol{r}')). \tag{10.20}$$

We note that $\Phi_n(r')$ equals $\widetilde{\psi}(r')$ plus higher order terms. We take the scalar product of Eq. (10.17) with $\widetilde{\psi}_n$ and substitute Eq. (10.19) and Eq. (10.20)

and obtain, to lowest order in the radiation field, the shift for the state N:

$$\Delta\widetilde{E}_N \equiv \widetilde{E}_N - \widetilde{E}_N^0 = \frac{1}{2m}(\widetilde{\psi}_N,\, \overline{M}^2(\widetilde{E}_N)\widetilde{\psi}_N), \tag{10.21}$$

which is shorthand for

$$\Delta\tilde{E}_{\mathrm{N}} = \frac{1}{2m}\int d^3r\, \tilde{\psi}^*_{\mathrm{N}}(\boldsymbol{r}') \int d^3r''\overline{M}^2(\tilde{E}_{\mathrm{N}}, \boldsymbol{r}', \boldsymbol{r}'')\tilde{\psi}_{\mathrm{N}}(\boldsymbol{r}''). \tag{10.22}$$

If we define the relativistic state $|\widetilde{n}\rangle$ such that $\tilde{\psi}_n(\boldsymbol{r}') \equiv \langle r'|\tilde{n}\rangle$ and note that

$$\overline{M}^2(\widetilde{E}_{\mathrm{n}}, \boldsymbol{r}', \boldsymbol{r}'') = \langle \boldsymbol{r}'|\overline{M}^2(\widetilde{E}_n)|\boldsymbol{r}''\rangle \tag{10.23}$$

then we obtain the simple and important result

$$\Delta\widetilde{E}_{\mathrm{N}} = \frac{1}{2\mathrm{m}}\langle\widetilde{N}|\overline{M}^2(\widetilde{E}_N)|\tilde{\mathrm{N}}\rangle. \tag{10.24}$$

The radiative shift of the level $\widetilde{E}_N$ is equal to $1/2m$ times the expectation value of the renormalized $(mass)^2$ operator $\overline{M}^2(\widetilde{E}_N)$ with respect to the state $\langle\widetilde{N}|$, where $\widetilde{E}$ is the relativistic energy.

In Sections 10.5 and 11.2, we derive an expression for $\overline{M}^2$ to order α in the radiation field by using the equations of motion for the meson in an external potential, a method we believe is closest to fundamental principles.

10.3 S Matrix Approach

As an alternative to our approach, we should mention that it is possible to use the S matrix formalism to find the radiative shift. As mentioned in Section 8.2, Dyson showed the equivalence of the QED formulations of Schwinger and Feynman with the S matrix formalism [195, 196]. For the Lagrangian interaction, we use

$$L_{\mathrm{int}} = \mathrm{e}j_\mu A^\mu_{rad}, \tag{10.25}$$

where A^μ_{rad} is the radiation field of the meson and j^μ is the current of the meson in the potential field. We calculate the S matrix element between pure bound states with the usual harmonic time dependence. Since we have a perturbation to a bound state, the matrix element must be expressed in the form $\langle S\rangle_{\mathrm{N}} = \mathrm{e}^{-\mathrm{iT}(\widetilde{\mathrm{E}}_N - \widetilde{\mathrm{E}}^0_{\mathrm{N}})}$, where T is the interaction time. To obtain the shift, we perform the integrations and use the usual trick of equating T and $2\pi\delta(0)$.

10.4 Derivation of $Mass^2$ Operator for a Relativistic Meson (Spinless Electron) in an External Potential

We calculate $\overline{M}^2(\widetilde{E})$ in a covariant gauge in which the meson radiation field A^{μ}_{rad} and the meson field ϕ obey the equations:

$$\begin{aligned}
\left[\dot{A}^{\mu}_{rad}(x'), A^{\nu}_{rad}(x'')\right] &= ig^{\mu\nu}\delta(x'-x'') \\
[A^{\mu}_{rad}(\boldsymbol{r'},t), A^{\nu}_{rad}(\boldsymbol{r''},t)] &= 0 \\
\left[A^{0}_{rad}(\boldsymbol{r}',t), \phi(\boldsymbol{r}'',t)\right] &= 0 \\
\left[\partial_0 A^{0}_{rad}(\boldsymbol{r}',t),\ \phi(\boldsymbol{r}'',t)\right] &= 0.
\end{aligned} \tag{10.26}$$

Since the results are gauge invariant, we can choose the Feynman gauge in order to simplify the calculation. In the final answer, we simply replace the Feynman propagator with the radiation gauge propagator. The derivation proceeds by converting the Klein–Gordon equation for a self-interacting meson in an external potential into an equation for the corresponding Green function $G(x', x'')$. An explicit form for $M^2(\widetilde{E})$ is then obtained by comparing this equation to the defining equation for G which includes M^2 (Eq. (10.9)). If desired, skip the mathematics and go to Section 10.5.

To take electromagnetic self-interactions into account in the Klein–Gordon equation, we make the substitution

$$\Pi'_{\mu} \to \Pi'_{\mu} - eA_{\mu,rad}(x'), \tag{10.27}$$

where Eq. (10.10) defines $\Pi'_{\mu} = (1/i)\partial'_{\mu} - V_{\mu}(x')$, with the result

$$(\Pi'^2 + m_0^2)\phi(x') = j(x'), \tag{10.28}$$

where

$$j\,(x') = e\left\{A^{rad}_{\mu}(x'), \Pi'^{\mu}\right\}\phi\,(x') - e^2 A^{\mu}_{rad}\,(x')\,A_{\mu,rad}\,(x')\,\phi(x'). \tag{10.29}$$

The anticommutator ensures that the term $\boldsymbol{A}\cdot\boldsymbol{p}$ is Hermitian. To convert Eq. (10.28) into an equation for $G(x', x'')$, we make use of the definition of $G(x', x'')$ Eq. (10.14). We multiply from the right by $\phi^{\dagger}(x'')$, time order, and take the vacuum expectation value. We use the equation

$$\begin{aligned}
\partial'^2(\mathrm{A}(x')\mathrm{B}(x''))_+ = {} & (\partial'^2\mathrm{A}(x')\mathrm{B}(x''))_+ \\
& + [\partial'_0\mathrm{A}(x'), \mathrm{B}(x'')]\delta(t'-t'') \\
& + \partial'_0[\mathrm{A}(x'), \mathrm{B}(x'')]\delta(t'-t'') \\
& + [\mathrm{A}(x'), \mathrm{B}(x'')]\delta'(t'-t''),
\end{aligned} \tag{10.30}$$

which follows from the lemma

$$\partial_0'(A(x')B(x''))_+ = (\partial_0 A(x')B(x''))_+ + [A(x'), B(x'')]\delta(t'-t'') \quad (10.31)$$

to obtain the result

$$(\Pi'^2 + m_0^2)G(x', x'') = +\delta(x'-x'') + i\langle(j(x')\phi^\dagger(x''))_+\rangle. \quad (10.32)$$

Since we are calculating $\overline{M}^2$ to order e^2 in the radiation field, the term $e^2\langle(A_\mu^{\rm rad}(x')\,A_{\rm rad}^\mu(x')\,\phi(x')\,\phi^\dagger(x''))_+\rangle$ in $\langle(j(x')\phi^\dagger(x''))_+\rangle$ can be calculated with the field of a free photon rather than with the radiation field. In essence, this follows since the radiation field is equal to the free field plus terms of higher order. This is essentially why we get the same result whether we assume the radiative shift is due to interaction with either the vacuum field or the radiation field of the atom. To show the formal justification, consider the matrix element

$$\sigma = \langle(A^\mu(\xi')A^\nu(\xi'')\phi(x')\phi^\dagger(x''))_+\rangle. \quad (10.33)$$

Recall

$$\partial_{\xi'}^2 A^\mu(\xi') = ej^\mu(\xi'), \quad (10.34)$$

thus

$$\begin{aligned}\partial_{\xi'}^2\sigma = {} & e\langle(j^\mu(\xi')A^\nu(\xi'')\phi(x')\phi^\dagger(x''))_+\rangle \\ & + ig^{\mu\nu}\delta(\xi'-\xi'')\langle(\phi(x')\phi^\dagger(x''))_+\rangle. \end{aligned} \quad (10.35)$$

To lowest order, we may drop the first term. Solving for σ gives

$$\sigma = \left[g^{\mu\nu}\frac{1}{\partial_{\xi'}{}^2}\delta(\xi'-\xi'')\right]G(x', x''). \quad (10.36)$$

Considering the boundary conditions, we realize that the term in brackets is just the usual Feynman propagator. Accordingly, we obtain

$$\sigma = -D^{\mu\nu}(\xi'-\xi'')G(x', x''). \quad (10.37)$$

This result is to be expected since to lowest order the complete Hilbert space factors into two independent spaces, one for $\phi(x')$ and one for $A(x')$.

Thus, we have shown that

$$\langle (j(x')\phi(x''))_+\rangle = ie^2\langle (A_\mu(x')A^\mu(x'))_+\rangle G(x',x'') + e\langle ((A_\mu^{rad}(x')\Pi'^\mu + \Pi'^\mu A_\mu^{rad}(x'))\phi(x')\phi(x''))_+\rangle. \tag{10.38}$$

We can rewrite the second term on the right side using the notation

$$\overrightarrow{\Pi}'^\mu A_\mu^{rad}(x')\phi(x') \equiv (A_\mu^{\rm rad}\ (x')\Pi'^\mu + \Pi'^\mu A_\mu^{rad}(x'))\phi(x') = \left(\frac{1}{i}\partial^\mu_{\xi'} + \frac{2}{i}\partial^\mu_{x'} - 2V^\mu(x')\right) A_\mu^{\rm rad}(\xi')\phi(x')|_{\xi'=x'}. \tag{10.39}$$

From Eq. (10.32), we have

$$(\Pi'^2 + m_0^2)G(x',x'') = \delta(x'-x'') + ie\overrightarrow{\Pi}'^\mu\langle (A_\mu^{rad}(x')\phi(x')\phi^\dagger(x''))_+\rangle - e^2\langle (A_\mu(x')A^\mu(x'))_+\rangle G(x',x''). \tag{10.40}$$

Using Eq. (10.9) and Eq. (10.11) for the unrenormalized $mass^2$ operator M^2 shows the last two terms on the right side of Eq. (10.40) are equal to

$$-M^2G(x',x'') = ie\overrightarrow{\Pi}'^\mu\langle (A_\mu^{rad}(x')\phi(x')\phi^\dagger(x''))_+\rangle - e^2\langle (A_\mu(x')A^\mu(x'))_+\rangle G(x',x''). \tag{10.41}$$

where $M^2G(x',x'')$ represents a convolution integral as in Eq. (10.13). To order e^2, we may replace the full propagator G by the Coulomb propagator G^c for a particle in the potential with the physical mass:

$$(\Pi'^2 + m^2)G^c(x',x'') = \delta(x'-x''). \tag{10.42}$$

Operating on Eq. (10.41) from the right with $\Pi^2(x'') + m^2$ therefore gives

$$M^2(x',x'') = -{\rm ie}\ \overrightarrow{\Pi}'^\mu\langle (A_\mu^{\rm rad}\ (x')\phi(x')\phi^\dagger(x''))_+\rangle(\Pi^2(x'') + m^2) + e^2\langle (A_\mu(x')A^\mu(x'))_+\rangle\delta(x'-x''). \tag{10.43}$$

Following the same procedure as before gives the result

$$M^2(x',x'') = -{\rm ie}^2\overrightarrow{\Pi'^\mu}(x')\langle (A_\mu(x')A^\nu(x'')\phi(x')\phi^\dagger(x''))_+\rangle\overleftarrow{\Pi}_\nu(x'') + e^2\langle (A_\mu(x')A^\mu(x'))_+\rangle\delta(x'-x''), \tag{10.44}$$

which is a shorthand notation for

$$M^2(x',x'') = ie^2\left(\frac{2}{i}\partial^{\mu}_{x'} + \frac{1}{i}\partial^{\mu}_{\xi'} - 2V^{\mu}(x')\right) D_{\mu\nu}(\xi'-\xi'')G^c(x',x'')$$
$$\times\left(\frac{2}{i}\partial^{\nu}_{x''} + \frac{1}{i}\partial^{\nu}_{\xi''} - 2V^{\mu}(x'')\right)|_{\xi''=x'',\,\xi'=x'}$$
$$-\,\mathrm{ie}^2 D^{\mu}_{\mu}(0)\delta(x'-x''). \tag{10.45}$$

Since our calculation is to order α or e^2, we have again substituted G^c for $G(x',x'')$. Now that we have derived the equation for $M^2(x',x'')$, we return to the radiation gauge.

10.5 The Expression for $M^2(\widetilde{E})$

For our calculation of the radiative shift, we need the operator corresponding to the time Fourier transform of $M^2(x',x'')$. To obtain this result, we use the expression for G^c which follows from Eq. (10.42) and the invariance for translations in time[2]:

$$G^c\,(x',x'') = \int_{-\infty}^{\infty}\frac{d\widetilde{E}}{2\pi}\left\langle r'\left|\frac{1}{\Pi^2+m^2-i\epsilon}\right|r''\right\rangle e^{-i\widetilde{E}(t'-t'')}, \tag{10.46}$$

where

$$\Pi^k = p^k, \quad \Pi^0 = \widetilde{E} - V(r). \tag{10.47}$$

If we substitute Eq. (10.46) and

$$D_{\mu\nu}\,(\xi'-\xi'') = \int\frac{d^4k}{(2\pi)^4}e^{ik(\xi'-\xi'')}D_{\mu\nu}(k) \tag{10.48}$$

into our expression for M^2, Eq. (10.45), and we note the derivative with respect to ξ'_{μ} brings down a factor of k_{μ}, we find, after some computation,

[2]To validate this expression for G^c we operate on the integral with Π'^2+m^2. We observe $\Pi'^k < r'| =< r'|\Pi^k$, $\Pi'^0 < r'| =< r'|\Pi^0$ so $(\Pi'^2+m^2) < r'| =< r'|(\Pi^2+m^2)$. With the normalization $< r'|r'' >= \delta(r'-r'')$, it follows the integral obeys the defining equation for G^c.

the important result for the unrenormalized relativistic $mass^2$ operator

$$M^2(\widetilde{E}) = \frac{ie^2}{2}\int \frac{d^4k}{(2\pi)^4} D_{\mu\nu}(k) T^{\mu\nu}, \tag{10.49}$$

where

$$T^{\mu\nu} = (2\Pi^\mu - k^\mu)\frac{1}{(\Pi - k)^2 + m^2}(2\Pi^\nu - k^\nu) + (2\Pi^\nu + k^\nu)\frac{1}{(\Pi + k)^2 + m^2}(2\Pi^\mu + k^\mu) - 2g^{\mu\nu}. \tag{10.50}$$

We exploit the symmetry of the photon propagator under $k \to -k$ to write $T^{\mu\nu}$ in a form that manifests crossing symmetry. From the Feynman rules we see that the diagrams corresponding to the operator $T^{\mu\nu}$ are shown in Fig. 10.7.

The double line in the figure refers to the meson propagating in an external potential. $T^{\mu\nu}$ is the operator Compton scattering amplitude in the forward direction. The seagull term on the right in Fig. 10.7 must be included to insure gauge invariance. At threshold, it gives the Thomson scattering amplitude. As Eq. (10.49) indicates, we obtain the diagrams for M^2 by contracting the diagrams for $T^{\mu\nu}$ with the diagram for the photon propagator $D_{\mu\nu}$, giving the resulting Feynman diagrams for M^2 in Fig. 10.8. The crossed diagram may be deformed into the uncrossed diagram; therefore, both diagrams give equal contributions to M^2. Note that, in a calculation of the shift between two levels, the bubble term gives no contribution since its matrix elements are independent of the state.

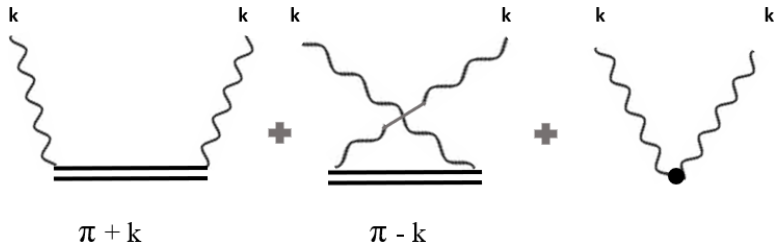

Fig. 10.7. Feynman diagrams for the Compton scattering amplitude $T^{\mu\nu}$ of a photon by a bound meson (double line).

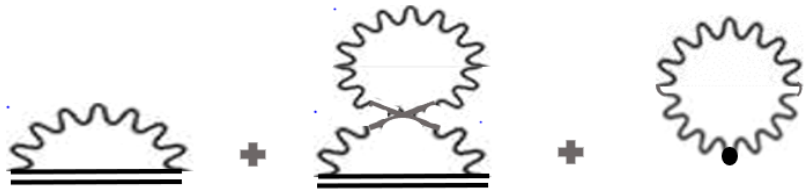

Fig. 10.8. Feynman diagrams for M^2 that give the radiative shift of a bound meson, The shift arises from the Compton scattering amplitude (Fig. 10.7) of virtual radiation photons by a bound meson (double line).

10.6 Gauge Invariance of the Shift $\widetilde{\Delta E_N}$ for a Relativistic Meson (Spinless Electron)

We must show that the most general gauge transformation [174]

$$D_{\mu\nu} \to D_{\mu\nu} + \lambda' n_\mu k_\nu + \mu' n_\nu k_\mu + \nu' k_\mu k_\nu \tag{10.51}$$

induces no change in the observed shift. Under a gauge transformation, the radiative shift changes by an amount

$$\delta(\Delta\widetilde{\mathrm{E}}_{\mathrm{N}}) = \frac{1}{2\mathrm{m}}\frac{\mathrm{ie}^2}{2}\int \frac{\mathrm{d}^4\mathrm{k}}{(2\pi)^4}\langle\widetilde{\mathrm{N}}|\lambda' n_\mu k_\nu T^{\mu\nu} + \mu' n_\nu k_\mu \mathrm{T}^{\mu\nu} + \nu' k_\mu k_\nu \mathrm{T}^{\mu\nu}|\widetilde{N}\rangle. \tag{10.52}$$

We contract $T^{\mu\nu}$ with k_μ and use the identities

$$\begin{aligned} k(2\Pi + k) &= (\Pi + k)^2 + m^2 - \left(\Pi^2 + m^2\right) \\ k(2\Pi - k) &= -[(\Pi - k)^2 + m^2] + \Pi^2 + m^2 \end{aligned} \tag{10.53}$$

to obtain

$$\begin{aligned} k_\mu T^{\mu\nu} = {} & (2\Pi^\nu + k^\nu) - (\Pi^2 + m^2)\frac{1}{(\Pi + k)^2 + m^2}(2\Pi^\nu + k^\nu) \\ & - (2\Pi^\nu - k^\nu) + (2\Pi^\nu - k^\nu)\frac{1}{(\Pi - k)^2 + m^2}(\Pi^2 + m^2) \\ & - 2k^\nu. \end{aligned} \tag{10.54}$$

For our unperturbed basis states, we have

$$\left(\Pi^2 + m^2\right)|\widetilde{N}\rangle = 0. \tag{10.55}$$

Consequently, $\langle\widetilde{N}\,|k_\mu T^{\mu\nu}|\,\widetilde{N}\rangle = 0$. Since $T^{\mu\nu}(k) = T^{\nu\mu}(-k)$ it follows that $\langle\widetilde{N}\,|k_\nu T^{\mu\nu}|\,\widetilde{N}\rangle = 0$. Accordingly, we see that $T^{\mu\nu}$ is gauge invariant between physical states and that $\delta(\widetilde{\Delta E_N})$ vanishes. Now that we have an expression for the $mass^2$ operator, we can evaluate it to determine the shift. In the next chapter, we make a non-relativistic approximation of the shift.

Chapter 11

Calculation of the Radiative Shifts in the Non-relativistic Approximation

In this chapter, we consider the expression for the radiative level shifts in the dipole approximation, clarifying the physical meaning of the approximation and its relationship to the non-relativistic approximations. We show that the shift is complex: the imaginary part corresponding to the width for decay by dipole emission and the real part corresponding to the displacement of the energy level. This result is an extension of Bethe's second-order perturbation theory calculation of just the level shift. We show that the real and imaginary parts satisfy a dispersion relation, which is fundamentally just an expression of causality [169]. We interpret the radiative shift as due to the virtual transitions induced by the interaction of the particle with its own radiation field. This interaction means that for a given energy level, there is a finite width and that the mean energy, averaged over time, is shifted. After developing the results for an arbitrary central force potential, we illustrate two particular cases: the harmonic oscillator potential and the Coulomb potential.

11.1 Relationship to the Dipole Approximation

The dipole approximation and the non-relativistic approximation are often considered as two separate approximations. In radiative shift calculations, the dipole approximation is often given by the prescription: In the radiation gauge compute the shift ignoring the dependence of $T^{\mu\nu}$ on the photon three-momentum $\boldsymbol{k}$. As a consequence, we find that the term $T^{00}D_{00}$ corresponding to the static Coulomb or longitudinal photon interaction gives a vanishing contribution to the shift. In this way, the dipole

approximation breaks gauge invariance, which is why we must specify the gauge.

Another form of the dipole approximation is to let $\boldsymbol{A}(\boldsymbol{r})$ be independent of $\boldsymbol{r}$. To understand the properties of this form of the dipole approximation under gauge transformations, consider the non-relativistic interaction Hamiltonian for radiation with a four-potential $(\phi(\boldsymbol{r}), \boldsymbol{A}(\boldsymbol{r}))$ and a scalar particle of charge e and mass m:

$$H_I = -\frac{e}{m}(\boldsymbol{p}\cdot\boldsymbol{A}) + e\phi. \tag{11.1}$$

Under a gauge transformation $\boldsymbol{A} \rightarrow \boldsymbol{A} + \boldsymbol{\nabla}\lambda$, $\phi \rightarrow \phi - \partial_t\lambda$, and H_I transforms into $H_I + \Lambda$, where

$$\Lambda = -\frac{e}{m}\boldsymbol{p}\cdot\boldsymbol{\nabla}\lambda - e\partial_t\lambda. \tag{11.2}$$

To obtain gauge invariance, the matrix elements of Λ between the initial and final states must vanish: $\langle f|\Lambda|i\rangle = 0$. If we let $\lambda = e^{i\boldsymbol{k}\cdot\boldsymbol{r}-i\omega t}$, then gauge invariance requires that

$$\left\langle f \left| \frac{1}{m}\boldsymbol{p}\cdot\boldsymbol{k}\, e^{i\boldsymbol{k}\cdot\boldsymbol{r}} - \omega\, e^{i\boldsymbol{k}\cdot\boldsymbol{r}} \right| i \right\rangle = 0. \tag{11.3}$$

Following the customary prescription for the dipole approximation, we set $exp(i\boldsymbol{k}\cdot\boldsymbol{r})$ equal to unity, then, since $\langle f|i\rangle = 0$, we conclude that the matrix element $\langle f|\boldsymbol{p}\cdot\boldsymbol{k}|i\rangle$ must vanish if we are to obtain gauge invariance. Clearly, this is not generally the case and gauge invariance is violated. The difficulty lies in the fact that setting the exponential equal to one resulted in approximating the change in the vector potential to the first order in k and the change in the scalar potential to zero order in k. If we approximate the change in the scalar potential to one order higher, then we find that the gauge invariance requires

$$\left\langle f \left| \frac{1}{m}\boldsymbol{p}\cdot\boldsymbol{k} - i\omega\boldsymbol{k}\cdot\boldsymbol{r} \right| i \right\rangle = 0. \tag{11.4}$$

In fact, this quantity vanishes since

$$\begin{aligned} \left\langle f \left| \frac{\boldsymbol{p}}{m} \right| i \right\rangle &= i\langle f|[H,\boldsymbol{r}]\rangle i\rangle = i\,(\mathrm{E}_f - \mathrm{E}_i)\,\langle f|\boldsymbol{r}|i\rangle \\ &= i\omega\langle f|\boldsymbol{r}|i\rangle. \end{aligned} \tag{11.5}$$

In the radiation gauge, the scalar potential vanishes, thus we circumvent these difficulties.

Alternatively, we may obtain the unrenormalized M^2 operator in the non-relativistic approximation from a different perspective, by noting that

the pole in the photon propagator in Eq. (10.49) ensures that the integration over k^0 leads to the result $|\boldsymbol{k}| = k^0$ but since $|\boldsymbol{k}|$ is a momentum it equals a frequency over the speed of light $|\boldsymbol{k}| = \omega/c$. As c increases the magnitude of the spatial momentum vanishes and we obtain the dipole approximation. Seen in this way, the dipole approximation is not gauge dependent but simply part of the non-relativistic approximation. If we work in the radiation gauge, then this method gives the same result obtained from the usual proscription.

From dynamical considerations we can show that in a bound system characterized by a small coupling constant the motion is non-relativistic and $|\boldsymbol{k}|$, the approximate change in momentum for radiative transitions between states, may be neglected with respect to the momentum p of the bound particle.

Consider a potential of the form

$$V(r) = \frac{1}{n} m g^{n+2} (mr)^{\mathrm{n}} \quad \mathrm{n} \geq -2. \tag{11.6}$$

The exponent of the mass m is chosen so that the coupling constant g is dimensionless; the exponent of g and the overall coefficient are chosen so that V agrees with the conventional expressions for the simple harmonic oscillator ($n = 2, g = \sqrt{\omega_0/m}$ and the Coulomb potential ($n = -1, g = Z\alpha$). The total non-relativistic energy of the atom is $E = T + V$. The virial theorem for our potential is $\bar{T} = -(n/2)\bar{V}$. Applying the uncertainty principle we find

$$p \approx \frac{1}{r} \approx gmc, \quad \mathrm{E} \approx \frac{n+2}{2n} g^2 mc^2, \tag{11.7}$$

where c is the speed of light. These results justify the use of non-relativistic dynamics for small g. The contribution to the shift of a bound state energy level will be greatest per Hz for resonant virtual transitions, that is, when the photon energy equals the difference between two energy levels. For these resonant transitions $E \approx |\boldsymbol{k}|c$ and

$$\left| \frac{\boldsymbol{k}}{\boldsymbol{p}} \right| \sim \frac{E}{pc} \sim \left| \frac{n+2}{2n} \right| g << 1 \tag{11.8}$$

for weak coupling. To insure that the non-relativistic approximations remain valid during integration over frequency, it may be necessary to use a cutoff which is proportional to the mass. The shift for greater frequencies for physically realistic situations can be calculated by neglecting the bound state energy and keeping only the lowest order terms in the coupling constant.

To understand the physical meaning of the dipole approximation more clearly, we employ the translation operator in momentum space $e^{i\boldsymbol{k}\cdot\boldsymbol{r}}$ to show that for a function $f(p)$, we have the identity

$$\begin{aligned}&\langle N|(2\boldsymbol{p}-\boldsymbol{k})f(\boldsymbol{p}-\boldsymbol{k})(2\boldsymbol{p}-\boldsymbol{k})|N\rangle\\&\quad=\langle N|e^{i\boldsymbol{k}\cdot\boldsymbol{r}})(2\boldsymbol{p}+\boldsymbol{k})f(\boldsymbol{p})(2\boldsymbol{p}+\boldsymbol{k})(e^{-i\boldsymbol{k}\cdot\boldsymbol{r}}|N\rangle.\end{aligned}\tag{11.9}$$

Applying this result to the expressions for $M^2(E)$ and $T^{\mu\nu}$ (Eq. (10.49) and Eq. (10.50)), we see that the matrix elements for the shift are between translated atomic states ($e^{-i\boldsymbol{k}\cdot\boldsymbol{r}}|N\rangle$) that have a center of mass momentum $-\boldsymbol{k}$ in order to conserve momentum when the virtual photon of momentum $+\boldsymbol{k}$ is emitted. In addition, from the Feynman rules for spinless mesons, we know that the $\boldsymbol{k}$ present in $2\boldsymbol{p}+\boldsymbol{k}$ ensures momentum conservation at the vertex. Accordingly, dropping the $\boldsymbol{k}$ dependence means that we are violating momentum conservation and neglecting the recoil of the particle, which is a reasonable approximation since we are dealing with long wavelength photons whose momentum is much less than the particle's momentum. For large momenta, near the end of the integration over frequency, the approximation breaks down. In more accurate calculations, we need to maintain center of mass momentum conservation and include the corresponding recoil terms [95, 152, 199, 214, 219, 231].

11.2 M^2 in the Non-relativistic Dipole Approximation

We first take the non-relativistic limit of our fully relativistic expression for $T^{\mu\nu}$ Eq. (10.50):

$$\begin{aligned}T^{\mu\nu}=&(2\Pi^\mu-k^\mu)\,\frac{1}{(\Pi-k)^2+m^2}\,(2\Pi^\nu-k^\nu)\\&+(2\Pi^\nu+k^\nu)\,\frac{1}{(\Pi+k)^2+m^2}\,(2\Pi^\mu+k^\mu)-2g^{\mu\nu}.\end{aligned}$$

We obtain the crossing symmetric, gauge invariant Compton scattering amplitude operator in the forward direction for a meson or a spinless Schrodinger electron in a potential V:

$$\begin{aligned}T^{ij}=&(2p_i-k_i)\,\frac{1}{(\boldsymbol{p}-\boldsymbol{k})^2+2mV-(E-k^0)\,2m}\,(2p_j-k_j)\\&+(2p_j+k_j)\,\frac{1}{(\boldsymbol{p}+\boldsymbol{k})^2+2mV-(E+k^\circ)\,2m}\,(2p_i+k_i)-2g^{ij},\end{aligned}\tag{11.10}$$

$$T^{00} = 4m^2 \frac{1}{(\boldsymbol{p}-\boldsymbol{k})^2 + 2mV - (E-k^\circ)\,2m} + 4m^2 \frac{1}{(\boldsymbol{p}+\boldsymbol{k})^2 + 2mV - (E+k^0)\,2m} - 2g^{00}, \tag{11.11}$$

$$T^{i0} = 2m(2p_i - k_i) \frac{1}{(\boldsymbol{p}-\boldsymbol{k})^2 + 2mV - (E-k^0)2m} + 2m \frac{1}{(\boldsymbol{p}+\boldsymbol{k})^2 + 2mV - (E+k^0)2m}(2p_i + k_i), \tag{11.12}$$

where E is the non-relativistic energy $E = \widetilde{E} - m$ (which is negative for the hydrogen atom). We have dropped the V^2 terms in the denominator of $T^{\mu\nu}$. As a check on the non-relativistic limit, we can prove gauge invariance by noting

$$\begin{aligned} \boldsymbol{k}\cdot(2\boldsymbol{p}+\boldsymbol{k}) &= (\boldsymbol{p}+\boldsymbol{k})^2 - \boldsymbol{p}^2 \\ \boldsymbol{k}\cdot(2\boldsymbol{p}-\boldsymbol{k}) &= -(\boldsymbol{p}-\boldsymbol{k})^2 + \boldsymbol{p}^2 \end{aligned} \tag{11.13}$$

and remembering that for matrix elements between physical states we can use the Schrodinger equation

$$(H-E)|N\rangle = 0, \tag{11.14}$$

where

$$H = \frac{p^2}{2m} - V. \tag{11.15}$$

The expression for the $(mass)^2$ operator in the non-relativistic limit is given by

$$M^2(E) = \frac{ie^2}{2}\int \frac{d^4k}{(2\pi)^4} D_{\mu\nu}(k) T^{\mu\nu}, \tag{11.16}$$

where $T^{\mu\nu}$ is given by the non-relativistic form in Eq. (11.10) to Eq. (11.12). We use the photon propagator in the radiation gauge:

$$D_{00} = \frac{g_{00}}{k^2} \quad D_{ij} = \frac{P_{ij}}{k^2}, \tag{11.17}$$

where

$$P_{ij} = \left(\delta_{ij} - \frac{k_i k_j}{\boldsymbol{k}^2}\right). \tag{11.18}$$

We first perform the k^0 integration. There are poles in the complex k^0 plane at $k^0 = E - V - (\boldsymbol{p}-\boldsymbol{k})^2/2m + i\epsilon$ (in the first quadrant) and $\pm(\omega/c - i\epsilon)$

(second and fourth quadrants), where $\omega = c|\boldsymbol{k}|$ and we display the speed of light c. Closing the contour in the lower half plane surrounds the single pole at $k_0 = \omega/c - i\epsilon$ and gives the result

$$M^2 = -\frac{\alpha c}{2m\pi}\int \omega d\omega \int \frac{d\Omega_k}{4\pi} \times \left\{ P_{ij}\left[\left(2p_i - \hat{n}_i\frac{\omega}{c}\right)\frac{1}{\frac{(\boldsymbol{p}-\hat{n}\frac{\omega}{c})^2}{2m} + V - (E-\omega)}\left(2p_j - \hat{n}_j\frac{\omega}{c}\right) - 2mg_{ij}\right] + 4m^2c^2\frac{1}{\frac{(\boldsymbol{p}-\hat{n}\frac{\omega}{c})^2}{2m} + V - (E-\omega)} - 2mg_{00}\right\}, \tag{11.19}$$

where $\hat{n} = \boldsymbol{k}/|\boldsymbol{k}|$ and we have combined cross terms since they give equal contributions to M^2. As we let $c \to \infty$, the terms in $\hat{n}\omega/c$ vanish leaving us with the expression for M^2 obtained by making the dipole approximation in the usual way ($|\boldsymbol{k}| \to 0$).

The angular integration for the term $g_{ij}P^{ij}$ is

$$\int \frac{d\Omega_k}{4\pi} g_{ij}P^{ij} = \frac{2}{3}\delta_{ij} \tag{11.20}$$

corresponding to the two transverse polarization states of a photon. Using the identity,

$$\frac{\omega}{H-(E-\omega)} = 1 - \frac{H-E}{H-(E-\omega)}, \tag{11.21}$$

we find

$$M^2 = -\frac{\alpha c}{\pi}\int d\omega \left[\frac{8}{3}\frac{p^2}{2m} - 3\omega + 2mc^2 - \frac{4}{3m}p_i\frac{H-E}{H-(E-\omega)}p_i - 2mc^2\frac{H-E}{H-(E-\omega)}\right]. \tag{11.22}$$

The expectation value of the last term, which comes from $g_{00}D^{00}$, vanishes for physical states. The first term can be interpreted as the change in kinetic energy due to mass renormalization in the non-relativistic limit [3]. The second and third terms compose the mass renormalization of free particles as they do not involve the Hamiltonian. The next to the last term is the only term that depends on the potential V and gives a vanishing shift in

the free particle limit $V \to 0$. Thus, the renormalized $mass^2$ operator in the non-relativistic limit is

$$\overline{M}^2(E) = \frac{4\alpha c}{3\pi m} \int d\omega p_i \frac{H - E}{H - (E - \omega) - i\epsilon} p_i. \tag{11.23}$$

11.3 Calculation of the Radiative Shift in the Non-relativistic Limit

The shift is given by the matrix elements of $\overline{M}^2$ between the non-relativistic states of the meson. To find the non-relativistic limit of the normalization in Eq. (10.19) of our relativistic meson wave functions $\langle r'|\widetilde{n}\rangle$, we use our definition of the non-relativistic energy $E = \bar{E} - m$ to write the normalization in the form

$$\int d^3r' |\langle r'|\widetilde{n}\rangle|^2 \left(1 + \frac{E_N}{mc^2} - \frac{V}{mc^2}\right) = 1, \tag{11.24}$$

where we make the factors of c explicit. Clearly, in the non-relativistic limit, we obtain the usual Schrodinger wave functions $\langle r'|n\rangle$ with the normalization

$$\int d^3r' |\langle r'|n\rangle|^2 = 1 \tag{11.25}$$

or

$$\langle nlm|n'l'm'\rangle = \delta_{nn'}\delta_{ll'}\delta mm'. \tag{11.26}$$

The effective shift in the unperturbed level E_N^0 due to the radiative interaction is the matrix element of the renormalized $(mass)^2$ operator with respect to $|N\rangle$:

$$\Delta E_N = E_N - E_N^0 = \frac{1}{2m}\langle N|\overline{M}^2(E_N)|N\rangle. \tag{11.27}$$

Substituting the expression for $\overline{M}^2$ (Eq. (11.23)) and inserting a complete set of intermediate states gives the result

$$\Delta E_N = \frac{2\alpha}{3\pi m^2} \sum_n^s \int_0^{\omega_C} \mathrm{d}\omega \frac{[(E_n - E_N)\,\langle N\,|p_i|\,n\rangle\,\langle n\,|p_i|\,N\rangle]}{E_n - E_N + \omega - i\epsilon}, \tag{11.28}$$

where the s in the summation indicates that we also include scattering states.[1] This is the same result as in Bethe's original paper and in his

[1] Note that the sign of the energy shift is positive. This seems to contradict the rule that a perturbation must lower the ground state energy. However, the rule holds if we consider the total perturbation to be the unrenormalized $(mass)^2$ operator, not the renormalized operator.

book [19, 158]. Note that a cutoff $\hbar\omega_C = mc^2$, where m is the mass of the electron has been introduced. No approximation has been used to evaluate the integral. Bethe justified the cutoff in the frequency integration on the grounds that the radiative shift is primarily a non-relativistic phenomena. Equation (11.28) can be easily derived from second-order perturbation theory, as shown in Section 9.3, Eq. (9.27). This was Bethe's approach, in which the complete set of states $|n\rangle$ represents intermediate states. This is often the method used in calculations of the radiative Lamb shift in textbooks [3]. We have derived this equation for the shift using only the fundamental equations of motion.

We now show that the term in brackets in this equation is proportional to the probability of a transition between state N and state n due to the emission or absorption of dipole radiation, which leads to a model for the radiative shift. The interaction Hamiltonian is

$$H_{int}(t) = \frac{e}{m}\boldsymbol{p}(t)\cdot\boldsymbol{A}^{rad}(\boldsymbol{r}(t),t), \tag{11.29}$$

where $\boldsymbol{A}^{rad}$ is the vector potential for the spinless electron's or meson's radiation field. The S matrix operator is

$$S = (e^{i\int_{-\infty}^{\infty}:dtH_{int}(t):})_{+}, \tag{11.30}$$

where the double dots mean that the Hamiltonian is normally ordered, with creation operators to the left of the annihilation operators. We want the matrix element ρ for a transition $n \to n', n' < n$ with the emission of a photon of momentum $\boldsymbol{k}$ and polarization $\boldsymbol{\epsilon}$:

$$\rho = \langle k\epsilon n'|S-1|n\rangle. \tag{11.31}$$

To lowest order, the Hilbert spaces are separable and $\boldsymbol{A}^{rad}$ equals the free field vector potential $\boldsymbol{A}$. The matrix element of $\boldsymbol{A}$ is the photon wave function:

$$\langle \mathrm{k}\epsilon|\boldsymbol{A}(\boldsymbol{r}(t),t)|0\rangle = \boldsymbol{\epsilon}\,\mathrm{e}^{-i\boldsymbol{k}\cdot\boldsymbol{r}+\mathrm{i}\omega t}. \tag{11.32}$$

In the interaction representation,

$$\boldsymbol{p}(t) = e^{+i\mathrm{H}t}\boldsymbol{p}(0)\,e^{-i\mathrm{H}t}. \tag{11.33}$$

Accordingly, we find

$$\rho = -2\pi i\frac{e}{m}\delta\left(E_{n'}+\omega-E_n\right)\langle n'|\boldsymbol{\epsilon}\cdot\boldsymbol{p}|n\rangle, \tag{11.34}$$

where we use the dipole approximation $\boldsymbol{k}\cdot\boldsymbol{r}\approx 1$. The decay rate for $n\to n'$ by dipole emission is

$$\Gamma^e_{n',n}=\frac{\text{total probability}}{\text{interaction time}}. \tag{11.35}$$

In the usual way, we take $2\pi\delta(0)$ as the interaction time, $|\boldsymbol{k}|=\omega$, giving

$$\Gamma^e_{n',n}=\sum_{pol}\int\frac{d^3k}{(2\pi)^3}\frac{1}{2\omega}\frac{|\rho|^2}{2\pi\delta(0)}. \tag{11.36}$$

Recalling

$$\sum_{\mu}\epsilon_{\mu i}\epsilon_{\mu j}=\delta_{ij}-\frac{k_ik_j}{k^2}, \tag{11.37}$$

we obtain

$$\Gamma^e_{n',n}=\frac{4\alpha}{3m^2}(E_n-E'_n)\langle n'|p_i|n\rangle\langle n|p_i|n'\rangle>0,\quad n'<n \tag{11.38}$$

for the decay rate from $n\to n'$ by dipole emission, where $E_n-E'_n=\omega_{nn'}$. Similarly, the rate for the transition $n\to n'$ for $n'>n$, by absorption of dipole radiation is

$$\Gamma^a_{n',n}=\frac{4\alpha}{3m^2}\left(E_{n'}-E_n\right)\left\langle n'\left|p_i\right|n\right\rangle\left\langle n\left|p_i\right|n'\right\rangle>0,\quad n'>n. \tag{11.39}$$

In accordance with the principle of detailed balance, we see

$$\Gamma^a_{n',n}=\Gamma^e_{n,n'}. \tag{11.40}$$

From our definition, $\Gamma^e_{n,n'}$ is defined only for $n'>n$ and then is always positive or zero. We see formally that $\Gamma^e_{n,n'}=-\Gamma^e_{n',n}$. Accordingly, if $n>n'$, we interpret $\Gamma^e_{n,n'}$ as $-\Gamma^e_{n',n}$. Using this convention with our expression for $\Gamma^e_{n,n'}$, we find that, after changing variables, the expression in Eq. (11.28) for the shift may be written in the simpler form:

$$\Delta E_N=\frac{1}{\pi}\sum_n^s\int_{E_n}^{E_n+\omega_C}d\omega\frac{-\frac{1}{2}\Gamma^e_{n,N}}{\omega-E_N-i\epsilon}. \tag{11.41}$$

Based on Eq. (11.10) to Eq. (11.12) for $T^{\mu\nu}$, it is clear that ΔE_N is an analytic function $f(N,E_N)$ of energy E_N, which is in the denominator. We define

$$\Delta E_N=f\left(N;E_N\right)=\sum_n^s f_n(N;E_N). \tag{11.42}$$

The partial shift $f_n(N;E_N)$ represents the contribution to the shift in level N from virtual transitions from level N to level n. We replace E_N by the

complex variable z and investigate the structure of the partial shift as a function of z:

$$f_n(N;z) = \frac{1}{\pi}\int_{E_n}^{E_n+\omega_C} d\omega \frac{-\frac{1}{2}\Gamma^e_{n,N}}{\omega - z - i\epsilon}. \tag{11.43}$$

We extend the lower limit of integration to E_1 and the upper limit to ∞ and multiply by the appropriate theta functions ($\theta(t) = 0$ if $t < 0, = 1$ if $t > 0$) so that the value of the integral is unchanged. After summing over all states, we find that the complex radiative shift obeys the dispersion relation [169]

$$f(N;z) = \frac{1}{\pi}\int_{E_1}^{\infty} d\omega \frac{Im\, f(N;\omega)}{\omega - z - i\epsilon}, \tag{11.44}$$

where

$$Im\, f(N;\omega) = \sum_n^s -\frac{1}{2}\Gamma^e_{n,N}\theta(\omega - E_n)\theta(\omega_C + E_n - \omega). \tag{11.45}$$

We can separate the integral into its real and imaginary parts

$$f(N;z) = \frac{1}{\pi}P\int_{E_1}^{\infty} d\omega \frac{Im\, f(N;\omega)}{\omega - z} + i\,\mathrm{Im}\, f(N;z). \tag{11.46}$$

Figure 11.1 shows the cut structure for $f(N;\omega)$ in the complex ω plane.

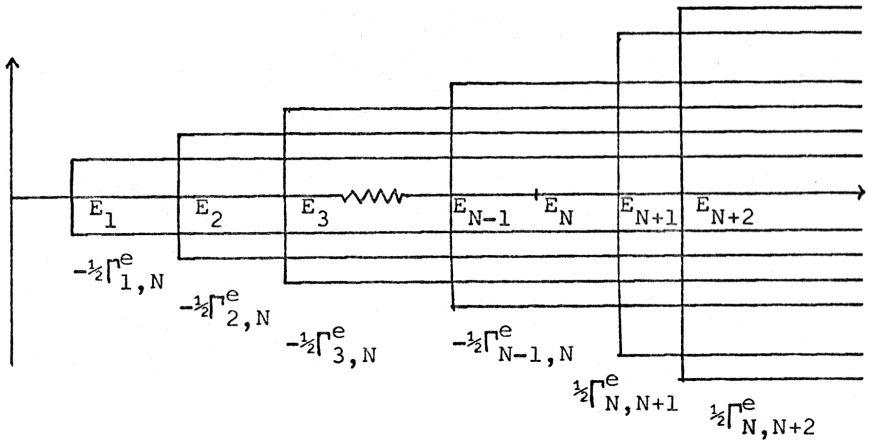

Fig. 11.1. Cut Structure of $f(N;\omega)$ in the complex ω plane. At each value of E_n which is less than E_N, there is a cut with a discontinuity of $-\frac{1}{2}\Gamma^e_{n,N}$; at E_N, there is no cut. At each value of E_n which is greater than E_N, there is a cut with a discontinuity of $\frac{1}{2}\Gamma^e_{N,n}$.

11.4 Radiative Shift for Physical Energy Levels

The function $f(N;z)|_{z=E_N}$ gives the radiative shift for the energy level E_N. The imaginary part of the shift is

$$\begin{aligned} \mathrm{Im}\Delta E_N &= \mathrm{Im}\, f\,(N;E_N) \\ &= -\frac{1}{2}\sum_{n<N}\Gamma^e_{n,N} \equiv -\frac{1}{2}\Gamma_N, \end{aligned} \tag{11.47}$$

where Γ_N is the total width for the decay of state N to state n by dipole radiation. The imaginary part of the shift equals the half-width in magnitude and is always negative, as it must be to ensure that the probability density decreases exponentially: $|e^{-it\left(E^0_N+\Delta E_N\right)}|^2 = e^{-\Gamma_N t}$. Only states to which the state N can decay by the emission of real radiation contribute to the width of the level E_N.

The real part of the shift $Re\, f(N;E_N)$ is given by the principal part of the integral. Since we integrate from E_1 to ∞, skipping the infinitesimal portion $|\omega - E_N| < \epsilon$, all cuts (or equivalently all intermediate states) contribute to the real part of the radiative shift. Integrating over ω, we obtain an expression for the real part of the partial shift $f_n(N;E_N)$:

$$Ref_n(N;E_N) = \begin{cases} -\Gamma^e_{n,N} & n<N \\ \Gamma^e_{N,n} & n>N \end{cases} \times \frac{1}{2\pi}\ln\frac{\omega_C - E_N + E_n}{|E_n - E_N|}. \tag{11.48}$$

We can approximate $Re\, f_n(N;E_N)$ by neglecting $E_n - E_N$ in the numerator of the log, similar to the approximation Bethe used. With this approximation, and writing the log of the ratio as a difference in logs, we can sum $Re\, f_n(N;E_N)$ over all states using the dipole sum rule and Eq. (11.38):

$$\frac{3m^2}{2\alpha}\sum_n^s \Gamma^e_{N,n} = 2\sum_n^s (E_n - E_N)\,\langle N\,|p_i|n\rangle\,\langle n\,|p_i|\,N\rangle \;= -\langle N|\nabla^2 V|N\rangle. \tag{11.49}$$

This gives the result

$$\begin{aligned} \mathrm{Re}\,\Delta E_N = \frac{2\alpha}{3\pi m^2}\Bigg\{ &\frac{1}{2}\langle N|\nabla^2 V|N\rangle \ln\frac{\omega_C}{E_0} \\ &+ \sum_n (E_n - E_N)\langle N|p_i|n\rangle\langle n|p_i|N\rangle \ln\frac{E_o}{|E_n - E_N|}\Bigg\}, \end{aligned} \tag{11.50}$$

where E_0 is an arbitrary energy parameter that we shall take to be some characteristic energy of the bound system, for example, the ground state

energy. We take the frequency cutoff ω_C to be $mc^2/\hbar$, as Bethe did. The first term is the same expression for the shift that we obtained by considering the motion of the particle in the zero-point field (Eq. 9.43) in Welton's model. Note that we have assumed only that the spinless electron is in a central force potential $V(r)$, not necessarily a Coulomb potential.

11.4.1 *A model to interpret the results*

We can construct a simple model (Fig. 11.2) to interpret the salient features of the partial radiative shifts $f_m(N; E_N)$, which give the shift in the energy E_N due to virtual transitions to level m. The features are expressed in the following equations, which hold for any positive integer $m < N$:

(1) $\mathrm{Re} f_m(N; E_N) + Re f_N(m; E_m) = 0.$
(2) $\mathrm{Re}\ f_m(N; E_N) < 0.$
(3) $\mathrm{Im}\ f_m(N; E_N) = \mathrm{Re} f_m(N; E_N)[\frac{1}{\pi}\ln\frac{\omega_C}{|E_N - E_m|}]^{-1}.$

The first relation shows that the average energy of two levels that shift each other is unchanged. Together, the first two relations show that virtual transitions to lower states cause downward shifts and transitions to upper states cause upward shifts. This is an important result, demonstrating that a radiative shift tends to conserve energy. Consider, for example, the radiative shift in the ground state of H. Many transitions to higher states will contribute to raising the ground state energy level. Each of the

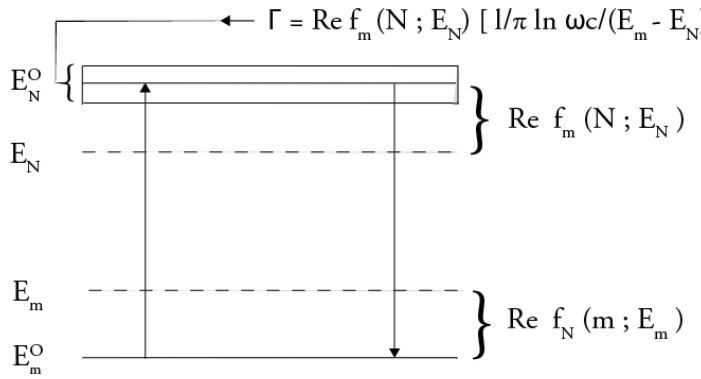

Fig. 11.2. The energy level E_N^0 is shifted to E_N by intermediate virtual transitions to E_m^0, which also increases the width of the level to Γ. The level E_m^0 is shifted to E_m by virtual transitions to E_N^0. The latter transition does not increase the width of the level for E_m.

higher levels experiences a very small shift downwards. The sum of all the downward shifts will equal the upward shift on the ground state, so the total of all the shifts is zero. To determine the net energy shift of the atom precisely, one would also have to consider the population of the various states. Since the ground state is heavily populated, there tends to be a net increase of energy.

The third statement shows that the contribution of a lower level to the width is less than its contribution to the level shift by the factor $(1/\pi)\ln(\omega_C/|E_N - E_m|)$. We can deduce relations (1) and (2) for the level shifts exactly and relation (3) for the level width in an approximation by assuming that the observed energy corresponds to a time-weighted average of the original energy and the energy of the state to which the system made a virtual transition. To make this interpretation quantitative, we consider a state N with a partial width $\Gamma = \Gamma^e_{N,m} = \Gamma^a_{m,N}$ for $m < N$. The system makes Γ transitions from N to m in one second and remains in the state m for a time allowed by the time-energy uncertainty principle:[2]

$$\delta t \approx \frac{1}{E_N - E_m}. \tag{11.51}$$

Therefore, for a system in which $\Gamma << E_N - E_m$ (e.g., atomic systems), the average energy E_{Nave} of level N is shifted and is approximately

$$E_{Nave} = \frac{\Gamma}{E_N - E_m} E_m + \left(1 - \frac{\Gamma}{E_N - E_m}\right) E_N = E_N - \Gamma. \tag{11.52}$$

The level shift for state N due to a transition from a state N to a lower state m is $E_{Nave} - E_N$ or $\mathrm{Re}f_m(N; E_N) = -\Gamma^e_{m,N}$. Similarly, we find that for a transition from a state m to a higher state N, the level shift is $\mathrm{Re}f_N(m, E_N) = \Gamma^a_{N,m}$ which is positive. From these two expressions, the relations (1) and (2) follow. Corresponding to the third relation we find using Eq. (11.45) and the results directly above that the model predicts a level width

$$\mathrm{Im}f_m(N; E_N) = -\frac{1}{2}\Gamma = \frac{1}{2}\mathrm{Re}f_m(N; E_N). \tag{11.53}$$

[2]The time-energy relationship is not an uncertainly principle in the same sense as the position-momentum uncertainty principle, which follows because the corresponding operators do not commute. The time-energy relationship arises from the properties of Fourier transforms [172, p. 201].

This result agrees with relation (3) only if we replace $\frac{1}{\pi} ln \frac{\omega_C}{|E_N - E_m|}$ by unity.[3] The difference between the equations for the level shift and the level width arises primarily because only states that can decay by the emission of real radiation contribute to the width of level E_N.

11.5 Two Examples: The Harmonic Oscillator and the Coulomb Potential

In our discussion thus far, we only assume we have a spinless particle of mass m and charge e in a central force potential $V(r)$ interacting with its own radiation field. Now, we can apply the results to these two specific potentials.

(1) Isotropic 3D Harmonic Oscillator

Consider a simple isotropic harmonic oscillator in three dimensions for which

$$V(r) = \frac{1}{2} m\omega_0^2 r^2 \tag{11.54}$$

with energy levels

$$E_N = \left(N + \frac{3}{2}\right)\omega_0, \quad N = n_1 + n_2 + n_3. \tag{11.55}$$

The fact that $V(r)$ increases formally with r without bound does not introduce difficulties since transitions are possible only between adjacent energy levels. Employing the matrix elements of the momentum operator

$$\langle n_i' \,|p_j|\, n_i\rangle = \sqrt{\frac{m\omega_0}{2}}(\sqrt{n_i + 1}\delta_{n_i' n_i + 1} - \sqrt{n_i}\delta_{n_i' n_i - 1}), \tag{11.56}$$

we can easily compute the real part of the radiative shift using Eq. (11.50) or the complex shift using Eqs. (11.38–11.39) and Eq. (11.42) and Eqs. (11.47–11.48). For the complex radiative shift of level E_N, we find

$$\Delta E_N = \frac{\alpha}{\pi} \frac{(\hbar\omega_0)^2}{mc^2} \left(\ln \frac{\omega_C}{\omega_0} - i\frac{2}{3}\pi N\right) \tag{11.57}$$

giving a corresponding width

$$\Gamma_N = \frac{2}{3}\alpha \frac{(\hbar\omega_0)^2}{mc^2} N, \tag{11.58}$$

[3]For the H atom, the value of $(1/\pi) ln(\omega_C/|E_n - E_m|)$ is roughly three assuming the cutoff is at $h\omega_c = mc^2$ and n and m are adjacent energy levels of the bound state.

where we have displayed the factors of $\hbar$ and c. In the dipole approximation, the shift is the same for all levels: no degeneracy is split. On the other hand, the radiative width Γ_N increases with N and is consistent with the width Eq. (9.18) obtained by applying the Bohr Correspondence Principle to the classical expression for the radiated power. The ratio of Γ_N/E_N approaches a constant for large N and equals $(2/3)\alpha\hbar\omega_0/mc^2$. In Chapter 13, we compute the radiative shift for a relativistic spinless electron in a harmonic potential and show that for some levels the degeneracy is lifted.

(2) The Coulomb Potential

We have

$$V(r) = -\frac{Z\alpha}{r} \tag{11.59}$$

and therefore

$$\nabla^2 V(r) = 4\pi Z\alpha\delta(r). \tag{11.60}$$

Since the matrix elements of the delta function vanish except for S states, we may isolate the L dependence of the shift by defining the Bethe log $\gamma(N,L)$(Eq. 9.34), where [158]

$$\begin{aligned} &\gamma(N,L)\sum_n^s (E_n - E_N)\langle N\,0\,|p_i|\,n\rangle\langle n\,|p_i|\,N\,0\rangle \\ &= \sum_n^s (E_n - E_N)\langle NL\,|p_i|\,n\rangle\langle n\,|p_i|\,NL\rangle \ln\tfrac{|E_n-E_N|}{\frac{1}{2}mc^2(Z\alpha)^2}\end{aligned}. \tag{11.61}$$

Using Eq. (11.50), setting the frequency cutoff to $\omega_C = m$, setting E_o to the ground state energy $(1/2)m(Z\alpha)^2$ and substituting the Schrodinger wave function

$$|\psi_N(0)|^2 = \frac{1}{\pi}\left(\frac{Z\alpha m}{N}\right)^3 \delta_{L0}, \tag{11.62}$$

we find the shift for level NL is

$$\mathrm{Re}\,\Delta \mathrm{E}_{NL} = \left[\frac{4m}{3\pi}\alpha(Z\alpha)^4\right]\frac{1}{N^3}\left\{\delta_{\mathrm{LO}}\ln\frac{2}{(Z\alpha)^2} - \gamma(N,L)\right\}, \tag{11.63}$$

where $\gamma(N,L)$ must still be numerically evaluated.[4] The result is the same result that Bethe obtained in his original calculation. The Bethe log is tabulated for a few energy levels in the original work in which it was introduced [158] and in various articles for additional levels and with a higher precision, for example [152, 227].

[4]The value of the Bethe log for the 2S state is about $\gamma(2,0) = ln(16.639)$.

To provide a scale of magnitude for the shift, we note that the term in square brackets is the energy radiated in one revolution of the electron in the ground state according to the laws of classical physics and equals Planck's constant times 1090 MHz. The currently accepted value for the $2s_{1/2}$–$2p_{1/2}$ Lamb shift is about 1057.87 MHz, which includes all effects, including vacuum polarization, to higher orders. The $2p$ shift is negative as we discuss in Chapter 14. We can estimate the relative shift

$$\Delta E_N/E_N \approx \alpha\frac{(Z\alpha)^2}{N}, \tag{11.64}$$

which is about one part in 1.3×10^6 for $N = 2$. The width for low-lying states may be obtained by computing the sum in Eq. (11.45) explicitly.

For both examples, the relative shifts go approximately as α x (bound state energy level)/(rest mass energy), reflecting the fundamental nature of radiative shifts (and that we are considering radiative shifts in lowest order).

In the limit of very large quantum numbers for any central force field for circular orbits, we can simplify the expression for the width Γ_N by assuming that the most important transitions are those for which $\Delta n << N$. The strongest transitions in the classical limit are between wave packets corresponding to the circular orbits $n = N$, $l = N - 1$ and $n = N-1$, $l = N-2$. This is equivalent to saying that the classical radiation is primarily in the fundamental band. Consequently, our sum collapses to

$$\Gamma_N = \omega_{cl} \left\langle N \left| p_i \right| N-1 \right\rangle \left\langle N-1 \left| p_i \right| N \right\rangle \frac{4\alpha}{3m^2}, \tag{11.65}$$

where ω_{cl} is the classical frequency of rotation. This matrix element can be obtained without direct computation by noting that

$$\langle N|p^2|N\rangle \cong \left\langle N \left| p_i \right| N+1 \right\rangle \left\langle N+1 \left| p_i \right| N \right\rangle + \left\langle N \left| p_i \right| N-1 \right\rangle \left\langle N-1 \left| p_i \right| N \right\rangle, \tag{11.66}$$

which follows from our assumption that the only significant transitions are those for which $\Delta N = \pm 1$ and from the fact that $\langle N|p_i|N\rangle = 0$ for a bound state. We assume that the matrix elements do not change rapidly with N, thus

$$\left\langle N \left| p_i \right| N-1 \right\rangle \left\langle N-1 \left| p_i \right| N \right\rangle \cong \left\langle N \left| p_i \right| N+1 \right\rangle \left\langle N+1 \left| p_i \right| N \right\rangle. \tag{11.67}$$

Therefore, our final expression for Γ_N is

$$\Gamma_{\mathrm{N}} = \frac{2\alpha}{3m^2}\omega_{c\ell} \left\langle N \left| p^2 \right| N \right\rangle. \tag{11.68}$$

For the Coulomb potential $\omega_{cl} = m(Z\alpha)^2/N^3$ (which is consistent with Eq. (9.7) and Eq. (9.10)), and $\langle N|p^2|N\rangle = (mZ\alpha/N)^2$, so we find

$$\Gamma_N = \frac{2}{3} m\alpha \frac{(Z\alpha)^4}{N^5}, \tag{11.69}$$

which is in agreement with the result obtained by the correspondence principle Eq. (9.11).

Note that nowhere in our derivation of Eq. (11.68) do we specify the detailed nature of the central force. We only assumed that the radiation was in the fundamental band, which is always true for classical circular orbits. In fact, this equation agrees with the expression for Γ obtained by applying the correspondence principle to the classical expression for the radiated power P_c for any circular orbit of a charged particle with momentum p:

$$P_c = \frac{2}{3} \frac{\alpha}{m^2} p^2 \omega_{cl}^2, \tag{11.70}$$

which, from the Bohr Correspondence Principle, has the width $\Gamma = P_c/\omega_{cl}$ so

$$\Gamma = \frac{2}{3} \frac{\alpha}{m^2} p^2 \omega_{cl}. \tag{11.71}$$

For exact non-relativistic calculations, the sum over states for the real part of the energy shift was trivial to compute for the harmonic oscillator since only two intermediate states contribute. Alternatively, if we compute the shift from Eq. (11.23) without inserting intermediate states, then from the equations of motion we can easily compute the contraction over p_i. We will follow this procedure in our calculations of the level shift for the relativistic harmonic oscillator in Chapter 13. Unfortunately, obtaining exact results for the Coulomb potential is more difficult. If we use Eq. (11.28), we must include an infinite number of intermediate states in our sum. If we do not use intermediate states but rather use Eq. (11.23) directly, then we find that the equations of motion are intractable unless we use group theoretical techniques, which are described in the next chapter [252].

This page intentionally left blank

Chapter 12

SO(4,2) Calculation of the Radiative Shift for the Schrodinger Hydrogen Atom

In Chapter 12, we compute the radiative shift in the non-relativistic dipole approximation and to first order in the radiation field, as did Bethe, but we use group theoretical methods based on the SO(4,2) symmetry of the non-relativistic hydrogen atom as developed in Chapter 7. The shifts are expressed as integrals over the frequency of the virtual electromagnetic field. This allows us to determine the contribution of different frequencies to the shift. The analytic expressions for the shifts are easy to evaluate numerically as discussed in Chapter 14. Bethe's calculation required the numerical sum over all intermediate states to obtain the average value of the energy of the states contributing to the shift. In our calculation, we do not use intermediate states, and we derive an integral equivalent to Bethe's log, and more generally derive the shift for all levels in terms of a double integral of an analytic function that we can readily evaluate.

12.1 SO(4,2) Expressions for the Radiative Shift

An expression for the radiative shift Δ_{NL} for energy level E_N of a hydrogen atom in a state $|NL\rangle$ can be easily obtained using second order perturbation theory (to first order in α the radiation field) [3, 19, 149, 158]

$$\Delta E_{NL} = \frac{2\alpha}{3\pi m^2} \sum_n^s \int_0^{\omega_C} d\omega \frac{(E_n - E_N)\langle NL|p_i|n\rangle\langle n|p_i|NL\rangle}{E_n - E_N + \omega - i\epsilon}, \qquad (12.1)$$

where ω_C is a cutoff frequency for integration that we will take as $\omega_C = m$. This equation is the same as Eq. (9.27) which we derived using perturbation theory and Eq. (11.28) which we derived using the $mass^2$ operator and the non-relativistic dipole approximation to the Klein–Gordon equation. This

expression, which is the same as Bethe's before any approximations were made, has been derived by inserting a complete set of states $|n\rangle\langle n|$ in Eqs. (11.23) and (11.27), a step that is not necessary with our group theoretical approach:

$$\Delta E_{NL} = \frac{2\alpha}{3\pi m^2}\int_0^{\omega_C} d\omega \langle NL|p_i \frac{H - E_N}{H - (E_N - \omega) - i\epsilon} p_i |NL\rangle. \tag{12.2}$$

If we add and subtract ω from the numerator, we find the real part of the shift is

$$Re\Delta E_{NL} = \frac{2\alpha}{3\pi m^2} Re \int_0^{\omega_C} d\omega [\langle NL|p^2|NL\rangle - \omega\Omega_{NL}], \tag{12.3}$$

where

$$\Omega_{NL} = \langle NL|p_i \frac{1}{H - E_N + \omega - i\epsilon} p_i |NL\rangle \tag{12.4}$$

and

$$H = \frac{p^2}{2m} - \frac{Z\alpha}{r}. \tag{12.5}$$

The imaginary part of the shift gives the width of the level as discussed in Secs. 11.3 and 11.4.

The matrix element Ω_{NL} can be converted to a matrix element of a function of the generators Γ_A taken between the eigenstates $|nlm)$ of $(Z\alpha)^{-1}$. To do this we insert factors of $1 = \sqrt{r}\frac{1}{\sqrt{r}}$ and use the definitions of Γ_A in terms of the canonical variables, Eqs. (7.45–7.47). Letting the parameter a take the value a_N, we obtain the result

$$\Omega_{NL} = \frac{m\nu}{N^2}\left(NL|\Gamma_i \frac{}{\Gamma n(\xi) - \nu}\Gamma_i|NL\right), \tag{12.6}$$

where $\Gamma n(\xi) = -\Gamma_0 n_0 + \Gamma_4 n_4$, and

$$n_0(\xi) = \frac{2+\xi}{2\sqrt{1+\xi}} = -\cosh\phi \quad n_i = 0 \quad n_4(\xi) = -\frac{\xi}{2\sqrt{1+\xi}} = -\sinh\phi \tag{12.7}$$

and

$$\xi = \frac{\omega}{|E_N|} \quad \nu = \frac{N}{\sqrt{1+\xi}} = Ne^{-\phi}. \tag{12.8}$$

From the definitions, we see $\phi = \frac{1}{2}ln(1+\xi) > 0$ and $n_A(\xi)n^A(\xi) = -1$. The quantity

$$\nu = \frac{mcZ\alpha}{\sqrt{-2m(E_N - \omega)}}$$

may be considered the effective principal quantum number for a state of energy $E_N - \omega$. The contraction over i in Ω_{NL} can be evaluated using the group theoretical formula Eq. (7.41):

$$\Gamma_A \frac{1}{\Gamma n - \nu} \Gamma^A = -2\nu \int_0^\infty ds\, e^{\nu s} \frac{d}{ds} \left(\sinh^2 \frac{s}{2}\, e^{-\Gamma n(\xi) s} \right).$$

Applying this equation to Eq. (12.6), we obtain

$$\begin{aligned} \Omega_{NL} = & -2\frac{m\nu^2}{N^2} \int_0^\infty ds e^{\nu s} \frac{d}{ds} \left(\sinh^2 \frac{s}{2} M_{NL}(s) \right) \\ & - m\frac{\nu}{N^2} \left(NL|\Gamma_4 \frac{1}{\Gamma n(\xi) - \nu} \Gamma_4 |NL \right) \\ & + m\frac{\nu}{N^2} \left(NL|\Gamma_0 \frac{1}{\Gamma n(\xi) - \nu} \Gamma_0 |NL \right), \end{aligned} \tag{12.9}$$

where

$$M_{NL}(s) = (NL|e^{-\Gamma n(\xi)\, s}|NL). \tag{12.10}$$

In order to evaluate the last-two terms in Ω_{NL}, we can express the action of Γ_4 on our states in terms of $\Gamma n(\xi) - \nu$. Substituting Eq. (7.44)

$$\Gamma_0 |NL) = N|NL) \tag{12.11}$$

into the expression for $\Gamma n(\xi) - \nu$, with $n(\xi)$ given by Eq. (12.7) gives

$$\Gamma_4 = N - \left(\frac{1}{\sinh \phi} \right) (\Gamma n(\xi) - \nu) \tag{12.12}$$

when acting on the state $|NL)$. If we substitute Eq. (12.12) into the expression for the $Re\Delta E_{NL}$, Eq. (12.3), use Eq. (12.9), and simplify using the virial theorem

$$(NL|p^2|NL) = a_N^2,$$

we find that the term in p^2 exactly cancels the last two terms in Ω_{NL}, yielding the result

$$\mathrm{Re}\Delta E_{NL} = \frac{4m\alpha(Z\alpha)^4}{3\pi N^4} \int_0^{\phi_c} d\phi \sinh\phi e^{\phi} \int_0^\infty ds\, e^{\nu s} \frac{d}{ds} \left(\sinh^2 \frac{s}{2} M_{NL}(s) \right), \tag{12.13}$$

where

$$\phi_c = \frac{1}{2}\ln\left(1+\frac{\omega_C}{|E_N|}\right) = \frac{1}{2}\ln\left(1+\frac{2N^2}{(Z\alpha)^2}\right) \tag{12.14}$$

and $\omega_C = m$.

This is a very convenient expression for the shift $Re\Delta E_{NL}$ for any state NL because we can derive an analytical expressions for M_{NL}. An unexpected feature of Eq. (12.13) is that the explicit dependence on the principal quantum number is $1/N^4$, whereas in the Bethe formalism (see Eq. 9.33) the dependence is $1/N^3$. The difference arises because in Eq. (12.13), the integrand contains ϕ and $\nu = Ne^{-\phi}$ which both depend on the energy $E_N = -(1/2N^2)m(Z\alpha)^2$ of the state. The numerical calculations of both equations agree.

Comparison to the Bethe logarithm

Comparing the SO(4,2) expression for the shift Eq. (12.13) to Eq. (11.63), which gives the shift in terms of a sum over states and the Bethe log, we find that the Bethe log is

$$\gamma(N,L) = -N\int_0^{\phi_c} d\phi \sinh\phi e^{\phi}\int_0^{\infty} ds e^{\nu s}\frac{d}{ds}\left(\sinh^2\frac{s}{2}M_{NL}(s)\right) + \delta_{L0}\ln\frac{2}{(Z\alpha)^2}. \tag{12.15}$$

Note that this expression for the Bethe log is not an approximation like the usual expression in which an approximate integration over energy has been done.

12.2 Generating Function for the Shifts

We can derive a generating function for the shifts for any eigenstate characterized by N and L if we multiply Eq. (12.13) by $N^4e^{\beta N}$ and sum over all $N, N \geq L+1$. To simplify the right side of the resulting equation, we use the fact that the O(2,1) algebra of Γ_0, Γ_4, and S closes (Section 7.4). We make the identifications $j_1 = \Gamma_4, j_2 = S$, and $j_3 = \Gamma_0$ to compute the sum on the right hand side using Eq. (12.10), $M_{NL} = (NL|e^{-\Gamma n(\xi)s}|NL)$, and use Eq. (7.44), $(\Gamma_0 - n)|nlm) = 0$:

$$\sum_{N=L+1}^{\infty} e^{-\beta N}M_{NL} = \sum_{N=L+1}^{\infty}(NL|e^{-\boldsymbol{j}\cdot\boldsymbol{\psi}}|NL), \tag{12.16}$$

where

$$e^{-\boldsymbol{j}\cdot\boldsymbol{\psi}} \equiv e^{-\beta\Gamma_0} e^{-s\Gamma n(\xi)}. \tag{12.17}$$

We perform $\boldsymbol{j}$ transformation, generated by a similarity transforamtion, such that

$$e^{-\boldsymbol{j}\cdot\boldsymbol{\psi}} \to e^{-j_3\psi} = e^{-\Gamma_0\psi}. \tag{12.18}$$

Remembering the cyclic symmetry of the trace, we find

$$\sum_{N=L+1}^{\infty} e^{-\beta N} M_{NL} = \sum_{N=L+1}^{\infty} (NL|e^{-j_3\psi}|NL) = \sum_{N=L+1}^{\infty} e^{-N\psi}, \tag{12.19}$$

$$\sum_{N=L+1}^{\infty} e^{-\beta N} M_{NL} = \frac{e^{-\psi(L+1)}}{1-e^{-\psi}}, \tag{12.20}$$

where we have used the identity

$$\frac{1}{1-e^{-\psi}} = \sum_{m=0}^{\infty} e^{-m\psi}.$$

Eq. (12.20) is a generating function for M_{NL}, which determines the radiative shift as shown in Eq. (12.13).

In order to find a particular M_{NL}, we must expand both sides of Eq. (12.20) in powers of $e^{-\beta}$ and equate the coefficients of the corresponding powers of $e^{-\beta}$. First, we need an equation for $e^{-\psi}$. This can be obtained using the isomorphism between $\boldsymbol{j}$ and the Pauli $\boldsymbol{\sigma}$ matrices:

$$(\Gamma_4, S, \Gamma_0) \to (j_1, j_2, j_3) \to \left(\frac{i}{2}\sigma_1,\ \frac{i}{2}\sigma_2,\ \frac{1}{2}\sigma_3\right). \tag{12.21}$$

Using Eqs. (12.17) and (12.18) and the formula

$$e^{\frac{i}{2}s\boldsymbol{n}\cdot\boldsymbol{\sigma}} = \cos\frac{s}{2} + i\boldsymbol{n}\cdot\boldsymbol{\sigma}\sin\frac{s}{2}, \tag{12.22}$$

where $|\boldsymbol{n}| = 1$, we find

$$\cosh\frac{\psi}{2} = \cosh\frac{\beta}{2}\cosh\frac{s}{2} + \sinh\frac{\beta}{2}\sinh\frac{s}{2}\cosh\phi. \tag{12.23}$$

We can rewrite this equation in a form easier for expansion

$$e^{+\frac{1}{2}\psi} = de^{\frac{1}{2}\beta} + be^{-\frac{1}{2}\beta} - e^{-\frac{1}{2}\psi}, \tag{12.24}$$

where

$$\begin{aligned} d &= \cosh\frac{s}{2} + \sinh\frac{s}{2}\cosh\phi \\ b &= \cosh\frac{s}{2} - \sinh\frac{s}{2}\cosh\phi \end{aligned} \quad . \tag{12.25}$$

Let β become very large and iterate the equation for $e^{-\frac{1}{2}\psi}$ to obtain the result

$$e^{-\psi} = Ae^{-\beta}\left[1 + A_1 e^{-\beta} + A_2 e^{-2\beta} + \cdots\right], \tag{12.26}$$

where

$$\begin{aligned} A = A_0 &= \frac{1}{d^2} \\ A_1 &= -\left(\frac{2}{d}\right)\left(b - d^{-1}\right) \\ A_2 &= 3d^{-2}\left(b - d^{-1}\right)^2 - 2^{-2}(b - d^{-1}). \\ &\vdots \end{aligned} \tag{12.27}$$

Note $b - d^{-1} = -d^{-1}\sinh^2\frac{s}{2}\sinh^2\phi$.

12.3 The Shift Between Degenerate Levels

Expressions for the energy shift between degenerate levels with quantum numbers (N, L) and (N, L') may be obtained directly from the generating function using Eq. (12.13) and Eq. (12.20). We find

$$\begin{aligned} &\sum_{N=L+1} e^{-\beta N} N^4 \operatorname{Re}\Delta E_{NL} - \sum_{N=L'+1}^{\infty} e^{-\beta N} N^4 \operatorname{Re}\Delta E_{NL'} \\ &\quad = \frac{4m\alpha(Z\alpha)^4}{3\pi}\int_0^{\phi_c} d\phi e^{\phi}\sinh\phi\int_0^{\infty} ds e^{\nu s}\frac{d}{ds} \\ &\qquad \times\left(\sinh^2\frac{s}{2}\frac{e^{-\psi(L+1)} - e^{-\psi\left(L'+1\right)}}{1 - e^{-\psi}}\right). \end{aligned} \tag{12.28}$$

For an example, consider $L = 1, L' = 0$. For the shifts between levels we obtain

$$\begin{aligned} &\sum_{N=2}^{\infty} e^{-\beta N} N^4 \operatorname{Re}\left(\Delta E_{NO} - \Delta E_{N1}\right) + \operatorname{Re}\Delta E_{10}\, e^{-\beta} \\ &\quad = \frac{4m\alpha(z\alpha)^4}{3\pi}\int_0^{\phi_c} d\phi\, e^{\phi}\sinh\phi\int_0^{\infty} ds e^{\nu s}\frac{d}{ds}\left(\sinh^2\frac{s}{2}e^{-\psi}\right). \end{aligned} \tag{12.29}$$

Substituting Eq. (12.26) for $e^{-\psi}$, which gives the coefficient AA_{N-1} of $e^{-N\beta}$, we find

$$Re(\Delta E_{N0} - \Delta E_{N1}) = \frac{4m\alpha(Z\alpha)^4}{3\pi N^4} \int_0^{\phi_c} d\phi e^{\phi} \sinh\phi \int_0^{\infty} ds e^{\nu s} \frac{d}{ds} \left(\sinh^2 \frac{s}{2} AA_{N-1}\right), \tag{12.30}$$

where A and A_{N-1} are given in Eq. (12.27) in terms of the integration variables s and ϕ.

General expression for M_{NL}

Once we have a general expression for M_{NL}, we can use Eq. (12.13) to calculate the shift for any level E_{NL}. We can obtain expressions for the values of M_{NL} by letting β become large, expanding the denominator in Eq. (12.20) and equating the coefficients of powers of $e^{-\beta}$. For large β, we have large ψ. We have

$$\frac{e^{-\psi(L+1)}}{1-e^{-\psi}} = \sum_{m=1}^{\infty} e^{-\psi(m+L)}$$

and for large β it follows from Eq. (12.26) that

$$\sum_{N=L+1}^{\infty} e^{-\beta N} M_{NL} = \sum_{m=1}^{\infty} \left[e^{-\beta} A \left(1 + A_1 e^{-\beta} + \ldots\right)\right]^{m+L}. \tag{12.31}$$

Using the multinomial theorem [129], the coefficient of $e^{-\beta(m+L)}$ in the exponent on the right side of the equation becomes

$$\sum_{m=1}^{\infty} A^{m+L} \sum_{r,s,t,\ldots} \frac{(m+L)!}{r!s!t!\ldots} {A_1}^s A_2^t \ldots e^{-\beta(m+L+s+2t+\ldots)}, \tag{12.32}$$

where $r + s + t + \cdots = m + L$.

To obtain the expression for M_{NL}, we note N is the coefficient of β on the left side of Eq. (12.31) so $N = m + L + s + 2t + \cdots = r + 2s + 3t + \cdots$ Accordingly we find

$$M_{NL} = \sum_{r,s,t,\ldots} A^{(r+s+t+\ldots)} \frac{(r+s+t+\ldots)!}{r!s!t!\ldots} A_1^s A_2^t \ldots, \tag{12.33}$$

where $r + 2s + 3t + \cdots = N$ and $r + s + t + \cdots > L$.

By applying this formula, we obtain the results:

$N = 1$:

$$M_{10} = A \tag{12.34}$$

$N = 2$:

$$\begin{aligned} M_{20} &= A^2 + AA_1 \\ M_{21} &= A^2 \end{aligned} \tag{12.35}$$

$N = 3$:

$$\begin{aligned} M_{30} &= A^3 + 2A^2A_1 + AA_2 \\ M_{31} &= A^3 + 2A^2A_1 \\ M_{32} &= A^3 \end{aligned} \tag{12.36}$$

Shifts for $N = 1$ and $N = 2$

To illustrate these results, we can calculate the shift for a given energy level using Eq. (12.13). For $N = 1$, we note from Eq. (12.34) that $M_{10} = A$, and from Eq. (12.27) that $A = 1/d^2$. We find that the real part of the radiative shift for the $1S$ ground state is

$$Re\Delta E_{10} = \frac{4m\alpha(Z\alpha)^4}{3\pi} \int_0^{\phi_c} d\phi e^{\phi} \sinh\phi \int_0^{\infty} ds e^{se^{-\phi}} \frac{d}{ds} \frac{1}{\left(\coth\frac{s}{2} + \cosh\phi\right)^2}, \tag{12.37}$$

where ϕ_c is given by Eq. (12.14).

Equation (12.30) can be used to obtain the shift between two states with the same N and with $L = 0$ and $L = 1$. For the $N = 2$ Lamb shift between 2S-2P states, the radiative shift to first order in α (one radiation field photon), is

$$\begin{aligned} &(\Delta E_{20} - \Delta E_{21}) \\ &\quad = \frac{m\alpha(Z\alpha)^4}{6\pi} \int_0^{\phi_c} d\phi e^{\phi} \sinh^3\phi \int_0^{\infty} ds e^{2se^{-\phi}} \frac{d}{ds} \frac{1}{\left(\coth\frac{s}{2} + \cosh\phi\right)^4}. \end{aligned} \tag{12.38}$$

The s integral can be computed in terms of a Jacobi function of the second kind [130][1] The shifts for 1S and 2S-2P are given in terms of integrals of simple analytic functions.

In Chapter 13, we compute the radiative shift for a harmonically bound relativistic particle without spin.

[1] As a check on our group theoretical methods, we can compare our matrix elements $(10|e^{iS\phi}|n0)$ with those of Huff [58]. To go from Eq. (12.20) to Eq. (12.21), we do a rotation $R(\phi) = e^{i\phi S}$ generated by S that transforms Γn into Γ_0. For $N, L = 1, 0$ we have

$$M_{10} = (10|e^{-\Gamma n s}|10) = (10|R(\phi)e^{-\Gamma_0 s}R^{-1}(\phi)|10) = \frac{1}{(\cosh\frac{s}{2} + \sinh\frac{s}{2}\cosh\phi)^2}. \tag{12.39}$$

Expanding the hyperbolic functions, we get

$$M_{10} = \frac{4e^{-s}}{(1+\cosh\phi)^2}\left[1 - e^{-s}\tanh^2\frac{s}{2}\right]^{-2} = \frac{4}{(1+\cosh\phi)^2}\sum_{n=1}^{\infty} ne^{-ns}\left(\tanh^2\frac{\phi}{2}\right)^{n-1}. \tag{12.40}$$

We can also compute M_{10} by inserting a complete set of states and using $\Gamma_0|n0) = n|n0)$ in Eq. (12.39). Because the generator S is a scalar, only states with $L = 0, m = 0$ can contribute:

$$M_{10} = \sum_{nlm} e^{-ns}|n(10|R(\phi)|n0)|^2. \tag{12.41}$$

Comparing this to Eq. (12.40), we make the identification

$$|(10|R(\phi)|n0)|^2 = \frac{4n}{(1+\cosh\phi)^2}\left(\tanh^2\frac{\phi}{2}\right)^{n-1}. \tag{12.42}$$

Huff computes this matrix element by analytically continuing the known $O(3)$ matrix element of $e^{iJ_y\phi}$ obtaining

$$|\langle 10|R(\phi)|n0\rangle|^2 = \frac{4n}{\cosh^2\phi - 1}\left(\tanh^2\frac{\phi}{2}\right)^n \cdot [{}_2F_1(0,-1;n;\frac{1}{2}(1-\cosh\phi))]^2. \tag{12.43}$$

Using $\tanh\phi/2 = \sinh\phi/(\cosh\phi + 1)$ and that ${}_2F_1 = 1$ for the arguments here, we can show that this result agrees with our much more simply expressed result from group theory.

This page intentionally left blank

Chapter 13

Radiative Shift of a Relativistic Meson (Spinless Electron) in a Harmonic Potential

13.1 Introduction

We compute the radiative shift for a spinless, relativistic meson with charge e in a three-dimensional harmonic potential $V = C^2r^2$, where C is a real constant. From consideration of the equations of motion, we compute the radiative shift of the energy levels that corresponds to the difference in the contribution to the mass renormalization of a mass m bound by the harmonic interaction and a free meson [253, 254]. We derive an integral expression for the complex radiative shift to order α in the radiation field and to all orders in C, the binding field. In Section 13.2, we perform the computations after making the simplifying assumption that the virtual photon is spinless. In Section 13.3, we include the effects of spin.

We assume the unperturbed meson state $|N\rangle = |N_1N_2N_3\rangle$ obeys the Klein–Gordon equation with the interaction term

$$(\boldsymbol{p}^2 - p_0^2 + C^2r^2 + m^2)|N\rangle = 0. \tag{13.1}$$

The equations of motion can be written in the form

$$(H - E_N^0)|N\rangle = 0, \tag{13.2}$$

where

$$H = \frac{\boldsymbol{p}^2}{2m} + \frac{m}{2}\left(\frac{C}{m}\right)^2 r^2 \tag{13.3}$$

and the relativistic energy is

$$E_N^0 = \frac{p_0^2 - m^2}{2m}. \tag{13.4}$$

This form shows that the equations of motion are the same as those of a simple harmonic oscillator with frequency

$$\omega = C/m. \tag{13.5}$$

Consequently, we know that the unperturbed energy levels are

$$E_N^0 = \left(N + \frac{3}{2}\right)\omega, \tag{13.6}$$

where $N = N_1 + N_2 + N_3$,
which implies that

$$p_0^2 = 2\left(N + \frac{3}{2}\right)C + m^2. \tag{13.7}$$

13.2 Relativistic Radiative Shift for a Scalar Photon Interaction

The shift is given by the equation

$$\Delta E_{\mathrm{N}} = \mathrm{E_N} - \mathrm{E_N^O} = \mathrm{ig}\int \frac{\mathrm{d^4k}}{(2\pi)^4}\frac{1}{\mathrm{k^2}}\left\langle \mathrm{N}\left|\frac{1}{\mathrm{D}(\boldsymbol{k}) - i\epsilon'}\right|\mathrm{N}\right\rangle, \tag{13.8}$$

where $g = 2me^2$, $1/k^2$ is the propagator for a scalar photon, and $D(\boldsymbol{k})$ is the inverse momentum space propagator for the bound meson:

$$D\left(\boldsymbol{k}, k_0\right) = D(k) = \left(\boldsymbol{p} - \boldsymbol{k}\right)^2 - \left(p_0 - k_0\right)^2 + C^2r^2 + m^2. \tag{13.9}$$

We employ the integral representations

$$\frac{1}{k^2 - i\epsilon} = i\int_0^\infty d\lambda e^{-i\lambda k^2 - \epsilon\lambda}, \quad \frac{1}{D(k) - i\epsilon'} = i\int_0^\infty dt e^{-itD(k) - \epsilon' t}. \tag{13.10}$$

By employing the translation operator in momentum space, we see that

$$\mathrm{e}^{-\mathrm{i\,t}\,D(k)} = \mathrm{e}^{\mathrm{i}\boldsymbol{k}\cdot\boldsymbol{r}}\mathrm{e}^{-\mathrm{i\,tD}(\mathbf{0},\,k_\mathrm{o})}\mathrm{e}^{-\mathrm{i}\boldsymbol{k}\cdot\boldsymbol{r}}, \tag{13.11}$$

where

$$D(\mathbf{0}, k_0) = 2mH + m^2 - (p_0 - k_0)^2. \tag{13.12}$$

By applying the equations of motion for the canonical variables for an elapsed time equal to mt, we find

$$\begin{aligned} e^{-itmH} r_i e^{itmH} &= r_i\cos(Ct) - p_i\sin(Ct) \\ e^{-itmH} p_i e^{itmH} &= p_i\cos(Ct) + r_i\sin(Ct) \end{aligned}. \tag{13.13}$$

We can compute the translations in Eq. (13.11) explicitly with the result

$$\frac{1}{D(k)-i\epsilon'} = i\int_0^\infty dt e^{-itmH} e^{i2\boldsymbol{k}\cdot\boldsymbol{p}\nu} e^{+itmH} \times e^{-i\mu k^2} e^{-it\left(m^2-(p_0-k_0)^2\right)} e^{-\epsilon' t}, \tag{13.14}$$

where

$$\begin{aligned} \mu &= \frac{\sin(Ct)\cos(Ct)}{C}, \\ \nu &= \frac{\sin(Ct)}{C}. \end{aligned} \tag{13.15}$$

The integration over scalar photon momentum can be performed by completing the square and employing the general formula

$$\int_{-\infty}^{\infty} dx e^{\pm(iax^2-2ibx)} = \frac{\pi}{a} e^{\mp\frac{b^2}{a}} e^{\pm i\frac{\pi}{4}}. \tag{13.16}$$

After taking matrix elements as indicated in Eq. (13.8), we find that the shift is

$$\Delta E_{N_1N_2N_3} = \int_O^\infty dt \int_0^\infty d\lambda \sigma_{\mathrm{N}} \Omega_{N_1\mathrm{N}_2\mathrm{N}_3}, \tag{13.17}$$

where we have used the product representation for the three-dimensional harmonic oscillator states $|N_1N_2N_3\rangle = |N_1\rangle|N_2\rangle|N_3\rangle$. The quantities σ and Ω are

$$\sigma_{\mathrm{N}} = -\frac{g}{16\pi^2}(\lambda+t)^{-\frac{1}{2}} e^{-ip_0^2\left(\frac{t^2}{t+\lambda}\right)} \tag{13.18}$$

$$\Omega_{N_1N_2N_3} = (\lambda+\mu)^{-\frac{3}{2}} \langle N_1N_2N_3|e^{i\boldsymbol{p}^2\left(\frac{\nu^2}{\lambda+\mu}\right)}|N_1N_2N_3\rangle. \tag{13.19}$$

We can calculate the matrix elements directly and express the results in terms of the quantity

$$\Omega(j) = \frac{\left(i\nu^2C\right)^j}{(\lambda+\mu-i\nu^2C)^{j+\frac{3}{2}}}. \tag{13.20}$$

We find

$$\begin{aligned} \Omega_{000} &= \Omega(0), \\ \Omega_{100} &= \Omega(0)+\Omega(1), \\ \Omega_{200} &= \Omega(0)+2\Omega(1)+\tfrac{3}{2}\Omega(2), \\ \Omega_{110} &= \Omega(0)+2\Omega(1)+\Omega(2). \end{aligned} \tag{13.21}$$

The radiative shifts lift the degeneracy for some levels, and this parameterization simplifies the calculation of shifts between degenerate levels. Renormalization of the free particle mass is contained in $\Omega(0)$ to all orders. This follows by noting that, for $j \geq 1$, as $C \to 0$

$$\lim_{C\to 0} \Omega(j) \to 0. \tag{13.22}$$

For calculations of the shift between the non-degenerate energy levels, we would use a different formulation, subtracting the free particle shift in the beginning.

To verify our equations, we consider the limit $C \to 0$, which should yield the free particle renormalization. In this limit, we have $\mu \to t$, $\nu \to t$ from Eq. (13.15), and $p_0^2 = m^2$ from Eq. (13.7) so the only non-vanishing Ω is

$$\Omega(0) \to (\lambda + t)^{-\frac{3}{2}}. \tag{13.23}$$

Substituting these quantities into the expression for the shift, Eq. (13.17), we find

$$\Delta \mathrm{E}_{\mathrm{free}} = -\frac{g}{16\pi^2} \int_0^1 dy \int_0^\infty \frac{dt}{t} \mathrm{e}^{-im^2 yt}, \tag{13.24}$$

where we have made the substitution

$$y = \frac{t}{t+\lambda}. \tag{13.25}$$

To avoid having a spurious imaginary term, we do not include the contribution from the pole at $t = 0$, but start our integration at $t = \epsilon$. Using the formula

$$\int_\epsilon^\infty dt \frac{e^{-iat}}{t} = -\ln(\epsilon a) - \gamma, \tag{13.26}$$

we find

$$\Delta E_{free} = \frac{g}{16\pi^2} \ln(\epsilon m^2) + \gamma - 1, \tag{13.27}$$

where ϵ in the infinitesimal cutoff for the t integration and γ is Euler' constant. This result has the same structure as the conventional result with respect to the divergences. The finite parts depend on the values of the cutoffs and on the particular procedures used to evaluate the integrals. The infinite terms cancel in the calculation of measurable shifts and consequently have no direct physical significance.

Equation 13.20 for the bound state shifts can be rewritten in terms of y and $\tau = 2Ct$:

$$\begin{aligned}\lambda + \mu - \mathrm{i}\nu^2\mathrm{C} &= \frac{\tau}{2\mathrm{Cy}}\left[1 - \frac{y}{i\tau}\left(\mathrm{e}^{-i\tau} + \mathrm{i}\tau - 1\right)\right] \\ \mathrm{i}\nu^2\mathrm{C} &= \frac{1}{4i\mathrm{C}}\left(\mathrm{e}^{\mathrm{i}\tau} + \mathrm{e}^{-\mathrm{i}\tau} - 2\right) \\ \mu &= \frac{1}{4\mathrm{iC}}\left(\mathrm{e}^{\mathrm{i}\tau} - \mathrm{e}^{-\mathrm{i}\tau}\right).\end{aligned} \tag{13.28}$$

The integral used to calculate the shifts is

$$\Delta E_N(j) \equiv \int_0^1 dy \int_0^\infty dt \sigma_N \Omega(j), \tag{13.29}$$

which equals

$$\Delta E_N(j) = -\frac{g}{16\pi^2}\frac{1}{(2i)^j}\int_0^1 dy \int_{2C\epsilon}^\infty \frac{d\tau}{\tau^{j+1}} \frac{y^j\left(e^{i\tau} + e^{-i\tau} - 2\right)^j e^{-iy\eta\tau}}{\left[1 - \frac{y}{i\tau}\left(e^{-i\tau} + i\tau - 1\right)\right]^{j+\frac{3}{2}}}, \tag{13.30}$$

where the lower limit of the τ integration is $2\epsilon C$ to avoid the pole at zero. The degree of coupling to the harmonic oscillator is given by the dimensionless parameter

$$\eta = \frac{p_0^2}{2C}. \tag{13.31}$$

The shift can be expressed as a single integral of a confluent hypergeometric function with two arguments. The structure is similar to that for the H atom, where the shift can also be expressed in terms of an integral over a confluent hypergeometric function [156].

13.3 Relativistic Radiative Shift for a Spin 1 Photon Interaction

The expression for the shift is

$$\Delta E_\mathrm{N} = E_\mathrm{N} - E_\mathrm{N}^0 = ig\int \frac{\mathrm{d}^4k}{(2\pi)^4}\frac{1}{k^2 - i\epsilon}\left\langle \mathrm{N}\left|\mathrm{T}_\mu^\mu\right|\mathrm{N}\right\rangle, \tag{13.32}$$

where we are using the spin 1 photon propagator and

$$\mathrm{T}_{\mu}^{\mu} = (2p-k)_{\mu}\frac{1}{D(k)-i\epsilon}(2p-k)^{\mu}. \tag{13.33}$$

Executing the trace gives

$$\begin{aligned} T_{\mu}^{\mu} = 4\left[p_i\frac{1}{D(k)}p_i - p_o^2\frac{1}{D(k)}\right] - 2\left\{\mathbf{p}\cdot\mathbf{k},\frac{1}{D(k)}\right\} \\ - 4\mathrm{p_o k_o}\frac{1}{D(k)} - \left(\mathbf{k}^2 - \mathrm{k_o^2}\right)\frac{1}{D(k)}. \end{aligned} \tag{13.34}$$

We can derive expressions for each of these quantities in terms of our previous results by employing the Heisenberg equations of motion for p_i and q_i (Eq. 13.13) and also our form of the Klein–Gordon equation (Eq. 13.1). Our final result is

$$\begin{aligned} \Delta E_{N_1N_2N_3} = 4\int_0^{\infty} d\lambda \int_0^{\infty} dt \left[-p_O^2 - C^2\nu^2 2C\left(\mathrm{N}+\frac{3}{2}\right) - 3i\mu C^2\right. \\ - p_0^2\frac{t}{t+\lambda} + \left(2\mu\nu C^2 + \frac{\lambda}{\nu}\right)\frac{1}{2i}\frac{\partial}{\partial\nu} \\ \left. + C^2\nu^2\left(2C^2\nu^2-1\right)\frac{1}{-i}\frac{\partial}{\partial(\lambda+\mu)}\right]\sigma_{\mathrm{N}}\Omega_{\mathrm{N}_1N_2N_3} \\ + \frac{1}{i}\int_0^{\infty} dt\sigma_N\Omega_{N_1N_2N_3}|_{\lambda=0}, \end{aligned} \tag{13.35}$$

where σ_N and $\Omega_{N_1N_2N_3}$ have the same meaning as before (Eqs. (13.18) and (13.19)).

In Chapter 14 we return to the hydrogen atom and we determine the contribution to the Lamb shift from the different frequency components in the quantum vacuum field. We find that 97% of the radiative shift is due to energies above the ionization energy, implying that transitions to scattering states dominate.

Chapter 14

New Insights into the Lamb Shift: The Spectral Density of the Shift

In an atom, the interaction of a bound electron with the vacuum fluctuations of the electromagnetic field leads to complex shifts in the energy levels of the electron, with the real part of the shift corresponding to a shift in the energy level and the imaginary part to the width of the energy level. The most celebrated radiative shift is the Lamb shift between the $2s_{1/2}$ and $2p_{1/2}$ levels of the hydrogen atom. We have done a calculation of the shift using a group theoretical approach which gives the shift as an integral over frequency of an analytic function, which we call a shift spectral density. The shift spectral density reveals how different frequencies contribute to the total energy shift. We find, for example, that half the radiative shift for $N = 1$ level in hydrogen comes from photon energies above 9700 eV, and that the expressions by Power and Welton for the radiative shift do not have the correct low frequency behavior, although they do give the correct value for the total shift.

14.1 Introduction

In astronomy, in quantum theory, in quantum electrodynamics (QED), there have been periods of great progress in which solutions to challenging problems have been obtained, and the fields have moved forward. However, in some cases, getting the right answers can still leave fundamental questions unanswered. The Big Bang explained the origin of the cosmic background radiation, but left the problem of why the universe appears to be made of matter and not equal amounts of matter and antimatter [255]. In quantum theory, we can compute the behavior of atoms, yet we cannot describe a measurement of a quantum system in a self-consistent way or

make sense of the collapse of a photon wavefunction from a nearly infinite volume to a point [256]. In quantum electrodynamics, we can compute the Lamb shift of the H atom to 15 decimal places [1], yet we are left with the paradox of using perturbation theory to remove infinite terms, or to understand a quantum vacuum with infinite energy. In this chapter, we examine some of the differences in the approaches to the computation of the non-relativistic Lamb shift. For all these approaches, the Lamb shift can be expressed in different ways as an integral over frequency of a spectral density that indicates the contribution to the shift from different frequency components in the quantum vacuum.

We compare the spectral densities for the different approaches of Bethe, Welton and Power to the group theoretical spectral density of the non-relativistic Lamb shift for the 1S ground state, the 2S and 2P levels. With this new picture of the Lamb shift, we have found differences between the various approaches. Knowing the spectral density of the shift provides new insights into understanding the Lamb shift.

14.2 Spectral Density of the Lamb Shift

Our goal is to develop an expression for the shift of an energy level, in terms of the generators of the group SO(4,2), that is an integral over frequency. Then the integrand will be the spectral density of the shift, and group theoretical techniques can be used to evaluate it [20]. We have derived a generating function for the shifts for all levels in Chapter 12. We first focus on the ground state 1S level as an illustration of the results. At ordinary temperatures and pressures, most atoms are in the ground state. The radiative shift for the 1S level is given in Eq. (12.37) [252]

$$\Delta E_1 = \frac{4mc^2\alpha(Z\alpha)^4}{3\pi}\int_0^{\phi_c} d\phi e^{\phi}\sinh\phi\int_0^{\infty} ds e^{se^{-\phi}}\frac{d}{ds}\frac{1}{\left(\coth\frac{s}{2}+\cosh\phi\right)^2}, \tag{14.1}$$

where the dimensionless normalized frequency variable ϕ is defined as

$$\phi = \frac{1}{2}\ln\left[1+\frac{\hbar\omega}{|E_1|}\right], \tag{14.2}$$

where E_1 is the ground state energy $-13.6\,\text{eV}$. The cutoff ϕ_c corresponds to $E = \hbar\omega_C = mc^2$, 511 keV, corresponding to the electron mass. The group theoretical expression for the Lamb shift Eq. 14.1 is directly derived from the Klein–Gordon equations of motion using a non-relativistic dipole

approximation, assuming infinite proton mass, and minimal coupling with the vacuum field. Basis states of $(1/Z\alpha)$ are used since they have no scattering states and have the same quantum numbers as the usual bound energy eigenstates [252]. The level shift is obtained as the difference between the mass renormalization for a spinless meson bound in the desired state and the mass renormalization for a free meson. Second order perturbation theory is not used. Near the end of the derivation, an equation which is identical to Bethe's result Eq. (9.27) for the radiative shift can be derived by inserting a complete set of Schrodinger energy eigenstates. Thus, we expect the fundamental results from Bethe's spectral density (with no approximations) and the group theoretical spectral density to be in agreement [20, 252].

We can write Eq. 14.1 as an integral over $E = \hbar\omega$, which is the energy of the vacuum field in eV, and evaluate the definite integral over s for different values of E. We measure the ground state Lamb shift ΔE_1 in eV so the spectral density of the shift $d\Delta E_1/dE$ is measured in eV/eV which is dimensionless:

$$\Delta E_1 = \int_0^{mc^2} \frac{d\Delta E_1}{dE} dE, \tag{14.3}$$

where the ground state spectral density from Eq. (14.1) is

$$\frac{d\Delta E_1}{dE} = \frac{4\alpha^3}{3\pi} e^{-2\phi} \sinh\phi \int_0^\infty ds e^{se^{-\phi}} \frac{1}{\sinh(\frac{s}{2})^2} \frac{1}{(\coth\frac{s}{2} + \cosh\phi)^3}. \tag{14.4}$$

Figure 14.1 shows a logarithmic plot (ordinate is a log, abscissa is linear) of the spectral density $\frac{d\Delta E_1}{dE}$ of the ground state Lamb shift with $Z = 1$ over the entire range of energy E computed from Eq. (14.4) using Mathematica. The spectral density is largest at the lowest energies and decreases monotonically by about 4 orders of magnitude as the energy increases to 511 eV. The ground state shift is the integral of the spectral density from energy 0 to 511 keV. Figure 14.2 is a loglog plot (both ordinate and abscissa are log) of the same information. The use of the loglog plot expands the energy range for each decade, revealing that for energy above about 100 eV the slope is approximately -1, indicating that the spectral density is nearly proportional to $1/E$. For energy below about 10 eV, the spectral density in Fig. 14.2 is almost flat, corresponding to a linear increase as energy decreases, with a maximum spectral density at the lowest energy computed, as shown in Fig. 14.3.

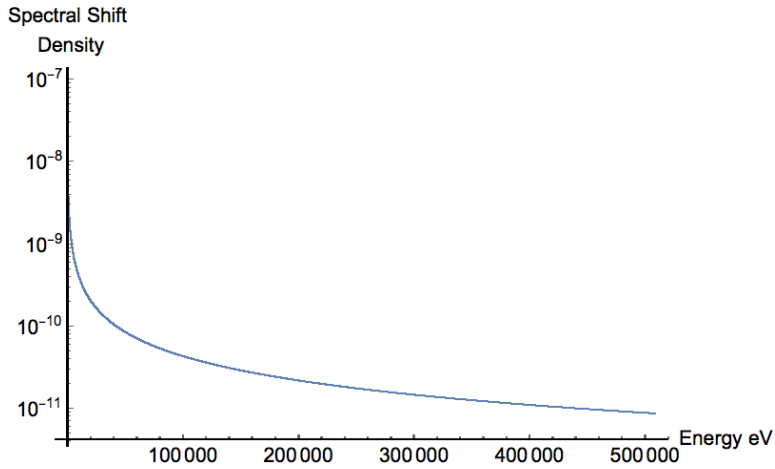

Fig. 14.1. Plot of the log of the spectral density of the ground state Lamb shift from the group theoretical expression Eq. (14.4) on the vertical axis versus the energy in eV from 0 to 511 keV on the horizontal axis.

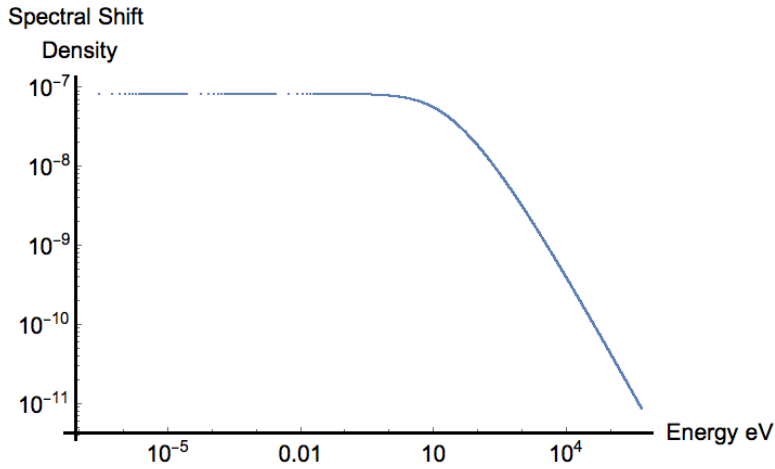

Fig. 14.2. This loglog plot shows the log of the spectral density of the ground state shift from the group theoretical expression Eq. (14.4) on the vertical axis versus the log of the energy in eV. From about 0 eV to 10 eV, there is a slow linear decrease in the spectral density. For energies above about 100 eV, the behavior is dominated by a 1/energy dependence.

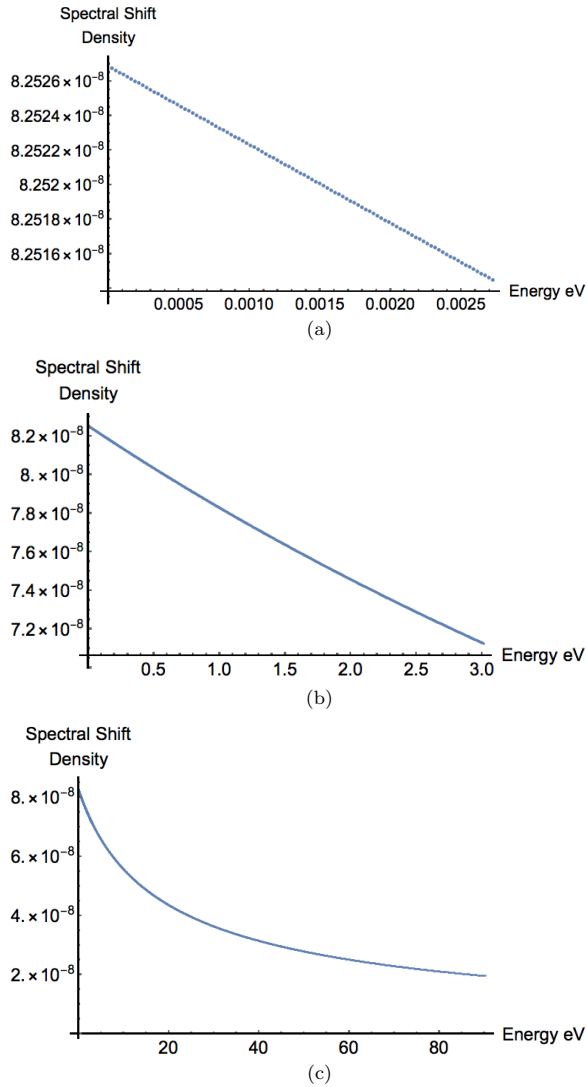

Fig. 14.3. Linear plot of the ground state spectral density as a function of eV calculated from group theory, plotted as a function of energy for low and mid energies. From about 0 eV to 10 eV, the spectral density decreases linearly from its maximum value at the origin which corresponds to 0 eV for all graphs. (a) Linear decrease in ground state spectral density at very low energies. Note ordinate changes very little over small energy region plotted. (b) Near linear change in ground state spectral density for visible and near IR energies. The contribution to the total shift for energies below 3 eV is about 0.7%. (c) Ground state spectral density calculated for energies below 80 eV, which contribute about 8.6% to the total shift.

Figure 14.2 shows that there are essentially two different behaviors of the spectral density. For values of the energy E of the vacuum field that are about 10 eV and below, in the range of the changes in energy for bound state transitions, the spectral density corresponds to the near horizontal portion of the spectral density in Fig. 14.2, and when E is much larger than the bound state energies, the spectral density goes as 1/E.

Figure 14.3 shows linear plots (linear in ordinate and abscissa) of the spectral density of the shift for the ground state computed from Eq. (14.4) for several lower energy regions. Fig. 14.3(a) shows a linear decrease in the spectral density as the energy increases over the small, low energy interval plotted. Figure 14.3(b) shows a linear decrease of about 15% as the energy increases from 0 eV to 3 eV. Figure 14.3(c) shows that the spectral density decreases by a factor of about 4 as the energy increases from 0 eV to 100 eV. In the low frequency limit, the spectral density decreases linearly as the energy increases from the asymptotic constant value at 0 eV.

It may seem somewhat surprising that the spectral shift density is a monotonically decreasing function as the energy increases. Bethe believed, and it seemed reasonable, that the contributions to the shift would be greatest for resonant transitions between the bound state energy levels, but there is no such effect in the computed spectral shift density. This conundrum suggests we may not have a precise understanding of the physical processes that are occurring despite the fact that our mathematics allow us to make a very precise computation of the shift. One of the challenges is that it is not possible to measure these computed transitions directly.

From explicit evaluations, we will show in Section 14.4 that for S states with principal quantum number n, the asymptotic spectral density for large E is proportional to $\alpha(Z\alpha)^4(1/n^3)(1/E)$, and show in Section 14.5 that as the energy E goes to zero, the spectral density increases linearly, reaching a maximum value that is proportional to $\alpha(Z\alpha)^2(1/n^2)$. An approximate fit to the ground state data in Fig. 14.1 is

$$\frac{d\Delta E_1^{Fit}(E)}{dE} = A\frac{(1+e^{-E/B})}{(E+C)}, \tag{14.5}$$

where $A = 4.4008 \times 10^{-6}$, $B = 11.841$ eV, $C = 106.79$ eV. The fit is quite good at the asymptotes and within 10% over the entire energy range.

We can use the spectral density shown in Figs. 14.1 or 14.2 to determine the contribution to the total ground state shift from different energy regions. If we integrate the spectral density from 0 eV to energy E, we obtain the

value of the partial shift $\Delta_1(E)$ in which these energies (0 eV to E eV) contribute to the total shift ΔE_1 for the ground state. In Fig. 14.4, we have plotted $\Delta_1(E)/\Delta E_1$, which is the fraction of the total shift ΔE_1 due to the contributions of energies below E, as a function of E. Figure 14.4(a) shows that almost 80% of the shift comes from energies below about 100,000 eV. Figure 14.4(b) shows that about half the total shift is from energies below 9050 eV. Figure 14.4(c) shows that energies below 100 eV contribute about 10% of the total shift. Energies below 13.6 eV contribute about 2.5% while energies below 1 eV contribute about 1/4% of the total. It is quite remarkable that over 96% of the contribution to the 1S radiative shift is from transitions to states that are ionized. As shown in Fig. 14.4(c), the fraction of the total shift increases linearly as E decreases from 10 ev to 0, corresponding to the nearly horizontal portion of the shift density as shown in Fig. 14.2. The contribution to the total 1S shift for the visible spectral interval 400–700 nm (1.770–3.10 eV) is about 1.00342×10^{-7} eV or about 3/10% of the total shift.

The relative contribution to the total shift per eV is much greater for lower energies. For example, half the 1S shift corresponds to energies 0 to 9000 eV, but only about 0.2% corresponds to 500,000 to 509,000 eV. The largest contribution to the shift per eV is at the lowest energies, which have the steepest slope of the spectral density curve in Fig. 14.1, about 1000 times greater than the slope for the largest values of the energy. But the total range for the large energies, from 9050 to 510,000 is so large that the absolute contribution to the total shift for large energies is significant.

For the ground state, Fig. 14.5 shows how the dominant terms for different m in the Bethe sum over states in Eq. (12.1) contribute to the full spectral density obtained from group theory Eq. (14.4). Each such term in the Bethe sum could be interpreted as corresponding to the shift resulting from virtual transitions from state n to state m occurring due to the vacuum field. Each term shown has a behavior similar to that of the full spectral density, but the magnitudes decrease as the transition probabilities decrease.

Figure 14.6 shows the spectral densities for the 1S (top curve) and 2S (middle curve) shifts. The shapes are similar, but the spectral density for the 1S shift is about eight times as large at high frequencies and about four times as large at low frequencies, factors that we will derive explicitly by considering the asymptotic forms of the spectra density for S states with different principal quantum numbers. Both have a $1/E$ high frequency behavior. The s integration in the group theoretical calculation

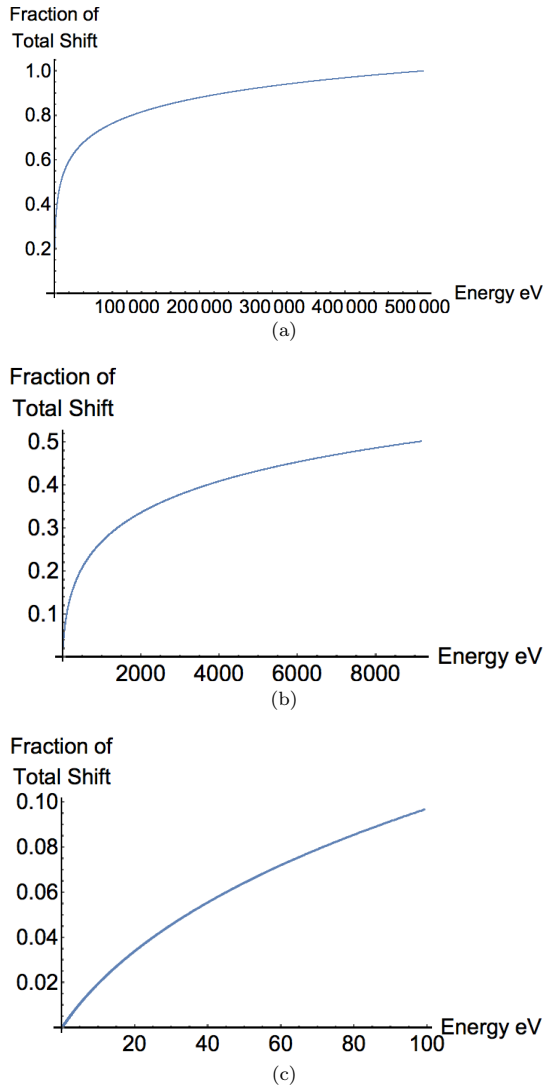

Fig. 14.4. The ordinate is the fraction of the ground state shift ΔE_1 due to vacuum field energies between 0 and E, plotted as a function of E on the abscissa. This plot is obtained by integration of the spectral density from Eq. (14.4), shown in Fig. 14.1. The plot is linear in the ordinate and abscissa. The origin corresponds to (0,0) for all plots. (a) Fraction of the 1S shift due to energies from 0 to E plotted versus E on the abscissa, for $0 < E < 510$ keV. (b) Fraction of the 1S shift due to energies below E plotted versus E, for $0 < E < 9000$ eV. (c) Fraction of the 1S shift due to energies from 0 to E plotted versus E on the abscissa, for $0 < E < 100$ eV. Energies below 30 eV account for about 0.05 of the total shift. The variation is linear for $E < 10$ eV.

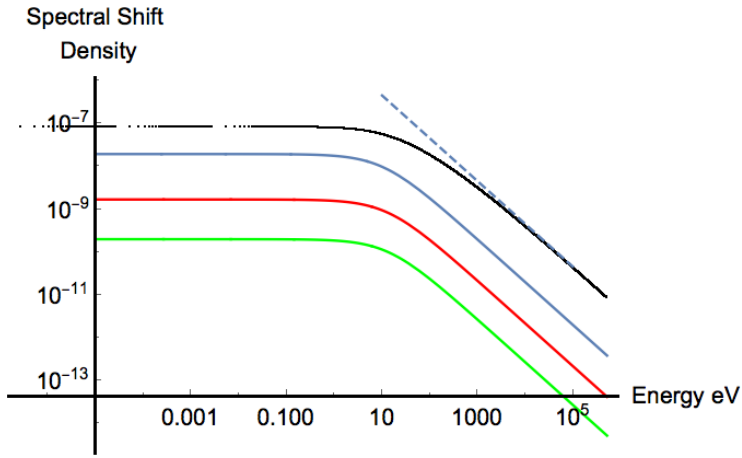

Fig. 14.5. This loglog plot shows the 1S spectral density from group theory Eq. (14.4) (top curve), and the contributions to this shift in the Bethe formalism for the transition $1S \to 2P$ (blue, just below top curve), $1S \to 4P$ (red, third curve from the top), $1S \to 8P$ (green, bottom curve). The dashed line shows the high frequency $1/E$ asymptote. The top curve is the complete 1S spectral density which is the summation of the contributions from all transitions.

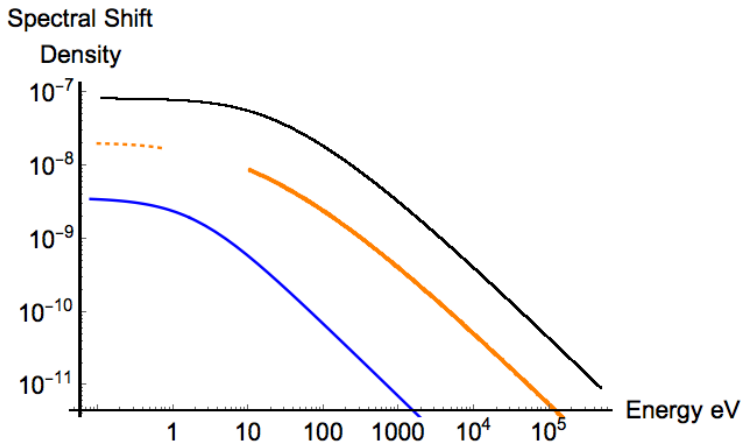

Fig. 14.6. This loglog plot shows the log of the group theoretical spectral density for the 1S (black, top curve) and 2S (red, middle curve) shifts on the vertical axis versus the log of the frequency in eV. The dashed curve below 1 eV is a 2S low energy approximation Eq. (14.24) from group theory or the Bethe formula. The bottom curve is the largest single contribution in the Bethe formalism to the 2S shift spectral density for the transition 2S → 3P.

for the 2S state diverges for energies below 10.2 eV due to a non-relativistic approximation, but the spectral density of the shift can be obtained from a low energy approximation, Eq. (14.24), to the group theory result, which we derive in Section 14.4.

We can define the spectral density $\frac{d\Delta E_n}{dE}$ for a state n in a convenient form suggested by Eq. (14.4),

$$\frac{d\Delta E_n}{dE} = \frac{4\alpha^3}{3\pi}\int_0^\infty ds W_n(s,\phi_n) \quad \text{where} \quad \phi_n = \ln\left[1+\frac{E}{|E_n|}\right], \tag{14.6}$$

where the energy for state n is $E_n = -mc^2(Z\alpha)^2/2n^2$. From our group theoretical results for the 2S-2P Lamb shift, Eq. (12.38), we have

$$W_{2S-2P}(s,\phi_2) = \frac{4e^{(2se^{-\phi_2}+\phi_2)}\sinh^3(\phi_2)\mathrm{csch}^2\left(\frac{s}{2}\right)}{\left(\cosh(\phi_2)+\coth\left(\frac{s}{2}\right)\right)^5} \tag{14.7}$$

and for the 2P shift [252]:

$$W_{2P}(s,\phi_2) \tag{14.8}$$

$$= -\frac{e^{(2se^{-\phi_2}+\phi_2)}\sinh(\phi_2)\mathrm{csch}^4\left(\frac{s}{2}\right)\left(\cosh(\phi_2)\sinh(s)+\cosh(s)-3\right)}{2\left(\cosh(\phi_2)+\coth\left(\frac{s}{2}\right)\right)^5}. \tag{14.9}$$

The spectral density of the 2P shift has a very different behavior from the spectral density of the 2S shift (Fig. 14.7). It is negative and drops off as $1/E^2$. The shift is negative because the dominant contribution to the shift is from virtual transitions from the 2P state to the lower 1S state, with an energy difference of about 10.2 eV. At 510 keV, the 2P spectral density is about five orders of magnitude smaller than the 2S spectral density. Below 20 eV, the absolute value of the 2P spectral density is greater than the 2S spectral density. Note that the 2P spectral density is actually negative and the 2S spectral density is positive. For energies below about 20 eV, the absolute value of the spectral density of the 2P shift increases rapidly in magnitude as the energy is reduced and is much larger than the spectral density for the 2S shift. The 2S shift cannot have a negative contribution from the lower 1S state since the transition 2S→1S is forbidden by conservation of angular momentum. The classic Lamb shift arises from the difference between the two spectral densities, so the negative 2P spectral density actually increases the 2S-2P Lamb shift as the energy decreases (Fig. 14.8). The total 2P shift is about 0.3% of the 2S shift. Bethe also computed a negative contribution for the shift from the 2P state [158].

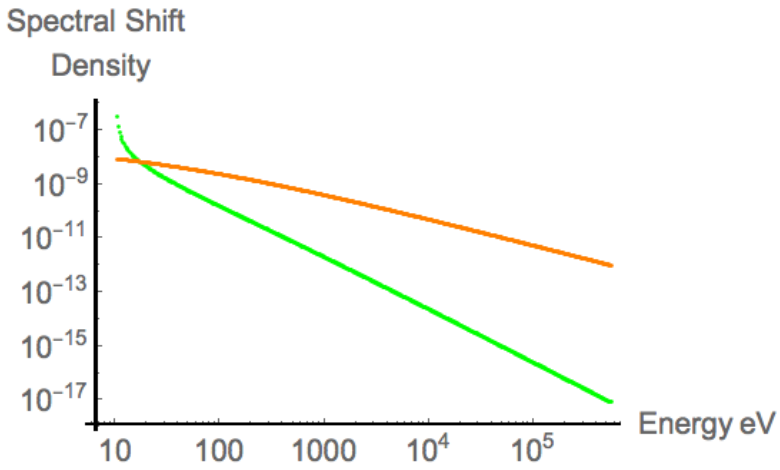

Fig. 14.7. This loglog plot shows the log of the absolute value of the spectral density on the vertical axis versus the log of the energy in eV for the 2S shift (red, top curve), which goes as $1/E$ for large E, and for the 2P shift (green, bottom curve), which goes as $1/E^2$ for large E.

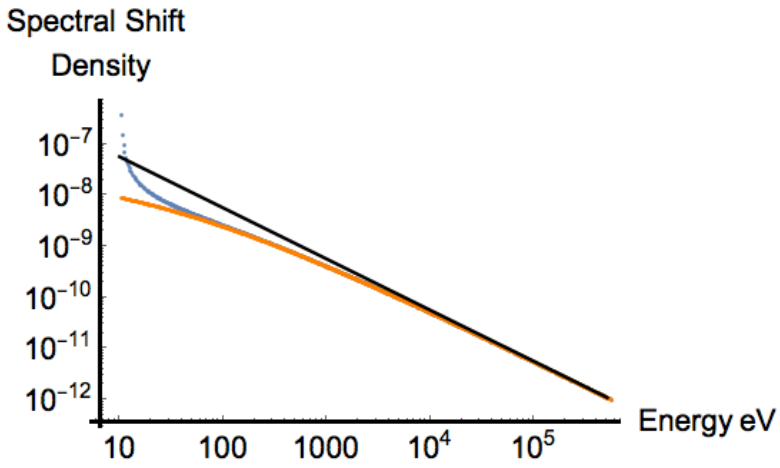

Fig. 14.8. This loglog plot shows the log of the spectral density for the 2S shift (red, bottom line) and the 2S-2P Lamb shift (blue, curved middle line) versus the log of the energy. The line at the top is the $1/E$ asymptote.

14.2.1 *Comparing the ground state group theoretical Lamb shift calculations to those of Bethe, Welton, and Feynman*

Integrating the group theoretical spectral density Eq. (14.4) from near zero energy (5.4×10^{-7} eV) to 511 keV, about the rest mass energy of the electron, gives the 1S shift of 3.4027×10^{-5} eV, in agreement with the numerical result of Bethe and Salpeter summing over states and using the Bethe log approximation, 3.392×10^{-5} eV, to about 0.3% [158].

Bethe and Salpeter reported that the ground state Bethe log Eq. (9.34), which is a logarithmically weighted average value of the excitation of the energy levels contributing to the radiative 1S shift, was 19.77 Ry or 269 eV [158]. Because of the weighting, it is not clear how one should interpret this value, other than it indicates that high energy photons and scattering states contribute significantly to the shift. As we have noted, our group theoretical method does not provide an equivalent weighted average value for direct comparison.

Although the methods of Bethe, Welton, and Power as defined all give approximately the same value for the 1S shift, which equals the integral of the spectral density in our approach, they differ significantly in their frequency dependence, which we will now examine.

14.3 The Spectral Density of the Lamb Shift at High Frequency

The form for $d\Delta E_n/dE$, which is the Lamb shift spectral density for level n, can be obtained at high energies from (1) the classic calculation by Bethe using second order perturbation theory, before any approximations are made to evaluate the integral; (2) the calculation by Welton of the Lamb shift; (3) the calculation of Power of the Lamb shift based on Feynman's approach; and (4) our group theoretical calculation.

The spectral density for level n can be written from Bethe's expression Eq. (11.28)

$$\frac{\Delta E_n^{Bethe}}{\Delta E} = \frac{2\alpha}{3\pi}\left(\frac{1}{mc}\right)^2 \sum_m |\mathbf{p}_{mn}|^2 (E_n - E_m)\frac{1}{E_n - E_m - E}. \qquad (14.10)$$

If we are evaluating the spectral density for the ground state $n = 1$, $Z = 1$, then $E_1 = -13.613$ eV and for the bound states $E_m = -13.613eV/m^2$. For scattering states E_m is positive. Hence, the denominator is negative for

all terms in the sum over m and never vanishes, and the spectral density is positive, and the ground state shift is positive as it must be. For large values of $E > E_n - E_m$, we can make the approximation

$$\frac{\Delta E_n^{Bethe}}{\Delta E}|_{E->\infty} = \frac{2\alpha}{3\pi}\left(\frac{1}{mc}\right)^2 \sum_m |\mathbf{p}_{mn}|^2 (E_m - E_n)\frac{1}{E}. \tag{14.11}$$

The summation can be evaluated using the dipole sum rule Eq. (9.30), and Eqs. (9.31) and (9.32) for the Coulomb S state wavefunction, obtaining the final result for the high frequency spectral density for S states with principal quantum number n

$$\frac{d\Delta E_n^{Bethe}}{dE}|_{E->\infty} = \frac{4mc^2}{3\pi}\alpha(Z\alpha)^4\frac{1}{n^3}\frac{1}{E}. \tag{14.12}$$

The result highlights the $1/E$ behavior at high frequencies, and shows the presence of a coefficient proportional to $1/n^3$. To put a scale on the coefficient, we note that the high frequency spectral density can be written as $(8/3\pi)(\alpha(Z\alpha)^2/n)(E_n/E)$.

The spectral density for *all* frequencies from Welton's model can be obtained from Eq. (9.44):

$$\Delta_N^{Welton} = \frac{4\alpha(Z\alpha)^4 mc^2}{3\pi}\frac{1}{N^3}\frac{1}{E}. \tag{14.13}$$

This is identical to this high frequency limit of Bethe's calculation. Thus, at low frequencies, the spectral density for Welton's calculation diverges as $1/E$. Because of the expectation value of the Laplacian, Welton's approach predicts a shift only for S states. Its appeal is that it gives a clear physical picture of the primary role of vacuum fluctuations in the Lamb shift and shows the presence of the $1/E$ characteristic behavior. To obtain a level shift, it requires providing a low energy limit for the integration. As we have noted, if the lower limit is Bethe's logarithmic average excitation energy, 269 eV for $n = 1$, and the upper limit mc^2, then Welton's total 1S shift agrees with Bethe's. A choice of this type works since (1) it does not include any contributions from energies below 269 eV and (2) it gives a compensating contribution for energies from 269 eV to about 1000 eV that is larger than the actual spectral density, as shown in Fig. 14.2, and (3) above about 1000 eV, Welton's model gives the same $1/E$ spectral density as Bethe.

The spectral density for Power's model can be obtained from Eq. (9.53)

$$\frac{\Delta E_n^{Power}}{dE} = -\frac{2\alpha}{3\pi}\left(\frac{1}{mc}\right)^2 \sum_m |\mathbf{p}_{mn}|^2 (E_m - E_n)\frac{E}{(E_m - E_n)^2 - E^2} \tag{14.14}$$

For large energy E, we see the result is identical to the high frequency limit Eq. (14.12) for the Bethe formalism and the Welton model so we have

$$\frac{\Delta E_n^{Power}}{dE}|_{E->\infty} = \frac{4mc^2}{3\pi}\frac{\alpha(Z\alpha)^4}{n^3}\frac{1}{E}. \tag{14.15}$$

Thus, we find for S states a $1/E$ dependence of the high frequency spectral density, corresponding to the logarithmic divergence at high frequency. We can write all the high energy theoretical results in a form allowing easy comparison to the calculated group theoretical spectral density eV/eV:

$$\frac{d\Delta E_n^{Bethe}}{dE}|_{E->\infty} = \frac{4mc^2}{3\pi}\frac{\alpha(Z\alpha)^4}{n^3}\frac{1}{E}. \tag{14.16}$$

The spectral density is $1/n^3$ for the S states. For the ground state $n = 1$, $Z = 1$, we have

$$\frac{d\Delta E_1^{Bethe}}{dE}|_{E->\infty} = 4.488 \times 10^{-6}\frac{1}{E}. \tag{14.17}$$

A fit to the last two data points near 510 KeV in the group theoretical calculations gives:

$$\frac{d\Delta E_1^{GTcalc}}{dE}|_{E->510\,\mathrm{keV}} = 4.4008 \times 10^{-6}\frac{1}{E}. \tag{14.18}$$

The coefficients differ by approximately 2%. The difference may be due to the fact that the Bethe result is a high frequency asymptotic result, whereas the group theory is for a finite limit of 510 eV. Figure 14.9 is a plot of the ground state group theoretical spectral density (top curve) from Eq. (14.4) and the theoretical high energy $1/E$ function from Bethe, Power and Welton, Eq. (14.17), (slightly below top curve), and the difference times a factor of 10 (bottom curve). The asymptotic theoretical result from Bethe, Power, and Welton agrees with the full group theoretical calculation from Eq. (14.4) to within about 2% at 511 keV and to within about 6% at 50 KeV. It is notable that the high frequency form is a reasonable approximation down to 50 keV. In fact, the Welton approach is based on this observation; it has the same $1/E$ energy dependence for all energies.

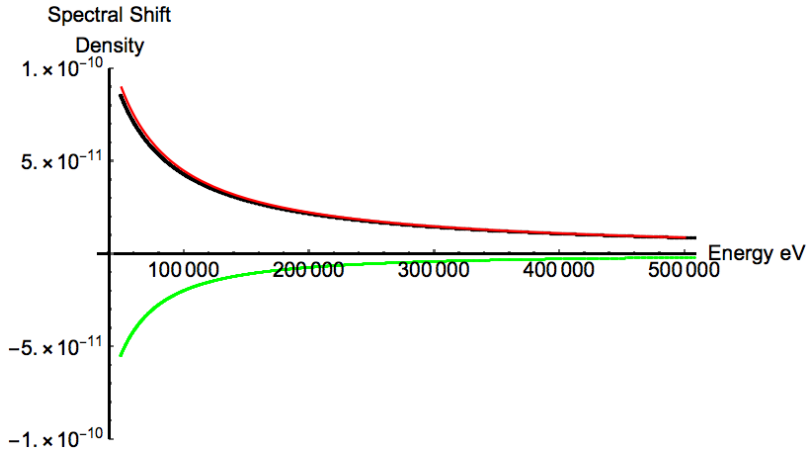

Fig. 14.9. Top curve is the 1S group theoretical calculated spectral density Eq. (14.4), slightly lower curve is the $1/E$ asymptotic model Eq. (14.17) of Bethe, Power and Welton, and the bottom negative curve is the difference times 10, plotted for the interval 50–510keV. Both axes are linear.

14.4 Spectral Density of the Lamb Shift at Low Frequency

We can obtain a low frequency limit of the spectral density of the Lamb shift from the Bethe spectral density Eq. (14.10). For small values of E, the spectral density can be expanded to the first order in E, giving

$$\frac{\Delta E_n^{Bethe}}{dE}|_{E->0} = \frac{2\alpha}{3\pi}\left(\frac{1}{mc}\right)^2 \sum_m |\mathbf{p}_{mn}|^2 \left(1 - \frac{E}{E_m - E_n}\right). \tag{14.19}$$

Since the sum is over a complete set of states m, including scattering states, we can evaluate the first term in parenthesis using the sum rule

$$\sum_m |\mathbf{p}_{mn}|^2 = -2mE_n = (mc)^2 \frac{(Z\alpha)^2}{n^2}. \tag{14.20}$$

For the second term we use Eq. 9.51

$$|\mathbf{p}_{mn}|^2 = m^2\omega_{mn}^2 |\mathbf{x}_{mn}|^2 = \frac{m^2\omega_{mn}^2}{e^2}|\mathbf{d}_{mn}|^2$$

and the Thomas–Reiche–Kuhn sum rule [259]

$$\sum_m \omega_{mn}|\mathbf{d}_{mn}|^2 = \frac{3e^2\hbar}{2m} \tag{14.21}$$

to evaluate the resulting summation. The final result for $E \to 0$ is

$$\frac{\Delta E_n^{Bethe}}{dE}|_{E->0} = \frac{2\alpha}{3\pi}\frac{(Z\alpha)^2}{n^2} - \frac{\alpha}{\pi mc^2}E. \tag{14.22}$$

The corresponding spectral density for $n = 1, Z = 1$ is

$$\begin{aligned}\frac{d\Delta E_1^{Bethe}}{dE}|_{E->0} &= \frac{4\alpha \times 13.6}{3\pi mc^2}\left(1 - \frac{3E}{4 \times 13.6}\right) \\ &= 8.253 \times 10^{-8}(1 - 0.0551E).\end{aligned} \tag{14.23}$$

As E decreases to zero, the spectral density increases linearly to a constant value $(4\alpha/3\pi)(|E_n|/mc^2) = 2\alpha^3 Z^2/3\pi n^2 = 8.253 \times 10^{-8}/n^2$. The intercept goes as $1/n^2$, but the slope, $\alpha/\pi mc^2$, which is constant and has a remarkably simple form, is independent of n.

If we take the low frequency limit of the group theoretical result Eq. (14.4) analytically, we obtain exactly the same result as in Eq. (14.23) from the Bethe formulation

$$\frac{d\Delta E_1^{GTheory}}{dE}|_{E->0} = \frac{d\Delta E_1^{Bethe}}{dE}|_{E->0} = \frac{2\alpha}{3\pi}\frac{(Z\alpha)^2}{n^2} - \frac{\alpha}{\pi mc^2}E. \tag{14.24}$$

Figure 14.3 shows the results of group theoretical calculations of the spectral density of the ground state Lamb shift for different energy regions, showing the near linear increase in the spectral density as the frequency decreases from 80 eV to 10^{-5} eV. For low values of E, the slopes and intercept from Eq. (14.24) agree within about two tenth of a percent with the exact theoretical values obtained from Eq. (14.4).

To explore Power's approach at low frequency, we can let E become very small in the spectral density Eq. (14.14), giving

$$\frac{\Delta E_n^{Power}}{dE}|_{E->0} = -\frac{2\alpha}{3\pi mc^3}\sum_m |\mathbf{p}_{mn}|^2 \frac{E}{E_m - E_n} \tag{14.25}$$

which is identical to the second term in Eq. (14.19), the low E approximation to the Bethe result Eq. (14.10), so we have from Eq. (14.22):

$$\frac{\Delta E_n^{Power}}{dE} = -\frac{1}{\pi}\frac{\alpha}{mc^2}E. \tag{14.26}$$

This result Eq. (14.26) is identical to the frequency dependent term in Eq. (14.24), which is the low frequency spectral density from the Bethe approach and from the group theoretical expression. However, in the low frequency limit based on Power's expression for the spectral density, the

constant term that is present in the other approaches does not appear. This is a consequence of the form used for the index of refraction, which assumes that real photons are present that can excite the atom with resonant transitions. The modified implementation of Feynman's proposal by Milonni *et al.*, noted in Section 9.3.3 would yield a low energy result that agrees with that of Bethe and group theory [244].

14.5 Conclusion

The non-relativistic Lamb shift can be interpreted as due to the interaction of an atom with the fluctuating electromagnetic field of the quantum vacuum. We introduce the concept of a spectral shift density which is a function of frequency ω or energy $E = \hbar\omega$ of the vacuum field. The integral of the spectral density from $E = 0$ to the rest mass energy of an electron, 511 keV, gives the radiative shift. We report on calculations of the spectral density of the level shifts for 1S, 2S and 2P states based on a group theoretical analysis and compare the results to the spectral densities implicit in previous calculations of the Lamb shift. The group theoretical calculation provides an explicit form for the spectral density over the entire spectral range. Bethe's approach requires a summation over an infinite number of states, all bound and all scattering, to obtain a comparable spectral density. We compare all approaches for asymptotic cases, for very large and very small energies E.

The calculations of the shift spectral density provide a new perspective on radiative shifts. The group theory approach as well as the approaches of Bethe, Power, and Welton all show the same $1/E$ high frequency behavior for S states above about $E = \hbar\omega = 1000$ eV to $E = 511$ keV, namely a spectral density for S states equal to $(4/3\pi)(\alpha(Z\alpha)^4 mc^2/n^3)(1/E)$ for states with principal quantum number n. Since our group theory calculation shows that about 76% of the ground state 1S shift is contributed by E above 1000 eV, this is essentially why all the approaches give approximately the same result for the 1S Lamb shift.

Only the Bethe and group theory calculations have the correct low frequency behavior. We find that for the S states the spectral density increases linearly as E approaches zero. Its maximum value is at $E = 0$ and for S states equals $(2\alpha/3\pi)(Z\alpha)^2/n^2$. This maximum value is about $1/(Z\alpha)^2$ or about 2×10^4 larger than the high frequency spectral density at $E = 510$ keV. Thus, low energies contribute much more to the shift for a given spectral interval than high energies. Energies below 13.6 eV

contribute about 2.5%. It is surprising that about 97.5% of the 1S radiative shift is due to fluctuation energies above the ionization potential, which means that intermediate scattering states dominate the shift. Because of the huge spectral range that contributes to the shift, contributions to the shift from high energies are very important. Half of the contribution to the 1S shift comes from energies above 9050 eV.

The 2P shift has a very different spectral density from an S state: it is negative and has an asymptotic behavior that goes as $1/E^2$ rather than as $1/E$. Below about 20 eV, the absolute value of the 2P spectral density is much larger than the 2S spectral density and dominates the 2S-2P shift spectral density, yet the total 2P shift is only about 0.3% of the total 2S shift.

In the last chapter, we discuss the field of virtual vacuum energy that surrounds the hydrogen atom due to its interaction with quantum vacuum fluctuations.

Chapter 15

The Cloud of Virtual Quanta Surrounding the H Atom

15.1 Introduction

This chapter focuses on the spectral interpretation of the dominant lowest-order non-relativistic radiative shift, which is what Bethe calculated, and which accounts for about 97% of the total shift. This shift can be interpreted as arising from virtual transitions of the H atom induced by quantum fluctuations of the electromagnetic field. Since the vacuum field contains all frequencies, virtual transitions to all states, bound and scattering, occur. Indeed, as we saw in Chapter 14, over 95% of the ground state shift arises from transitions to scattering states. These short-lived virtual transitions result in a slight shift in the average energy of the atom, the radiative Lamb shift [20]. This continuous process of absorption and emission of virtual photons produces a cloud of virtual energy around the atom [243]. When only one atom is present, the interaction results in the field around the atom corresponding to the Lamb shift. If multiple atoms are present, these clouds affect neighboring atoms; along with the zero-point field, this interaction leads to the van der Waals force and the Casimir force. The van der Waals forces arise because the vacuum fluctuations cause a correlation in the induced dipole moments of the atoms.

We have calculated the non-relativistic Lamb shift using SO(4,2) group theory. In Chapter 14, Eqs. (14.3) and (14.4) give an expression for the level shift as an integral of a spectral shift density over the frequency of the vacuum fluctuations [252, 260]. There is no sum over states as in Bethe's evaluation of the shift. This approach provides an analytical expression for the contribution of each frequency of the vacuum fluctuations to the radiative Lamb shift. This expression allows us to compute the volume

that corresponds to the spectral components present in the Lamb shift by considering the energy density of the zero-point vacuum field.

The calculations by Power and Milonni show that for the ground state 1S Lamb shift, which is positive since all transitions are to states with energy greater than the ground state, the energy density of the fluctuating zero point field around the atom must increase so that the integral of the energy over the volume surrounding the atom gives the 1S Lamb shift [3, 203, 244]. The increased energy is supplied by the quantum fluctuations of the electromagnetic field. By comparing the needed vacuum energy, which we determine from our calculation of the spectral shift density in Chapter 14, with the known energy density of the zero-point vacuum fluctuations, we can calculate the volume of vacuum energy needed for each spectral component of the shift. In Sec. 15.2, we will show that for energies above about 100 eV, the spectral volume is much smaller than the region occupied by the ground state wavefunction; for energies less than about 1 eV the spectral volume is significantly larger than the ground state wavefunction. Consequently, the focus of this paper is on the low energy regime. For this regime, we will show that the radius of the spherical spectral volume for a vacuum fluctuation of wavelength λ is approximately $(\alpha/2\pi)\lambda$, where α is the fine structure constant. A simple estimate of the size of the virtual photon cloud based on the uncertainty relation for energy and time predicts a maximum radius of the spectral volume which is larger than that predicted by the Lamb shift model by a factor of $1/4\alpha$ [257, 261].

15.2 Computing the Size of the Vacuum Energy Field

Consider a large box containing one H atom in the ground state. We know both the spectral density $\frac{d\Delta E_1}{dE}$ of the radiative shift in the ground state, given by Eq. (14.4), and the energy density of the quantum vacuum without an H atom present. In the box containing the H atom, the vacuum field density must increase such that the integral of the energy density over the volume provides the 1S Lamb shift. This increase in vacuum energy results from the vacuum fluctuations, which have a free-field spectral energy density (energy/volume - frequency) equal to [3]

$$\rho_0(\omega) = \frac{\hbar\omega^3}{2\pi^2 c^3}, \tag{15.1}$$

where c is in cm/s, ω is the radial frequency in s^{-1} and ρ has units of erg/cm^3–sec^{-1}. If the frequency is measured in eV then it is the

energy $E = \hbar\omega$, and the vacuum spectral energy density has units of $(\text{eV/cm}^3 - \text{eV}) = 1/\text{cm}^3$ and is

$$\rho_0(E) = \frac{E^3}{2\pi^2\hbar^3c^3}. \tag{15.2}$$

The integral $\int_{E_1}^{E_2} \rho_0(E)dE$ represents the energy density eV/ cm^3 in the energy interval E_1 to E_2. The question being addressed here is: what volume of vacuum energy of density $\rho_0(E)$ is required to supply the amount of energy required for the radiative shift?

The total renormalized radiative shift ΔE_1 can be expressed as the integral of the vacuum energy density $\rho_0(E)$ over an effective volume $V_1(E)$:

$$\Delta E_1 = \int_0^{mc^2} dE\rho_0(E)V_1(E), \tag{15.3}$$

with the same upper limit for E as used previously [3]. Recall the definition of the spectral shift density Eq. (14.3):

$$\Delta E_1 = \int_0^{mc^2} dE\frac{\Delta E_1}{dE}. \tag{15.4}$$

Comparing Eq. (15.3) with Eq. (15.4) shows that the effective spectral volume $V_1(E)$ needed to insure energy balance at each energy E is

$$V_1(E) = \frac{d\Delta E_1}{dE}\frac{1}{\rho_0(E)}. \tag{15.5}$$

The spectral volume $V_1(E)$ has dimensions of cm^3 and contains the amount of vacuum energy at energy value E that corresponds to the ground state spectral density at the same energy E. To compute the spectral volume $V_1(E)$, we use the results for the spectral shift density $d\Delta E_1/dE$ described in Chapter 14, Eqs. (14.4) for the 1S shift and (14.6–14.8) for the 2S and 2P shifts. The spectral volume, $V_1(E)$, in Eq. (15.5) is assumed to be spherical since the ground state is an S state, so the radius can be calculated from the known spectral volume. In Section 15.4, this assumption is discussed in more detail.

Equations (15.3)–(15.5) are general equations and apply to any calculation of the radiative Lamb shift that can be expressed as an integral over the vacuum energy, as in Eq. (15.4). The utility of Eqs. (15.3)–(15.5) lies in our ability to provide an explicit analytical expression for the spectral shift using our group theoretical results.

An example of Eq. (15.3) is in the calculation of the Lamb shift as a Stark effect by Milonni [3]. Consider the energy $W = -\frac{1}{2}\mathbf{d}\cdot\mathbf{E}(\omega)$ for a

dipole $\mathbf{d}$ in an isotropic field, $\mathbf{E}(\omega)$. Assuming that the dipole is induced by the field, then $\mathbf{d}(\omega) = \alpha(\omega)\mathbf{E}(\omega)$. The energy for an atom A at $\mathbf{x}_a$ with polarizability $\alpha_A(\omega)$ can be expressed as [3]

$$W_A = -\frac{1}{2}\int_0^\infty d\omega \alpha_A(\omega)\langle \mathbf{E}^2(\omega)\rangle. \tag{15.6}$$

For the Lamb shift, $\langle \mathbf{E}(\omega)^2\rangle = 4\pi\rho_0(\omega)$, where ρ_0 is the zero-point vacuum spectral energy density, one obtains

$$W_A = -2\pi\int_0^\infty d\omega \alpha_A(\omega)\rho_0(\omega). \tag{15.7}$$

The polarizability is provided by the Kramers–Heisenberg formula and has units of volume. This expression for the Lamb shift has the same form as Eq. (15.3). To complete the Stark shift calculation, the contribution from the free electron needs to be subtracted, after which the final result is identical to that of Bethe [3].

In Fig. 15.1, for the 1S ground state radiative shift, we plot the log of the radius in Å of the spectral volume $V_1(E)$ on the y-axis versus the log of the energy E in eV on the x-axis.

For energies above about 100 eV, the spectral volume is less than 1 cubic Angstrom, approximately the volume of the ground state wavefunction. For an energy of 1 eV, the spectral volume is 11850 A^3, corresponding to a sphere of radius about 14 A, meaning that there is a sphere of positive vacuum energy of radius 14 A around the atom corresponding to the 1 eV shift spectral density.

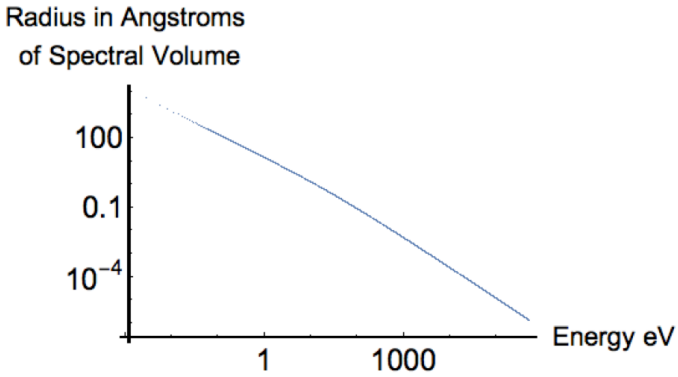

Fig. 15.1. The log of the radius of the spherical spectral volume $V_1(E)$ for the 1S state, Eq. (15.5), as a function of the log of the vacuum field energy E, from 0.0027 eV (where the radius is 5330 Å) to 511,000 eV (where the radius is 10^{-17} Å).

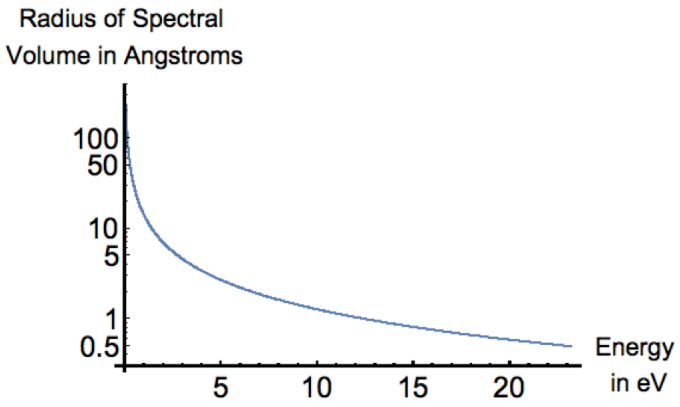

Fig. 15.2. The log of the radius of the spherical spectral volume $V_1(E)$ for the 1S state, Eq. (15.5) as a function of the vacuum field energy E, from 0.05 eV to 23 eV, with corresponding radii of 288 Å and 0.5 Å. The radius approximately follows $1/E$ behavior.

Figure 15.2 shows the radius of the spherical spectral volume for energies below 23 eV. For an energy of 21.7 eV, the spectral radius equals the mean radius of the ground-state wave function of 0.53 Å. For energies less than 21.7 eV, the radius will be greater than the radius of the ground state. For an energy of 0.054 eV, the radius is 288 Å. For these low energies, the radius goes approximately as $1/E$.

For low-energy vacuum fluctuations, the spectral density from Eq. 14.24 can be approximated for an S state with the principal quantum number n as constant, dropping the energy dependent term:

$$\frac{d\Delta E_n}{dE}|_{E\to 0} = \frac{2\alpha}{3\pi}\frac{(Z\alpha)^2}{n^2}. \tag{15.8}$$

Equation (15.8) is accurate to about 5% at 1 eV, and the precision increases as the energy decreases. This approximation corresponds to the end point $E = 0$ of the nearly horizontal portion of the spectral density in Fig. 14.2. For these low energies, the spectral volume, $V_n(E)$, from Eq. (15.5) is

$$V_n(E) = \frac{4\pi}{3}\frac{\alpha(Z\alpha)^2}{n^2}\frac{(\hbar c)^3}{E^3}. \tag{15.9}$$

Assuming a spherical spectral volume of radius $R_V(E)$ for a state n, one finds:

$$R_V(E) = \left[\frac{\alpha(Z\alpha)^2}{n^2}\right]^{1/3}\frac{\hbar c}{E}, \tag{15.10}$$

which for low E for the 1S state of hydrogen gives

$$R_V(E) = \alpha \frac{\hbar c}{E} = \frac{14.4\,\text{Å}}{E\ \text{eV}}. \tag{15.11}$$

The H atom is surrounded by a steady-state cloud of virtual quanta; this cloud has a radius $R_V(E)$ in Angstroms for a quantum energy E in eV and is continuously emitted and absorbed by the field. This vacuum energy density of the cloud is positive in the sense that it is above the free-field vacuum energy density.

It is remarkable that the asymptotic low energy spectral radius, $R_V(E)$, in Eq. (15.11) has such a simple form. This result can be rewritten using the definition, $\alpha = e^2/\hbar c$, with e the elementary charge as

$$E = \frac{e^2}{R_V(E)}. \tag{15.12}$$

Thus, the Coulomb energy for two electrons separated by a distance $R_V(E)$ equals the energy $E = \hbar\omega$ of the corresponding vacuum virtual photon.

It is interesting to compare the radius $R_V(E)$ of the spectral volume with the wavelength, λ, of the vacuum fluctuation corresponding to $E = \hbar\omega = 2\pi\hbar c/\lambda$. For the ground state, this gives

$$R_V(E) = \frac{\alpha}{2\pi}\lambda = \frac{\lambda}{861}. \tag{15.13}$$

The radius of the spectral volume is equal to $\alpha/2\pi$ times the wavelength of the corresponding vacuum fluctuation. That the radius is so much smaller than the wavelength of the corresponding vacuum fluctuation may seem puzzling, but we need to remember that the energy in the volume is an integral overall the wavelengths in the vacuum field. Long-wavelength vacuum fluctuations produce macroscopic regions of positive vacuum energy for the hydrogen ground state. For a fluctuation wavelength of 1 km, which corresponds to a radio wave, the vacuum field around the atom would extend for over one meter.

15.3 Comparison to Predictions from the Uncertainty Relation

A simple analysis using the uncertainty relation can provide an order of magnitude estimate of the largest extent of the positive energy vacuum field. The hydrogen atom is a quantum system, and its energy in the ground state can consequently vary for a time interval τ by an amount ΔE_u which is restricted by the uncertainty relation [172, p. 201]

$$\Delta E_u \tau < \hbar/2. \tag{15.14}$$

The variation in energy is modeled by the emission and absorption of virtual photons of energy $\Delta E_u = \hbar\omega_u$ and frequency ω_u. Since the velocity of the photon is c, in the time τ it can travel a distance $2R_u$ where [257]

$$R_u < \frac{\hbar c}{4\Delta E_u} = \frac{c}{4\omega_u} = \frac{\lambda}{8\pi}, \tag{15.15}$$

where λ is the wavelength of the virtual photon. Comparison of Eq. (15.15) to Eq. (15.13) shows that for the same energy virtual photon we have

$$R_V = 4\alpha R_u. \tag{15.16}$$

For vacuum fluctuations of energy E below about 1 eV, the dimension R_V of the virtual cloud predicted by an analysis of the ground state Lamb shift is 4α times smaller than the maximum extent, R_u, allowed by the Uncertainty Relation. Ref. [257] has suggested that $(4\pi/3)\alpha$ can be considered the mean density of virtual photons in the region around the atom, which may explain the difference between R_u and R_V.

15.4 Significance of the Zero-Point Field Around the Atom

The cloud of quantum fluctuations surrounding the H atom can be interpreted as resulting from the scattering of the free-field vacuum fluctuations by the atom. The zero-point field activates the atom in a continuous process, creating the steady-state cloud of quantum fluctuations that has been described in this chapter. As the derivation of the Lamb shift in terms of the Stark effect suggests, the zero-point field induces an instantaneous dipole moment in the atom that leads to a dipole field. The continuous stochastic excitation from the zero-point field leads to a sum of incoherent dipole contributions that average to a spherically symmetric cloud [172].

One can imagine the atom undergoing virtual transitions from the ground state to all higher energy states and then returning to the ground state in accordance with the time–energy uncertainty relation. For a zero-point fluctuation of the wavelength λ, our calculations in Section 15.2 have show that the cloud extends about $\alpha\lambda/2\pi$ from the nucleus, which can be a macroscopic distance. Probably the easiest way to detect the vacuum field, at least for short distances, is by the presence of Casimir-Polder or van der Waals forces. Direct measurement of vacuum fluctuations is challenging but there have been several recent direct measurements in the terahertz range using femtosecond electro-optic detection in a cryogenic non-linear crystal [262–264].

For the cloud of vacuum energy that we have calculated, there are several ways of exploring its significance: first, by computing estimates of the mean

energy density, which we do in Section 15.5; and second, by explaining its role in the creation of van der Waals forces under the assumption that another H atom is nearby, which we do in Section 15.6.

15.4.1 *Does the field of vacuum fluctuations around the atom have any biological significance?*

There are similar fields of quantum vacuum energy around all atoms, and for macroscopic matter, the fields are more energetic, so it is reasonable to ask this question. We know these fields induce significant dispersion forces and interactions, for example in protein folding, DNA stacking, and nucleic acid stability [281].

Recent research has suggested that Casimir forces, Casimir-Polder forces, van der Waals forces and quantum entanglement may play a pervasive role in biological systems. For example, Casimir forces have been proposed as the force that stabilizes the lipid bilayer structure of cell membranes [279].

To organize data from diverse fields, neurology, biophysics, psychology, mind-body medicine, psychoimmunology, energy medicine, researchers have proposed the concept of an energetic biofield, "a complex organizing field engaged in the generation, maintenance, and regulation of biological homeodynamics" [280]. It is very likely that the ubiquitous field of quantum fluctuations plays a role in the biofield. There is increasing evidence of quantum signaling, entanglement, communication in biological systems [282] and in the cytoskeleton of networks of microtubules [280]:

"Together these results describe the mind-body as an interconnected system in which electromagnetic and quantum interactions act through field-coherent oscillatory activity to regulate biological processes and mediate interactions correlated with sentience and mental activity."

It is very possible that future research will involve extensive exploration of the role of vacuum fluctuations in biological systems. The discovery of a simple, reliable method to measure vacuum fluctuations would certainly catalyze this research.

15.5 Energy Density of the Zero-Point Field Around the Atom

Using the results in Section 15.3, it is possible to compute the energy density of this field as a function of distance for different wavelengths or energy intervals of the zero-point field. Consider a spherical shell: the inner radius corresponds to one energy and is given by Eq. (15.11). The outer radius

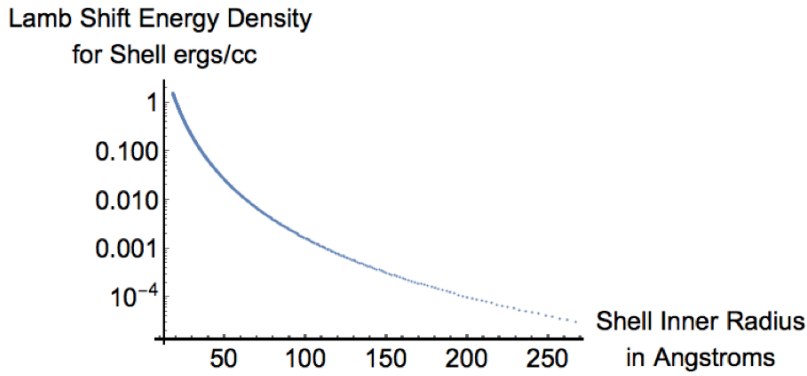

Fig. 15.3. The Lamb shift energy density, $\rho_{\rm LS}^{\rm shell}$ from Eq. (15.19) as a function of the inner radius, $R_1 = \alpha\hbar c/(\beta E)$, of the shell. The outer radius, $R = \alpha\hbar c/E$, is 1.03 times the inner radius; thus, $g(\beta) = 11.3$ (see Eq. (15.21)).

corresponds to a slightly smaller energy. For this energy interval, one can estimate the contribution to the total Lamb shift by integrating the curve in Fig. 14.1 [260]. For energies below 1 eV the contribution to the ground state Lamb shift is about 0.24% of the total shift. In this low energy range, the contribution to the shift scales linearly with the energy, as shown in Fig. 14.3(b). This allows us to compute a mean energy density, $\rho_{\rm LS}^{\rm shell}$, of the quantum fluctuations in a spherical shell.

The density of the Lamb shift energy in the spherically symmetric region of vacuum energy surrounding the H atom can be analyzed in terms of shells with an outer radius of $R = \alpha\hbar c/E$ and inner radius of $R_1 = \alpha\hbar c/E_1$. It is convenient to let $E_1 = \beta E$, where $\beta > 1$. Assuming that both energies are less than 1 eV, one can integrate the Lamb shift (LS) spectral density from Eq. (15.8) for the ground state and $Z = 1$ to obtain the enegy contained in the shell

$$\Delta E_{\rm LS}^{\rm shell}(E) = \int_E^{\beta E} dE \frac{2\alpha^3}{3\pi} = \frac{2\alpha^3}{3\pi} E(\beta - 1) \tag{15.17}$$

to an accuracy of about 5%. The volume of the shell is

$$V^{\rm shell}(E) = \frac{4\pi}{3}(\alpha\hbar c)^3 \left(1 - \frac{1}{\beta^3}\right) \frac{1}{E^3}. \tag{15.18}$$

Therefore, the Lamb shift energy density (in erg/cm^3) in the shell is

$$\rho_{\rm LS}^{\rm shell}(E) = \frac{\Delta E_{\rm LS}^{\rm shell}(E)}{V^{\rm shell}(E)} = \frac{1}{2\pi^2} \frac{1}{(\hbar c)^3} \frac{\beta - 1}{1 - 1/\beta^3} E^4. \tag{15.19}$$

The Lamb shift energy density for a shell with outer radius $R = \alpha\hbar c/E$, and inner radius $R_1 = \alpha\hbar c/(\beta E)$, is proportional to E^4 or $1/R_V^4(E)$. Figure 15.3 shows the value of $\rho_{\rm LS}^{\rm shell}$ as a function of the inner radius (in Å), where the outer radius is 1.03 times the inner radius ($\beta = 1.03$).

One can compare the energy density $\rho_{\rm LS}^{\rm shell}(E)$ from Eq. (15.19) (in erg/cm^3) to the energy density $\rho_0^{\rm shell}(E)$ (in erg/cm^3) of the free zero-point vacuum field for the same spectral interval, i.e., from E to βE:

$$\rho_0^{\rm shell}(E) = \int_E^{\beta E} dE\rho_0(E) = \frac{1}{8\pi^2\hbar^3c^3}E^4(\beta^4 - 1). \tag{15.20}$$

One finds that the ratio

$$\frac{\rho_{\rm LS}^{\rm shell}(E)}{\rho_0^{\rm shell}(E)} = 4\frac{\beta - 1}{1 - 1/\beta^3}\frac{1}{\beta^4 - 1} = g(\beta), \tag{15.21}$$

is a constant that depends on β. The Lamb shift energy density for the shell is directly proportional to the free vacuum energy density for the same energy interval. This result follows for low E since the spectral density, $\frac{d\Delta E_1}{dE}$ from Eq. (15.8), is a constant. Comparison with Eq. (15.5) shows that $\rho_0(E)V_1(E)$ is therefore constant and independent of E for low E values.

The function $g(\beta)$ is singular at $\beta = 1$ and decreases rapidly as β increases. For $1 < \beta < 1.35$, $g(\beta)$ is greater than 1. For β of (1.01, 1.02 1.03, 1.05, 1.1), the corresponding values of $g(\beta)$ are $(33.5, 16.8, 11.3, 6.8, 3.5)$. For these shells, $\rho_{\rm LS}^{\rm shell}(E)$ is always greater than $\rho_0^{\rm shell}(E)$. Just as free-field vacuum fluctuations are important in many physical systems, the field of fluctuations due to the Lamb shift must be equally important.

Table 15.1 shows the results of computing the energy densities for different spherical shells. The first row corresponds to a shell with the frequency range of the visible spectrum (400 nm to 700 nm), for which the energy density in the shell, $\rho_{\rm LS}^{\rm shell}$, is 98.7 erg/cm^3, which is 45% of the corresponding $\rho_0^{\rm shell}$ (the free field energy density for the shell) of 218 erg/cm^3. For cases with $\beta < 1.35$, the ratio $\rho_{\rm LS}^{\rm shell}/\rho_0^{\rm shell}$ in the fifth column is greater than one.

The energy densities $\rho_{\rm LS}^{\rm shell}$ for the shells are significant, for example, compared to the energy densities, $\rho_{\rm bb}$, for black body radiation over the same spectral intervals. For a temperature of 600 K (for which the peak intensity is at about five micrometers or 0.25 eV) the ratio of $\rho_{\rm LS}^{\rm shell}/\rho_{\rm bb}$ is $2.8 \times 10^4, 148$, and 10.1, respectively, for the shells with radii 20 –30 Å, 50–60 Å, and 200–210 Å. Of course black body radiation is ordinary electromagnetic radiation, while the Lamb shift energy consists of vacuum fluctuations of the electromagnetic field.

Table 15.1. The inner and outer radii for a spherical shell around the atom, the corresponding fluctuation energies $\rho_{\rm LS}^{\rm shell}$ Eq. (15.19) and $\rho_0^{\rm shell}$ Eq. (15.20), and the ratio of $\rho_{\rm LS}^{\rm shell}$ to $\rho_0^{\rm shell}$.

Inner and Outer Radii of Spherical Shell (in Å)	**Quantum Fluctuation Energy Range (in eV)**	**Mean Shell Lamb Shift Energy Density, $\rho_{\rm LS}^{\rm shell}$ (in erg/cm^3)**	**Mean Shell Free Field Energy Density, $\rho_0^{\rm shell}$ (in erg/cm^3)**	$\rho_{\rm LS}^{\rm shell}/\rho_0^{\rm shell}$
4.64 to 8.13	Visible 3.10 to 1.77	98.7	218	0.45
10 to 20	0.72 to 1.44	3.34	10.65	0.314
20 to 30	0.48 to 0.72	0.399	0.570	0.700
30 to 40	0.36 to 0.48	0.1024	0.0959	1.068
40 to 50	0.288 to 0.36	0.0373	0.0262	1.16
50 to 60	0.240 to 0.288	0.0167	0.00941	1.77
60 to 70	0.2057 to 0.240	0.00852	0.00403	2.12
70 to 80	0.180 to 0.2057	0.00480	0.00196	2.45
80 to 90	0.160 to 0.180	0.00291	0.00104	2.79
90 to 100	0.144 to 0.16	0.00186	0.000595	3.13
140 to 150	0.096 to 0.1029	0.000344	0.0000718	4.78
200 to 210	0.0686 to 0.072	8.59×10^{-5}	1.25×10^{-5}	6.87
300 to 310	0.0465 to 0.048	1.76×10^{-5}	1.67×10^{-6}	10.49
400 to 410	0.0351 to 0.036	5.63×10^{-6}	4.27×10^{-7}	13.16
1000 to 1020	0.01412 to 0.0144	1.46×10^{-7}	8.58×10^{-9}	16.97

15.6 Relationship between the Zero-Point Field Around the Atom and van der Waals Forces

Zero-temperature Lamb shifts and van der Waals interactions have straightforward physical interpretations in terms of fluctuating zero-point fields [3]. Here, we consider an isolated atom A and describe the fluctuating field around this atom that arises from its interaction with the free field vacuum fluctuations. The field around atom A corresponds to the non-relativistic Lamb shift for atom A. If another atom is present, the field around A plays an essential role in the van der Waals forces between the atoms.

To illustrate this, generalize Eq. (15.6) for the energy of an induced dipole at A to include a second atom B. The total field is $\mathbf{E}_{\mathbf{k},\omega}$ and the combined energy is [3, Sec. 3.11]

$$W_{AB} = -\frac{1}{2}\sum_{\mathbf{k}\omega} \alpha_A(\omega_k)\langle \mathbf{E}^2_{\mathbf{k}\omega}(\mathbf{x}_A, t)\rangle, \tag{15.22}$$

where $\alpha_A(\omega_k)$ is the polarizability of atom A at frequency ω_k, $\mathbf{k}$ is the wave vector, and t denotes the time. The total field acting on A is assumed to be the sum of the zero-point field $\mathbf{E}_{0,\mathbf{k}\omega}(\mathbf{x}_A, t)$ acting on A and the field at A

that is produced by atom B from its interaction with the quantum vacuum field:

$$\mathbf{E}_{\mathbf{k}\omega}(\mathbf{x}_A, t) = \mathbf{E}_{0,\mathbf{k}\omega}(\mathbf{x}_A, t) + \mathbf{E}_{B,\mathbf{k}\omega}(\mathbf{x}_A, t). \tag{15.23}$$

The presence of the second atom breaks the spherical symmetry, so a summation over $\mathbf{k}$ for the non-isotropic field is included. Each atom is "driven" by the zero-point field at its location, creating a fluctuating dipole field about the atom. The field about atom B affects atom A and vice versa so the total energy is

$$W_{AB}^{total} = -\frac{1}{2}\sum_{\mathbf{k}\omega} \alpha_A(\omega_k)\langle \mathbf{E}_{0,\mathbf{k}\omega}^2(\mathbf{x}_A, t) + \mathbf{E}_{B,\mathbf{k}\omega}^2(\mathbf{x}_A, t) + \mathbf{E}_{0,\mathbf{k}\omega}(\mathbf{x}_A, t)\mathbf{E}_{B,\mathbf{k}\omega}(\mathbf{x}_A, t) + \mathbf{E}_{B,\mathbf{k}\omega}(\mathbf{x}_A, t)\mathbf{E}_{0,\mathbf{k}\omega}(\mathbf{x}_A, t)\rangle. \tag{15.24}$$

The portion of the energy W_{AB}^{total} that depends on the distance between the atoms corresponds to the van der Waals force, and is

$$W_{AB}^{\text{vdW}} = -\frac{1}{2}\sum_{\mathbf{k}\omega} \alpha_A(\omega_k)\langle \mathbf{E}_{0,\mathbf{k}\omega}(\mathbf{x}_A, t)\mathbf{E}_{B,\mathbf{k}\omega}(\mathbf{x}_A, t) + \mathbf{E}_{B,\mathbf{k}\omega}(\mathbf{x}_A, t)\mathbf{E}_{0,\mathbf{k}\omega}(\mathbf{x}_A, t)\rangle. \tag{15.25}$$

The term $\alpha_A(\omega_k)\langle \mathbf{E}_{0,\mathbf{k}\omega}(\mathbf{x}_A, t)\rangle^2$ in the summation in Eq. (15.24) does not depend on the separation between the atoms and corresponds to the Lamb shift for atom A. This is the field of vacuum fluctuations about the atom that represents the atom's response to the vacuum field that we have described. From Eq. (15.25) one can immediately see that this field also plays an essential role in the van der Waals force. Similarly, this field would be essential for the Casimir–Polder force between an atom and a surface.

The term $\mathbf{E}_{B,\mathbf{k}\omega}(\mathbf{x}_A, t)$ represents the field at atom A that is from the induced dipole at atom B, and is proportional to the polarizability $\alpha_B(\omega_k)$ of atom B. After computation, the final expression for the van der Waals force is shown to be a symmetric integral over ω of the product $\alpha_A(\omega)\alpha_B(\omega)$ times a function of ω and $r = |\mathbf{x}_A - \mathbf{x}_B|$ [3]. Detailed calculations of the renormalized electric and magnetic field fluctuations around a dressed H atom are given in [243].

To clarify the physical origin of the van der Waals force, we note that the field about atom B corresponding to the Lamb shift induces a fluctuating dipole moment in the nearby atom A. The correlation between the fluctuating dipole moments at the two locations gives rise to the van

der Waals forces. The correlation falls off rapidly with frequency and with the distance r between the two locations, giving the r^{-6}-dependence of the non-retarded van der Waals interaction. The cloud of zero-point fluctuations about the H atom described is fundamental to van der Waals forces as well as to the Lamb shift. These phenomena are linked in that they both arise from the interaction between atoms and the fluctuating zero-point field.

The van der Waals forces tend to become retarded for distances greater than about a_0/α (a_0 being the Bohr radius of the ground-state wavefunction), or about 70 Å. Retarded van der Waals forces are described as Casimir forces [3]. From the calculations in Table 15.1, one can see that lower energy fluctuations are responsible for these dispersion forces.

15.7 Conclusions

The nonrelativistic Lamb shift can be interpreted as being due to the interaction between atoms and the fluctuating zero-point electromagnetic field of the quantum vacuum. The renormalized radiative Lamb shift can be expressed in terms of a spectral shift density, which is a function of the frequency ω or energy $E = \hbar\omega$ of the vacuum field. The integral of the spectral density from $E = 0$ to the rest of the mass energy of an electron, 511 keV, gives the non-relativistic radiative shift for that state of the atom.

Feynman, Power, and Milonni showed that the radiative shift equals the change in the energy of the vacuum fluctuations in the region containing the H atom. Using this result with our group-theoretical calculation of the contribution to the Lamb shift from each frequency of the vacuum fluctuations, we derived an expression for the size of the region of vacuum energy corresponding to each value of the vacuum energy E around the H atom. The spectral volume for the energy E around an H atom contains vacuum fluctuations of energy E; the total energy of these fluctuations equals the radiative shift corresponding to that energy E. For the ground state, the energy density in the spectral volume is positive, which means that it is above the energy density of the free field. For $E > 23$ eV, the radius of the region of positive energy vacuum fluctuations is less than the atomic radius; on the other hand, for energies less than 1 eV the radius is shown to be approximately $R_V(E) = \alpha\hbar c/E = 14.4/E$ Å, and can be much larger than the ground-state wavefunction.

The radius of the spectral volume can also be expressed in terms of the wavelength of the corresponding vacuum fluctuations as $\alpha\lambda/2\pi = \lambda/861$.

An estimate of the extent of photons from virtual transitions based on the uncertainty relation for time and energy predicts a maximum radius that is about $1/4\alpha$ larger than the radius based on the radiative shift calculations.

The vacuum energy field around the H atom described in this chapter plays an essential role in the van der Waals forces and Casimir forces as well as in the Lamb shift. These phenomena are linked since both arise from the interaction between atoms and the fluctuating zero-point field. The calculations in this paper were performed for the ground state of H, which has a positive radiative shift. States with a negative radiative shift, such as 2P, would also have a spectral volume as well; however, the energy would be negative, i.e., below the free-field vacuum energy. Notably, this analysis is complicated by the fact that the 2P state decays to the 1S state.

15.8 Final Comments about the H atom and Radiative Shifts and Future Research

We have discussed the history of Lamb shift and Bethe's pivotal calculation and how it influenced the direction of theoretical physics for over half a century.

Measurement and computation of the properties of the hydrogen atom have been central to the development of modern physics over the last century. One of the most useful and profound ways to understand its properties is through its symmetries, which we have explored, beginning with the symmetry of the Hamiltonian, which reflects the symmetry of the degenerate levels, then the larger non-invariance and spectrum-generating groups, which include all of the states. The successes in using symmetry to explore the hydrogen atom led to use of symmetry to understand and model other physical systems, particularly elementary particles.

We have discussed the general nature of radiative shifts of bound state energy levels from the classical and the quantum perspectives, examining in some detail results for the harmonic oscillator and the hydrogen atom. The radiative shifts are complex; the real part is the level shift and the imaginary part is the level width. The shifts arise due to the emission and absorption of virtual photons which occurs because of the interaction of the charged particle with its own radiation field or with the vacuum zero-point fluctuations. We know that vacuum fluctuations are affected by geometry and therefore radiative shifts differ from free space values for atoms in a cavity or near a surface [245–249, 265]. Lamb shifts have even been used to model gravitational energy in black holes [266].

Today, the calculation of radiative shifts and atomic energy levels can be done very precisely, from 1 part in 10^{12} to 1 part in 10^{15} for certain energy levels, one of the the most precise computations for any physical system [1]. Today, the corresponding experiments demonstrate comparable precision and agreement with theory. Because of this high precision, measurements of radiative shifts and atomic energy levels reveal detailed information about phenomena causing shifts aside from radiative effects. Some see the opportunity for developing metrology [205, 267–270]. This favorable situation allows atomic systems to be a platform for the discovery of new physics beyond the standard model.

Theoreticians are already calculating the effect on energy levels due to the quantization of space and space-time fluctuations for H atoms, muonic atoms, and Rydberg states [4, 6, 14, 15, 267, 271–274]. Measurements are being done on cooperative Lamb shifts for mesoscopic arrays [275, 276].

Researchers are exploring the relationship between the hydrogen atom and quantum information [12], the effect of non-commuting canonical variables $[x_i, x_j] \neq 0$ on energy levels [13–15], muonic hydrogen spectra [4], and new physics using Rydberg states [5–8, 10, 277]. The ultra high precision of the measurement of energy levels has led to a new understanding of the two body systems with low Z, including muonium, positronium, and tritium [149]. As mentioned in the introduction, measurements of levels shifts are currently being used to measure the radius of the proton [1]. We can expect that atomic energy level measurements and computations will continue to contribute significantly to the development of quantum physics in the future. Investigations of the hydrogen atom and hydrogen-like atoms will continue to reveal new vistas of physics, and symmetry considerations will likely play an important part.

This page intentionally left blank

Appendix A

Appendix: Brief Derivation of the Group Theoretical Formula for the Radiative Shift

The group theoretical approach is based solely on the Schrodinger and Klein–Gordon equations of motion in the non-relativistic dipole approximation. We obtain a result

$$\Delta E_{NL} = \frac{2\alpha}{3\pi(mc)^2}\int_0^{\hbar\omega_c} dE\langle NL|p_i\frac{H-E_N}{H-(E_N-E)-i\epsilon}p_i|NL\rangle, \quad \text{(A.1)}$$

where $E=\hbar\omega$ and ω_C is a cutoff frequency for the integration that we will take as $\hbar\omega_c = mc^2$. If we insert a complete set of states in this expression we obtain Bethe's result Eq. (12.1). If we add and subtract E from the numerator in Eq. (A.1), we find the real part of the shift is

$$\Delta E_{NL} = \frac{2\alpha}{3\pi(mc)^2}Re\int_0^{\hbar\omega_c} dE[\langle NL|p^2|NL\rangle - E\Omega_{NL}], \quad \text{(A.2)}$$

where

$$\Omega_{NL} = \langle NL|p_i\frac{1}{H-E_N+\hbar\omega-i\epsilon}p_i|NL\rangle. \quad \text{(A.3)}$$

The matrix element Ω_{NL} can be converted to a matrix element of a function of SO(4,2) generators taken between the basis states $|nlm;a)$ of $(Z\alpha)^{-1}$ [110]. To obtain these basis states $|nlm;a)$ we write Schrodinger's equation for a particle of energy $E=-\frac{a^2}{2m}$ in a Coulomb potential as

$$\left[p^2+a^2-\frac{2m\hbar cZ\alpha}{r}\right]|a\rangle = 0. \quad \text{(A.4)}$$

There are solutions for $|a\rangle$ for certain critical values of the energy $E_n = -\frac{a_n^2}{2m}$ or for $a_n = \frac{mcZ\alpha}{n}$. By inserting factors of $1 = \sqrt{ar}\frac{1}{\sqrt{ar}}$ and making a scale change from a_n to a we obtain the eigenvalue equation

$$\left(\frac{1}{n} - K_1(a)\right) \ |nlm;a) = 0, \tag{A.5}$$

where

$$K_1(a) = \frac{1}{\sqrt{ar}}\frac{2a^2\hbar}{p^2+a^2}\frac{1}{\sqrt{ar}} \quad \rho(a) = n\hbar/ar \quad \sqrt{\rho(a_n)}|nlm\rangle = |nlm;a_n). \tag{A.6}$$

The complete basis functions $|nlm;a)$ have the same quantum numbers as the ordinary bound states [110]. The kernel $K_1(a)$ is bounded and finite, so there are no continuum solutions. We define a generator of SO(4,1) as $\Gamma_0 = 1/K_1(a)$ so

$$(\Gamma_0 - n)|nlm) = 0. \tag{A.7}$$

We need to define several more generators. The generator S is a dimensionless dilation operator that can change the value of the parameter a in the basis states:

$$S = \frac{1}{2\hbar}(\boldsymbol{p}\cdot\boldsymbol{r} + \boldsymbol{r}\cdot\boldsymbol{p}). \tag{A.8}$$

To find Γ_4, we calculate $\Gamma_4 = -i[S,\Gamma_0]$, obtaining

$$\Gamma_4 = \frac{1}{2\hbar}\left(\frac{\sqrt{r}p^2\sqrt{r}}{a} - ar\right) \quad \Gamma_0 = \frac{1}{2\hbar}\left(\frac{\sqrt{r}p^2\sqrt{r}}{a} + ar\right). \tag{A.9}$$

The generators $(\Gamma_4, S, \Gamma_0) = (j_1, j_2, j_3)$ form a O(2,1) subgroup and $S = i[\Gamma_4,\Gamma_0], \Gamma_0 = -i[S,\Gamma_4]$ and for our representations $\Gamma_0^2 - \Gamma_4^2 - S^2 = \boldsymbol{L^2} = l(l+1)$. The scale change S transforms Γ_0 according to the equation

$$e^{i\lambda S}\Gamma_0(a)e^{-i\lambda S} = \Gamma_0(e^\lambda a) = \Gamma_0\cosh\lambda - \Gamma_4\sinh\lambda \tag{A.10}$$

with the corresponding equation for Γ_4. Finally, we have

$$\Gamma_i = \frac{1}{\hbar}\sqrt{r}p_i\sqrt{r}. \tag{A.11}$$

The quantity $\boldsymbol{\Gamma} = (\Gamma_0,\Gamma_1,\Gamma_2,\Gamma_3,\Gamma_4)$ is a five vector under transformations generated by SO(4,2). For the representation of SO(4,2) based on the states $|nlm)$, all generators are Hermetian, and $\boldsymbol{\Gamma}^2 = \Gamma_A\Gamma^A = -\Gamma_0^2 + \Gamma_1^2 + \Gamma_2^2 + \Gamma_3^2 + \Gamma_4^2 = 1$. The commutators of the components of the five vector are generators of $SO(4,2)$ transformations.

Inserting factors of $1 = \sqrt{ar}\frac{1}{\sqrt{ar}}$ and using the definitions of the generators we can transform Eq. (A.3) to

$$\Omega_{NL} = \frac{m\nu}{N^2}(NL|\Gamma_i \frac{}{\Gamma n(\xi) - \nu}\Gamma_i|NL), \tag{A.12}$$

where

$$n^0(\xi) = \frac{2+\xi}{2\sqrt{1+\xi}} = \cosh\phi \quad n^i = 0 \quad n^4(\xi) = -\frac{\xi}{2\sqrt{1+\xi}} = -\sinh\phi \tag{A.13}$$

and

$$\xi = \frac{\hbar\omega}{|E_N|} \quad \nu = \frac{N}{\sqrt{1+\xi}} = Ne^{-\phi}. \tag{A.14}$$

From the definitions, we see $\phi = \frac{1}{2}ln(1+\xi) > 0$ and $n_A(\xi)n^A(\xi) = -1$. The contraction over i in Ω_{NL} may be evaluated using our group theoretical formula for a contraction Eq. 7.31

$$\sum_B \Gamma_B f(n\Gamma)\Gamma^B = \frac{1}{2}(n\Gamma+1)^2 f(n\Gamma+1) + \frac{1}{2}(n\Gamma-1)^2 f(n\Gamma-1) - (n\Gamma)^2 f(n\Gamma). \tag{A.15}$$

We apply the contraction formula to the the integral representation

$$f(n\Gamma) = \frac{1}{\Gamma n - \nu} = \int_0^\infty ds e^{\nu s} e^{-n\Gamma s} \tag{A.16}$$

and obtain the result Eq. 7.41

$$\Gamma_A \frac{1}{\Gamma n - \nu}\Gamma^A = -2\nu \int_0^\infty ds\, e^{\nu s}\frac{d}{ds}\left(\sinh^2\frac{s}{2}\, e^{-n\Gamma s}\right). \tag{A.17}$$

Applying this to our expression Eq. (A.12) for Ω_{NL} gives

$$\begin{aligned}\Omega_{NL} = &-2\frac{m\nu^2}{N^2}\int_0^\infty ds e^{\nu s}\frac{d}{ds}\left(\sinh^2\frac{s}{2}M_{NL}(s)\right) \\ &- m\frac{\nu}{N^2}(NL|\Gamma_4\frac{1}{\Gamma n(\xi)-\nu}\Gamma_4|NL) \\ &+ m\frac{\nu}{N^2}(NL|\Gamma_0\frac{1}{\Gamma n(\xi)-\nu}\Gamma_0|NL),\end{aligned} \tag{A.18}$$

where

$$M_{NL}(s) = (NL|e^{-\Gamma n(\xi)s}|NL). \tag{A.19}$$

In order to evaluate the last two terms in Eq. (A.19), we use $\Gamma_0 = N|NL)$ and express the action of Γ_4 on our states as $\Gamma_4 = N-(1/\sinh\phi)(\Gamma n(\xi)-\nu)$. Using the virial theorem $(NLM|p^2|NLM) = a_N^2$, we find that the term in p^2 in Eq. (A.2) exactly cancels the last two terms in Ω_{NL}, yielding the result

$$Re\Delta E_{NL} = \frac{4mc^2\alpha(Z\alpha)^4}{3\pi N^4}\int_0^{\phi_c} d\phi \sinh\phi e^{\phi}\int_0^{\infty} ds\, e^{\nu s}\frac{d}{ds}\Big(\sinh^2\frac{s}{2}M_{NL}(s)\Big), \tag{A.20}$$

where

$$\phi_c = \frac{1}{2}ln\left(1+\frac{\hbar\omega_c}{|E_N|}\right) = \frac{1}{2}ln\left(1+\frac{2N^2}{(Z\alpha)^2}\right). \tag{A.21}$$

We can derive a generating function for the shifts for any eigenstate characterized by N and L if we multiply Eq. (A.20) by $N^4e^{-\beta N}$ and sum over all $N, N \geq L+1$. To simplify the right side of the resulting equation, we use the fact that Γ_4, S, and Γ_0 form an O(2,1) algebra so we have:

$$\sum_{N=L+1}^{\infty} e^{-\beta N}M_{NL} = \sum_{N=L+1}^{\infty}(NL|e^{-\boldsymbol{j}\cdot\boldsymbol{\psi}}|NL), \tag{A.22}$$

where

$$e^{-\boldsymbol{j}\cdot\boldsymbol{\psi}} \equiv e^{-\beta\Gamma_0}e^{-s\Gamma n(\xi)}. \tag{A.23}$$

We perform a $\boldsymbol{j}$ transformation generated by $e^{i\phi S}$, such that $e^{-\boldsymbol{j}\cdot\psi} \rightarrow e^{-j_3\psi} = e^{-\Gamma_0\psi}$. The trace is invariant with respect to this transformation so we have

$$\sum_{N=L+1}^{\infty} e^{-\beta N}M_{NL} = \sum_{N=L+1}^{\infty}(NL|e^{-j_3\psi}|NL) = \sum_{N=L+1}^{\infty} e^{-N\psi} = \frac{e^{-\psi(L+1)}}{1-e^{-\psi}}, \tag{A.24}$$

where we have used $(NL|\Gamma_0)|NL) = N$.

In order to find a particular M_{NL}, we must expand the right hand side of the equation in powers of $e^{-\beta}$ and equate the coefficients to those on the left hand side. Using the isomorphism between $\boldsymbol{j}$ and the Pauli $\boldsymbol{\sigma}$ matrices $(\Gamma_4, S, \Gamma_0) \rightarrow (j_1, j_2, j_3) \rightarrow (\frac{i}{2}\sigma_1,\ \frac{i}{2}\sigma_2,\ \frac{1}{2}\sigma_3)$ we find

$$e^{+\frac{1}{2}\psi} = de^{\frac{1}{2}\beta} + be^{-\frac{1}{2}\beta} - e^{-\frac{1}{2}\psi}, \tag{A.25}$$

where

$$\begin{aligned} d &= \cosh\frac{s}{2} + \sinh\frac{s}{2}\cosh\phi \\ b &= \cosh\frac{s}{2} - \sinh\frac{s}{2}\cosh\phi \end{aligned} . \tag{A.26}$$

Let β become very large and iterate the equation for $e^{-\frac{1}{2}\psi}$ to obtain the result

$$e^{-\psi} = Ae^{-\beta}\left[1 + A_1 e^{-\beta} + A_2 e^{-2\beta} + \cdots\right], \tag{A.27}$$

where $A = 1/d^2$ and $A_1 = -(2/d)(b - d^{-1})$. To obtain M_{NL}, we expand the right side of Eq. (A.24) using Eq. (A.27), and use the multinomial theorem and collect terms in powers of β. For the 1S shift, we want the matrix element M_{10} which corresponds to $e^{-\beta}$ so $M_{10} = A$. For $N = 2$, $M_{20} = A^2 + AA_1$, $M_{21} = A^2$. Therefore, the radiative shift for the $1S$ ground state is

$$Re\Delta E_{10} = \frac{4mc^2\alpha(Z\alpha)^4}{3\pi}\int_0^{\phi_c} d\phi e^{\phi}\sinh\phi\int_0^{\infty} dse^{se^{-\phi}}\frac{d}{ds}\frac{1}{\left(\coth\frac{s}{2} + \cosh\phi\right)^2}. \tag{A.28}$$

The shift for the 2S-2P level is

$$\begin{aligned} Re(\Delta E_{20} - \Delta E_{21}) = \frac{m\alpha(Z\alpha)^4}{6\pi}\int_0^{\phi_c} d\phi e^{\phi}\sinh^3\phi \\ \times\int_0^{\infty} dse^{2se^{-\phi}}\frac{d}{ds}\frac{1}{\left(\coth\frac{s}{2} + \cosh\phi\right)^4}. \end{aligned} \tag{A.29}$$

This page intentionally left blank

References

[1] A. Beyer, L. Maisenbacher, A. Matveev, R. Pohl, K. Khabarova, A. Grinin, T. Lamour, D. Yost, T. Hansch, N. Kolachevsky and T. H. Udem, The Rydberg constant and proton size from atomic hydrogen, *Science* **358**, p. 79 (2017).

[2] S. Karshenboim, F. Pavone, F. Bassani, M. Inguscio, T. Hänsch and V. Smirnov (eds.), *The Hydrogen Atom: Precision Physics of Simple Atomic Systems*. Springer, Berlin/Heidelberg, Germany (2001).

[3] P. Milonni, *The Quantum Vacuum*. Academic Press, San Diego, CA, USA (1994).

[4] M. Haghighat and M. Khorsandi, Hydrogen and muonic hydrogen atomic spectra in non-commutative space-time, *Eur. Phys. J. C* **75**, 4 (2015).

[5] L. Praxmeyer, Hydrogen atom in phase space: The Wigner representation, *J. Phys. A: Math. Gen.* **39**, p. 14143 (2006).

[6] M. Jones, R. M. Potvliege and M. Spannowsky, Probing new physics using Rydberg states of atomic hydrogen, *Phys. Rev. Research* **2**, p. 013244 (2020).

[7] U. Jentschura, P. Mohr and J. Tan, Fundamental constants and tests of theory in Rydberg states of one-electron ions, *J. Phys. B: At. Mol. Opt. Phys.* **43**, p. 074002 (2010).

[8] U. Jentschura and P. Mohr, Calculation of hydrogenic Bethe logarithms for Rydberg states, *Phys. Rev. A* **72**, p. 012110 (2002).

[9] U. D. Jentschura, E. O. L. Bigot, J. Evers, P. J. Mohr and C. H. Keitel, Relativistic and radiative energy shifts for Rydberg states, *J. Phys. B: At. Mol. Opt. Phys.* **38**, pp. S97–S105 (2005).

[10] S. H. Cantu, A. V. Venkatramani and W. Xu, Repulsive photons in a quantum nonlinear medium, *Nat. Phys.* **16**, pp. 921–925 (2020). https://doi.org/10.1038/s41567-020-0917-6.

[11] M. I. Eides and V. A. Shelyuto, Hard three-loop corrections to hyperfine splitting in positronium and muonium, *Phys. Rev. D* **92**, p. 013010 (2015).
[12] A. Rau and G. Alber, Shared symmetries of the hydrogen atom and the two-bit system, *J. Phys. B: At. Mol. Opt.* **50**, p. 242001 (2017).
[13] P. Castro and R. Kullock, Physics of the $SO_q(4)$ hydrogen atom, *Theo. Math. Phys.* **185**, p. 1678 (2015).
[14] A. Alavi and N. Rezaei, Dirac equation, hydrogen atom spectrum and the Lamb shift in dynamical non-commutative spaces, *Pramana-J. Phys.* **88** (2017), available as https://arxiv.org/abs/1612.05942v1.
[15] K. P. Gnatenko, Y. S. Krynytskyi and V. M. Tkachuk, Perturbation of the ns levels of the hydrogen atom in rotationally invariant non-commutative space, *Mod. Phys. Lett. A* **30**, 08 (2015).
[16] P. Mohr, D. B. Newell and B. N. Taylor, Codata recommended values of the fundamental physical constants: 2014, *Rev. Mod. Phys.* **88**, 3, p. 035009 (2016), arxiv:1507.07956 [physics.atom-ph].
[17] J. Rigden, *Hydrogen, The Essential Element*. Harvard University Press, Cambridge, MA, USA (2002).
[18] W. Lamb and R. Retherford, Fine structure of the hydrogen atom by a microwave method, *Phys. Rev.* **72**, p. 241 (1947).
[19] H. Bethe, The electromagnetic shift of energy levels, *Phys. Rev.* **72**, p. 339 (1947).
[20] G. J. Maclay, History and some aspects of the Lamb shift, *Physics* **2**, pp. 105–149 (2020).
[21] E. Noether, Invariant variation problems, *Transport Theory and Statistical Physics* **1**, 3, pp. 186–207 (1971), doi:10.1080/00411457108231446, arXiv:physics/0503066, original in Gott. Nachr. 1918: 235–257.
[22] M. Hamermesh, *Group Theory*. Addison-Wesley Publishing Co., Reading, MA (1962).
[23] H. Weyl, *The Theory of Groups and Quantum Mechanics*, second edition, Dover Publications, New York, NY (1928), originally published in German in 1928.
[24] E. Wigner, *Group Theory and Its Application to the Quantum Mechanics of Atomic Spectra*. Academic Press, New York, NY (1959).
[25] V. Bargmann, Zur theorie des wasserstoffatoms, *Z. Phys.* **99**, p. 576 (1936).
[26] P. Laplace, *A Treatise of Celestial Mechanics*. Dublin (1827).
[27] W. Pauli, Ãber das wasserstoffspektrum vom standpunkt der neuen quantenmechanik, *Z. Phys.* **36**, p. 336 (1926), eng. trans.: Sources of

Quantum Mechanics (North-Holland, Amsterdam, 1967, B. van der Waerden, Ed.).
[28] G. Valent, The hydrogen atom in electric and magnetic fields: Pauli's 1926 article, *Am. J. Phys.* **71**, p. 171 (2003).
[29] H. Goldstein, *Classical Mechanics*. Addison-Wesley Publishing C., Cambridge, MA (1950).
[30] H. McIntosh, On accidental degeneracy in classical and quantum mechanics, *Am. J. Phys.* **27**, p. 620 (1959).
[31] E. Hulthen, Ãber die quantenmechanische herleitung der balmerterme, *Z. Phys.* **86**, p. 21 (1933).
[32] V. Fock, Zur theorie des wasserstoffatoms, *Z. Phys.* **98**, p. 145 (1935).
[33] P. Dirac, *Quantum Mechanics*, fourth edition edn. Oxford University Press, Oxford, England (1958), first Edition, 1930.
[34] M. Gell-Mann, Symmetries of baryons and mesons, *Phys. Rev.* **125**, p. 1067 (1962).
[35] J. Schwinger, Coulomb's Green's function, *J. Math. Phys.* **5**, p. 1606 (1964).
[36] Y. Ne'eman, *Algebraic Theory of Particle Physics*. W.A. Benjamin, New York, NY (1967).
[37] M. Gell-Mann, A schematic model of baryons and mesons, *Phys. Lett.* **8**, p. 214 (1964).
[38] M. Gell-Mann and Y. Ne'eman, *The Eightfold Way*. W.A. Benjamin, New York, NY (1964).
[39] Y. Dothan, M. Gell-Mann and Y. Ne'eman, Series of hadron energy levels as representations of non-compact groups, *Phys. Lett.* **17**, p. 148 (1965).
[40] Y. Nambu, Infinite-component wave equations with hydrogenlike mass spectra, *Phys. Rev.* **160**, p. 1171 (1967).
[41] F. Dyson, *Symmetry Groups in Nuclear and Particle Physics*. W.A. Benjamin, New York, NY (1966).
[42] L. Thomas, On the unitary representations of the group of de Sitter space, *Ann. Math.* **42**, p. 113 (1941).
[43] Harish-Chandra, Representations of semisimple lie groups II, *Trans. Am. Math. Soc.* **76**, p. 26 (1954).
[44] A. Barut, P. Budini and C. Fronsdal, Two examples of covariant theories with internal symmetries involving spin, *Proc. Roy. Soc. (London) A* **291**, p. 106 (1966).
[45] I. Malkin and V. Man'ko, Symmetry of the hydrogen atom, *Soviet Physics JETP Lett.* **2**, p. 146 (1966).
[46] A. Barut and K. Kleinert, Transition probabilities of the hydrogen atom from noncompact dynamical groups, *Phys. Rev.* **156**, p. 1541 (1967a).

[47] A. Barut and K. Kleinert, Transition form factors in the H atom, *Phys. Rev.* **160**, p. 1149 (1967b).
[48] M. Bander and C. Itzykson, Group theory and the hydrogen atom (I), *Rev. Mod. Phys.* **38**, p. 330 (1966a).
[49] M. Bander and C. Itzykson, Group theory and the hydrogen atom (II), *Rev. Mod. Phys.* **38**, p. 330 (1966b).
[50] C. Fronsdal, Infinite multiplets and local fields, *Phys. Rev.* **156**, p. 1653 (1967a).
[51] C. Fronsdal, Infinite multiplets and the hydrogen atom, *Phys. Rev.* **156**, p. 1665 (1967b).
[52] A. Barut and C. Fronsdal, On non-compact groups. II Representations of the 2+1 Lorentz group, *Proc. Roy. Soc. (London) A* **287**, p. 532 (1965).
[53] C. Fronsdal, Relativistic Lagrangian field theory for composite systems, *Phys. Rev.* **171**, p. 1811 (1968).
[54] R. Pratt and T. Jordan, Coulomb group theory for any spin, *Phys. Rev.* **188**, p. 2534 (1969).
[55] C. Fronsdal, Relativistic and realistic classical mechanics of two interacting point particles, *Phys. Rev. D* **4**, p. 1689 (1971).
[56] R. Kyriakopoulos, Dynamical groups and the Bethe-Salpeter equation, *Phys. Rev.* **174**, p. 1846 (1968).
[57] M. Lieber, O(4) symmetry of the hydrogen atom and the Lamb shift, *Phys. Rev.* **174**, p. 2037 (1968).
[58] R. Huff, Simplified calculation of Lamb shift using algebraic techniques, *Phys. Rev.* **186**, p. 1367 (1969).
[59] R. Musto, Generators of SO(4,1) for the quantum mechanical hydrogen atom, *Phys. Rev.* **148**, p. 1274 (1966).
[60] A. Barut and G. Bornzin, SO(4,2)-formulation of the symmetry breaking in relativistic Kepler problems with or without magnetic charge, *J. Math. Phys.* **12**, p. 841 (1971).
[61] A. Barut and H. Kleinert, Current operators and Majorana equation for the hydrogen atom from dynamical groups, *Phys. Rev.* **157**, p. 1180 (1967).
[62] G. Mack and I. Todorov, Irreducibility of the ladder representations when restricted to the Poincare subgroup, *J. Math. Phys.* **10**, p. 2078 (1969).
[63] A. Decoster, Realization of the symmetry groups of the nonrelativistic hydrogen atom, *Nuovo Cimento* **68A**, p. 105 (1970).
[64] M. Englefield, *Group Theory and the Coulomb Problem.* Wiley-Interscience, New York (1972).
[65] A. Barut, *Dynamical Groups.* University of Canterbury Press, Christchurch, New Zealand (1972).

[66] M. Bednar, Algebraic treatment of quantum-mechanical models with modified Coulomb potentials, *Ann. Phys.* **75**, p. 305 (1973).

[67] C. Wulfman and Y. Takahata, Noninvariance groups in molecular quantum mechanics, *J. Chem. Phys.* **47**, p. 4888 (1967).

[68] B. Wybourne, Symmetry principles in atomic spectroscopy, *J. Phys.* **31**, pp. C4–33 (1970), from his book *Symmetry Principles in Atomic Spectroscopy*, John Wiley and Sons, 1970.

[69] K. Mariwalla, Dynamical symmetries in mechanics, *Phys. Rep.* **20**, p. 287 (1975).

[70] Y. Akyildiz, On the dynamical symmetries of the Kepler problem, *J. Math. Phys.* **21**, p. 665 (1980).

[71] C. Fronsdal and R. Huff, Two-body problem in quantum field theory, *Phys. Rev. D* **3**, p. 933 (1971).

[72] E. Loebl (ed.), *Group Theory and Its Applications*. Academic Press, New York (1971).

[73] A. Barut and W. Rasmussen, The hydrogen atom as a relativistic elementary particle I. The wave equation and mass formulae, *J. Phys. B* **6**, p. 1695 (1973a).

[74] A. Barut and W. Rasmussen, The hydrogen atom as a relativistic elementary particle II. Relativistic scattering problems and photoeffect, *J. Phys. B* **6**, p. 1713 (1973b).

[75] A. Barut and G. Bornzin, Unification of the external conformal symmetry group and the internal conformal dynamical group, *J. Math. Phys.* **15**, p. 1000 (1974).

[76] A. Barut, C. Schneider and R. Wilson, Quantum theory of infinite component fields, *J. Math. Phys.* **20**, p. 2244 (1979).

[77] T. Shibuya and C. Wulfman, The Kepler problem in two-dimensional momentum space, *Am. J. Phys.* **33**, p. 570 (1965).

[78] J. Dahl, Physical interpretation of the Runge-Lenz vector, *Phys. Lett. A* **27**, p. 62 (1968).

[79] P. Collas, Algebraic solution of the Kepler problem using the Runge-Lenz vector, *Am. J. Phys.* **38**, p. 253 (1970).

[80] H. Rodgers, Symmetry transformations of the classical Kepler problem, *J. Math. Phys.* **14**, p. 1125 (1973).

[81] S. Majumdar and D. Basu, O(3,1) symmetry of the hydrogen atom, *J. Phys. A: Math. Nuc. Gen.* **7**, p. 787 (1974).

[82] J. Stickforth, The classical Kepler problem in momentum space, *Am. J. Phys.* **46**, p. 74 (1978).

[83] T. Ligon and M. Schaaf, On the global symmetry of the classical Kepler problem, *Rep. Math. Phys.* **9**, p. 281 (1976).

[84] M. Lakshmanan and H. Hasegawa, On the canonical equivalence of the Kepler problem in coordinate and momentum space, *J. Phys. Math. Gen.*, p. L889 (1984).
[85] R. O'Connell and K. Jagannathan, Illustrating dynamical symmetries in classical mechanics: The Laplace-Runge-Lenz vector revisited, *Am. J. Phys.* **71**, p. 243 (2003).
[86] J. Morehead, Visualizing the extra symmetry of the Kepler problem, *Am. J. Phys.* **73**, p. 234 (2005).
[87] L. Huntington and M. Nooijen, An SO(4) invariant Hamiltonian and the two body bound state. I: Coulomb interaction between two spinless particles, *Intl. J. Quant. Chem.* **109**, p. 2885 (2009).
[88] A. Barut, A. Bohm and Y. Neeman, *Dynamical Groups and Spectrum Generating Algebras*. World Scientific, Singapore (1986).
[89] W. Greiner and B. Muller, *Quantum Mechanics, Symmetries*. Springer-Verlag, Berlin (1989).
[90] R. Gilmore, *Lie Groups, Lie Algebras and Some of their Applications*, Dover Books on Mathematics. Dover, Mineola, NY (2005).
[91] M. Kibler, On the use of the group SO(4,2) in atomic and molecular physics, *Mol. Phys.* **102**, p. 1221 (2004).
[92] I. Hammond and S. Chu, Irregular wavefunction behavior in dimagnetic Rydberg atoms: a dynamical SO(4,2) group study, *Chem. Phys. Lett.* **182**, p. 63 (1991).
[93] F. Lev, Symmetries in foundation of quantum theory and mathematics, *Symmetry* **12**, p. 409 (2020).
[94] C. Wulfman, *Dynamical Symmetry*. World Scientific Publishing, Singapore (2011).
[95] S. G. Karshenboim, Precision physics of simple atoms: QED tests, nuclear structure and fundamental constants, *Phys. Rep. Rev. Sect. Phys. Lett.* **422**, pp. 1–63 (2005).
[96] M. Johnson and B. A. Lippmann, Relativistic Kepler problem, *Phys. Rev.* **78**, p. 329 (1950).
[97] L. Biedenharn, Remarks on the relativistic Kepler problem, *Phys. Rev.* **126**, pp. 845–851 (1962).
[98] J. Lanik, The reformulations of the Klein-Gordon and Dirac equations for the hydrogen atom to algebraic forms, *Czech. J. Phys. B* **19**, p. 1540 (1969).
[99] J. Chen, D. Deng and M. Hu, SO(4) symmetry in the relativistic hydrogen atom, *Phys. Rev. A* **77**, p. 034102 (2008).
[100] A. Stahlhofen, Comment on "SO(4) symmetry in the relativistic hydrogen atom", *Phys. Rev. A* **78**, p. 036101 (2008).

[101] T. Khachidze and A. Khelashvili, The hidden symmetry of the Coulomb problem in relativistic quantum mechanics: from Pauli to Dirac, *Am. J. Phys.* **74**, p. 628 (2006).
[102] F. Zhang, B. Fu and J. Chen, Dynamical symmetry of Dirac hydrogen atom with spin symmetry and its connection to Ginocchio's oscillator, *Phys. Rev. A* **78**, p. 040101(R) (2008).
[103] V. Heine, *Group theory in Quantum Mechanics*. Dover Publications, New York, NY (1993), originally published by Pergamon Press in 1960.
[104] D. E. Neuenschwander, *Emmy Noether's Wonderful Theorem*. Johns Hopkins University Press (2010).
[105] J. Hanca, S. Tulejab and M. Hancova, Symmetries and conservation laws: Consequences of noether's theorem, *Am. J. Phys.* **72**, 4, pp. 428–435 (2004).
[106] N. Byers, E. Noether's discovery of the deep connection between symmetries and conservation laws, (1998), arXiv:physics/9807044, proceedings of a Symposium on the Heritage of Emmy Noether, held on 2–4 December 1996, at the Bar-Ilan University, Israel, Appendix B.
[107] Y. Dothan, Finite-dimensional spectrum-generating algebras, *Phys. Rev. D* **2**, p. 2944 (1970).
[108] O. Mukanda, N. and E. Sudarshan, Characteristic noninvariance groups of dynamical systems, *Phys. Rev. Let.* **15**, p. 1041 (1965).
[109] E. Kyriakopoulos, Algebraic equations for Bethe-Salpeter and Coulomb Green's functions, *J. Math. Phys.* **13**, p. 1729 (1972).
[110] L. S. Brown, Bounds on screening corrections in beta decay, *Phys. Rev.* **135**, p. B314 (1964).
[111] H. Lipkin, *Lie Groups for Pedestrians*. Dover Publications, Mineola, New York (2001).
[112] L. S. Brown, Classical limit of the hydrogen atom, *Am. J. Phys.* **41**, p. 525 (1973).
[113] G. Bois, *Tables of Indefinite Integrals*. Dover Pub1ications, Inc., New York (1961).
[114] H. Bacry, in W. E. Brittin, A. O. Barut and M. Guenin (eds.), *Lectures in Theoretical Physics, Vol. IXA*. Gordon and Breach, New York, NY (1967).
[115] M. Boiteux, The three-dimensional hydrogen atom as a restricted four-dimensional harmonic oscillator, *Physica* **65**, p. 381 (1972).
[116] J. Hughes, The harmonic oscillator: values of the SU(3) invariants, *J. Phys. A: Math. Gen.* **6**, p. 453 (1973).

[117] A. Chen, Hydrogen atom as a four-dimensional oscillator, *Phys. Rev. A* **22**, p. 333 (1980).
[118] A. Chen, Homomorphism between SO(4,2) and SU(2,2), *Phys. Rev. A* **23**, p. 1653 (1981).
[119] M. Kibler and T. Negadi, Connection between the hydrogen atom and the harmonic oscillator: The zero-energy case, *Phys. Rev. A* **29**, p. 2891 (1984).
[120] A. Chen and M. Kibler, Connection between the hydrogen atom and the four-dimensional oscillator, *Phys. Rev. A* **31**, p. 3960 (1985).
[121] C. Gerry, Coherent states and the Kepler-Coulomb problem, *Phys. Rev. A* **33**, pp. 2207–2211 (1986).
[122] A. Chen, Coulomb Kepler problem and the harmonic oscillator, *Am. J. Phys.* **55**, p. 250 (1987).
[123] J. van der Meer, The Kepler system as a reduced 4d oscillator, *J. Geom. Phys.* **92**, p. 181 (2015).
[124] H. Bacry, The de Sitter group $L_{4,1}$ and the bound states of the hydrogen atom, *Nuovo Cimento* **41**, p. A222 (1966).
[125] L. Biedenharn, Wigner coefficients for the R_4 group and some applications, *J. Math. Phys.* **2**, p. 433 (1961).
[126] L. I. Schiff, *Quantum Mechanics*. McGraw Hill, New York, NY (1955).
[127] L. Biedenharn and N. Swamy, Remarks on the relativistic Kepler problem. II. approximate Dirac-Coulomb Hamiltonian possessing two vector invariants, *Phys. Rev.* **133**, p. B1353 (1964).
[128] S. Karshenboim, Simple atoms, quantum electrodynamics, and fundamental constants, in S. G. Karshenboim and V. B. Smirnov (eds.), *Precision Physics of Simple Atomic Systems*. Springer, Berlin/Heidelberg, Germany, pp. 141–162 (2003).
[129] P. Morse and H. Feshbach, *Methods of Theoretical Physics*, Vol. 1. McGraw-Hill, New York (1953).
[130] A. Erdeli (ed.), *Higher Transcendental Functions, Bateman Manuscript Project, Vol. 2*. McGraw-Hill Book Co., NY, NY (1953).
[131] A. Makowski and P. Peplowski, Zero-energy wave packets that follow classical orbits, *Phys. Rev. A* **86**, p. 042117 (2012).
[132] P. Bellomo and J. C. Stroud, Classical evolution of quantum elliptical orbits, *Phys. Rev. A* **59**, p. 2139 (1999).
[133] M. Berry and K. Mount, Semiclassical approximations in wave mechanics, *Rep. Prog. Phys.* **35**, p. 315 (1972).
[134] J. Eberly and C. R. Stroud, Jr. *Chapters 14 (Rydberg Atoms) and Chapter 73 (Coherent Transients) in Springer Handbook of Atomic, Molecular, and Optical Physics, Ed. G. Drake*. Springer Science and Business Media, NY, NY (2006).

[135] M. Lakshmanan and K. Ganesan, Rydberg atoms and molecules-testing grounds for quantum manifestations of chaos, *Curr. Sci.* **68**, p. 38 (1995).
[136] K. Kay, Exact wave functions for the Coulomb problem from classical orbits, *Phys. Rev.* **25**, p. 5190 (1999).
[137] D. D. Lena, C. and J. Gay, Wave functions of atomic elliptic states, *Europhys. Lett.* **15**, p. 697 (1991).
[138] B. D.-R. Bhaumik, D. and G. Ghosh, Classical limit of the hydrogen atom, *J. Phys. A: Math. Gen.* **19**, p. 1355 (1986).
[139] D. McAnally and A. Bracken, Quasiclassical states of the Coulomb system and SO(4, 2), *J. Phys. A: Math. Gen.* **23**, p. 2027 (1990).
[140] A. Pitak and J. Mostowski, Classical limit of position and matrix elements for Rydberg atoms, *Eur. J. Phys.* **39**, p. 025402 (2018).
[141] M. Nauenberg, Quantum wavepackets on Kepler elliptical orbits, *Phys. Rev. A* **401** (1989).
[142] U. Leonhardt, *Measuring the Quantum State of Light*. Cambridge University Press, Cambridge, UK (1997).
[143] A. Barut and L. Girardello, New "coherent" states associated with non-compact groups, *Commun. Math. Phys.* **21**, p. 41 (1971).
[144] M. Satyanarayana, Squeezed coherent states of the hydrogen atom, *J. Phys. A: Math. Gen.* **19**, p. 1973 (1986).
[145] Q. Liu and B. Hu, The hydrogen atom's quantum-to-classical correspondence in Heisenberg's correspondence principle, *J. Phys. A: Math. Gen.* **34**, p. 5713 (2001).
[146] V. Zverev and B. Rubinstein, Dynamical symmetries and well-localized hydrogenic wave packets, *Proc. of Inst. of Math. of NAS of Ukraine* **50, Part 2**, p. 1018 (2004).
[147] S. Nandi and C. Shastry, Classical limit of the two-dimensional and three-dimensional hydrogen atom, *J. Phys. A: Math. Gen* **22** (1989).
[148] L. Pauling and E. B. Wilson, *Introduction to Quantum Mechancis*. McGraw-Hill, New York, New York (1935).
[149] H. G. Eides, M. and V. Shelyuto, *Theory of Light Hydrogenic Bound States*. Springer Tracts in Modern Physics 222, Springer, Berlin, Germany (2007).
[150] G. W. F. Drake (ed.), *Springer Handbook of Atomic, Molecular and Optical Physics*. Springer, New York, NY, USA (2006).
[151] H. Grotch and D. A. Owen, Bound states in quantum electrodynamics: Theory and application, *Found. Phys.* **32**, pp. 1419–1457 (2002).
[152] M. I. Eides, H. Grotch and V. Shelyoto, Theory of light hydrogenic atoms, *Phys. Rep.* **342**, pp. 63–261 (2001).
[153] H. Grotch, Status of the theory of the hydrogen Lamb shift, *Found. Phys.* **24**, pp. 249–272 (1994).

[154] J. Sapirstein and D. Yennie, Theory of hydrogenic bound states, in T. Kinoshita (ed.), *Quantum Electrodynamics*. World Scientific, Singapore (1990), both perturbative and nonperturbative approaches to the self-energy calculations as well as recoil corrections are summarized.

[155] R. Szafron, Radiative corrections in bound states, *Acta Phys. Pol. B* **48**, p. 2183 (2017).

[156] L. Labzowski and D. Solovyev, Coulomb Green function and its application in atomic theory, in S. G. Karshenboim and V. B. Smirnov (eds.), *Precision Physics of Simple Atomic Systems*. Springer, Berlin/Heidelberg, Germany, pp. 141–162 (2003).

[157] G. Erickson and D. Yennie, Radiative level shifts, I. formulation and lowest order Lamb shift, *Ann. Phys.* **36**, pp. 271–313 (1965).

[158] H. Bethe and E. Salpeter, *The Quantum Mechanics of One and Two Electron Atoms*. Springer-Verlag, Berlin, Germany (1957).

[159] W. Lamb and R. Retherford, Fine structure of the H atom, part I, *Phys. Rev.* **79**, p. 549 (1950).

[160] W. Lamb and R. Retherford, Fine structure of the H atom, Part II, *Phys. Rev.* **81**, p. 222 (1951).

[161] W. Lamb and R. Retherford, Fine structure of the H atom, Part III, *Phys. Rev.* **85**, p. 259 (1952a).

[162] W. Lamb and R. Retherford, Fine structure of the H atom, Part IV, *Phys. Rev.* **86**, p. 1014 (1952b).

[163] J. Rauch and F. Rohrlich, *Theory of Photons and Electrons*. Addison-Wesley, Reading, Mass. (1959).

[164] B. Taylor, W. Parker and D. Langenberg, *The Fundamental Constants and Quantum Electrodynamics*. Academic Press, New York (1969).

[165] T. Appelquist and S. Brodsky, Order α^2 electrodynamic corrections to the Lamb shift, *Phys. Rev. Lett.* **24**, p. 562 (1970).

[166] S. G. Karshenboim, The Lamb shift in the hydrogen atom: Shift of S-states, *Phys. At. Nucl.* **58**, pp. 262–266 (1995).

[167] S. G. Karshenboim and V. A. Shelyuto, Three-loop radiative corrections to the 1s Lamb shift in hydrogen, *Phys. Rev. A* **100**, p. 032513 (2019).

[168] S. G. Karshenboim, A. Ozawa and V. G. Ivanov, Higher-order logarithmic corrections and the two-loop self-energy of a 1s electron in hydrogen, *Phys. Rev. A* **100**, p. 032515 (2019).

[169] F. Low, Natural line shape, *Phys. Rev.* **88**, p. 53 (1952).

[170] P. J. Mohr, D. B. Newell and B. N. Taylor, Codata recommended values of the fundamental physical constants: 2014, *Rev. Mod. Phys.* **88**, p. 035009 (2016), arxiv:1507.07956.

[171] J. F. Babb and N. Brickhouse (eds.), *Eleventh International Conference on Atomic and Molecular Data and Their Applications*, Atoms. MDPI, Basel, Switzerland (2020).

[172] P. Milonni, *An Introduction to Quantum Optics and Quantum Fluctuations*. Oxford Univ. Press, Oxford, UK (2019), chapter 4 gives a careful and complete discussion of radiative shifts.

[173] S. Weinberg, *The Quantum Theory of Fields*, Vol. 1. Cambridge University Press, Cambridge, UK (1995).

[174] L. S. Brown, *Quantum Field Theory*. Cambridge University Press, Cambridge, UK (1992).

[175] J. Bjorken and S. Drell, *Relativistic Quantum Mechanics*. McGraw Hill, New York, NY, USA (1964), classic discussion of renormalization in terms of Feynman diagrams.

[176] J. R. Oppenheimer, Note on the theory of the interaction of field and matter, *Phys. Rev.* **35**, p. 461 (1930).

[177] H. A. Kramers, Subtraction of infinities, *Nuovo Cim.* **15**, p. 108 (1938).

[178] H. Bethe, Calculating the Lamb shift, webofstories.com (2020), videos 104–107 of Hans Bethe Scientist. Recorded by Sam Schweber, December 1996.

[179] H. Bethe, Energy on earth and in the stars, in A. Salam, H. Bethe, P. Dirac, W. Heisenberg, E. Wigner, O. Klein and E. Lifshitz (eds.), *From a Life in Physics*. World Scientific, Singapore (1989).

[180] V. Weisskopf, The development of field theory in the last 50 years, *Phys. Today* **34**, pp. 69–85 (1981).

[181] V. Weisskopf, On the self-energy and the electromagnetic field of the electron, *Phys. Rev.* **56**, p. 72 (1939).

[182] P. Milonni, Personal communication, (2020), theoretical Division, Los Alamos National Laboratory, Los Alamos, New Mexico 87545.

[183] W. Lamb, Super classical quantum mechanics: The best interpretation of nonrelativistic quantum mechanics, *Am. J. Phys.* **69**, pp. 413–422 (2001).

[184] F. Dyson, Videos of Freeman Dyson 64-65 discussing Hans Bethe, (1998), recorded by Sam Schweber, June 1998. Available online: we bofstories.com (accessed on 15 March 2020).

[185] F. Dyson, Hans Bethe and quantum electrodynamics, *Phys. Today* **58**, p. 48 (2005).

[186] R. Feynman, The development of the space-time view of quantum electrodynamics, *Phys. Today* **19**, p. 31 (1966).

[187] S. Schweber, *QED and the Men Who Made It: Dyson, Feynman, Schwinger, and Tomonaga*. Princeton University Press, Princeton, NJ, USA (1994).

[188] S. Schweber, The happy thirties, *Phys. Today* **58**, p. 38 (2005).
[189] R. Serber, Linear modifications in the Maxwell field equations, *Phys. Rev.* **48**, p. 49 (1935).
[190] E. Uehling, Polarization effects in the positron theory, *Phys. Rev.* **48**, p. 55 (1935).
[191] F. Dyson, The electromagnetic shift of energy levels, *Phys. Rev.* **73**, p. 617 (1948).
[192] J. French and V. Weisskopf, The electromagnetic shift of energy levels, *Phys. Rev.* **75**, p. 1240 (1949).
[193] N. Kroll and J. W. E. Lamb, On the self-energy of a bound electron, *Phys. Rev.* **75**, p. 388 (1949).
[194] J. Schwinger, Quantum electrodynamics. I. a covariant formulation, *Phys. Rev.* **74**, p. 1439 (1948).
[195] F. Dyson, The radiation theories of Tomonaga, Schwinger, and Feynman, *Phys. Rev.* **75**, p. 486 (1949a).
[196] F. Dyson, The S-matrix in quantum mechanics, *Phys. Rev.* **75**, p. 1736 (1949b).
[197] F. Dyson, *Makers of Patterns: An Autobiography through Letters*. Liveright Publishing, New York, NY, USA (2018).
[198] T. Welton, Some observable effects of the quantum-mechanical fluctuations of the electromagnetic field, *Phys. Rev.* **74**, p. 1157 (1948).
[199] M. Baranger, H. A. Bethe and R. P. Feynman, Relativistic correction to the Lamb shift, *Phys. Rev.* **92**, p. 482 (1953).
[200] R. Karplus, A. Klein and J. Schwinger, Electrodynamic displacement of atomic energy levels. II. Lamb shift, *Phys. Rev.* **86**, p. 288 (1952).
[201] E. H. Wichmann and N. M. Kroll, Vacuum polarization in a strong Coulomb field, *Phys. Rev.* **101**, p. 843 (1956).
[202] W. Erickson, Improved Lamb-shift calculation for all values of $Z\alpha$, *Phys. Rev. Lett.* **27**, p. 780 (1971).
[203] E. Power, Zero-point energy and the Lamb shift, *Am. J. Phys.* **34**, p. 516 (1966).
[204] V. Weisskopf, *The Privilege of Being a Physicist*. W. H. Freeman and Co., New York, NY, USA (1989).
[205] P. J. Mohr, G. Plunien and G. Soff, QED corrections in heavy atoms, *Phys. Rep.* **293**, p. 227 (1998).
[206] P. J. Mohr, Self-energy correction to one-electron energy levels in a strong Coulomb field, *Phys. Rev. A* **46**, p. 4421 (1992).
[207] S. G. Karshenboim, The Lamb shift of excited S-levels in hydrogen and deuterium atoms, *Z. Phys. D* **39**, p. 109 (1997).

[208] S. G. Karshenboim, Two-loop logarithmic corrections in the hydrogen Lamb shift, *J. Phys. B: At. Mol. Opt. Phys.* **29**, pp. L29–L31 (1996).

[209] D. Berkeland, E. Hind and M. Boshier, Precision optical measurement of Lamb shifts in atomic hydrogen, *Phys. Rev. Lett.* **75**, p. 2470 (1995).

[210] S. G. Karshenboim, Lamb shift in the hydrogen atom: Leading logarithmic corrections, *Phys. At. Nucl.* **58**, pp. 649–653 (1995a).

[211] S. G. Karshenboim, Lamb shift in the hydrogen atom: Lifetime of the 2p(1/2) level, *Phys. At. Nucl.* **58**, pp. 835–838 (1995b).

[212] M. I. Eides and H. Grotch, Corrections of order $\alpha^2(Z\alpha)^4$ and $\alpha^2(Z\alpha)^6$ to the Lamb shift, *Phys. Rev. A* **52**, p. 3360 (1995).

[213] S. G. Karshenboim, The Lamb shift in the hydrogen atom, *Zh. Eksp. Teor. Fiz.* **106**, pp. 414–424 (1994).

[214] K. Pachucki, Higher-order binding corrections to the Lamb shift, *Annals of Physics (New York)* **226**, pp. 1–87 (1993), doi:10.1006/aphy.1993.1017.

[215] V. Palchikov, Y. Sokolov and V. Yakovlev, Lifetime of the 2P state and Lamb shift in the hydrogen-atom, *JETP Lett.* **38**, pp. 418–420 (1983).

[216] S. R. Lundeen and F. M. Pipkin, Measurement of the Lamb shift in hydrogen, n = 2, *Phys. Rev. Lett.* **46**, p. 232 (1981).

[217] G. Drake, Quantum electrodynamic effects in few-electron atomic systems, *Adv. At. Mol. Phys.* **18**, p. 399 (1982).

[218] H. Grotch, Lamb shift in nonrelativistic quantum electrodynamics, *Am. J. Phys.* **49**, pp. 48–51 (1981).

[219] J. Sapirstein, Higher-order binding corrections to the Lamb shift, *Phys. Rev. Lett.* **47**, p. 1723 (1981).

[220] S. Schwebel, Interaction theory: Relativistic hydrogen atom and the Lamb shift, *Int. J. Theor. Phys.* **17**, pp. 931–939 (1978).

[221] B. Davies, Note on the Lamb shift, *Am. J. Phys.* **50**, p. 331 (1982).

[222] J. H. Noble and U. D. Jentschura, Dirac equations with confining potentials, *Int. J. Mod. Phys. A* **30**, p. 1550002 (2015).

[223] M. I. Eides and V. A. Shelyuto, Polarization operator contributions to the Lamb shift and hyperfine splitting, *Phys. Rev. A* **68**, p. 042106 (2003).

[224] R. Szafron, E. Y. Korzinin, V. A. Shelyuto, V. G. Ivanov and S. G. Karshenboim, Virtual Delbrück scattering and the Lamb shift in light hydrogenlike atoms, *Phys. Rev. A* **100**, p. 032507 (2019), arXiv:1909.04116. Many papers of Prof. Karshenboim and collaborators are available on ArXiv.

[225] J. Zamastil and V. Patkos, Self-energy of an electron bound in a Coulomb field, *Phys. Rev. A* **88**, p. 032501 (2013).
[226] J. Zamastil, Approximate numerical calculation of the self-energy of a bound electron, *Ann. Phys.* **327**, pp. 297–328 (2012).
[227] U. D. Jentschura and P. J. Mohr, Calculation of hydrogenic Bethe logarithms for Rydberg states, *Phys. Rev. A* **72**, p. 012110 (2005).
[228] U. D. Jentschura, Techniques in analytic Lamb shift calculations, *Mod. Phys. Lett. A* **20**, pp. 2261–2276 (2005).
[229] U. D. Jentschura, P. J. Mohr and G. Soff, Electron self-energy for the K and L shells at low nuclear charge, *Phys. Rev. A* **63**, p. 042512 (2001).
[230] U. D. Jentschura and P. J. Mohr, Electron self-energy for higher excited S levels, *Phys. Rev. A* **69**, p. 064103 (2004).
[231] M. I. Eides, H. Grotch and V. A. Shelyuto, Radiative-recoil corrections of order $\alpha(Z\alpha)^5(m/M)m$ to the Lamb shift revisited, *Phys. Rev. A* **63**, p. 052509 (2002).
[232] B. R. Holstein, Effective interactions and the hydrogen atom, *Am. J. Phys.* **72**, pp. 333–344 (2004).
[233] A. I. Agafonov, Hydrogen energy-level shifts induced by the atom motion: Crossover from the Lamb shifts to the motion-induced shifts, *Mod. Phys. Lett. B* **32**, p. 1850273 (2018).
[234] G. Kelkar, T. Mart and M. Nowakowski, Extraction of the proton charge radius from experiments, *Makara J. Sci.* **20**, pp. 119–126 (2016).
[235] A. P. Martynenko, Proton-polarizability effect in the Lamb shift for the hydrogen atom, *Phys. At. Nucl.* **69**, pp. 1309–1316 (2006).
[236] R. Feynman, *QED: The Strange Theory of Light and Matter*. Princeton University Press, Princeton, NJ, USA (1988).
[237] J. Jackson, *Classical Electrodynamics*. Wiley and Sons, New York, NY, USA (1962), Chapter 17.
[238] D. Cole and Y. Zou, Quantum mechanical ground state of hydrogen obtained from classical electrodynamics, *Phys. Lett. A* **317**, pp. 14–20 (2003).
[239] T. Boyer, Classical zero-point radiation and relativity: The problem of atomic collapse revisited, *Found. Phys.* **46**, pp. 880–890 (2016).
[240] J. Maclay, The role of vacuum fluctuations and symmetry in the hydrogen atom in quantum mechanics and stochastic electrodynamics, *Atoms* **7**, p. 39 (2019), Stochastic Electrodynamics (SED) posits that the vacuum fluctuations are a real electromagnetic field.
[241] H. Puthoff, Ground state of hydrogen as a zero-point fluctuation-determined state, *Phys. Rev. D* **35** (1987).

[242] V. Weisskopf, Recent developments in the theory of the electron, *Rev. Mod. Phys.* **21**, p. 305 (1949).
[243] R. Passante and L. Rizzuto, Vacuum self-dressing of an atom and its physical effects, *Physics* **7** (2025).
[244] P. Milonni, P. R. Berman and K. Sinha, Effect of self-interaction on Feynman's interpretation of the Lamb shift, *Phys. Rev. A* **111**, p. 062208 (2025).
[245] G. Barton, New aspects of the Casimir effect: Fluctuations and radiative reaction, in P. Berman (ed.), *Cavity Quantum Electrodynamics*. Academic Press, San Diego, CA, USA, pp. 425–455 (1994), this gives a clear discussion of how changes in the vacuum field due to surfaces affect charge, magnetic moment, mass and energy levels.
[246] M. Bordag, G. Klimchitskaya, U. Mohideen and V. Mostepanenko, *Advances in the Casimir Effect*. Oxford Univ. Press, New York, NY, USA (2009), this book gives a very complete discussion of how surfaces affect vacuum energy and can lead to Casimir forces between surfaces.
[247] K. Milton, *The Casimir Effect, Physical Manifestations of Zero-Point Energy*. World Scientific, Singapore (2001).
[248] K. Milton and M. Bordag, *Quantum Field Theory Under the Influence of External Conditions*. World Scientific, Singapore (2010), this book discusses a broad variety of systems, including gravitational and nuclear.
[249] B. Billaud and T.-T. Truong, Lamb shift of non-degenerate energy level systems placed between two infinite parallel conducting plates, *J. Phys. A: Math. Theor.* **46**, p. 025306 (2013).
[250] P. Milonni, M. Shaden and L. Spruch, Lamb shift of an atom in a dielectric medium, *Phys. Rev. A* **59**, p. 4259 (1998).
[251] J. Maclay, *The Symmetry of the Energy Levels of the Hydrogen Atom and the Application of the Symmetry to the Calculation of Radiative Level Shifts*, Ph.D. thesis, Yale University, New Haven, CT, USA (1972).
[252] G. J. Maclay, Dynamical symmetries of the H atom, one of the most important tools of modern physics: SO(4) to SO(4,2), background, theory, and use in calculating radiative shifts, *Symmetry* **12**, p. 1323 (2020).
[253] N. Došlić and S. Danko, Harmonic oscillator with the radiation reaction interaction, *Phys. Rev. A* **51**, p. 3485 (1995).
[254] M. Daeimohamad and M. Mohammadi, Quantum dynamics of a harmonic oscillator in a deformed bath in the presence of Lamb shift, *Int. J. Theor. Phys.* **51**, pp. 3052–3061 (2012).

[255] A. Choudhuri, *Astrophysics for Physicists*. Cambridge University Press, Cambridge, England (2010).

[256] B. d'Espagnat, *Veiled Reality, An Analysis of Present-Day Quantum Mechanical Concepts*. Addison-Wesley, Reading, MA, USA (1995).

[257] G. Campagno, R. Passante and F. Persico, *Atom-Field Interactions and Dressed Atoms*. Cambridge University Press, Cambridge, UK (1995).

[258] R. P. Feynman, The present status of quantum electrodynamics, in R. Stoops (ed.), *Institut International de Physique Solvay 1962. La Théorie Quantique des Champs: Douzième Conseil de Physique, tenu à l'Université Libre de Bruxelles du 9 au 14 octobre 1961*. Interscience Publishers/John Wiley & Sons, Inc., New York, NY, USA, pp. 61–99 (1962), available online: http://www.solvayinstitutes.be/pdf/Proceedings_Physics/1961.pdf (accessed on 15 July 2023).

[259] J. J. Sakurai, *Modern Quantum Mechanics*. Addison-Wesley, New York, New York (1994).

[260] G. J. Maclay, New insights into the Lamb shift: The spectral density of the shift, *Physics* **4**, pp. 1253–1277 (2022).

[261] G. J. Maclay, Is the H atom surrounded by a cloud of virtual quanta due to the Lamb shift? *Physics* **5**, pp. 883–894 (2023).

[262] C. Riek, D. V. Seletskiy, A. S. Moskalenko, J. F. Schmidt, P. Krauspe, S. Eckart, S. Eggert, G. Burkard and A. Leitenstorfer, Direct sampling of electric-field vacuum fluctuations, *Science* **350**, 6259, pp. 420–423 (2015).

[263] C. Riek, D. Seletskiy and A. Leitenstorfer, Femtosecond measurements of electric fields: From classical amplitudes to quantum fluctuations, *Eur. J. Phys.* **38** (2017).

[264] I. Benea-Chelmus, F. Settembrini, G. Scalari and J. Faist, Electric field correlation measurements on the electromagnetic vacuum state, *Nature* **568** (2019).

[265] K. Koshino and Y. Nakamura, Control of the radiative level shift and linewidth of a superconducting artificial atom through a variable boundary condition, *New J. Phys.* **14**, p. 043005 (2012).

[266] R. A. Porto, Lamb shift and the gravitational binding energy for binary black holes, *Phys. Rev. D* **96**, p. 024063 (2017).

[267] G. Hagel, C. Schwob, L. Jozefowski, B. de Beauvoir, L. Hilico, F. Nez, L. Julien, F. Biraben, O. Acef and A. Clairon, Metrology of hydrogen atom: Determination of the Rydberg constant and Lamb shifts, *Laser Phys.* **11**, pp. 1076–1082 (2001).

[268] B. Cagnac, Hydrogen metrology: Up to what limit? *Phys. Scr.* **T70**, pp. 24–33 (1997).

[269] B. Cagnac, Progress on the Rydberg constant: The hydrogen atom as a frequency standard, *IEEE Trans. Instrum. Meas.* **42**, pp. 206–213 (1993).

[270] B. Cagnac, M. D. Plimmer, L. Julien and F. Biraben, The hydrogen atom: A tool for metrology, *Rep. Prog. Phys.* **57**, pp. 853–893 (1994).

[271] I. Rivas, A. Camacho and E. Goklu, Quantum spacetime fluctuations: Lamb shift and hyperfine structure of the hydrogen atom, *Phys. Rev. D* **84**, p. 055024 (2011).

[272] S. Zaim, L. Khodja and Y. Delenda, Second-order corrections to the noncommutative Klein-Gordon equation with a Coulomb potential, *Int. J. Mod. Phys. A* **26**, pp. 4133–4144 (2011).

[273] D. Bouaziz and N. Ferkous, Hydrogen atom in momentum space with a minimal length, *Phys. Rev. A* **82**, p. 022105 (2010).

[274] M. Chaichian, M. M. Sheikh-Jabbari and A. Tureanu, Hydrogen atom spectrum and the Lamb shift in noncommutative QED, *Phys. Rev. Lett.* **86**, pp. 2716–2719 (2001).

[275] M. O. Scully, Collective Lamb shift in single photon Dicke superradiance, *Phys. Rev. Lett.* **102**, p. 143601 (2009).

[276] Z. Meir, O. Schwartz, E. Shahmoon, D. Oron and R. Ozeri, Cooperative Lamb shift in a mesoscopic atomic array, *Phys. Rev. Lett.* **113**, p. 193002 (2014).

[277] U. Jentschura, E. LeBigot, J. Evers, P. Mohr and C. Keitel, Relativistic and radiative shifts for Rydberg states, *J. Phys. B: At. Mol. Opt. Phys.* **38**, p. S97 (2005).

[278] A. Cho, Atomic explosion, *Science* **389**, pp. 121–125 (2025).

[279] P. Pawlowski and P. Zielenkiewicz, The quantum Casimir effect may be a universal force organizing the bilayer structure of the cell membrane, *J. Membr. Biol.* **246**(5), pp. 383–389 (2013).

[280] B. Rubik, D. Muehsam, R. Hammerschlag and S. Jain, Biofield science and healing: History, terminology, and concepts, *Global Adv Health Med.* **4**(suppl), pp. 8–14 (2015). DOI:10.7453/gahmj.2015.038.supp.

[281] A. Altun, M. Garcia-Ratés, F. Neese and G. Bistoni, Unveiling the complex pattern of intermolecular interactions responsible for the stability of the DNA duplex, *Chem. Sci.* **12**, pp. 12785–12793 (2021).

[282] M. Bischof and M. E. Del Giudice, Communication and the emergence of collective behavior in living organisms: A quantum approach, *Mol. Biol. Int.* **2013**, pp. 987549 (2013).

This page intentionally left blank

Index